

# **Development of Composites for Tooth and Bone Repair**

Piyaphong Panpisut

DDS, MSc

**UCL**

**Doctor of Philosophy (PhD)**

**2017**

## Candidate declaration

I, Piyaphong Panpisut confirm that the work presented in this thesis is my own. Where information has been derived from other sources, I confirm that this has been indicated in the thesis.

Signature: \_\_\_\_\_

Date: 31<sup>nd</sup> August 2017

## Acknowledgements

Firstly, I would like sincerely to thank my primary supervisor, Professor Anne Young, for her invaluable advice, support, guidance, and encouragement throughout my PhD project. I would like also to thank my secondary supervisor, Dr Lambis Petridis, for his guidance, advice, and help throughout the project.

I would like to acknowledge Dr Wendy Xia, Dr Graham Palmer, Dr George Georgio, Dr Nicola Mordan, and Dr Cécile Dreiss for their training and technical assistance. I also want to acknowledge Dr Caitriona O'Rourke for performing cytocompatibility test. I am very grateful to my friends and colleagues in BTE particularly, Mrs Mayda Arshad, Dr Adnan Khan, Dr Nick Walters, Dr Saad Liaqat, Dr Hesham Ben Nuba, Dr Anas Aljabo, Dr Mustafa Alqaysi, and Dr Nabih Alkhouri for their support.

I am very grateful to Thai Royal Government Scholarship, Dr Weerachai Singhatanadgit, and Faculty of Dentistry, Thammasat University for offering me a great opportunity to study at UCL Eastman Dental Institute.

Finally, I would like to thank my family for supporting and encouraging me to finish my PhD.

## Abstract

Currently used composites for tooth and bone repair share a similar composition. A major issue with dental composites is polymerisation shrinkage leading to bond damage and increased risk of bacterial microleakage. Concerns with bone composites for vertebral fracture repair (vertebroplasty) include low monomer conversion, high stiffness, and lack of antibacterial agent release. The aim of this study was to develop novel dental composites and injectable bone composites to overcome these limitations. The effects of components on various properties of the materials were also examined.

The main components of experimental composites consisted of dimethacrylate monomers mixed with dental glass, mono calcium phosphate monohydrate (MCPM), tristrontium phosphate (TSrP), and polylysine (PLS). The experimental dental composites exhibited higher monomer conversion than a commercial material. The addition of MCPM with TSrP and PLS promoted hygroscopic expansion, apatite precipitation, and early polylysine release. These properties are expected to reduce bacterial microleakage. The incorporation of these additives reduced the monomer conversion and strength of the composites but these were still within an acceptable range.

To produce bone composites, the dental composites were modified by replacing a light activated initiator with a chemically activated initiator and decreasing powder to liquid ratio. The pre-cured bone composites exhibited viscoelastic properties and shear-thinning behaviour which are desirable for injectable materials. The use of high molecular weight diluent monomer (polypropylene glycol dimethacrylate, PPGDMA) increased monomer conversion and shelf life of the bone composites. The addition of MCPM and PPGDMA increased strontium release, which is known to promote *in vivo* bone formation. The use of small glass fillers and fibres improved mechanical properties

of the composites. Furthermore, the composites showed fatigue properties that compared favourably with commercially available materials.

Modulus of elasticity of the experimental bone composites was, however, too high compared with that of cancellous bone. This could potentially lead to increased adjacent vertebral fracture risk. An attempt was made to decrease the modulus by raising the level of PPGDMA, phosphates, and polylysine. Increasing of PPGDMA improved monomer conversion and reduced the injection force required for the composites. Furthermore, the increase of PPGDMA and phosphates enhanced surface apatite precipitation which is known to enable *in vivo* bone bonding. The increase of these components also increased polylysine release. This may reduce postoperative infection, which is a life-threatening complication of vertebroplasty. Increasing PPGDMA and phosphates, however, reduced metabolic activity of mesenchymal stem cells limiting optimal levels.

# Table of Contents

<b>List of Symbols .....</b>	<b>14</b>
<b>List of Abbreviations .....</b>	<b>17</b>
<b>List of Tables.....</b>	<b>20</b>
<b>List of Figures .....</b>	<b>23</b>
<b>Chaper 1 Literature Review .....</b>	<b>37</b>
<b>1.1 Human tooth and Bone .....</b>	<b>37</b>
1.1.1 Tooth: Enamel .....	37
1.1.2 Tooth: Dentine-pulp complex .....	38
1.1.3 Bone .....	39
<b>1.2 Dental Caries.....</b>	<b>41</b>
1.2.1 Epidemiology .....	41
1.2.2 Aetiology of dental caries .....	41
<b>1.3 Current direct restorative materials .....</b>	<b>45</b>
1.3.1 Dental amalgam.....	45
1.3.2 Conventional glass ionomer cement (GIC) and resin modified glass ionomer cement (RMGIC) .....	46
1.3.3 Dental composites .....	48
<b>1.4 Components of dental composites .....</b>	<b>48</b>
1.4.1 Matrix phase .....	48
1.4.2 Filler phase .....	53
<b>1.5 Failure of dental composites due to secondary caries. ....</b>	<b>55</b>
1.5.1 Improper marginal sealing .....	56
1.5.2 Polymerisation shrinkage .....	56
1.5.3 Tooth-composite interfaces degradation .....	56
1.5.4 Surface properties and the composite-biofilm interaction .....	57

<b>1.6</b>	<b>Modification of dental composites to reduce the risk of secondary caries.</b>	<b>57</b>
1.6.1	Remineralising agents .....	58
1.6.2	Antimicrobial agents.....	62
<b>1.7</b>	<b>Regulatory approval for the dental / bone composites.....</b>	<b>65</b>
<b>1.8</b>	<b>Osteoporotic vertebral fractures .....</b>	<b>66</b>
1.8.1	Epidemiology .....	66
1.8.2	Aetiology.....	67
<b>1.9</b>	<b>Vertebroplasty (VP) and kyphoplasty (KP) .....</b>	<b>68</b>
1.9.1	Vertebroplasty (VP) .....	69
1.9.2	Kyphoplasty .....	70
<b>1.10</b>	<b>Current bone cements for VP and BKP.....</b>	<b>71</b>
1.10.1	Polymethyl methacrylate (PMMA) .....	72
1.10.2	Calcium phosphate cements (CPCs) .....	73
1.10.3	Bone composites .....	74
<b>1.11</b>	<b>Complications after VP and KP .....</b>	<b>75</b>
1.11.1	Cement leakage.....	75
1.11.2	Subsequent adjacent fractures .....	76
1.11.3	Postoperative infection.....	76
<b>1.12</b>	<b>Development of low stiffness, mineralising, and antibacterial bone cement .....</b>	<b>77</b>
1.12.1	Low stiffness bone cement.....	77
1.12.2	Calcium phosphate containing bone composite .....	78
1.12.3	Strontium-substituted bone cement.....	79
1.12.4	Antibiotic-loaded bone cement.....	80
<b>1.13</b>	<b>Statement of the problem, aims, objectives, and hypotheses.....</b>	<b>81</b>
<b>Chaper 2</b>	<b>Materials and Methods .....</b>	<b>84</b>
<b>2.1</b>	<b>Materials preparation .....</b>	<b>84</b>
<b>2.2</b>	<b>Storage solutions .....</b>	<b>87</b>
<b>2.3</b>	<b>Methods.....</b>	<b>88</b>

2.3.1 Rheological properties .....	89
2.3.2 Injectability .....	91
2.3.3 Stability of the composite .....	92
2.3.4 Monomer conversion and calculated polymerisation shrinkage/ heat generation .....	93
2.3.5 Mass and volume change .....	96
2.3.6 Polylysine release .....	97
2.3.7 Strontium release .....	102
2.3.8 Surface apatite formation .....	103
2.3.9 Mechanical properties .....	105
2.3.10 Cytocompatibility test using MTS assay .....	110
2.3.11 Statistical analysis .....	111

### **Chaper 3 UDMA / TEGDMA Dental Composites containing Calcium /**

#### **Strontium Phosphate and Polylysine.....113**

<b>3.1 Abstract.....</b>	<b>113</b>
<b>3.2 Introduction.....</b>	<b>115</b>
<b>3.3 Hypotheses .....</b>	<b>116</b>
<b>3.4 Aims and objectives .....</b>	<b>118</b>
<b>3.5 Materials and Methods .....</b>	<b>119</b>
<b>3.6 Statistical analysis.....</b>	<b>120</b>
<b>3.7 Results .....</b>	<b>120</b>
3.7.1 Monomer conversion and calculated polymerisation shrinkage.....	120
3.7.2 Mass and volume changes upon water sorption .....	122
3.7.3 Apatite formation.....	124
3.7.4 Polylysine release .....	127
3.7.5 Biaxial flexural strength (BFS) and modulus of elasticity .....	128
<b>3.8 Discussion .....</b>	<b>129</b>
3.8.1 Monomer conversion .....	129
3.8.2 Mass and volume changes .....	131
3.8.3 Apatite formation.....	132
3.8.4 Polylysine release .....	133



3.8.5	Biaxial flexural strength and modulus of elasticity .....	134
3.9	Conclusions .....	136
<b>Chaper 4 Effect of Powder to Liquid Ratio, Polypropylene Glycol</b>		
<b>Dimethacrylate (PPGDMA) level, and Glass Particle Size on</b>		
<b>Rheological Properties and Physical Stability of Novel Bone</b>		
<b>Composites .....137</b>		
4.1	Abstract.....	137
4.2	Introduction.....	139
4.3	Hypotheses .....	141
4.4	Objectives .....	142
4.5	Materials and Methods .....	143
4.5.1	Material preparation .....	143
4.5.2	Rheological testing .....	144
4.6	Statistical analysis.....	145
4.7	Results .....	146
4.7.1	Apparent viscosity.....	146
4.7.2	Strain sweep measurement .....	147
4.7.3	Frequency sweep measurement.....	153
4.7.4	Flow curve measurement.....	156
4.8	Discussion .....	158
4.8.1	Apparent viscosities .....	158
4.8.2	Strain sweep measurement .....	159
4.8.3	Frequency sweep measurement.....	160
4.8.4	Flow curve measurement.....	160
4.9	Conclusions .....	162
<b>Chaper 5 Assessment of High Temperature Aging on Concentrated</b>		
<b>Active Ingredient Dispersions and Bone Composite Pastes to</b>		

<b>Aid Prediction of Long-Term Chemical Stabilities of New Component Mixtures. ....</b>	<b>163</b>
<b>5.1 Abstract.....</b>	<b>163</b>
<b>5.2 Introduction.....</b>	<b>165</b>
<b>5.3 Hypotheses .....</b>	<b>166</b>
<b>5.4 Objectives .....</b>	<b>168</b>
<b>5.5 Materials and method.....</b>	<b>168</b>
5.5.1 Stability of active ingredients in monomers .....	168
5.5.2 Stability of experimental bone composites .....	171
<b>5.6 Results .....</b>	<b>173</b>
5.6.1 Stability of active ingredients in monomers .....	173
5.6.2 Stability of initiator and activator pastes .....	177
5.6.3 Effect of ageing on monomer conversion of the experimental bone composites.....	181
<b>5.7 Discussion .....</b>	<b>185</b>
5.7.1 Stability of chemical components.....	185
5.7.2 Stability of initiator paste .....	186
5.7.3 Effect of aging on monomer conversion of the experimental bone composites containing PPGDMA or TEGDMA .....	187
<b>5.8 Conclusions.....</b>	<b>188</b>
 <b>Chaper 6 Effect Glass Filler Size / Shape, MCPM, and Level of PPGDMA on Mechanical Properties of Injectable Bone Composites ....</b>	 <b>189</b>
<b>6.1 Abstract.....</b>	<b>189</b>
<b>6.2 Introduction.....</b>	<b>191</b>
<b>6.3 Hypotheses .....</b>	<b>193</b>
<b>6.4 Objectives .....</b>	<b>194</b>
<b>6.5 Material preparation .....</b>	<b>195</b>

6.5.1	Formulations containing different levels of MCPM, fibres, and glass particle size .....	195
6.5.2	Formulations containing varying level of PPGDMA diluent monomer .....	196
<b>6.6</b>	<b>Statistical analysis.....</b>	<b>197</b>
<b>6.7</b>	<b>Results .....</b>	<b>198</b>
6.7.1	Effect of MCPM level, fibre addition, and glass particle size.....	198
6.7.2	Effect of PPGDMA level on biaxial flexural strength and modulus of elasticity .....	203
<b>6.8</b>	<b>Discussion .....</b>	<b>205</b>
6.8.1	Effect of MCPM level, fibre addition, and glass particle size and on biaxial flexural strength (BFS) and fracture toughness ( $K_{IC}$ ) .....	205
6.8.2	Effect of PPGDMA level on biaxial flexural strength and modulus of elasticity .....	207
<b>6.9</b>	<b>Conclusions .....</b>	<b>209</b>
 <b>Chaper 7 Effect of Diluent Monomer and MCPM level on Monomer Conversion, Volumetric stability, Strontium release, Apatite formation, and Fatigue Resistance of Bone Composites.....</b>		
<b>7.1</b>	<b>Abstract.....</b>	<b>210</b>
<b>7.2</b>	<b>Introduction.....</b>	<b>212</b>
<b>7.3</b>	<b>Hypotheses .....</b>	<b>215</b>
<b>7.4</b>	<b>Objectives .....</b>	<b>217</b>
<b>7.5</b>	<b>Materials and Methods .....</b>	<b>218</b>
<b>7.6</b>	<b>Statistical analysis.....</b>	<b>219</b>
<b>7.7</b>	<b>Results .....</b>	<b>220</b>
7.7.1	Monomer conversion .....	220
7.7.2	Mass and volume changes .....	227
7.7.3	Surface apatite formation .....	229
7.7.4	Strontium ( $Sr^{2+}$ ) release .....	230
7.7.5	Biaxial flexural fatigue .....	231

<b>7.8 Discussion .....</b>	<b>237</b>
7.8.1 Monomer conversion .....	237
7.8.2 Mass and volume changes .....	242
7.8.3 Surface apatite formation .....	243
7.8.4 Sr <sup>2+</sup> release.....	243
7.8.5 Biaxial flexural fatigue .....	244
<b>7.9 Conclusions .....</b>	<b>247</b>

## **Chaper 8 Development of Low Stiffness, Polylysine Releasing, and Mineralising Injectable Bone Composites for Vertebroplasty248**

<b>8.1 Abstract.....</b>	<b>248</b>
<b>8.2 Introduction.....</b>	<b>250</b>
<b>8.3 Hypotheses .....</b>	<b>253</b>
<b>8.4 Aim and objectives .....</b>	<b>255</b>
<b>8.5 Materials and Methods .....</b>	<b>256</b>
<b>8.6 Statistical analysis.....</b>	<b>258</b>
<b>8.7 Results .....</b>	<b>259</b>
8.7.1 Injectability.....	259
8.7.2 Monomer conversion .....	261
8.7.3 Mass and volume changes .....	269
8.7.4 Polylysine release.....	274
8.7.5 Apatite formation.....	280
8.7.6 Mechanical properties.....	286
8.7.7 Cytocompatibility test.....	303
<b>8.8 Discussion .....</b>	<b>305</b>
8.8.1 Injectability.....	305
8.8.2 Monomer conversion .....	306
8.8.3 Mass and volume change .....	307
8.8.4 Polylysine release.....	308
8.8.5 Apatite formation.....	310
8.8.6 Mechanical properties.....	311

8.8.7 Cytocompatibility test .....	314
<b>8.9 Conclusions .....</b>	<b>316</b>
<b>Chaper 9 Summary .....</b>	<b>317</b>
<b>Chaper 10 Future Projects.....</b>	<b>322</b>
<b>Bibliography .....</b>	<b>324</b>

# List of Symbols

## Greek letters

$\beta_c$	Centre of deflection
$\delta$	Phase angle
$\varphi$	Volumetric shrinkage
$\epsilon$	Heat generation
$\omega$	Oscillatory frequency
$\rho$	Density
$\nu$	Poisson ratio
$\tau$	Shear stress

## English letters

$a_i$	Variable effect
$A$	Frequency factor
$A$	Absorbance
$b$	Crack length
$B$	Absorbance of C-O peak ( $1320\text{ cm}^{-1}$ ) above background level at $1335\text{ cm}^{-1}$
$C_i$	Concentration of component i
$C_s$	Compressive strength
$d$	Specimen's thickness
$D$	Diffusion coefficient
$D_c$	Monomer conversion

$e_i$	Error functions related to random errors measured at wavelength $i$
$E$	Modulus of elasticity
$E_a$	Activation energy
$F$	Maximum load
$f(a)$	Geometry calibration factor
$G'$	Storage modulus
$G''$	Loss modulus
$G$	Geometric average of property
$\frac{\Delta H}{\Delta W_c}$	Rate of change of load with regard to central deflection gradient of force versus displacement curve
hr	Hour
$K_{IC}$	Fracture toughness
$I$	Radius of specimen
$M$	Mass of a composite disc
$M_t$	Cumulative amount of drug release
$n$	Number of sample
$n_i$	Number of C=C bonds per molecule
$P$	Property of material in factorial analysis
$p$	Level of significance
$q$	Ratio of support radius to the radius of disc
$Q$	Percentage effect of each variable
$r$	Radius of circular support
$R_p$	Rate of polymerisation
$R_p^{\max}$	Maximum rate of polymerisation
$R$	Universal gas constant

$P_t$	Amount of polylysine release
$s$	Second
$S$	Biaxial flexural strength
$S_t$	Amount of $Sr^{2+}$ release
$t$	Time
$t_d$	Delay time
$t_{50}$	Time when monomer conversion of bone composites reaches 50%
$T$	Temperature (Kelvin)
$T_g$	Glass transition temperature
$V$	Volume
$w$	Specimen's width
$W_i$	Molecular weight of each monomer
$W_{PLS}$	Amount of polylysine in a composite disc



## List of Abbreviations

4-META	4-methacryloyloxyethyl trimellitate anhydrous
4-MET	4-methacryloyloxyethyl trimellitate
ACP	Amorphous calcium phosphate
ACN	Acetonitrile
AU	Absorbance unit
ATR	Attenuated total reflectance
BAG	Bioactive glass
BFS	Biaxial flexural strength
BHT	Butylated hydroxyl methacrylate
Bis-EMA	Bisphenol A ethoxy dimethacrylate
Bis-GMA	Bisphenol A glycidyl methacrylate
BP	Benzoyl peroxide
$\beta$ -TCP	$\beta$ -Tricalcium phosphate
CaF <sub>2</sub>	Calcium fluoride
CaP	Calcium phosphate
CDHA	Calcium-deficient hydroxyapatite
CHX	Chlorhexidine
CI	Confidence interval
CPCs	Calcium phosphate cements
CQ	Camphoroquinone
DCPA	Dicalciumphosphate anhydrous (Monetite)
DCPD	Dicalciumphosphate dehydrate (Brushite)
DMPT	N, N-dimethyl-p-toluidine
EDX	Energy dispersive X-ray

FA	Fluoroapatite
FTIR	Fourier transform spectroscopy
GBD	Global Burden of Disease
HA	Hydroxyapatite
HEMA	Hydroxyethyl methacrylate
HILIC	Hydrophilic interaction liquid chromatography
HPLC	High performance liquid chromatography
ICP-MS	inductively couple plasma – mass spectroscopy
KP	Balloon kyphoplasty
MCPM	Monocalcium phosphate monohydrate
MEHQ	4-Methoxyphenol
MHRA	Medicines and Healthcare Regulatory Agency
MMA	Methylmethacrylate
NACP	Nanoparticle amorphous calcium phosphate
NAg	Nano silver particle
Na-NTGGMA	Na-N-tolyglycine glycidyl methacrylate
OCP	Octacalcium phosphate
PLR	Powder to liquid ratio
PLS	$\epsilon$ -Poly-L-lysine
PMMA	Polymethylmethacrylate
PO	Phosphates (combination of monocalcium phosphate monohydrate and tristrontium phosphate)
PPGDMA	Polypropylene glycol dimethacrylate (PPG)
PPRF	Pre-polymerised filler
QAMs	Quaternary ammonium methacrylate
RANKL	Receptor activator of nuclear factor $\kappa$ B ligand

rpm	Revolutions per minute
SBF	Simulated body fluid
S/N	Stress versus number of failure cycle
SQRT (t/hr)	Square root of time (hour)
SEM	Scanning electron microscope
TEGDMA	Triethylene glycol dimethacrylate
TSrP	Tristrontium phosphate
UDMA	Urethanedimethacrylate
UV	Ultraviolet
VP	Vertebroplasty

## List of Tables

Table 1-1 Chemical structure of bulk and diluent monomers (Walters et al., 2016). ....	49
Table 1-2 Chemical structure of adhesion promoting monomers. ....	50
Table 1-3 Chemical structure of initiators and activators. ....	51
Table 1-4 Calcium phosphate compounds (Dorozhkin, 2009; Layrolle, 2011) .....	59
Table 1-5 Summary of recent studies on dental composites containing remineralising and/or antibacterial agents.....	61
Table 1-6 Desirable properties of an injectable bone cement for VP / KP. ....	71
Table 2-1 Chemical components used in the liquid phase. ....	84
Table 2-2 Chemical components used in the powder phase.....	85
Table 2-3 Chemical components of commercial products (Khan, 2015; Guo et al., 2016) used in this thesis. ....	85
Table 2-4 Ion concentration of SBF and human blood plasma.....	87
Table 2-5 Chemicals for preparing 100 mL simulated body fluid.....	88
Table 2-6 Concentration of mobile phases. Solvent A and B were acetonitrile with 0.1 vol% phosphoric acid and deionised water with 0.1 vol% phosphoric acid respectively. ....	99
Table 3-1 Composition of powder phase of experimental composites.....	119

Table 4-1 Formulations of experimental bone composites for rheological test. Liquid phase contained fixed level of HEMA (5 wt%). Powder phase contained fixed level of active fillers (10 wt% MCPM, 15 wt% TSrP, and 5 wt% PLS.....	144
Table 4-2 Apparent viscosity and stability of the mixed composite pastes. Light, medium, and dark shades represent low, medium, and high apparent values respectively. Stars indicate sedimentation of the composite paste after storage in a fridge for 24 hr. ....	146
Table 5-1 Formulations of the composites for chemical stability test. ....	168
Table 5-2 FTIR peaks powder and liquid phase. Reported positions were obtained from published studies (Young et al., 2004; Rozenberg and Shoham, 2007; Young et al., 2008; Shukla and Rai, 2013; Azam et al., 2015). ....	170
Table 5-3 Components of liquid phases before mixing with the powder phase. ....	171
Table 5-4 The powder phase of each formulation was mixed with PPGDMA (PPG) or TEGDMA (TEG) liquid phases presented in Table 5-3.....	172
Table 5-5 Predicted $t_{50}$ at 4, 23, and 37 °C obtained using Arrhenius method and observed times of solidification of initiator pastes.....	180
Table 6-1 Components of liquid phases before mixing with the powder phase. ....	195
Table 6-2 Formulations with varying glass particle sizes, MCPM, and fibre level. Powder phases were mixed with PPGDMA-liquid phase presented in Table 4-1. Activator paste glass sizes were the same as in the initiator pastes.....	196
Table 6-3 Formulations with varying level of PPGDMA. Liquid phases of each formulation were mixed with powder phases of $M_{10}F_{20}G_{0.7}$ .....	197
Table 7-1 Components of liquid phases before mixing with the powder phase. ....	218
Table 7-2 Results from mass and volume changes of each material. Errors are 95 %CI (n=3). ....	228

Table 8-1 Formulations of experimental bone composites. HEMA was fixed at 5 wt%. BP and NTGGMA after mixing were fixed at 1.5 wt% and 1 wt%. Total amount of MCPM and TSrP (PO) in powder phase will be halved after mixing with liquid phase..... 257

## List of Figures

Fig 1-1 Structure of enamel. a) The keyhole-shaped structure consisting of enamel rods. b) The enamel rod contains highly packed of apatites (crystallites). Reprinted from *Biomaterials*, vol 31(7), Ang S. F., Bortel E. L., Swain M. V., Klocke A. & Schneider G. A. *Size-dependent elastic/inelastic behavior of enamel over millimeter and nanometer length scales*, page 1956, Copyright (2010), with permission from Elsevier. .... 37

Fig 1-2 Structure of dentine. a) Dentinal tubules surrounded by peritubular (white rings) and intertubular dentine (light grey). b) Schematic representation of the dentinal tubule (light green) lining by mineralised collagen fibres (dark green). c) These fibres are made of mineral-containing nanofibrils. d) Each nanofibril deposited by biological apatites which are plate-like structure. Reprinted from *Journal of the Mechanical Behavior of Biomedical Materials*, vol 50, Forien J.-B., Fleck C., Krywka C., Zolotoyabko E. & Zaslansky P. *In situ compressibility of carbonated hydroxyapatite in tooth dentine measured under hydrostatic pressure by high energy X-ray diffraction*, page 172, Copyright (2015), with permission from Elsevier. .... 39

Fig 1-3 Structure of Bone. Cortical bone and cancellous (trabeculae) bone consist of osteon. Nanostructure of bone contains collagen fibrils that are filled or surrounded by biological apatite. Reprinted from *Biomaterials*, vol 83, Wang X., Xu S., Zhou S., Xu W., Leary M., Choong P., Qian M., Brandt M. & Xie Y. M. *Topological design and additive manufacturing of porous metals for bone scaffolds and orthopaedic implants: A review*, page 129, Copyright (2016), with permission from Elsevier. .... 40

Fig 1-4 a) Acids produced via sugar metabolism of bacteria from the biofilm causes the reduction of pH and the dissolution of tooth minerals, b) ions from various sources such as saliva or biofilm buffer the acid and increase the pH. This then promotes mineral precipitation. Reprinted from *Dental materials*, vol 32, Curry J. A. et al. *Are fluoride releasing dental materials clinically effective on caries control*, page 325, Copyright (2016), with permission from Elsevier. .... 43

Fig 1-5 The progression of carious lesions. A) Early carious lesion which can be managed by non-surgical approaches, B) the lesion progresses and becomes a frank

cavity that requires restorative treatments, C) the lesion encroaches to the pulp which requires more invasive treatments such as root canal treatment or extraction. Reprinted from <i>Journal of Endodontics</i> , volume 32, Bjørndal L., et al. <i>Depth and activity of carious lesions as indicators for the regenerative potential of dental pulp after intervention</i> , page S77, Copyright (2014), with permission from Elsevier. ....	44
Fig 1-6 Cusps fractured in amalgam filled permanent molar. Multiple cracks (arrows) seen on the remaining cusps. Reprinted from <i>Operative Dentistry</i> , volume 41, Lenhard M. <i>Restoration of Severely Compromised Teeth with Modern Operative Techniques</i> . Page s89, Copyright (2015), with permission from Academy of Operative Dentistry. ...	45
Fig 1-7 Schematic representing the radical polymerisation process. ....	53
Fig 1-8 Different type of dental composites classified by filler composition. Reprinted from <i>Dental materials</i> , volume 27, Ferracane, J. L., <i>Resin composite—State of the art</i> , page 32, Copyright (2011), with permission from Elsevier. ....	54
Fig 1-9 a) Recurrent (secondary) caries around composite restoration. b) Old composite with additional sound tooth structures were removed to prepare a cavity for new restoration. Reprinted from <i>Clinical Oral Investigations</i> , <i>Five-year retrospective clinical study of indirect composite restorations luted with a light-cured composite in posterior teeth</i> , volume 18(2), 2014, page 617, D'arcangelo C., Zarow M., De Angelis F., Vadini M., Paolantonio M., Giannoni M. & D'amario, Copyright (2014), with permission of Springer. ....	55
Fig 1-10 Chemical structure of epsilon poly-L-lysine .....	64
Fig 1-11 Comparison of (a) normal and (b) osteoporotic bone from 3 <sup>rd</sup> lumbar vertebra. Credited to © Tim Arnett, University College London (t.arnett@ucl.ac.uk). ....	67
Fig 1-12 The schematic representing percutaneous vertebroplasty (VP) a) a collapse vertebra, b-c) needles are inserted into the vertebral body, d) bone cement is injected to stabilise the vertebra. Reprinted from <i>Biomaterials</i> , volume 27, Verlann et al., <i>Anterior spinal column augmentation with injectable bone cements</i> , page 292, Copyright (2006), with permission from Elsevier. ....	69



Fig 1-13 Schematic representing balloon kyphoplasty a) cannulas with balloon tamps are inserted into the vertebral body, b) bone tamps are inflated to correct the height and create space for the cement, c-d) the bone cement was injected. Reprinted from *Biomaterials*, volume 27, Verlann et al., *Anterior spinal column augmentation with injectable bone cements*, page 293, Copyright (2006), with permission from Elsevier. 70

Fig 1-14 A) Chemical structure of PMMA. B) The PMMA cement is supplied as powder and liquid phase..... 72

Fig 1-15 Example of a commercial calcium phosphate cement (BoneSource®, Stryker, New Jersey, USA) (Source: <http://www.stryker.com>) ..... 73

Fig 1-16 Example of a commercial bone composite supplied with automatic mixing tip and mixing gun (Cortoss®, Stryker, New Jersey, USA) (Source: <http://www.stryker.com>) ..... 74

Fig 1-17 CT image obtained after vertebroplasty showing the leakage of PMMA cement (red arrow) to right intercostal artery. Reprinted from *The Spine Journal*, volume 11(8), Yazbeck P. G., Al Rouhban R. B., Slaba S. G., Kreichati G. E. & Kharrat K. E., page e7, Copyright (2011), with permission from Elsevier. .... 75

Fig 1-18 Transmission electron microscope image of the interface between bioactive glass (A-W) and rat tibia after 8 weeks of implantation. Layer of apatite at the interface mediating integration between the glass and bone. Reprinted from *Biomaterials*, vol 24(13), Kokubo T., Kim H.-M. & Kawashita M. *Novel bioactive materials with different mechanical properties*, page 2163, Copyright (2003), with permission from Elsevier. . 78

Fig 2-1 Double-barrel syringes equipped with the automatic mixing tip and the mixing gun. .... 86

Fig 2-2 The stress and strain relation in viscoelastic materials during the dynamic rheological test. b) The stress can be separated into two independent components: stress that is exactly in phase with strain and stress that is  $\pi/2$  out of phase. Reprinted from *Cement and Concrete Research*, volume 36(2), Sun Z., Voigt T. & Shah S. P., *Rheometric and ultrasonic investigations of viscoelastic properties of fresh Portland cement pastes*, page 279, Copyright (2006), with permission from Elsevier..... 89

Fig 2-3 Example result from Injectability test. a) The composite paste was injected. b) Load decreased due possibly to shear-thinning behavior of the composites. c) Load increased as the plunger reaching the end of syringe. ....	91
Fig 2-4 FTIR spectra upon polymerisation obtained from the bottom of composites. ..	94
Fig 2-5 A) Example monomer conversion and B) rate of polymerisation versus time of an experimental bone composite. ....	95
Fig 2-6 Disc sample of dental and bone composite .....	96
Fig 2-7 A) UV spectra of the standard PLS solutions and B) PLS concentration calibration curve of absorbance versus PLS concentration. ....	98
Fig 2-8 Chromatograms of PLS from different batches. Retention time of PLS from 2 <sup>nd</sup> and 3 <sup>rd</sup> batch was broader than that of 1 <sup>st</sup> batch. ....	100
Fig 2-9 Plot of area under the curve of PLS retention time (19 – 27 min) versus concentration of PLS (3 <sup>rd</sup> batch).....	100
Fig 2-10 Example of PLS release profiles from experimental bone composites. ....	101
Fig 2-11 Calibration curve for Sr <sup>2+</sup> release .....	102
Fig 2-12 Example Raman mapping. Blue and green areas represent the polymer plus glass regions versus an apatite coating respectively. Yellow and red areas represent regions of brushite and TSrP. ....	104
Fig 2-13 Raman spectra of each pure chemical (Young et al., 2008; Mehdawi et al., 2009). ....	104
Fig 2-14 A) schematic of ball on ring test, B) example of force versus displacement diagram from BFS testing. ....	106

Fig 2-15 Schematic of fracture toughness testing and required dimensions of specimen according to BS ISO 13586:2000+A1:2003, Plastics-Determination of fracture toughness ( $G_{IC}$ and $K_{IC}$ )-Linear elastic fracture mechanics (LEFM) approach. ....	108
Fig 2-16 Testing performed under circulated SBF at the controlled temperature of $37 \pm 1$ °C .....	109
Fig 2-17 Example of plot between stresses versus number of log (cycles) from biaxial flexural fatigue testing to generate S/N curve.....	110
Fig 3-1 (A) Monomer conversion versus time (light turned on at 10 s and cured for 40 s), (B) final monomer conversion of each material, (C) light cured composite discs showing different translucencies and (D) calculated polymerisation shrinkage. Lines indicate no significant difference ( $p > 0.05$ ). Error bars are 95% CI (n=5). Adapted from Panpisut P, Liaqat S, Zacharaki E, Xia W, Petridis H, Young AM (2016) <i>Dental Composites with Calcium / Strontium Phosphates and Polylysine</i> . PLoS ONE 11(10): e0164653. doi:10.1371/journal.pone.0164653.g001.....	121
Fig 3-2 Changes of composite's mass and volume upon immersion in SBF or deionised water as a function of square root of hour. Error bars are 95% CI (n=3). Adapted from Panpisut P, Liaqat S, Zacharaki E, Xia W, Petridis H, Young AM (2016) <i>Dental Composites with Calcium / Strontium Phosphates and Polylysine</i> . PLoS ONE 11(10): e0164653. doi:10.1371/journal.pone.0164653.g002. ....	123
Fig 3-3 Acquired average Raman spectra and Raman maps from surfaces of $PO_{25}PLS_{2.5}$ and $PO_{25}PLS_0$ after immersion in SBF for 1 day, 1 week, and 4 weeks. Polymer plus glass regions and apatite are represented by blue and green areas. Brushite and TSrP are represented by yellow and red areas. MCPM was not observed in the mapping process. In both formulations, blues areas indicate polymer and glass peaks between 1300 and 1500 $cm^{-1}$ are dominant in point spectra. A substantial increase in the apatite scattering peak is observed with $PO_{25}PLS_{2.5}$ at 1 week, but this can be seen for both formulations at 4 weeks. Adapted from Panpisut P, Liaqat S, Zacharaki E, Xia W, Petridis H, Young AM (2016) <i>Dental Composites with Calcium / Strontium Phosphates and Polylysine</i> . PLoS ONE 11(10): e0164653. doi:10.1371/journal.pone.0164653.g00. ....	125

Fig 3-4 SEM images of PO<sub>25</sub>PLS<sub>2.5</sub> and PO<sub>25</sub>PLS<sub>0</sub> composite surfaces after immersion in SBF for 1 day, 1 week or 4 weeks. Adapted from Panpisut P, Liaqat S, Zacharaki E, Xia W, Petridis H, Young AM (2016) *Dental Composites with Calcium / Strontium Phosphates and Polylysine*. PLoS ONE 11(10): e0164653. doi:10.1371/journal.pone.0164653.g004. .... 126

Fig 3-5 Cumulative PLS release from the composite discs immersed in deionised water for up to 6 weeks. Error bars are 95% CI (n=3). Adapted from Panpisut P, Liaqat S, Zacharaki E, Xia W, Petridis H, Young AM (2016) *Dental Composites with Calcium / Strontium Phosphates and Polylysine*. PLoS ONE 11(10): e0164653. doi:10.1371/journal.pone.0164653.g004. .... 127

Fig 3-6 A) Biaxial flexural strength and B) modulus of elasticity of composites. Same letters indicate no significant difference ( $p > 0.05$ ). Error bars are 95% CI (n=8). Adapted from Panpisut P, Liaqat S, Zacharaki E, Xia W, Petridis H, Young AM (2016) *Dental Composites with Calcium / Strontium Phosphates and Polylysine*. PLoS ONE 11(10): e0164653. doi:10.1371/journal.pone.0164653.g006. .... 128

Fig 4-1 Storage modulus (G'), loss modulus (G''), and tangent of phase angle ( $\tan\delta$ ) plotted on log-log scales from strain sweep measurement of experimental bone composites and Cortoss. The frequency was fixed at 6.28 rad/s. .... 148

Fig 4-2 An average of G' (plotted on log scale) at strain between 0.01 to 0.1 % from strain sweep measurement. Error bars are 95 %CI (n=2). .... 150

Fig 4-3 Factorial analysis describing effect of PLR, PPGDMA, glass particle size, and their interaction effects on G' of experimental bone composites. Error bars are 95 %CI (n=2). .... 150

Fig 4-4 Critical strain (i.e. strain level where storage modulus drops) of all materials. .... 152

Fig 4-5 Factorial analysis describing effect of PLR, PPGDMA, glass particle size, and their interaction effects on critical strain of experimental composites. .... 152

Fig 4-6 Storage modulus ( $G'$ ), loss modulus ( $G''$ ), and tangent of phase angle ( $\tan\delta$ ) plotted on log-log scales from frequency measurement of experimental bone composites and Cortoss. The strain was fixed at 0.05 %.	154
Fig 4-7 Average of $G'$ (plotted on log scale) at frequency between 0.1 to 1 $\text{rad.s}^{-1}$ from strain sweep measurement. Error bars are 95 %CI (n=2).	155
Fig 4-8 Factorial analysis describing effect of PLR, PPGDMA, glass particle size, and their interaction effects on $G'$ of experimental composites from frequency sweep measurement.	155
Fig 4-9 Viscosity versus shear rate ( $\text{s}^{-1}$ ) plotted on log-log scales of each material. All material showed a reduction of viscosity upon increasing shear rate.	156
Fig 4-10 Average of viscosities (plotted on log scale) at shear rate between 0.1 and 1 $\text{s}^{-1}$ . Error bars are 95 % CI (n=2).	157
Fig 4-11 Factorial analysis describing effects of PLR, PPGDMA, glass particle size, and their interactions on viscosity of experimental bone composites. Error bars are 95 % CI (n=2).	157
Fig 5-1 A) Initial, 1 hour 80 °C stored, and expected FTIR spectra of a mixture of equal masses of MCPM, TSrP, and PPGDMA. B) Spectra of pure phosphates and Residual spectrum (difference between final and initial spectra). Labels indicate phosphate peaks ( $\text{PO}_4$ ).	174
Fig 5-2 A) Initial, 1 hour 80 °C stored, and expected FTIR spectra of a mixture of equal masses of PLS and UDMA. B) Spectra of pure components and Residual spectrum (difference between final and initial spectra).	175
Fig 5-3 A) Initial, 1 hour 80 °C stored, and expected FTIR spectra of a mixture of equal masses of PLS and PPGDMA. B) Spectra of pure components and Residual spectrum (difference between final and initial spectra).	176
Fig 5-4 Example polymerisation profiles for initiator and activator pastes of $\text{M}_{10}\text{PPG}$ at 80 °C. After 5 min, the initiator paste showed rapid monomer conversion levelling off at	

>90% after 20 min. In contrast, the conversion of the activator paste was negligible even after 1 hour at 80 °C. ....	177
Fig 5-5 Polymerisation profiles of A) M <sub>10</sub> PPG and B) M <sub>10</sub> TEG initiator pastes at different temperatures. Time when monomer conversion reached 50% (t <sub>50</sub> ) was used in the Arrhenius plots.....	178
Fig 5-6 Arrhenius plots of ln 1/t <sub>50</sub> versus inverse temperature (T) in Kelvin. ....	179
Fig 5-7 An average of inhibition time of the experimental bone composites kept at different storage temperature measured at early time (1 day – 3 months) and late time (9-12 months). ....	182
Fig 5-8 Average maximum rate of polymerisation (R <sub>p</sub> <sup>max</sup> ) of the experimental bone composites kept at different storage temperatures for either short (1 day – 3 months) or longer (9-12 months) time periods. ....	183
Fig 5-9 Average final monomer conversion of the experimental bone composites kept at different storage temperature for either short (1 day – 3 months) or longer time periods (9-12 months). ....	184
Fig 6-1 Biaxial flexural strength after immersion in SBF for 24 hr. Error bars are 95% CI (n=8). Lines indicate significant difference ( $p < 0.05$ ). ....	199
Fig 6-2 Factorial analysis describing the effect of MCPM level, glass fibre, glass filler size, and interaction effects on BFS of experimental bone composites. Error bars are 95 %CI (n =8). ....	199
Fig 6-3 Fracture toughness of all materials after immersion in SBF for 24 hr. Error bars are 95% CI (n=8). Lines indicate significant difference ( $p < 0.05$ ). ....	201
Fig 6-4 Factorial analysis describing the effect of MCPM level, glass fibre, glass filler size and interaction effects on fracture toughness of the experimental bone composites. Error bars are 95 %CI (n =8). ....	201

Fig 6-5 Representative fracture surface of commercial materials. Multiple porosities with small particles were seen with Simplex. ....	202
Fig 6-6 Representative fracture surface of the experimental composite from fracture toughness test. Circles and triangle represent fibre that oriented perpendicular and parallel to the fracture surface respectively. Squares represent areas of brushite precipitation. ....	202
Fig 6-7 Biaxial flexural strength and modulus of elasticity of the experimental bone composites and Cortoss after immersion in SBF for 24 hr. Error bars are 95 %CI (n=8). Solid lines indicate no significant difference ( $p > 0.05$ ). ....	204
Fig 6-8 Biaxial flexural strength and modulus of elasticity of the experimental bone composites versus level of PPGDMA. Error bars are 95 %CI (n=8). ....	204
Fig 7-1 Example polymerisation profiles of experimental bone composites measured at controlled temperature of 25 °C. ....	220
Fig 7-2 Inhibition time of experimental bone composites. Lines indicate no significant difference ( $p > 0.05$ ). Error bars are 95 %CI (n =3). ....	221
Fig 7-3 Factorial analysis describing the effect of MCPM level, diluent monomers, and their interaction effects on inhibition time. Error bars are 95 %CI (n =3). ....	221
Fig 7-4 Maximum rate of polymerisation ( $R_p^{\max}$ ) of experimental bone composites. Error bars are 95 %CI (n =3). ....	222
Fig 7-5 Factorial analysis describing the effect of MCPM level, diluent monomers, and their interaction effects on $R_p^{\max}$ . Error bars are 95 %CI (n =3). ....	223
Fig 7-6 Final monomer conversion of experimental bone composites. Lines indicate no significant difference ( $p > 0.05$ ). Error bars are 95 %CI (n =3). ....	224
Fig 7-7 Factorial analysis describing the effect of MCPM level, diluent monomers, and their interaction effects on monomer conversion. Error bars are 95 %CI (n =3). ....	224

Fig 7-8 Calculated polymerisation shrinkage and heat generation. Lines indicate no significant difference ( $p > 0.05$ ). Error bars are 95 %CI (n =3). .....	226
Fig 7-9 Factorial analysis describing the effect of MCPM level, diluent monomers, and their interaction effects on calculated polymerisation shrinkage/heat generation. Error bars are 95 %CI (n =3). .....	226
Fig 7-10 Mass and volume changes versus square root of time (hr) of all materials immersed in SBF up to 7 weeks. Error bars are 95% CI (n=3). .....	227
Fig 7-11 Representative SEM images for each material after 1 week immersion in SBF. ....	229
Fig 7-12 Cumulative $\text{Sr}^{2+}$ release versus hr from bone composites immersed in deionised water up to 4 weeks. Error bars are 95% CI (n=3). .....	230
Fig 7-13 Factorial analysis describing the effect of MCPM level, diluent monomers, and their interaction effects on the cumulative $\text{Sr}^{2+}$ release at 4 weeks. Error bars are 95 %CI (n =3). Stars indicate negative effect from variables.....	231
Fig 7-14 BFS of all materials after immersion in SBF for 4 weeks tested in wet condition at 37 °C. Error bars are 95% CI (n=5). Same letters indicate no significant difference ( $p > 0.05$ ) .....	232
Fig 7-15 Factorial analysis describing the effect of MCPM level, diluent monomers, and interaction effects on BFS at 4 weeks. Error bars are 95 %CI (n =5). .....	232
Fig 7-16 Plots of BFS versus log (cycle) (n=20). Gradients of regression lines (S/N curve) were used to compare fatigue performances. ....	234
Fig 7-17 Gradient of S-N curves. Error bars are 95% CI (n=5). Same letters indicate no significant difference ( $p > 0.05$ ). .....	235
Fig 7-18 Factorial analysis describing the effect of MCPM level, diluent monomers, and their interaction effects gradient of S/N curve. Error bars are 95 %CI (n =5). .....	235



Fig 7-19 Fatigue life upon applied stress of 10 MPa of the experimental composites and commercial products. Error bars are 95% CI (n=5). Line indicates no significant difference ( $p > 0.05$ ).....	236
Fig 7-20 Factorial analysis describing the effect of MCPM level, diluent monomers, and their interaction effects on fatigue life. Error bars are 95 %CI (n =5). Stars indicate negative effect from variables. ....	236
Fig 7-21 Schematics representing the polymerisation of methylmethacrylate (MMA) and dimethacrylate monomers. The methacrylate group of all MMA monomers have to be polymerised to prevent the release of unreacted monomers. In contrast, polymerisation of 50 % of methacrylate groups in dimethacrylate monomers may be sufficient to prevent leaching of the monomers.....	240
Fig 8-1 Injection force required for experimental bone composites. Lines indicate no significant difference ( $p > 0.05$ ). Error bars are 95% CI (n=3). ....	260
Fig 8-2 Factorial analysis describing the effect of PPGDMA, PO, PLS, and their interactions on required injection force of experimental bone composites. Error bars are 95% CI (n=3). ....	261
Fig 8-3 A) Inhibition time of each material. Lines indicate no significant difference ( $p > 0.05$ ). B) Factorial analysis describing the effect of PPGDMA, PO, PLS, and their interactions on inhibition time of experimental bone composites. Error bars are 95% CI (n=3).....	262
Fig 8-4 A) Maximum rate of polymersation ( $Rp^{max}$ ) of experimental bone composites and commercial materialss. Lines indicate significant difference ( $p < 0.05$ ). B) Factorial analysis describing the effect of PPGDMA, PO, PLS, and their interactions on $Rp^{max}$ of experimental bone composites. Error bars are 95% CI (n=3). ....	264
Fig 8-5 A) Final monomer conversion of experimental bone composites and commercial products. Lines indicate no significant difference ( $p > 0.05$ ). B) Factorial analysis describing the effect of PPGDMA, PO, PLS, and their interactions on final monomer conversion of experimental bone composites. Error bars are 95% CI (n=3). ....	266

Fig 8-6 A) Calculated polymerisation shrinkage and heat generation. Lines indicate significant difference ( $p < 0.05$ ). B) Factorial analysis describing the effect of increasing PPGDMA, PO, PLS, and their interactions on calculated polymerisation shrinkage and heat generation of experimental bone composites. Error bars are 95% CI (n=3). ....	268
Fig 8-7 Mass and volume changes of experimental bone composites in SBF versus square root of time. Error bars are 95% CI (n=3). .....	270
Fig 8-8 A) Rate of mass increase ( $\% \cdot \text{hr}^{-0.5}$ ) and maximum mass increase. B) Factorial analysis describing the effect PPGDMA, PO, PLS, and their interactions on rate of mass increase and maximum mass increase of experimental bone composites. Error bars are 95% CI (n=3). .....	271
Fig 8-9 A) Rate of volume increase ( $\% \cdot \text{hr}^{-0.5}$ ) and volume changes at late time, B) factorial analysis describing the effect of increasing PPGDMA, PO, PLS, and their interactions on rate of volume increase and volume changes at late time of experimental bone composites. Error bars are 95% CI (n=3). .....	273
Fig 8-10 PLS release in deionised water versus square root of hour. Error bars are 95% CI (n=3). .....	274
Fig 8-11 A) Delay time ( $t_d$ ) of each formulation and B) factorial analysis describing the effect of PPGDMA, PO, PLS, and their interactions on the $t_d$ of PLS. Error bars are 95% CI (n=3). .....	275
Fig 8-12 A) Diffusion coefficient PLS, and B) factorial analysis describing the effect of PPGDMA, PO, PLS, and interactions on the diffusion coefficient of PLS release. Lines indicated no significant difference ( $p > 0.05$ ) Error bars are 95% CI (n=3). .....	277
Fig 8-13 A) Cumulative release of PLS at 1 week, and B) factorial analysis describing the effect of increasing PPGDMA, PO, and PLS on the cumulative release of PLS. Error bars are 95% CI (n=3). .....	279
Fig 8-14 Representative of surface SEM images of composite discs after immersion in SBF for 1 day, 1, and 4 weeks (n=1). .....	282

Fig 8-15 Representative of surface SEM images of disc samples from experimental bone composites and Cortoss after immersion in SBF for 1 day, 1, and 4 weeks (n=1). Ca/Si and Ca/P ratio of Cortoss did not show due to the large variation in Ca, Si, and P ions across the surface. ....	283
Fig 8-16 A) Ca/P ratio of representative surface precipitates. B) Factorial analysis describing the effect of increasing PPGDMA, PO, and PLS on Ca / P ratio. Error bars are 95% CI (n=3). ....	284
Fig 8-17 A) Ca/Si ratio of representative surface precipitates. B) Factorial analysis describing the effect of increasing PPGDMA, PO, and PLS on Ca / Si ratio. Error bars are 95% CI (n=3). ....	285
Fig 8-18 A) Compressive strength and B) factorial analysis describing the effect of PPGDMA, PO, and PLS on compressive strength. Error bars are 95% CI (n = 5). Same letters indicate statistically insignificance ( $p > 0.05$ ). ....	287
Fig 8-19 BFS of all materials after immersion in SBF for 1 day and 4 weeks. Error bars are 95% CI (n=5). (*) and (**) indicate statistically significance ( $p < 0.05$ ) and statistically not significance ( $p > 0.05$ ) respectively. ....	290
Fig 8-20 Factorial analysis describing the effect of decreasing PPGDMA, PO, and PLS on biaxial flexural strength of the composites after immersion in SBF up to 4 weeks. Error bars are 95% CI (n=5).....	291
Fig 8-21 Modulus of elasticity of all materials for 1 day and 4 weeks. Error bars are 95% CI (n=5). (*) and (**) indicate statistically significance ( $p < 0.05$ ) and statistically not significance ( $p > 0.05$ ) respectively. ....	294
Fig 8-22 Factorial analysis describing the PPGDMA, PO, PLS, and their interactions on modulus of elasticity of the composites after immersion in SBF for up to 4 weeks. Error bars are 95% CI (n=3). ....	295
Fig 8-23 A) BFS of materials tested in air at room temperature from Fig 8-19 and in SBF at 37 °C after immersion in SBF for 4 weeks. B) Factorial analysis describing the effect	

of PPGDMA, PO, and PLS on BFS of the experimental bone composites. Error bars are 95% CI (n = 5). .....	298
Fig 8-24 Plots of BFS versus log (cycle) of experimental bone composites containing 75 or 50 wt% of PPGDMA (n=20). .....	299
Fig 8-25 Plots of BFS versus log (cycle) of experimental bone composites containing 25 wt% of PPGDMA and commercial materials (n=20). .....	300
Fig 8-26 A) Gradient of S / N curve and B) Factorial analysis describing the effect of PPGDMA, PO, PLS, and their interactions on gradient of S/N curve. Error bars are 95% CI (n=5). Line indicates no statistically significant difference ( $p > 0.05$ ).....	301
Fig 8-27 A) Fatigue life of materials upon BFS of 10 MPa and B) factorial analysis describing the effect of PPGDMA, PO, PLS, and their interactions on fatigue life of the experimental bone composites. Error bars are 95% CI (n=3). Line indicates no statistically significant difference ( $p > 0.05$ ).....	302
Fig 8-28 A) Metabolic activity (relative to the corresponding control) of surviving MSCS after cultured in solutions previously immersed by experimental bone composite discs for 24 hr. B) Factorial analysis describing the effect of PPGDMA, PO, PLS, and their interactions on the metabolic activity (relative to the corresponding control) of MSCS. Lines indicate no significant difference ( $p > 0.05$ ). Error bars are 95% CI (n=5). .....	304

## Chaper 1 Literature Review

### 1.1 Human tooth and Bone

#### 1.1.1 Tooth: Enamel

The upper part of the human tooth (crown) is composed of enamel and dentine-pulp complex (Fig 1-1 a). Enamel is the outer most layer and is the most highly mineralised tissue in the body. It contains more than 90 % inorganic material in the form of biological apatite,  $\text{Ca}_{10}(\text{PO}_4)_6(\text{OH})_2$ , (Abou Neel et al., 2016). This feature allows enamel to withstand masticatory forces and acids from diet or bacteria. Apatites in enamel are hexagonal in shape with a cross section of  $\sim 30$  nm in thickness and  $\sim 55 - 90$  nm in width (Ang et al., 2010). The apatites are highly packed into units called enamel prisms or rods in a keyhole-shaped structure with a diameter of  $5 \mu\text{m}$  when viewed in cross-section (Fig 1-1 b).

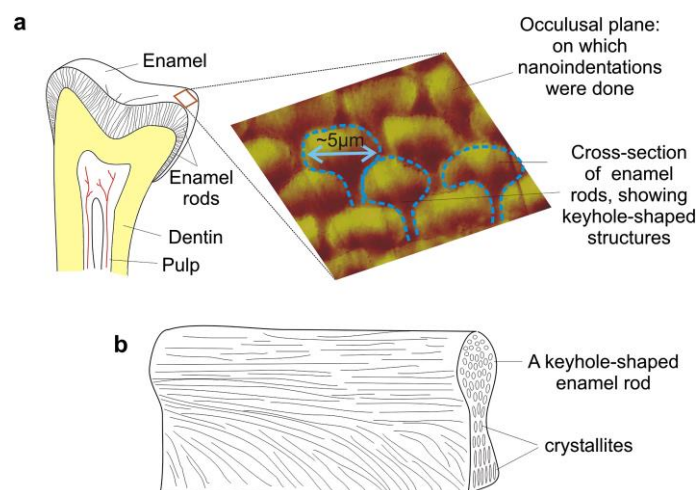


**Fig 1-1 Structure of enamel. a) The keyhole-shaped structure consisting of enamel rods. b) The enamel rod contains highly packed of apatites (crystallites).** Reprinted from *Biomaterials*, vol 31(7), Ang S. F., Bortel E. L., Swain M. V., Klocke A. & Schneider G. A. Size-dependent elastic/inelastic behavior of enamel over millimeter and nanometer length scales, page 1956, Copyright (2010), with permission from Elsevier.

Biological apatites of enamel contain a variety of substitutions and vacancies. Hence, its calcium to phosphorous ratio is usually lower than that of stoichiometric hydroxyapatite (1.67) (Abou Neel et al., 2016). The apatites in enamel, however, contain fewer ionic substitutions than that of dentine and bone. Additionally, crystals or apatites in the tooth regularly go through natural periods of mineral loss (demineralisation) and mineral gain (demineralisation)(Gonzalez-Cabezas, 2010).

### **1.1.2 Tooth: Dentine-pulp complex**

The brittleness of tooth is due to high enamel stiffness (modulus of elasticity of ~ 100 GPa). This can be mitigated, however, by supporting the enamel with more resilient tissue such as dentine (modulus of elasticity of ~ 10 to 20 GPa) (Zhang et al., 2014). Dentine encloses the dental pulp (Fig 1-1 a), which is a neurovascular connective tissue that contains living cells including osteoblasts, fibroblasts, and undifferentiated mesenchymal stem cells.

Dentine is the largest portion of tooth structure. Mature dentine consists of approximately 70 % inorganic material, 20 % of organic content, and 10% of water. Inorganic dentine mainly consists of type I collagen and substituted hydroxyapatite in the form of small plates (50 nm in length, 20 nm in width, and 2-5 nm in thickness) (Abou Neel et al., 2016).

Microscopic structure of dentine reveals tubules surrounded by more mineralised peritubular dentine (white ring) and less mineralised intertubular dentine (grey area) (Fig 1-2 a) (Forien et al., 2015). Dentinal tubules contain processes extended from osteoblasts in dental pulp (odontoblastic processes). Peritubular and intertubular dentine comprise of mineralised collagen matrix (Fig 1-2 b,c). The collagen fibres act as a scaffold that accommodates deposition of biological apatites (Fig 1-2 d).

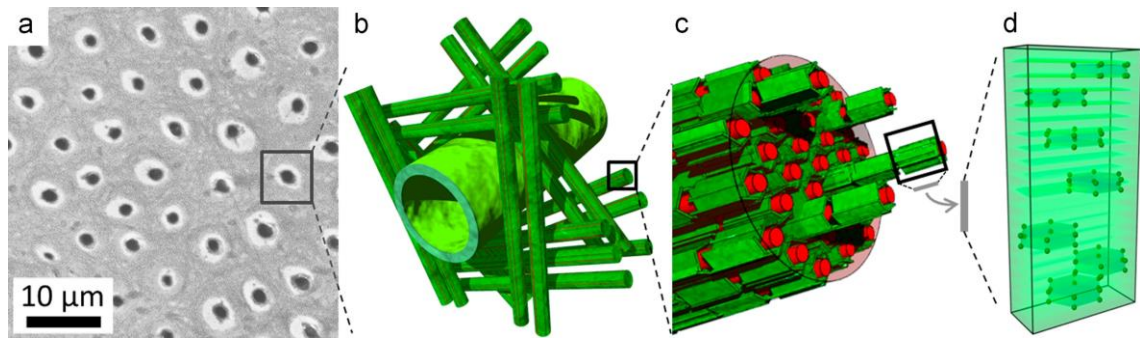


**Fig 1-2 Structure of dentine.** a) Dentinal tubules surrounded by peritubular (white rings) and intertubular dentine (light grey). b) Schematic representation of the dentinal tubule (light green) lining by mineralised collagen fibres (dark green). c) These fibres are made of mineral-containing nanofibrils. d) Each nanofibril deposited by biological apatites which are plate-like structure. Reprinted from *Journal of the Mechanical Behavior of Biomedical Materials*, vol 50, Forien J.-B., Fleck C., Krywka C., Zolotoyabko E. & Zaslansky P. *In situ compressibility of carbonated hydroxyapatite in tooth dentine measured under hydrostatic pressure by high energy X-ray diffraction*, page 172, Copyright (2015), with permission from Elsevier.

### 1.1.3 Bone

Bone is a mineralised connective tissue containing 67 % of inorganic content (mainly substituted hydroxyapatite), 28 % of type I collagen, and 5 % of noncollagenous protein. Bone can be divided macroscopically into two types; 1) cortical/compact bone (10 % of pores) and 2) cancellous/trabecular bone (50-90 % of pores). The primary anatomical unit of bone is osteon (Fig 1-3). The bone can be woven or lamella in structure depending on the collagen fibrils arrangement. Bone apatites may be formed within individual type I collagen fibrils, along the fibril surface, or between packed collagen fibrils. The apatites are plate-shaped with approximately 50 nm long, 25 nm wide, and 3 nm thick (Wang et al., 2016)

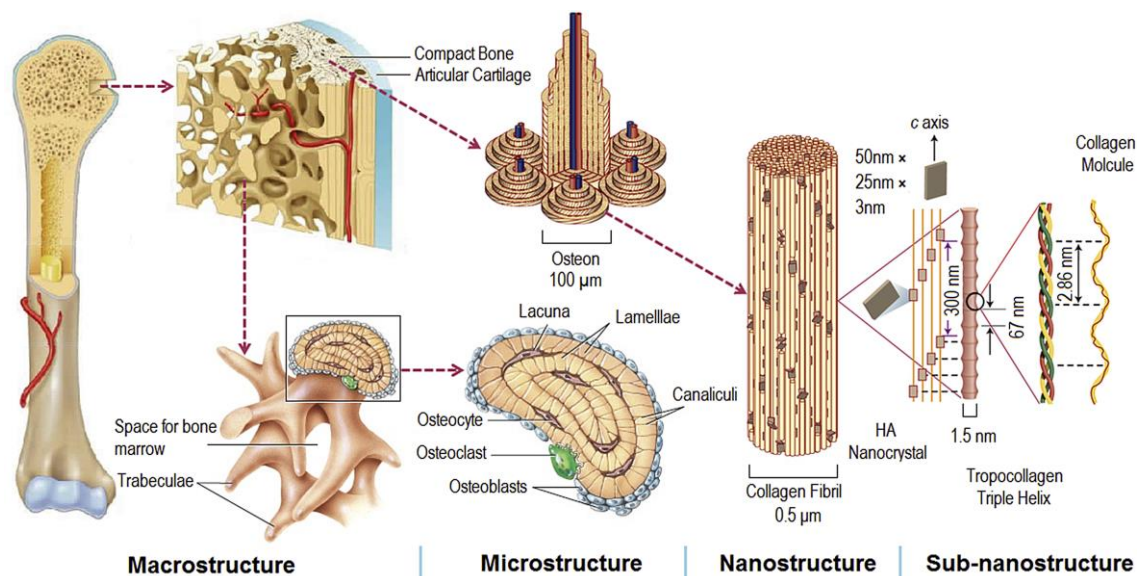


**Fig 1-3 Structure of Bone.** Cortical bone and cancellous (trabeculae) bone consist of osteon. Nanostructure of bone contains collagen fibrils that are filled or surrounded by biological apatite. Reprinted from *Biomaterials*, vol 83, Wang X., Xu S., Zhou S., Xu W., Leary M., Choong P., Qian M., Brandt M. & Xie Y. M. *Topological design and additive manufacturing of porous metals for bone scaffolds and orthopaedic implants: A review*, page 129, Copyright (2016), with permission from Elsevier.

Bone can respond to mechanical loads by adapting its mass, architecture, and mechanical properties. The reconstruction of bone occurs through a remodeling process. This remodeling process comprises of coordinated and sequential actions of bone-resorbing osteoclasts and bone-forming osteoblasts to repair micro damage and to enable adaptation of bone structure suitable for mechanical or metabolic needs (Eastell et al., 2016).

It can be seen that human dentine and bone are natural composite materials comprising primarily of inorganic biological apatites. Diseases associated with teeth and bone often involve loss of inorganic minerals or the alteration of their microstructure. Examples include dental caries and osteoporosis.



## **1.2 Dental Caries**

### **1.2.1 Epidemiology**

Dental caries is a common health challenge worldwide. According to the World Health Organisation (WHO), dental caries affects 2.4 billion adults and 621 million children globally (Kassebaum et al., 2015). Untreated caries lesions may lead to severe tooth pain, pulpal infection, or tooth loss. In 2010, Global Burden of Disease (GBD) figures put untreated caries as one of the most prevalent worldwide diseases which requires a large budget for management (Marcenes et al., 2013; Listl et al., 2015). In the same year, the global economic impact arising from productivity loss due to dental caries was estimated at US\$ 27 million. In the UK, the National Health Service (NHS) spends ~ £3.4 billion per year for treating dental diseases in adults and children (Claxton et al., 2016). Dental phobia can also lead to children needing hospital-based extraction, which additionally costs ~ £30 million per year from the NHS (de Souza et al., 2017).

### **1.2.2 Aetiology of dental caries**

Dental hard tissues consist of enamel, dentine-pulp complex, and cementum. Enamel contains the highest inorganic content (~90 wt%), followed by dentine (~70 wt%), and cementum (45 wt%) (Abou Neel et al., 2016). Dental caries is characterised by the localised, chemical dissolution of tooth structures via metabolic activity in dental biofilms. These biofilms metabolise sugar from carbohydrate and produce acids that can demineralise dental hard tissues (Fontana et al., 2010). The aetiology of dental caries is multifactorial. The ecological plaque hypothesis suggests that dental caries is developed due to the imbalance between the loss or gain of tooth minerals and the formation of dental biofilms (Takahashi and Nyvad, 2016). Additionally, the formation of

dental caries is influenced by various factors on an individual or population level. For example, education and socioeconomic status may determine the quality of oral hygiene and type of diets that will affect the progression of the disease (Costa et al., 2012; dos Santos Junior et al., 2014).

The acids produced by bacterial biofilms decrease the pH of the tooth environment and create unsaturated conditions with respect to tooth minerals in the surroundings. Minerals from the teeth dissolve (demineralisation) when the pH is below 5.5 and 6.5 for enamel and dentine respectively (Cury et al., 2016) (Fig 1-4 a). These acids, however, can be naturally buffered by ions from multiple sources such as saliva, dental biofilms, calculus, calcium-fluoride formation, or the tooth surface itself (Gonzalez-Cabezas, 2010). Increase of pH and ion concentration provides the supersaturated conditions suitable for mineral precipitation (remineralisation) (Fig 1-4 b). The demineralisation and remineralisation are therefore in equilibrium under physiological conditions (Tanaka et al., 2017).

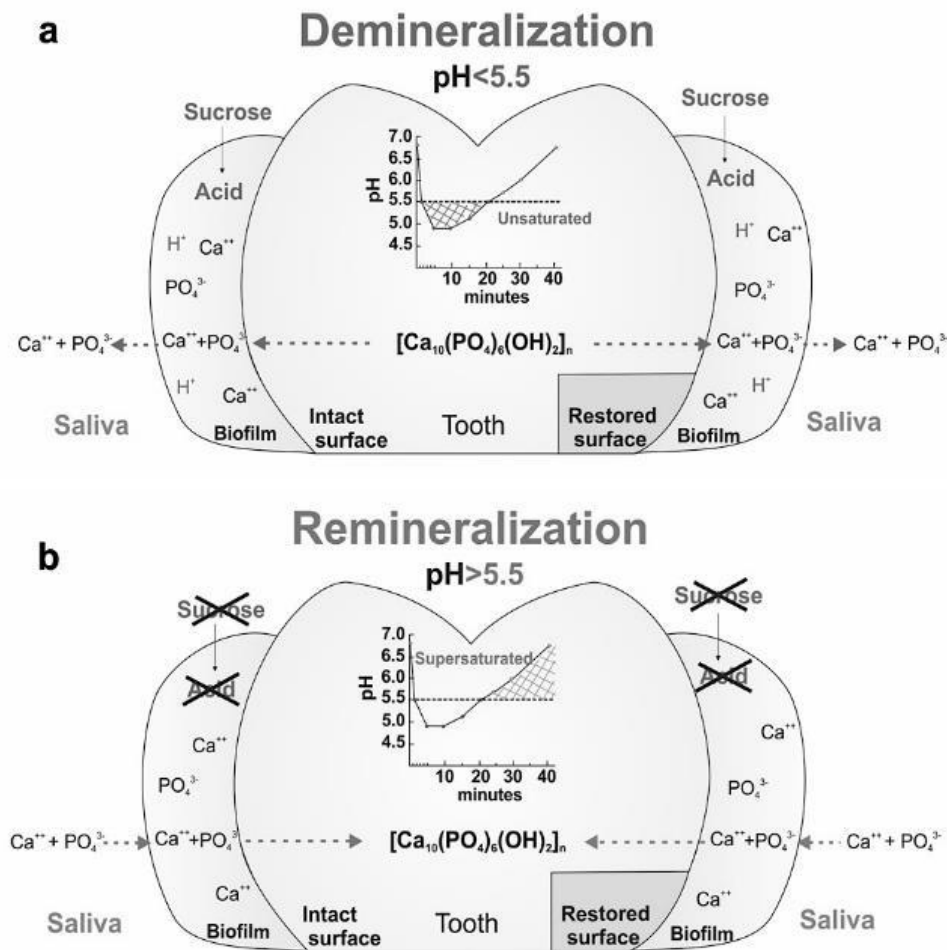


**Fig 1-4 a) Acids produced via sugar metabolism of bacteria from the biofilm causes the reduction of pH and the dissolution of tooth minerals, b) ions from various sources such as saliva or biofilm buffer the acid and increase the pH. This then promotes mineral precipitation.** Reprinted from *Dental materials*, vol 32, Curry J. A. et al. Are fluoride releasing dental materials clinically effective on caries control, page 325, Copyright (2016), with permission from Elsevier.

The mineral equilibrium can be tipped toward demineralisation by either an increase of fermentable carbohydrates intake or decrease in salivary flow. This leads to an increase of highly cariogenic bacteria (*Streptococcus mutans*, lactobacilli, *Actinomyces*, *Bifidobacteria*, and aciduric non-mutan streptococci) and enhances their acid-tolerating and acid-producing phenotypes (Marsh, 2010; Takahashi and Nyvad, 2011). Prolonged acidity continues the tooth demineralisation process and subsequently progresses the disease to a carious lesion.

The initial carious lesion is macroscopically intact (non-cavitated lesion) (Fig 1-5 A) and can be treated with minimally invasive approaches such as oral hygiene instruction or application of topical fluoride (Holmgren et al., 2014). If proper treatments are not provided, the lesion may eventually progress to the cavitated lesion (Fig 1-5 B,C), which requires irreversible treatments using restorative materials.

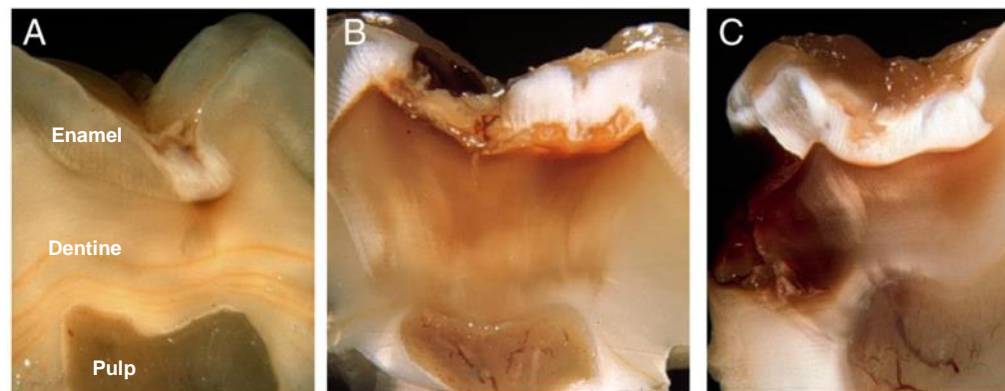


**Fig 1-5 The progression of carious lesions. A) Early carious lesion which can be managed by non-surgical approaches, B) the lesion progresses and becomes a frank cavity that requires restorative treatments, C) the lesion encroaches to the pulp which requires more invasive treatments such as root canal treatment or extraction.** Reprinted from *Journal of Endodontics*, volume 32, Bjørndal L., et al. *Depth and activity of carious lesions as indicators for the regenerative potential of dental pulp after intervention*, page S77, Copyright (2014), with permission from Elsevier.

## 1.3 Current direct restorative materials

### 1.3.1 Dental amalgam

Dental amalgam has been used in dentistry for over a century. Its placement technique is relatively simple. It is also a cost-effective restorative material for NHS dental care, and has seen widespread use in the UK for over a century (Lynch and Wilson, 2013; Austin et al., 2016). Additionally, dental amalgam exhibits high mechanical strength making it suitable for restoration of large cavities or high stress-bearing areas (Shaini et al., 2001). Moreover, this material may provide some antibacterial effects due to gradual release of metal ions, such as Ag, Hg, and Cu. These ions may also interfere with the metabolic activity of plaque biofilms (Wang et al., 2014).

The limitations of dental amalgam include its metallic colour and incapacity for effective bonding to tooth structure (Agnihotry et al., 2016). Furthermore, amalgam restorations require the removal of healthy tooth tissue to create mechanical retention. This reduces the tooth rigidity and may subsequently cause tooth fracture or cracking (Fig 1-6) (Banerji et al., 2010). Furthermore, dental amalgam can produce delayed hypersensitivity reactions in some patients resulting in oral lichenoid lesions (McParland and Warnakulasuriya, 2012).



**Fig 1-6 Cusps fractured in amalgam filled permanent molar. Multiple cracks (arrows) seen on the remaining cusps.** Reprinted from *Operative Dentistry*, volume 41, Lenhard M. *Restoration of Severely Compromised Teeth with Modern Operative Techniques*. Page s89, Copyright (2015), with permission from Academy of Operative Dentistry.

The mercury contained in amalgam fillings has raised concerns regarding both occupational health and environmental hazards. Intake of fish contaminated with mercury from industrial wastewater from 1950-1968 in Japan led to Minamata disease affecting the neurological system in thousands of people consuming the fish (Ekino et al., 2007). The Minamata Convention on Mercury in October 2013 was therefore convened to reduce effects from mercury (Bakhurji et al., 2017). According to the agreement, by 2020, a number of mercury-containing products will be banned. Dental amalgam, which was included in the agreement, is to be phased-down. Research on the development of alternative materials is therefore urgently needed (Mackey et al., 2014; Austin et al., 2016).

### **1.3.2 Conventional glass ionomer cement (GIC) and resin modified glass ionomer cement (RMGIC)**

Glass ionomer cements (GIC) were invented by Wilson and Kent in 1969. The main components of GIC are glass, organic acids, and water. The glass is typically a fluoroaluminosilicate glass and the liquid is an aqueous polyacrylic acid solution. The cement setting process involves an acid-base reaction. The acid attacks the glass surface leading to the release of cations such as  $\text{Ca}^{2+}$ ,  $\text{Al}^{3+}$ , and  $\text{Sr}^{2+}$ . These ions then form salt bridges between acid chains which result in the formation of a hydrogel. The remaining glass core acts as a reinforcing filler in the cement (Sidhu and Nicholson, 2016).

The balance of water sorption and desorption plays an important role in the setting process (Sidhu, 2011). Excessive water uptake during the hydrogel forming stage causes the dissolution of cations from the cement which leads to poor mechanical

properties (Lohbauer, 2010). Furthermore, the loss of water after this stage causes micro crack formation, which results in a poor aesthetic outcome.

Resin modified glass ionomer cements (RMGIC) were developed by incorporating a light activated initiator and a methacrylate monomer, which allows a photo-initiated polymerisation process. These materials exhibit higher strength than conventional GICs (Xie et al., 2000). Additionally, in some formulations a redox curing reaction is made possible through addition of a chemical cure initiator and activator (Sidhu, 2011; Sidhu and Nicholson, 2016).

Both conventional GIC and RMGIC can bond to dentine via micro mechanical interlocking, and chemical bonding through formation of an ion-exchange layer (Sidhu, 2011). The ability to release and recharge fluoride is usually considered an attractive feature of these materials. They can exhibit a burst release of fluoride initially followed by a low and sustained release (Sidhu and Nicholson, 2016).

Some reports argue, however, that the clinical benefit of fluoride release of the materials on caries prevention has not been proven (Cury et al., 2016; Raggio et al., 2016). Furthermore, Kim et al. (2010) found that GIC failed to encourage mineral precipitation in the mineral-depleted dentine. GIC and RMGIC also exhibited low initial strength with flexural strengths of only ~ 33 and ~ 59 MPa respectively (Bonifacio et al., 2009; Kumar and Shivrayan, 2015). As a consequence, high failure rates due to fracture can be observed from these materials (Kielbassa et al., 2016). These materials are therefore generally not considered suitable for load-bearing areas.

### **1.3.3 Dental composites**

The use of dental composites has increased rapidly primarily due to their aesthetic appeal and the development of more reliable adhesive systems (Lubisich et al., 2011). Over the years since their first development in the 1960s their composition has been modified to significantly enhance their performance and treatment outcome. The main components of a dental composite are described below.

## **1.4 Components of dental composites**

### **1.4.1 Matrix phase**

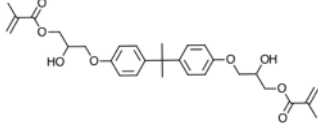
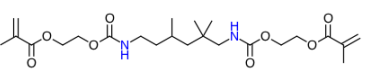
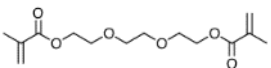
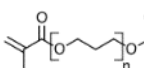
The matrix phase of the current dental composites may contain three main types of monomers: base, diluent, and functional. The base and diluent monomer (Table 1-1) generally contain two polymerisable groups (vinyl group or C=C). These C=C bonds can polymerise and form a cross-linked polymer. Functional monomers (Table 1-2) contain specific chemical groups to improve certain properties of the composites such as wettability or chemical bonding (Van Landuyt et al., 2007).

#### **1.4.1.1 Base monomers**

Bisphenol A diglycidyl methacrylate (Bis-GMA) (Table 1-1) is a commonly used base monomer in many commercial dental composites. It consists of two aromatic rings in the monomer chain. These result in a highly rigid monomer chain. The restricted movement of active monomer chains can negatively affect the polymerisation process of the composites (Van Landuyt et al., 2007). Urethane dimethacrylate (UDMA) is a commonly used alternative as it has a comparable molecular weight to that of Bis-GMA but, due to the lack of bulky groups which can have enhanced polymerisation (Du and Zheng, 2008). Furthermore, it has a lower viscosity to aid flow.



**Table 1-1 Chemical structure of bulk and diluent monomers (Walters et al., 2016).**

Chemicals	Chemical structure	Molecular weight (g/mol)	Viscosity (Pa.s)	Glass transition temperature (°C)	Refractive index
Bis-GMA		512	700	-7.7	1.54
UDMA		479	8.5	-35.3	1.48
TEGDMA		286	0.05	-83.4	1.46
PPGDMA (n ~ 7)		600	0.09	-62.0	1.45

#### 1.4.1.2 Diluent monomers

High viscosity of bulk monomers limits the handling properties of dental composites. Hence, mixing with a low molecular weight monomer (diluent monomer) is required to reduce the viscosity, improve the handling properties, and increase monomer conversion. Triethyleneglycol dimethacrylate (TEGDMA) (Table 1-1) is a commonly used diluent monomer. Incorporation of this monomer contributes to the high strength and high monomer conversion of composites. This may, however, increase volumetric shrinkage and heat generation due to its high double bond concentration (Goncalves et al., 2009).

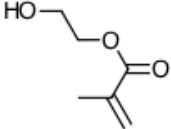
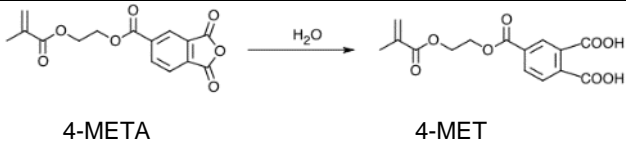
The lower double bond concentration of polypropylene glycol dimethacrylate (PPGDMA) (Table 1-1) compared to that of TEGDMA may provide a more flexible polymer network. Walters et al. (2016) showed that composites containing PPGDMA exhibited higher monomer conversion, greater depth of cure, and lower cytotoxicity compared with composites containing TEGDMA.

### 1.4.1.3 Adhesion promoting monomers

2-hydroxyethyl methacrylate (HEMA) (Table 1-2) is a surfactant monomer used for enhancing the surface wetting ability of the composite. It also helps to improve miscibility and solubility of components with different polarity. Polymerised HEMA in a polymer network, however, increases hydrophilicity and promotes water uptake into a dental composite (Moszner and Hirt, 2012).

4-methacryloyloxyethyl trimellitate anhydrous (4-META) reacts with water to form 4-MET (Table 1-2). The two carboxylic groups of 4-MET provide hydrophilic groups that enhance wetting of the dentine surface (Van Landuyt et al., 2007). Furthermore, carboxylic groups may replace phosphate ions of hydroxyapatite providing a chemical bond and thus improving dentine/enamel adhesion (Yoshida et al., 2000; Giannini et al., 2015).

**Table 1-2 Chemical structure of adhesion promoting monomers.**

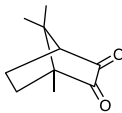
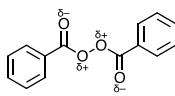
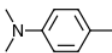
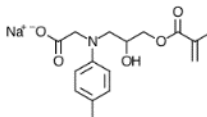
Chemicals	Chemical structure	Molecular weight (g/mol)
HEMA		130
4-META		304

#### 1.4.1.4 Initiators

Camphorquinone (CQ) (Table1-3) is used as a photo initiator in many commercial light-activated dental composites. This initiator absorbs blue light between 360 to 510 nm with the maximum absorption at 465-475 nm. A perceived disadvantage is the inherent yellowish hue, affecting the final colour of the composites (Moszner and Hirt, 2012). Upon irradiation, CQ absorbs visible light and decomposes into colourless products (Asmusen et al., 2009). This photo-bleaching, however, can partially improve the yellowish colour caused by this initiator.

Benzoyl peroxide (BP) (Table1-3) is an initiator used in chemical-activated or heat-activated polymerisation. The electron-withdrawing power of the adjacent oxygen and carbonyl groups weakens the central oxygen-oxygen bond. This compound is then susceptible to dissociation by heat ( $> 60\text{ }^{\circ}\text{C}$ ) or upon mixing with a reducing agent (activator) such as tertiary amines. Free radicals are produced upon its dissociation (Fig 1-7) and the polymerisation reaction is then started.

**Table 1-3 Chemical structure of initiators and activators.**

Chemicals	Chemical structure	Molecular weight (g/mol)
CQ		162
BP		242
DMPT		135
NTGGMA		329

#### 1.4.1.5 Activators

An aromatic amine, such as N-dimethyl-p-toluidine (DMPT) (Table1-3) is usually used as an activator or co-initiator. This chemical has proven to be an efficient hydrogen donating amine (Van Landuyt et al., 2007). Its toxicity and carcinogenicity are, however, of concern (Dunnick et al., 2014). The molecule has no methacrylate group and can be released from the polymerised composite.

Na-N-tolyglycine glycidyl methacrylate (Na-NTGGMA) (Table1-3) contains a tertiary amine and methacrylate group. This monomer therefore functions as the activator but can additionally be polymerised within the polymer network (Van Landuyt et al., 2007). This may lower the risk of its release from the composites (Khan et al., 2014).

#### 1.4.1.6 Polymerisation of composites

The polymerisation process is started when free radicals ( $R\bullet$ ) are produced due to the dissociation of an initiator triggered by light or chemical reaction (Fig 1-7). The free radicals then attack monomers and create monomer radicals. This initiation step is followed by the rapid addition of other monomer molecules, i.e. propagation step, which results in linkage between monomers by methylene bridges. This chain propagation process continues to build molecular weight and crosslink density. Free radical chains and the reaction are terminated either by direct coupling of two radicals (combination) or the abstraction of hydrogen (disproportionation) (Darvell, 2009).

The reported monomer conversions of current dental composites are 50 - 75 % (Alshali et al., 2013). High level of monomer conversion is required for enhancing mechanical properties and reducing cytotoxicity of dental composites (Goldberg, 2008; Ferracane, 2013). The high conversion, however, usually associates with high polymerisation shrinkage and shrinkage stress (Braga et al., 2005; Hui et al., 2010).

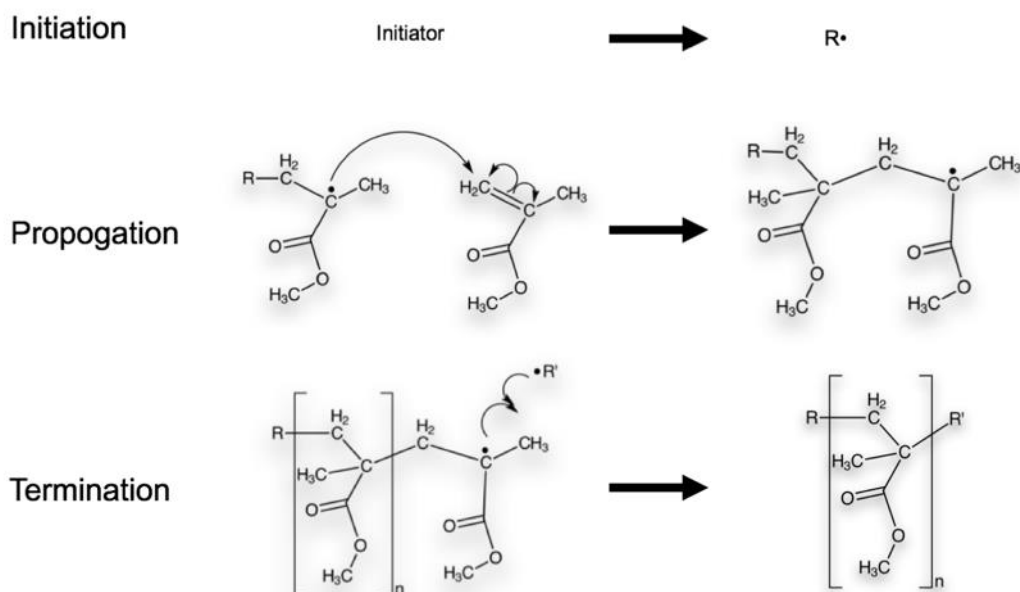


Fig 1-7 Schematic representing the radical polymerisation process.

#### 1.4.2 Filler phase

The incorporation of fillers improves both physical and mechanical properties of the dental composites. The fillers also help by reducing heat and shrinkage stress generated from polymerisation (Leprince et al., 2013; Hurle et al., 2014). Commonly used fillers are aluminosilicate glass or quartz which are chemically bonded to the polymer matrix via silane coupling agents.

The sizes of the fillers can be used to classify dental composites (Fig 1-8). The early-developed composites included particle sizes of 10 - 50  $\mu\text{m}$  (macrofill). These macrofilled composites exhibited high strength but poor polishability. Hence, the smaller filler composites (microfilled) were formulated to improve aesthetic properties (Ferracane, 2011). The incorporation of smaller fillers improved polishability but decreased mechanical properties of the composite (Beun et al., 2007). Furthermore, the

high surface area of small fillers (40 -50 nm) decreased filler loading of the composites (43 wt% filler load). Hence, flexural strength of the composites was relatively low (~ 70 MPa) compared to other composites (Ilie and Hickel, 2009). Large, small fillers, and pre-polymerised filler (PPRF) were combined (hybrid / microhybrid composite) to enhance both mechanical and physical properties (Blackham et al., 2009). Flexural strength of hybrid composites was ~ 120 MPa (Ilie and Hickel, 2009).

More recent dental composites contain only nanosize filler (nanofilled / nanohybrid composites). Nanofill and nanohybrid composites exhibited flexural strength of 103.7-144.4 MPa (Ilie and Hickel, 2009; Sideridou et al., 2011). These composites are generally used in both anterior and posterior teeth due to their high strength and good aesthetics (Ferracane, 2011).

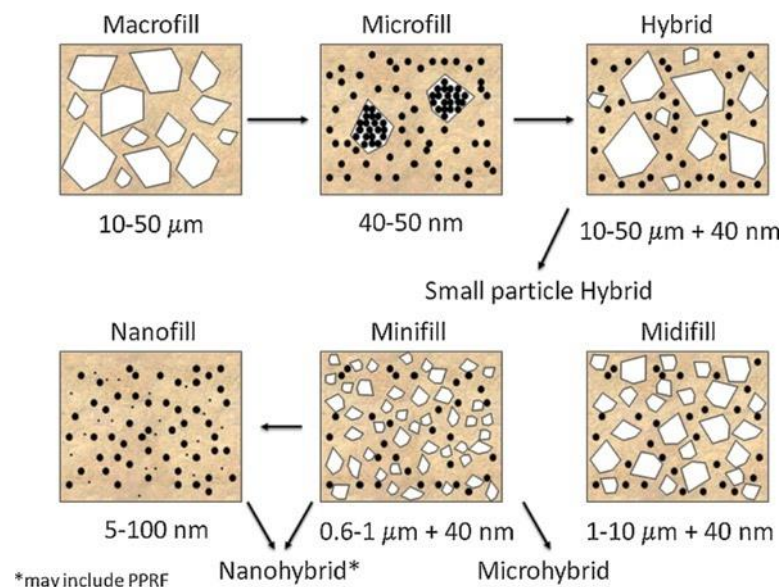


**Fig 1-8 Different type of dental composites classified by filler composition.** Reprinted from *Dental materials*, volume 27, Ferracane, J. L., *Resin composite—State of the art*, page 32, Copyright (2011), with permission from Elsevier.

## 1.5 Failure of dental composites due to secondary caries.

Tooth restorations have a limited lifetime. Factors affecting the outcome of restorations include patient, operator skills, treatment facilities, and the properties of restorative materials (Burke et al., 2005a; Burke et al., 2005b; Lucarotti et al., 2005). In general, glass ionomer restorations tend to exhibit highest annual failure rates (12 %) followed by dental composite (3 – 8 %) and dental amalgam restorations (2 – 4 %) (Opdam et al., 2010; Kopperud et al., 2012; Pinto Gdos et al., 2014; Laske et al., 2016). For dental composites, secondary caries or recurrent infection has been reported as a major reason for failure (70%) (Kopperud et al., 2012)(Fig 1-9).

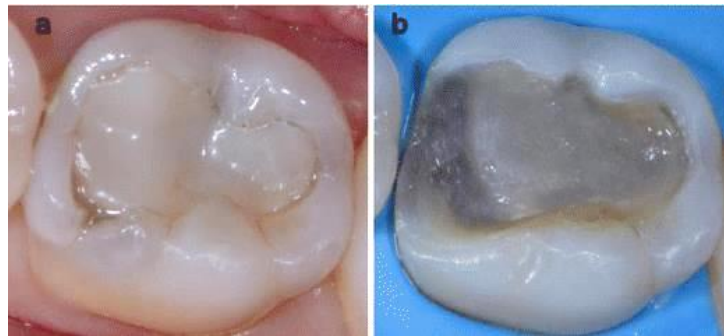


**Fig 1-9 a) Recurrent (secondary) caries around composite restoration. b) Old composite with additional sound tooth structures were removed to prepare a cavity for new restoration.** Reprinted from *Clinical Oral Investigations, Five-year retrospective clinical study of indirect composite restorations luted with a light-cured composite in posterior teeth*, volume 18(2), 2014, page 617, D'arcangelo C., Zarow M., De Angelis F., Vadini M., Paolantonio M., Giannoni M. & D'amario, Copyright (2014), with permission of Springer.

Secondary caries is more evident in high caries risk groups (Opdam et al., 2014). Aetiology of secondary caries is not largely different from that of primary caries. Bacterial microleakage has been proposed as the reason for secondary caries formation around dental composite restorations (Jokstad, 2016). Several reasons for the high incidence of secondary caries around dental composites have been proposed as shown below.

### **1.5.1 Improper marginal sealing**

Bacterial microleakage may be enhanced by the formation of micro gaps at the tooth-composite interface (Nedeljkovic et al., 2015). A successful dental composite restoration relies on an adequate seal between the restoration and tooth structure via adhesives. The application of these agents and the placement of the composite into the cavity are very technique-sensitive. Hence, marginal gaps could be formed around an improperly sealed composite restoration due to errors of placing technique (Irie et al., 2006; Yalcin et al., 2006; Demarco et al., 2012).

### **1.5.2 Polymerisation shrinkage**

The polymer-based material is associated with a volumetric reduction upon polymerisation. The shrinkage of commercial dental composites was reported to be 1–6 vol% (Schneider et al., 2010). This shrinkage is developed when the monomers previously existing at Van der Waals's force distances become closely packed with shorter covalent bonds. The contraction stress thus generated and transferred to the surrounding bonded surfaces, lead to an interfacial debonding, gap formation (Figure 1-4), postoperative sensitivity, and bacterial microleakage (Ferracane, 2008; Ferracane and Hilton, 2016).

### **1.5.3 Tooth-composite interfaces degradation**

Even if an adequate seal of the composite restoration is initially achieved, tooth-restoration interfaces can be degraded over time due to the following mechanisms; 1) Water absorbed into the polymer network of the hybrid layer at the interfaces and may cause chain scission of the susceptible groups, such as ester groups (Hashimoto, 2010). 2) The enzymatic degradation of exposed collagen in the hybrid layer by host-derived



collagenase also contributes to the disruption of interfacial integrity (Hu et al., 2015). 3) In addition, tooth-restoration interfaces are subjected to repetitive occlusal forces and oral temperature changes (Deng et al., 2014). This causes fatigue and disruption of the interfaces, subsequently leading to bacterial microleakage.

#### **1.5.4 Surface properties and the composite-biofilm interaction**

Unlike dental amalgam and GIC, dental composites have no anticariogenic properties. On the contrary, the composites may encourage biofilm formation (Zhang et al., 2016c). This could be due to the composite's surface properties such as roughness and surface free energy that favour bacterial adhesion (Cazzaniga et al., 2015). Furthermore, the release of un-polymerised monomers or biodegradable products from the composite could also promote the growth of the highly cariogenic bacteria (Nedeljkovic et al., 2015; Nedeljkovic et al., 2016a).

### **1.6 Modification of dental composites to reduce the risk of secondary caries**

Treatment of failed restorations has been estimated to account for 50% of all restorative works (Javidi et al., 2015). Frequently, the removal of a failed restoration leads to further destruction of sound tooth structures. This will subsequently weaken the tooth and may shorten the longevity of the new restoration (Frencken et al., 2012). An improvement of composite restorations to minimise the risk of failure due to secondary caries is therefore needed. This may be achieved by the addition of remineralising and / or antimicrobial agents (Tables 1-4,5).

### **1.6.1 Remineralising agents**

#### **1.6.1.1 Fluoride**

Fluoride has long been used to provide anticariogenic effects and increase acid resistance of dental hard tissues by the formation of fluoroapatite. Fluoride has therefore been incorporated into some dental composites as fluoridated glass, inorganic fluoride compounds, or pre-reacted glass ionomer (S-PRG) filler particles. The fluoride release from these composites was demonstrated to be low and probably not sufficient to provide clinical benefits (Wiegand et al., 2007; Cury et al., 2016). Incorporation of  $\text{CaF}_2$  nanoparticles enabled high fluoride release due to their high surface area. With 20-30 wt% addition to the filler phase, fluoride release from the composite was comparable to a commercial GIC and RMGIC (Melo et al., 2013a).

#### **1.6.1.2 Bioactive glass**

In several studies, a bioactive glass (BAG) containing oxides of silicon, calcium and phosphorous, plus fluoride have been included in dental composites. A silicon-rich layer can form on the surface of such glasses and acts as a template for apatite precipitation (Yli-Urpo et al., 2004). Fluoride-containing BAG may provide a single source for both calcium and fluoride release (Davis et al., 2014). Dental composites containing BAG exhibited higher flexural strength (117 – 124 MPa) compared to a commercial microfill composite (Khvostenko et al., 2013). Addition of BAG also helped to reduce biofilm formation within marginal gaps in simulated tooth restorations (Khvostenko et al., 2016).

Strontium has been incorporated into BAG for bone repair material. It has been shown that apatite formation was increased upon replacing Ca with Sr. This could be due to the fact that the strontium ions increased the potential nucleation sites for HA formation and stabilised the HA precursor phase (Drouet et al., 2008). Additionally, strontium may

also provide an antibacterial effect. It also has enhanced radiopacity in comparison with calcium (Lippert and Hara, 2013; Shahid et al., 2014).

### 1.6.1.3 Calcium phosphates (CaP)

An alternative remineralising agent to fluoride is a compound that releases calcium and phosphate ions. CaP compounds have been incorporated into dental composites to enable mineral release (Table 1-4). The rate of release of these ions is determined by the solubility of the compounds which increases with decreasing Ca/P ratio. As release also increases with decreasing pH (Young, 2010), there is also the potential to provide tooth remineralisation upon acid attack.

**Table 1-4 Calcium phosphate compounds (Dorozhkin, 2009; Layrolle, 2011)**

Name	Abbreviation	Formula	Ca/P ratio	Solubility at 25 °C (g/L)
Monocalcium phosphate monohydrate	MCPM	$\text{Ca}(\text{H}_2\text{PO}_4)_2 \cdot \text{H}_2\text{O}$	0.50	18
Dicalcium phosphate dihydrate (brushite)	DCPD	$\text{CaHPO}_4 \cdot 2\text{H}_2\text{O}$	1.00	0.088
Dicalcium phosphate anhydrous (monetite)	DCPA	$\text{CaHPO}_4$	1.00	0.048
Octacalcium phosphate	OCP	$\text{Ca}_8(\text{HPO}_4)_2(\text{PO}_4)_4 \cdot 5\text{H}_2\text{O}$	1.33	0.0081
Calcium-deficient hydroxyapatite	CDHA	$\text{Ca}_{10-x}(\text{HPO}_4)_x(\text{PO}_4)_{6-x}(\text{OH})_{2-x}$ ( $0 < x < 2$ )	1.33- 1.67	0.0094
Amorphous calcium phosphate	ACP	$\text{Ca}_x(\text{HPO}_4)_y(\text{PO}_4)_z \cdot n\text{H}_2\text{O}$ ( $n=3-4.5$ ; 15-20 wt% $\text{H}_2\text{O}$ )	1.20- 2.20	<sup>a</sup>
$\beta$ -Tricalcium phosphate	$\beta$ -TCP	$\beta\text{-Ca}_3(\text{PO}_4)_2$	1.50	0.0005
Hydroxyapatite	HA	$\text{Ca}_{10}(\text{PO}_4)_6(\text{OH})_2$	1.67	0.0003
Fluoroapatite	FA	$\text{Ca}_{10}(\text{PO}_4)_6\text{F}_2$	1.67	0.0002

<sup>a</sup> The solubility cannot be measured precisely.

The released ions may precipitate as several types of calcium phosphate depending on ions saturation degree and pH of the surrounding solution (Aoba, 2004). It has been shown that a material that promotes apatite precipitation on its surface could potentially encourage the remineralisation of demineralised dentine (Gandolfi et al., 2011).

In early studies, highly soluble amorphous calcium phosphate (ACP) particles of relatively large diameter were employed. The addition of this compound inevitably reduced the mechanical strength of the composites (Regnault et al., 2008). More recently, nanoparticle ACP (NACP, particle diameter ~ 116 nm) has been synthesised to address this issue. Composites incorporated with this filler gave rechargeable calcium / phosphate ion release for 6 weeks and initial strength comparable to a commercial hybrid composite (Xu et al., 2010b; Zhang et al., 2016a).

A previous study has shown that dental composites containing monocalcium phosphate monohydrate (MCPM) and tricalcium phosphate (TCP) encouraged the formation of calcium deficient hydroxyapatite upon immersion in simulated body fluid (SBF) (Aljabo et al., 2016). The addition of these compounds also encouraged water sorption which induced expansion to compensate polymerisation shrinkage (Aljabo et al., 2015). The degree of strength reduction upon water immersion of these composites was not significantly different from that observed with a microhybrid commercial dental composite.

**Table 1-5 Summary of recent studies on dental composites containing remineralising and/or antibacterial agents.**

Authors	Remineralising compounds (mean particle size)	Antibacterial agents	Flexural strength at 24 hr (MPa)	Comments
<b>Skrtic and Antonucci (2007)</b>	ACP (7 - 9 $\mu\text{m}$ )	-	~ 51	The maximum water sorption was 5 wt%.
<b>(Regnault et al., 2008)</b>		-	40-60	The strength was decreased by 25-45 % after 2 weeks
<b>Xu et al. (2010a)</b>	CaF <sub>2</sub> (56 nm)	-	100-160	The fluoride release of the composites was comparable to GIC and RMGIC
<b>Melo et al. (2013b)</b>	NACP (116 nm)	-	-	- The composites had increased CaP ions release at low pH - Reduced depth of mineral loss in enamel by ~ 30% compared to the control composite
<b>Cheng et al. (2016)</b>		QAMs and NAg	~ 70	- Strength was decreased to ~50 MPa after 3 months and stable for 12 months - Antibiofilm activity was maintained for 12 months
<b>Zhang et al. (2016a)</b>		-	60 – 90	The composites exhibited rechargeability of CaP ions and re-released same level of ions for 6 cycles
<b>(Khvostenko et al., 2013)</b>	Bioactive glass (0.04 - 3 $\mu\text{m}$ )	-	113-117	The strength was stable for 2 months
<b>Oral et al. (2014)</b>	Bioactive glass (300 – 1000 $\mu\text{m}$ )	-	70 - 106	Silanisation increased strength but may prevent the leaching of the ions from BAG.
<b>Mehdawi et al. (2013)</b>	MCPM (15 $\mu\text{m}$ ) + TCP (29 $\mu\text{m}$ )	Chlorhexidine	79 -160	The CaP release was increased upon raising hydrophilic monomer
<b>Aljabo et al. (2015); Aljabo et al. (2016)</b>		Chlorhexidine	137-160	- The strength was reduced to ~ 100 MPa after four weeks - The degree of apatite precipitation was increased upon raising CaP level - The level of CHX release depends on the level of MCPM and TCP

## **1.6.2 Antimicrobial agents**

### **1.6.2.1 Silver nanoparticles (NAg)**

Silver ions kill bacteria by targeting their respiratory chain and DNA replication processes (Rai et al., 2009). NAg can be combined with nanoparticle ACP to obtain composites with both antibacterial and remineralising properties. In one study a composite containing both agents exhibited mechanical properties comparable to that of a commercial product (Cheng et al., 2012).

Limitations of NAg include particle agglomeration and the discoloration of the composite (Cheng et al., 2011; Melo et al., 2013b). Another study has reported that bacteria can develop resistance to silver nanoparticles via genomic changes (Graves et al., 2015). Furthermore, these nanoparticles can pass the blood-brain barrier and subsequently accumulate in the brain (Padovani et al., 2015).

### **1.6.2.2 Quaternary ammonium methacrylates (QAMs)**

QAMs cause bacterial cell lysis by the interaction between its positively charged N<sup>+</sup> site and negatively charged bacterial cell membrane (Cheng et al., 2015). The polymerisable methacrylate monomer containing QAMs (12-methacryloyloxy dodecylpyridinium bromide; MDPB) has been successfully synthesised and used in the commercial dental primer such as Clearfil SE Protect (Kuraray Medical Inc, Japan)(Imazato et al., 2014). The antibacterial component is not released after light curing. Hence, their mechanical properties were maintained (Imazato, 2009).

Due to the immobilisation of QAMs molecule in the polymerised monomer, the resin polymer exhibited bacteriostatic effects only to the contacting bacteria (Imazato et al., 2014). Hence, it needed to combine with other antibacterials such as NAg to enable the

remote killing of bacteria (Zhang et al., 2013). The combination of these agents may further reduce mechanical properties of composites (Cheng et al., 2016).

### 1.6.2.3 Chlorhexidine

Chlorhexidine (CHX) has been generally used in oral infection control. It provides a wide-range of antimicrobial activity with comparable minimum inhibitory concentrations to antibiotics (Young, 2010). The release of CHX from dental composites is governed by the amount of water sorption of the composites (Leung et al., 2005; Mehdawi et al., 2013; Aljabo et al., 2016). High level of hydrophilic components in the material is therefore required to enable high CHX release.

Nevertheless, the high levels of hydrophilic components might then reduce the physical and mechanical properties of the composites (Leung et al., 2005; Mehdawi et al., 2009). Furthermore, recent studies have demonstrated increasing antibiotic resistance to chlorhexidine (Smiline et al., 2012; Kulik et al., 2015). Some severe hypersensitivity reactions resulting in death have also been reported (Pemberton, 2016).

### 1.6.2.4 $\epsilon$ -Poly-L-lysine (PLS)

$\epsilon$ -Poly-L-lysine (PLS) is hydrophilic cationic linear homopolymer of lysine amino acids (Fig 1-7). The one produced by bacteria typically comprises of 25-35 L-lysine residues. The peptide bond in this polymer links between the carboxyl groups and  $\epsilon$ -amino group of L-lysine residues. PLS was first biosynthesized by *S. albulus* (Shima et al., 1984). It is now industrially synthesised by the fermentation of a mutated *S. albulus* 110011A. The polymer is water soluble, stable in acid or basic conditions, and has low toxicity (Yoshida and Nagasawa, 2003)

PLS has been approved by FDA as a food preservative. The repetition of L-lysine residues is related to the antibacterial properties of PLS. At least 10 residues are required to exert antibacterial properties (Hyldgaard et al., 2014). Its antibacterial action involves the disruption of bacterial cell membrane. Cationic PLS interacts with negatively charged bacterial cell membrane leading to the stripping of lipopolysaccharides and permeability of the cell membrane (Shukla et al., 2012). Other antibacterial actions include the increase in reactive oxygen species and interruption of RNA transcription processes (Ye et al., 2013).

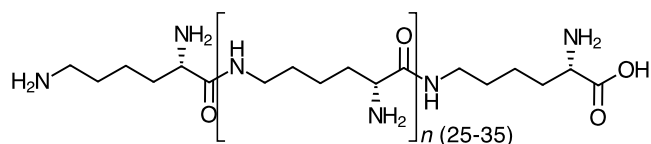


**Fig 1-10 Chemical structure of epsilon poly-L-lysine**



## **1.7 Regulatory approval for the dental / bone composites**

A dental composite is classified as a class IIa medical device (European Commission, 2015). To obtain regulatory approval for a material in this classification is easier than for a class III device that requires clinical studies (National Patient Safety Agency, 2008). To claim antibacterial and remineralising action, however, the device according to recent Medicines and Healthcare Regulatory Agency (MHRA) advice (personal communications) may need to be converted to class III. Bone composites are generally class IIb (under rule 8) but may become class III if they have a biological effect or undergo longer-term chemical changes (European Commission, 2010). Hence, the approval process for these materials will be more complicated than for conventional dental composites.

The goal of our research group is to obtain regulatory approval for clinical trials with a novel dental composite followed by a similar material for bone repair. The development of bone composites based on dental composites should be expected to assist the bone composite approval process. The application of the bone composite for vertebral bone fracture repair will be described in the next section.

## **1.8 Osteoporotic vertebral fractures**

### **1.8.1 Epidemiology**

The WHO considers osteoporosis a major health concern due to its high prevalence and severe complications. It affects approximately 200 million people worldwide (Lane, 2006). Worldwide, osteoporosis causes ~ 9 million fractures annually (Johnell and Kanis, 2006). It has been estimated that osteoporosis led to 1.5 million fractures per year in the US (Black and Rosen, 2016). Studies estimate the current number of osteoporotic vertebral fractures in the UK as 65,000 per year (Svedbom et al., 2013). Additionally, the incidence of vertebral fractures will increase by 23% by 2025 (Bouza et al., 2015). The five years survival rate after hip and vertebral fracture were approximately 80% (Harvey et al., 2010).

In the US, the estimated direct medical cost for osteoporosis and related fracture treatment is 20 billion dollars per year. In Europe, the economic burden of osteoporosis in 2010 was estimated to be 30.7 billion euro. This medical cost has been predicted to reach 76.7 billion euro in 2050 (Pisani et al., 2016). The estimated direct medical costs for treating osteoporotic fractures currently in the UK is ~ £1.8 billion per year but this could increase to £2.2 billion per year by 2025 (Burge et al., 2008).

### 1.8.2 Aetiology

Osteoporosis is a systemic skeletal disease resulting in a decrease of bone mineral density and profound changes in the bony micro architecture (Fig 1-11). The reduction of oestrogen either due to menopause or surgery leads to an increase in the production of the receptor activator of nuclear factor  $\kappa$ B (RANKL). The increase in this ligand and its reaction with the receptor initiates the proliferation and maturation of osteoclast precursors (Favus, 2010). This subsequently leads to an imbalance of bone remodelling.

The decrease of oestrogen production also leads to reduced intestinal calcium absorption and increase in calcium loss (Armas and Recker, 2012). Hence, the bone becomes weaker and susceptible to fracture from normal physiologic loads. Osteoporotic fractures are the most common complication found in osteoporotic patients. Frequently affected sites include hip, spine, and forearm (Rachner et al., 2011). The incidence of osteoporotic fractures varies by region. It has been estimated that up to 50 % of women older than 50 years will experience osteoporotic fractures during their lifetime (Eastell et al., 2016).

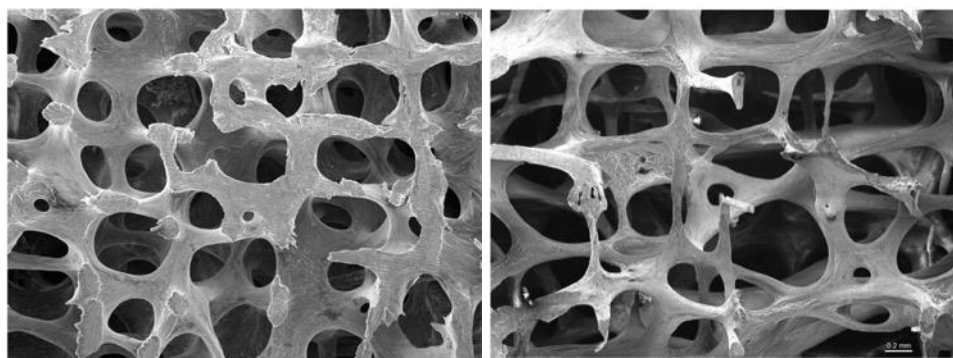


**Fig 1-11 Comparison of (a) normal and (b) osteoporotic bone from 3<sup>rd</sup> lumbar vertebra. Credited to © Tim Arnett, University College London (t.arnett@ucl.ac.uk).**

## 1.9 Vertebroplasty (VP) and kyphoplasty (KP)

An osteoporotic vertebral fracture causes pain, height loss, limited mobility, kyphosis, and reduced pulmonary function. The traditional non-operative treatments are bed rests, analgesics, and bracing. These non-operative managements failed to relieve severe pain in one-third of patients (Benzel, 2012; Lin et al., 2016). Furthermore, they also lead to the disease condition worsening and more complications.

Minimally invasive surgical treatments, vertebroplasty (VP) and balloon kyphoplasty (KP), have been employed to stabilise fractures, relieve pain, and increase mobility for patients who have failed to response from conservative treatments (McDonald et al., 2017). The currently accepted indications for VP and KP are painful osteoporotic vertebral compressive fracture, painful metastatic/malignant vertebral body lesions, and vertebral traumatic fracture (Wong and McGirt, 2013; Yimin et al., 2013).

Studies showed that patients treated surgically experienced rapid and significant pain reduction, improved pulmonary function, and had longer survival rates (Diamond et al., 2006; Lee et al., 2011; Blasco et al., 2012; Xu et al., 2012; Chen et al., 2013; Takura et al., 2017). Furthermore, a recent multicentre, randomised, double-blind, and placebo-controlled trial also revealed a superior pain reduction for patients that received vertebroplasty compared to patients that recieved simulated vertebroplasty (placebo intervention) (Clark et al., 2016). It has been estimated that the cost of VP and BKP is £800 and £2600 per procedure respectively (NICE, 2013). Both treatments, however, showed a comparable outcome in pain reduction and functional recovery (Ates et al., 2016).

### 1.9.1 Vertebroplasty (VP)

VP was introduced in 1984 by Gakibert and Deramond (Hulme et al., 2006). This treatment can be performed under local or general anaesthesia. Briefly, a cannula is inserted into the affected area (Fig 1-12). A bone cement is then injected into the collapsed vertebra under fluoroscopy control (Mukherjee and Lee, 2011). The treatment aims of VP, however, are not to restore the height of collapsed vertebra, but rather pain relief and the prevention of further spinal mal-alignment (Benneker and Hoppe, 2013; Yimin et al., 2013).

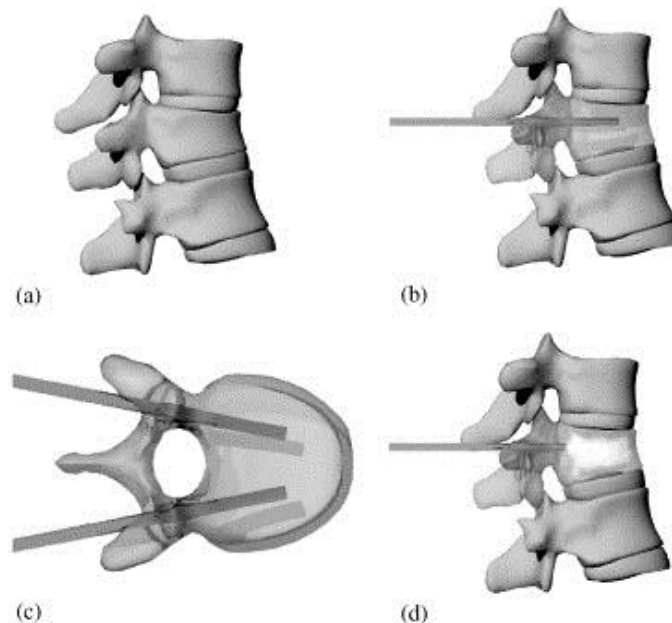


**Fig 1-12 The schematic representing percutaneous vertebroplasty (VP) a) a collapse vertebra, b-c) needles are inserted into the vertebral body, d) bone cement is injected to stabilise the vertebra.** Reprinted from *Biomaterials*, volume 27, Verlann et al., Anterior spinal column augmentation with injectable bone cements, page 292, Copyright (2006), with permission from Elsevier.

### 1.9.2 Kyphoplasty

Kyphoplasty or balloon kyphoplasty (KP) was introduced by Mark Reily in 1998 as an alternative to VP for restoring vertebral height and realigning the spine (Yimin et al., 2013). The inflatable bone tamp is inserted into the fracture site under fluoroscopy control (Fig 1-13 a). After creating the cavity and restoring the height of the collapsed vertebra (Fig 1-13 b), the balloon tamp is removed followed by the injection of bone cement (Fig 1-13 c,d) (Taylor et al., 2006; Vallejo and Benyamin, 2010).

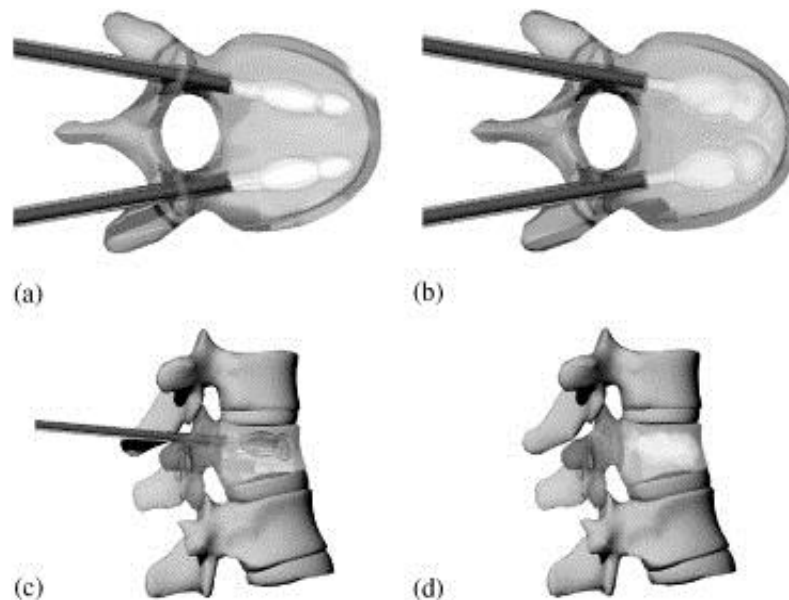


**Fig 1-13 Schematic representing balloon kyphoplasty a) cannulas with balloon tamps are inserted into the vertebral body, b) bone tamps are inflated to correct the height and create space for the cement, c-d) the bone cement was injected.** Reprinted from *Biomaterials*, volume 27, *Verlann et al., Anterior spinal column augmentation with injectable bone cements*, page 293, Copyright (2006), with permission from Elsevier.

## 1.10 Current bone cements for VP and BKP

Currently there are no specific requirements for a bone cement used in VP and KP. (Lewis, 2006) has proposed several required properties for the cement which are presented in Table 1-6. The currently used bone cements for VP and KP are described as follow.

**Table 1-6 Desirable properties of an injectable bone cement for VP / KP.**

Properties	Requirements
Handling / setting characteristics	<ul style="list-style-type: none"> <li>- High radiopacity</li> <li>- Ease of preparation and injection</li> <li>- Low viscosity during injection then quickly set once the cement reaches the vertebra</li> <li>- Working time ~ 6-10 min</li> <li>- Low curing temperature</li> <li>- Low cost</li> <li>- Long shelf life</li> </ul>
Mechanical properties	<ul style="list-style-type: none"> <li>- Comparable strength to vertebral bone</li> <li>- Appropriate adhesion, not dissociate during setting</li> </ul>
Bioactivity	<ul style="list-style-type: none"> <li>- Microporosity (&lt;10 <math>\mu\text{m}</math>) to allow circulation of fluid</li> <li>- Macroporosity (&gt;100 <math>\mu\text{m}</math>) to provide scaffold for blood-cell colonisation</li> <li>- Appropriate resorption rate</li> <li>- Osteoconductivity, osteoinductivity,</li> <li>- Low toxicity</li> </ul>

### 1.10.1 Polymethyl methacrylate (PMMA)

PMMA (Fig 1-14), the polymer of methylmethacrylate (MMA), is a commonly used bone cement for various orthopaedic applications. A commercial example of PMMA cement is Simplex P® or Spineplex® (Stryker, Newbury, Berkshire, UK). The powder phase contains PMMA, MMA-styrene copolymer, radiopacifier (barium sulphate) and benzoyl peroxide (BP). The monomer phase contains methylmethacrylate and N-dimethyl-p-toluidine (DMPT). Advantages of PMMA bone cement include familiarity for the orthopaedic surgeons, high strength (flexural strength ~ 150 MPa), and cost-effectiveness.

Disadvantages of this cement include handling difficulty, rapid changing of viscosity after mixing, high heat generation (82 - 86 °C), high shrinkage, lack of bone bonding potential, and risk of toxic residual monomer release (Lewis, 2006; Boyd et al., 2008; Benzel, 2012; Vaishya et al., 2013; Khan et al., 2014). Another serious concern of PMMA cement is its mechanical mismatch with the vertebral bone. The elastic modulus of PMMA cement (1.7 - 3.7 GPa) (Boger et al., 2007) is much higher than that of cancellous bone (0.1 - 0.7 GPa) (Banse et al., 2002). The differences in modulus of elasticity between treated and untreated vertebra may then subsequently increase the risk of adjacent vertebral fracture (Hadley et al., 2010).





### 1.10.2 Calcium phosphate cements (CPCs)

The main advantage of CPCs (Fig 1-15) is their osteoconductivity that may promote apposition at bone-cement interfaces (Tamimi et al., 2012). After the powder phase is mixed with the liquid phase, the paste then solidifies via a dissolution-precipitation process. The cements can be classified by their end product which is either apatite or brushite (Cama, 2014). In 2012, however, illegal testing of a CaP cement (Norian XR, Synthase, West Chester, Pa, USA) for vertebroplasty was performed on humans. This led to the death of five patients on the operating room table (Kimes, 2012). and put into serious question any use of CPCs in this application.

A common problem of the CPCs is separation of the liquid phase and powder phase during injection (O'Neill et al., 2016). Incomplete set can lead to pulmonary embolism (Bernards et al., 2004). The cements also tend to disintegrate upon exposure to fluids or blood (Wang et al., 2007). Furthermore, their excessive modulus of elasticity (8 -14 GPa) at early time may increase the risk of adjacent vertebral fracture (O'Hara et al., 2014). Moreover, inconsistency of resorption rate also led to rapid reduction in strength (Yang and Zou, 2011).



**Fig 1-15 Example of a commercial calcium phosphate cement (BoneSource®, Stryker, New Jersey, USA)**  
(Source: <http://www.stryker.com>)

### 1.10.3 Bone composites

An example of a commercial bone composite used in vertebroplasty is Cortoss<sup>®</sup> (Stryker, Newbury, Berkshire, UK) (Fig 1-16). Its monomer phase contains Bis-GMA, Bisphenol-A-ethoxy dimethacrylate (Bis-EMA), and TEGDMA. The powder phase contains bioactive glass (combeite,  $\text{Na}_2\text{O}-\text{CaO}-\text{P}_2\text{O}_5-\text{SiO}_2$ ) to enhance bone bonding, and barium boroaluminosilicate glass to improve mechanical properties and radiopacity (He et al., 2015). This composite is supplied in a double-barrelled syringe with mixing gun which could facilitate the handling process.



**Fig 1-16 Example of a commercial bone composite supplied with automatic mixing tip and mixing gun (Cortoss<sup>®</sup>, Stryker, New Jersey, USA) (Source: <http://www.stryker.com>)**

This bone composite is believed to be bioactive as some *in vivo* studies showed new bone apposition at the bone-composite interface without fibrous interposition (Mehbod et al., 2003; Sanus et al., 2013). A randomised controlled clinical trial showed that patients treated with Cortoss exhibited early pain reduction but in addition better long-term preservation of function compared to that of the patient treated with PMMA (Bae et al., 2012).

Concerns of this composite cement include its high exothermic reaction (63 °C), high stiffness (~ 2 GPa), and lack of antibacterial or therapeutic properties (Boyd et al., 2008; Anselmetti et al., 2009). Additionally, an *in vitro* study found that Cortoss showed a cytotoxic effect on human cells (Becker et al., 2006).

## 1.11 Complications after VP and KP

### 1.11.1 Cement leakage

Cement leakage (Fig 1-17) is the most common complication associated with VP and KP. The leakage depends on the fracture characteristic of the vertebra, injection method, and physicochemical properties of the bone cement (Xin et al., 2016). The incidence of this complication observed from normal radiograph of the patients was 31 % and 11 % for VP and KP respectively (Du et al., 2014). The incidence observed from normal radiograph was underestimated as it could increase up to 77 % when patients were assessed with CT scan (Tome-Bermejo et al., 2014).

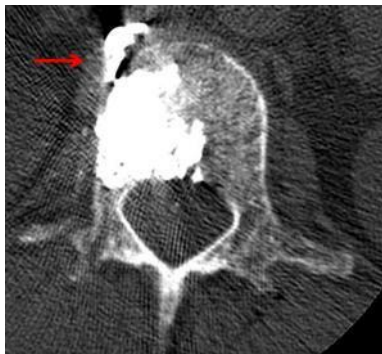


**Fig 1-17 CT image obtained after vertebroplasty showing the leakage of PMMA cement (red arrow) to right intercostal artery.** Reprinted from *The Spine Journal*, volume 11(8), Yazbeck P. G., Al Rouhban R. B., Slaba S. G., Kreichati G. E. & Kharrat K. E., page e7, Copyright (2011), with permission from Elsevier.

Despite the fact that the majority of the leakage occurrences may not pose a clinical problem, some can have severe consequences (Hulme et al., 2006). The severity of the complication depends on the site that cement leaks to. For example, cement leaking into the neural foramen may result in neurologic complications (Boonen et al., 2011). Cement leaking into paravertebral veins may cause embolism at pulmonary or cardiovascular systems (Arnaiz-Garcia et al., 2014; Janssen et al., 2017).

### **1.11.2 Subsequent adjacent fractures**

The second most common complication after VP and KP is an adjacent vertebral fracture. This complication was found in 12 – 50 % of patients (Li et al., 2012). The majority of those fractures were symptomatic and detected within one month (Takahara et al., 2016). The risk of developing adjacent vertebral fracture is similar following both VP and KP procedures (Du et al., 2014).

Researchers have not yet been able to provide conclusive evidence that the high risk of adjacent fractures is caused by the treatments. Several studies have, however, suggested that the fracture risk may be exacerbated by the alteration of load transfer due to the increase of stiffness of the injected vertebra (Klazen et al., 2010; Fahim et al., 2011; Cho et al., 2015; Holub et al., 2015). The high stiffness of the injected cement may affect the load transferred to the adjacent bone. The lack of applied loads may lower the bone density and subsequently reduce the strength of the adjacent bone: a problem known as stress shielding (Papanastassiou et al., 2014). The fracture, however, could be caused by the natural progression of the disease, improper technique, and patient factors (Aquarius et al., 2013; Takahara et al., 2016).

### **1.11.3 Postoperative infection**

Although postoperative infections are not common (< 1 %), they often require further invasive surgical intervention associated with high mortality rate (33 %) (Abdelrahman et al., 2013). The most common isolated organism from patients was *S. aureus* (Abdelrahman et al., 2013). Patient comorbidities such as multiple systemic diseases or immunosuppression may allow the low-virulence organism to colonise at the operation site. Hence, bone cement mixed with antibiotics such as gentamycin or vancomycin has been recommended for the medically compromised patient (Walker et al., 2004;

Hashimoto, 2010). However, the use of antibiotic loaded bone cement as a prophylaxis is not yet widely accepted. Some clinicians routinely mix a bone cement with an antibiotic to prevent this serious complication (Lee et al., 2007).

## **1.12 Development of low stiffness, mineralising, and antibacterial bone cement**

Due to above mentioned complications, several studies have been conducted to develop injectable bone cements for VP and KP that provide adequate mechanical matching to bone, bone-bonding ability, and antibacterial properties. Methods employed to improve those properties are described below.

### **1.12.1 Low stiffness bone cement**

Studies have shown that the application of a low stiffness bone cement in *ex vivo* human spinal segments can reduce the risk of adjacent vertebral fracture. Pressure concentrations adjacent to the injected cement were smaller with low modulus cement compared with standard cement (Kinzl et al., 2012a; Kolb et al., 2013a). Several methods to lower the stiffness/modulus of elasticity have been proposed.

(Boger et al., 2007) developed a low modulus bone cement by mixing a commercial PMMA with 35% sodium hyaluronate. This technique reduced the modulus of elasticity by 74% without causing any collapse of the injected vertebra. Lopez et al. (2011) mixed the PMMA cement with castor oil, reducing the modulus of elasticity by ~ 60 %. The castor oil however negatively affected polymerisation of the cement. Kolb et al. (2013b) managed to lower the modulus of elasticity of the PMMA cement by 51 % by mixing the cement with fetal bovine serum. The spinal segment injected with modified cement showed a higher fatigue fracture force than the group treated with standard PMMA.

Schröder et al. (2016) modified a standard PMMA cement by addition of normal saline. Modulus of elasticity of the cement was reduced by almost three times upon adding 30 vol% of normal saline. This, however, was associated with an increase of setting time.

These modifications decreased the stiffness of bone cements but may interfere with the fluid structure and the setting mechanism of the cements. This may lead to other problems such as poor handling properties and injectability, phase separation, and cement toxicity, and cement extravasation.

### 1.12.2 Calcium phosphate containing bone composite

Due to the superior bioactivity of CPCs, calcium phosphate compounds (CaP) have been incorporated into bone cements. The addition of these compounds promoted additional benefits such as low setting temperature and improved bioactivity (Rodriguez et al., 2014; Wu et al., 2016a). When this composite is exposed to an aqueous environment, ions are exchanged and re-precipitate as a calcium phosphate apatite. The apatite composition depends mainly on the local pH and ion saturation. The apatite is believed to promote *in vivo* bone bonding (Fig 1-18)(Kokubo et al., 2003; LeGeros, 2008).

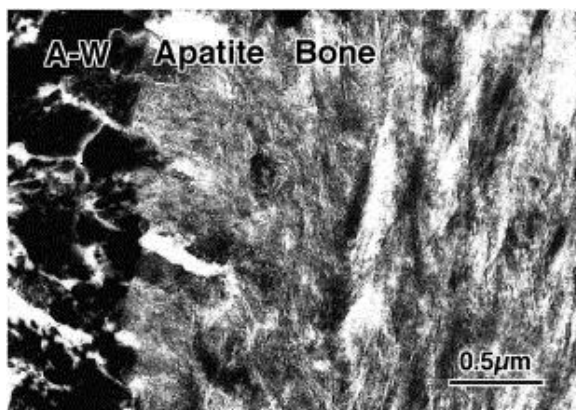


**Fig 1-18** Transmission electron microscope image of the interface between bioactive glass (A-W) and rat tibia after 8 weeks of implantation. Layer of apatite at the interface mediating integration between the glass and bone. Reprinted from *Biomaterials*, vol 24(13), Kokubo T., Kim H.-M. & Kawashita M. *Novel bioactive materials with different mechanical properties*, page 2163, Copyright (2003), with permission from Elsevier.

Bone bonding ability of the cement is required to promote new bone apposition at the bone-cement interface. The formation of the biomimetic bone substrate or an adsorption of bone specific proteins by this layer may promote osteoblast adhesion and its activity (Alves et al., 2010). Hence, the addition of calcium phosphate compounds is a simple method to encourage bioactivity of the bone cement.

An *in vivo* study showed that incorporation of  $\beta$ -TCP to PMMA promoted osseointegration with no obvious local toxicity signs (Dall'Oca et al., 2014). The addition of CaP compounds unfortunately caused a reduction of mechanical properties, increased cement viscosity, and poor handling properties of the cement. It has been shown that addition of 40 wt% brushite into PMMA cement led to poor handling properties and injectability, and reduced strength (Rodriguez et al., 2014).

### 1.12.3 Strontium-substituted bone cement

Strontium is an alkaline earth metal and is directly beneath calcium in the periodic table. Systemic administration of strontium ranelate has been prescribed for post-menopausal osteoporotic patients. Strontium exhibits treatment effect by stimulating osteoblast proliferation and maturation while inhibiting osteoclast formation and activity (Schumacher and Gelinsky, 2015; Liu et al., 2016). Hence, a bone cement that released strontium locally to the fracture area would be of benefit. This may help to reduce some adverse effects of systemic administration such as nausea, diarrhoea, headache, venous thromboembolism, and hypersensitivity reactions (Reginster et al., 2005; Rizzoli et al., 2011).

The incorporation of Sr into CPCs has previously increased bone-bonding strength (Zhang et al., 2011; Shepherd et al., 2012). In addition, an *in vivo* study showed faster bone healing and bone formation with Sr-substituted bone cement compared to that of

the traditional CPC (Kyllonen et al., 2015). Another benefit of the incorporation of Sr is the enhanced radiopacity of the cement to facilitate the surgical procedure and enable follow up with radiographs.

#### **1.12.4 Antibiotic-loaded bone cement**

Postoperative infection after VP or KP is a serious complication. Systemic antibiotic prophylaxis has been recommended for high-risk patients. Antibiotics, such as gentamycin, have been incorporated into bone cements to minimise the occurrence of infection. Bone cement with added antibiotics may provide local release of antibiotic. Antibiotic concentration may then exceed that obtained with systemic administration and reduce systemic adverse reactions (Anagnostakos, 2017). The addition of this agent has reduced the rate of infection after total joint arthroplasty (Chang et al., 2013). The addition of antibiotic however reduced mechanical properties of the cement (Wang et al., 2013). Moreover, the slow release of sub inhibitory amount of antibiotics over time may also increase the risk of developing antibiotic resistance (Walker et al., 2016). For patients who need revision surgery an alternative antibiotic to that used in any original bone cement is therefore needed (Jiranek et al., 2006).



### **1.13 Statement of the problem, aims, objectives, and hypotheses**

After the phase out of dental amalgam, dental composites would eventually become the only direct filling material suitable for large restorations in posterior teeth. The major problem of dental composite restorations is high failure rates due to secondary caries caused by bacterial microleakage and the material property shortcomings. To address this issue, remineralising and antibacterial agents have been incorporated into the composites.

Previous studies have developed dental composites containing MCPM with TCP and chlorhexidine. The composites encouraged apatite precipitation and water sorption induced expansion that matched with the polymerisation shrinkage. However, a severe allergic reaction and the development of antibiotic resistance to chlorhexidine are of concern. Polylysine has been approved by FDA as a food preservative. This agent has low cytotoxicity and has demonstrated a wide antimicrobial spectrum. The Sr substitution in bioactive glass for bone repair application has shown to enhance apatite precipitation. Additionally, strontium may help to increase the radiopacity of the composite which is important for radiographic examination. Hence, the development of a dental composite containing calcium / strontium and polylysine is of interest.

A dental composite can then potentially be modified for use as bone composite for osteoporotic vertebral fracture repair. Currently, PMMA bone cement is the commonly used material for orthopaedic surgeons. Limitations of this cement are handling difficulty, rapid changing of viscosity after mixing, high heat generation, toxic monomer leaching, and lack of bone bonding ability. Furthermore, the significant mismatch of mechanical properties compared to vertebral cancellous bone can potentially lead to adjacent

vertebral fractures. The recent development of commercial bone composites may have partially overcome these issues. However, bone composites still exhibit some of the shortcomings of the PMMA bone cement. Additionally, the lack of antibacterial properties of the composite may fail to reduce postoperative infections, which is a life-threatening complication. Hence, the development of novel bone composite is therefore needed.

The aim of this study was therefore to develop dental and bone composites containing calcium / strontium phosphates as remineralising agents and polylysine as an antibacterial agent to overcome limitations of currently available materials. Furthermore, the development of the bone composite based on the composition of the dental composite would also facilitate the regulatory approval process for the bone composites.

It is proposed that.

- 1) The novel remineralising and antibacterial releasing dental composites can be developed by the addition of remineralising agents (MCPM and TSrP) and polylysine (PLS). The addition of remineralising agents should promote hygroscopic expansion to compensate polymerisation shrinkage in addition to surface apatite precipitation. Furthermore, the addition of PLS should enable antibacterial PLS release from the composite. The mechanical properties of the composite should be sufficient to pass a requirement from the ISO standard 4049 (Chapter 3).
- 2) The novel bone composites can be produced by decreasing powder to liquid ratio of dental composites. Additionally, the bone composite pastes should exhibit rheological properties suitable for injection and long-term storage (Chapter 4).

- 3) Chemically activated novel bone composites can be developed by the addition of chemically activated initiator. Active ingredients and initiator paste of the composites should be stable upon ageing. Additionally, the use of high molecular weight diluent monomer should improve shelf life and monomer conversion of the bone composites (Chapter 5).
- 4) The novel bone composites should exhibit high strength at early time. Stiffness of the composites should be comparable to that of cancellous bone (Chapter 6).
- 5) The novel bone composites should exhibit high monomer conversion with any polymerisation shrinkage comparable with their hygroscopic expansions. The addition of MCPM and TSrP into bone composites should enable surface apatite formation for on the composite surfaces. The addition of TSrP should allow  $\text{Sr}^{2+}$  release from the bone composites. Furthermore, the composites should exhibit long-term strength and fatigue that are comparable or greater than commercial materials (Chapters 7).
- 6) The novel bone composites with increasing level of diluent monomer and active ingredients should exhibit high monomer conversion with low polymerisation shrinkage that is comparable with their hygroscopic expansion. The composites should be easy to inject, promote PLS release and surface apatite formation in addition to long-term mechanical properties that are comparable with cancellous bone. Furthermore, the composite should be cytocompatible with human cells (Chapter 8).

## Chaper 2 Materials and Methods

### 2.1 Materials preparation

The chemical components used in this study are provided in Tables 2-1,2. Compositions of commercial materials are provided in Table 2-3. Powder and monomer components were weighed using a four-figure balance (OHAUS PA214, Pine Brook, USA). The monomer was mixed in an amber bottle, then stirred until the mixture was clear. They were then kept in a fridge (4 °C) to reduce any heat or light exposure that may activate an initiator.

**Table 2-1 Chemical components used in the liquid phase.**

Name	Abbreviation	Batch/Lot number	Suppliers
Urethane dimethacrylate	UDMA	90761	DMG, Hamburg, Germany
Tri ethylene glycol dimethacrylate	TEGDMA	88661	DMG, Hamburg, Germany
Polypropylene glycol dimethacrylate	PPGDMA	626208	Polyscience, PA, USA
4-Methacryloyloxyethyl trimellitate anhydride	4-META	595697	Polyscience, PA, USA
Hydroxyethyl methacrylate	HEMA	88161	DMG, Hamburg, Germany
Camphorquinone	CQ	90339	DMG, Hamburg, Germany
Benzoyl peroxide	BP	593397	Polyscience, PA, USA
N, N-dimethyl-p-toluidine	DMPT	MKBR6240V	Sigma Aldrich, Gillingham, UK
N-tolyglycine dimethacrylate	NTGGMA	X8630050	Esschem, UK

**Table 2-2 Chemical components used in the powder phase**

Name	Filler size (µm)	Abbreviation	Batch/Lot number	Suppliers
Boroalumino silicate glass	0.7	G <sub>0.7</sub>	688344	DMG, Hamburg, Germany
	7	G <sub>7</sub>	680326	DMG, Hamburg, Germany
Glass fibres	30 (diameter) 150 (length)	F	88661	Mo-Sci, PA, USA
Monocalcium phosphate monohydrate	53	MCPM	MCP-B26	Himed, NY, USA
Tristrontium phosphate	10	TSrP	MKBPO162V	Sigma Aldrich, Gillingham, UK
Polylysine (Molecular weight of 4700 g/mol)	20-50	PLS	1 <sup>st</sup> batch 09010203 2 <sup>nd</sup> batch 593397 3 <sup>rd</sup> batch 020420140520	Handary, Brussel, Belgium

N.B. PLS used in Chapters 3 to 7 was 2<sup>nd</sup> batch whilst that in Chapter 8 was 3<sup>rd</sup>

**Table 2-3 Chemical components of commercial products (Khan, 2015; Guo et al., 2016) used in this thesis.**

Materials	Products (mode of applications)	Compositions	Suppliers
Dental composite	Z250® (single syringe)	Monomers: Bis-GMA, UDMA, Bis-EMA, CQ  Fillers: Zirconia/silica glass particles (82 wt%, diameter of 0.01 - 3.5 µm)	3M ESPE, USA
PMMA cement	Simplex P® (powder and liquid)	Liquid: DMPT, MMA, inhibitor  Powder: BP, PMMA, MMA-styrene copolymer beads (diameter of ~25 µm), barium sulphate (diameter ~ 2 µm)	Stryker, Newbury, Berkshire, UK
Bone composite	Cortoss® (double barrel syringes)	Monomer phase: Bis-GMA, Bis-EMA, TEGDMA, BP, DMPT, inhibitors  Filler phase: glass ceramic particles (combeite, diameter of ~ 5-30 µm)	

Experimental dental composites were prepared using a powder to liquid ratio (PLR) of 4:1. The powder and monomer phases were mixed using a planetary mixer (SpeedMixer, DAC 150.1 FVZ, Hauschild Engineering, Germany) at 3500 rpm for 10 s followed by 2000 rpm for 2 min. Consistency of the mixed composite pastes was comparable to commercial hybrid dental composites. The mixed composites were stored in an amber bottle to avoid light exposure and kept in a fridge.

For bone composites, the PLR was decreased in order to control rheology and allow injection of the paste through a fine mixing tip (tip diameter of 2 mm). The powder was mixed with the liquid containing either initiator or activator. The mixing speed for bone composite was 2000 rpm for 2 min. The initiator and activator paste were then poured into a double-barrel syringe (Fig 2-1) (MIXPAC, Sulzer, Switzerland) over a vibrator to reduce air entrapment. The syringe was left in an upright position for 24 hr to allow the release of air bubbles. The initiator and activator pastes were injected and mixed through an automatic mixing tip using a mixing gun (MIXPAC Dispenser, Sulzer, Switzerland).

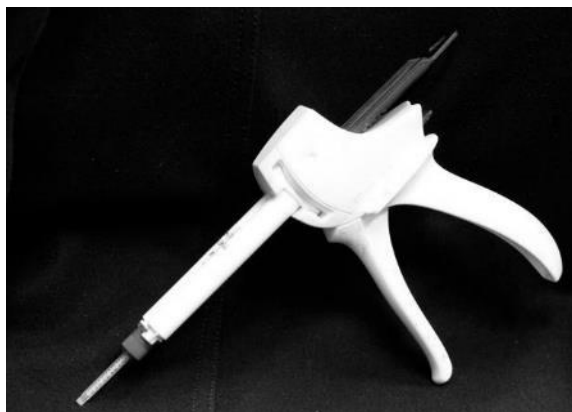


**Fig 2-1 Double-barrel syringes equipped with the automatic mixing tip and the mixing gun.**

## 2.2 Storage solutions

Deionised water and simulated body fluid (SBF) were used as storage solutions to age composite specimens. Ion concentrations in SBF were comparable to human blood plasma (Table 2-4). The SBF was prepared according to the BS ISO 23317:2012 (British Standard, 2012). All SBF chemicals (Table 2-5) were supplied by Sigma Aldrich (Gillingham, UK). Briefly, each chemical was gradually added in the order given in Table 2-4 into a plastic bottle containing 700 mL deionised water. The temperature of the solution was controlled at  $36.5 \pm 1.5$  °C. Prior to dissolving Tris (2-amino-2-(hydroxymethyl)-1,3-propanediol), total volume was made up to 900 mL and the pH was maintained at  $2 \pm 1$ . If the pH exceeded 7.45 while dissolving Tris, 1 molar HCl was added to adjust the pH. This procedure was repeated until all of Tris was dissolved. The final pH of the solution should be exactly 7.4 at 36.5 °C. The solution was then left to cool at ambient temperature, then kept in the fridge (4 °C). The SBF should be used within 30 days after preparation.

**Table 2-4 Ion concentration of SBF and human blood plasma.**

Ions	Concentration ( $10^{-3}$ mol)	
	SBF (pH 7.4)	Blood plasma (pH 7.2 - 7.4)
Na <sup>+</sup>	142.0	142.0
K <sup>+</sup>	5.0	5.0
Mg <sup>2+</sup>	1.5	1.5
Ca <sup>2+</sup>	2.5	2.5
Cl <sup>-</sup>	147.8	103.0
HCO <sub>3</sub> <sup>-</sup>	4.2	27.0
HPO <sub>4</sub> <sup>2-</sup>	1.0	1.0
SO <sub>4</sub> <sup>2-</sup>	0.5	0.5

**Table 2-5 Chemicals for preparing 100 mL simulated body fluid.**

Reagents	Amount (g)
NaCl	8.035
NaHCO <sub>3</sub>	0.355
KCl	0.255
K <sub>2</sub> PO <sub>4</sub> ·3H <sub>2</sub> O	0.231
MgCl <sub>2</sub> ·6H <sub>2</sub> O	0.311
1 molar HCl	39 mL
CaCl <sub>2</sub>	0.292
Na <sub>2</sub> SO <sub>4</sub>	0.072
Tris	6.118

## 2.3 Methods

Composite properties assessed included rheology, injectability, monomer conversion, calculated polymerisation shrinkage and heat generation, and accelerated aging to predict shelf life. Additionally, mineralisation promotion ability of the composites was tested using gravimetric and SEM studies to assess apatite precipitation in SBF. PLS release from the composites was analysed using UV spectroscopy and high performance liquid chromatography (HPLC). Sr<sup>2+</sup> release was measured using inductively coupled plasma – mass spectroscopy (ICP-MS). Assessed mechanical properties were compressive strength, biaxial flexural strength, fracture toughness, and biaxial flexural fatigue.



### 2.3.1 Rheological properties

Rheological properties of the experimental bone composite pastes were measured using a strain-controlled oscillatory rheometer (ARES, TA instruments, DE, USA) with parallel plates (25 mm) geometry. During dynamic testing mode, bottom plate was rotated applying an oscillatory (sinusoidal) shear deformation to the pastes. The fixed top plate then measured the resultant stress response from the pastes (Fig 2-2). For static testing mode, the direction of shear deformation is constant.

For viscoelastic materials, the response strain and stress are not in phase during small-amplitude oscillatory shear. The strain lags behind the stress by an angle ( $\delta$ ) which is known as the phase angle (Fig 2-2 a).

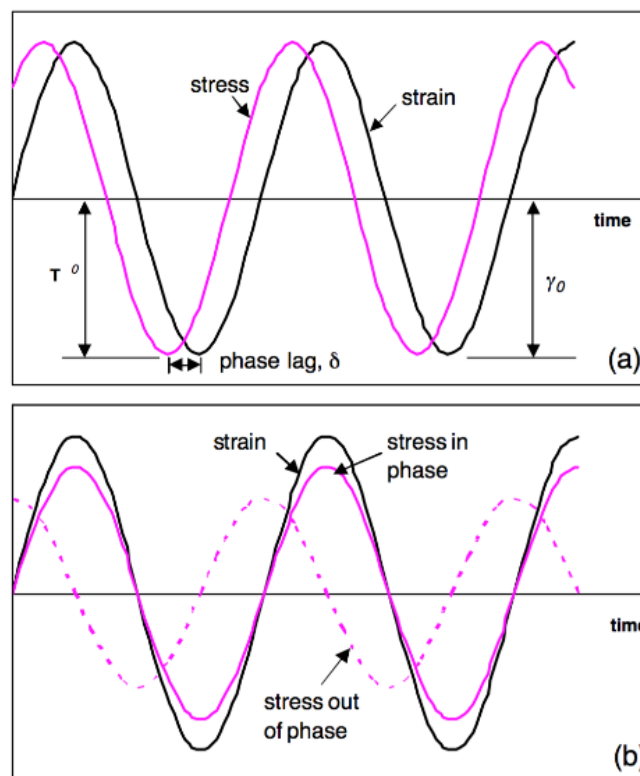


**Fig 2-2 The stress and strain relation in viscoelastic materials during the dynamic rheological test.**  
**b) The stress can be separated into two independent components: stress that is exactly in phase with strain and stress that is  $\frac{\pi}{2}$  out of phase.** Reprinted from *Cement and Concrete Research*, volume 36(2), Sun Z., Voigt T. & Shah S. P., *Rheometric and ultrasonic investigations of viscoelastic properties of fresh Portland cement pastes*, page 279, Copyright (2006), with permission from Elsevier.

Shear stress and phase angle ( $\delta$ ) are described by the following equations (Nicholas et al., 2007).

$$\tau = \tau_0 \sin \omega t \quad \text{Equation 2-1}$$

Where  $\tau$  is shear stress (Pa);  $\tau_0$  is stress amplitude;  $\omega$  is angular frequency (rad.s<sup>-1</sup>);  $t$  is time.

$$\gamma = \gamma_0 \sin(\omega t - \delta) \quad \text{Equation 2-2}$$

Where  $\gamma$  is shear strain;  $\gamma_0$  is strain amplitude. Equation 2-2 can be further analysed to gives

$$\tau = \tau_0 \sin \omega t \cos \delta + \tau_0 \cos \omega t \sin \delta \quad \text{Equation 2-3}$$

Therefore, shear stress can be divided into two components (Fig 2-2 b). The responding stress ( $\tau_0 \cos \delta$ ) that is in phase with the strain and that ( $\tau_0 \sin \delta$ ) which is  $\frac{\pi}{2}$  out of phase with the strain (Fig 2-2 b). Hence, two dynamic shear moduli can be defined which include the shear modulus that is in phase with the strain ( $G'$ , Pa) and the modulus that is  $\frac{\pi}{2}$  out of phase with the strain ( $G''$ , Pa).

$$G' = \left( \frac{\tau_0}{\gamma_0} \right) \cos \delta \quad \text{Equation 2-4}$$

$$G'' = \left( \frac{\tau_0}{\gamma_0} \right) \sin \delta \quad \text{Equation 2-5}$$

Where  $G'$  is the storage shear modulus that represents the elastic behaviour or energy storage of the material.  $G''$  is the loss shear modulus, which represents the viscous behaviour or energy dissipation of the material (Sun et al., 2006). These lead to the equation for phase angle ( $\delta$ ) as in the following equation.

$$\tan \delta = \frac{G''}{G'} \quad \text{Equation 2-6}$$

Curves of viscosity ( $\eta$ , Pa.s) can be obtained by equation 2-7 using continuous shear (static mode) instead of oscillatory shear (Liu et al., 2006).

$$\eta = \tau / \dot{\gamma}$$

Equation 2-7

Where  $\tau$  and  $\dot{\gamma}$  are shear stress (Pa) and shear rate ( $\text{s}^{-1}$ ) respectively.

### 2.3.2 Injectability

To assess maximum injection force and injectability, bone composites (3 g) were mixed and weighed using a four figure balance (Ohaus PA214, Parsippany, NJ, USA) then injected through a 5 mL plastic syringe with an outlet diameter of 1.8 mm (BD Plastipak, Fischer Scientific, UK) (BD Plastipak, Fischer Scientific, UK) (Wynn-Jones et al., 2014). The sample was subjected to a compressive load using a universal testing machine (Shimadzu AGSX, Kyoto, Japan). The load was applied at a crosshead speed of 15 mm/min. The test was terminated when the entire paste was injected or the maximum applied force (100 N) was reached (Liu et al., 2013). The average of maximum force (N) was recorded (Fig 2-3) and the injectability (%) was calculated using equation 2-8.

$$\text{Injectability (\%)} = \frac{\text{mass of injected material}}{\text{original mass in syringe}} \times 100$$

Equation 2-8

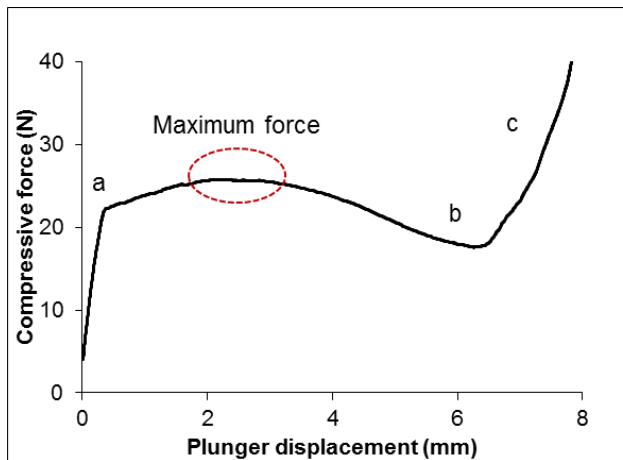


Fig 2-3 Example result from Injectability test. a) The composite paste was injected. b) Load decreased due possibly to shear-thinning behavior of the composites. c) Load increased as the plunger reaching the end of syringe.

### 2.3.3 Stability of the composite

#### 2.3.3.1 Stability of the chemical components

To assess the stability of chemical components, FTIR of mixtures of components were obtained to assess if any new chemicals were produced. These spectra were compared with predicted spectra. The predicted spectra were generated from the FTIR spectrum of each pure component using a modified Beer-Lambert law (equation 2-9) (Griffiths, 2002).

$$A_s = \sum_{i=1}^N A_i C_i \quad \text{Equation 2-9}$$

Where  $A_s$  is the absorbance of a mixture consisting of  $N$  components,  $A_i$  and  $C_i$  are absorbance and concentration of component  $i$ .

#### 2.3.3.2 Predicted shelf life

To predict the shelf life of experimental bone composites, FTIR spectra of initiator pastes were measured at temperatures of 50, 60, 70, and 80 °C. Rate of polymerisation ( $R_p$ ) is expected to be inversely proportional to  $t_{50}$  (time when monomer conversion reached 50%) which can then be expressed using an Arrhenius type equation (equation 2-10) (Shim et al., 2005).

$$R_p \propto \frac{1}{t_{50}} = A[\exp(-\frac{E_a}{RT})] \quad \text{Equation 2-10}$$

In the following,  $A$  is a frequency factor ( $\text{mol}^{-1}\text{s}^{-1}$ ),  $E_a$  is the activation energy (kJ/mol),  $R$  is the universal gas constant,  $T$  is temperature (Kelvin). Straight-line plots were generated by using the logarithmic version of equation 2-11 which gives.

$$\ln\left(\frac{1}{t_{50}}\right) = \ln(A) - \frac{E_a}{RT} \quad \text{Equation 2-11}$$

From this relationship,  $t_{50}$  which was assumed to be the time at which spontaneous polymerisation of initiator or activator paste of bone composites occurs at low temperatures (4, 2, and 37 °C) can be obtained by extrapolation.

#### **2.3.3.3 Observed shelf life**

To assess the actual shelf life of experimental bone composites, initiator and activator pastes of composites were prepared and loaded into double-barreled syringes. They were then stored at temperatures of 4, 25, and 37 °C. At 1 day, 1, 3, 9, and 12 months, the syringes were assessed for any solidification of composite pastes. If the pastes were not solidified, a portion of the composites was mixed and polymerisation kinetics at 25 °C determined by FTIR. The remaining composite was returned to its required storage test condition.

### **2.3.4 Monomer conversion and calculated polymerisation shrinkage/heat generation**

#### **2.3.4.1 Monomer conversion**

An FTIR (Perkin-Elmer Series 2000, Beaconsfield, UK) with ATR (3000 Series RS232, Specac Ltd., UK) was used to assess monomer conversion of the composites. Unpolymerised composite pastes were placed in a metal circlip (1 mm depth and 10 mm diameter) on the ATR diamond and covered with an acetate sheet. After spectra were recorded for 10 s, dental composite was light cured for 40 s from the top surface with a LED light curing unit (1,100-1,330 mW/cm<sup>2</sup>, Demi Plus, Kerr, USA). Bone composite were cured chemically after mixing initiator with activator paste. FTIR spectra between 700-4000 cm<sup>-1</sup> of the bottom surfaces of both dental and bone composite were recorded for every 4 s at a resolution of 4 cm<sup>-1</sup> (see for example Fig 2-4). The temperature was controlled at 25 °C. The measurement time for dental composites and bone composites were 20 min and 40 min respectively.

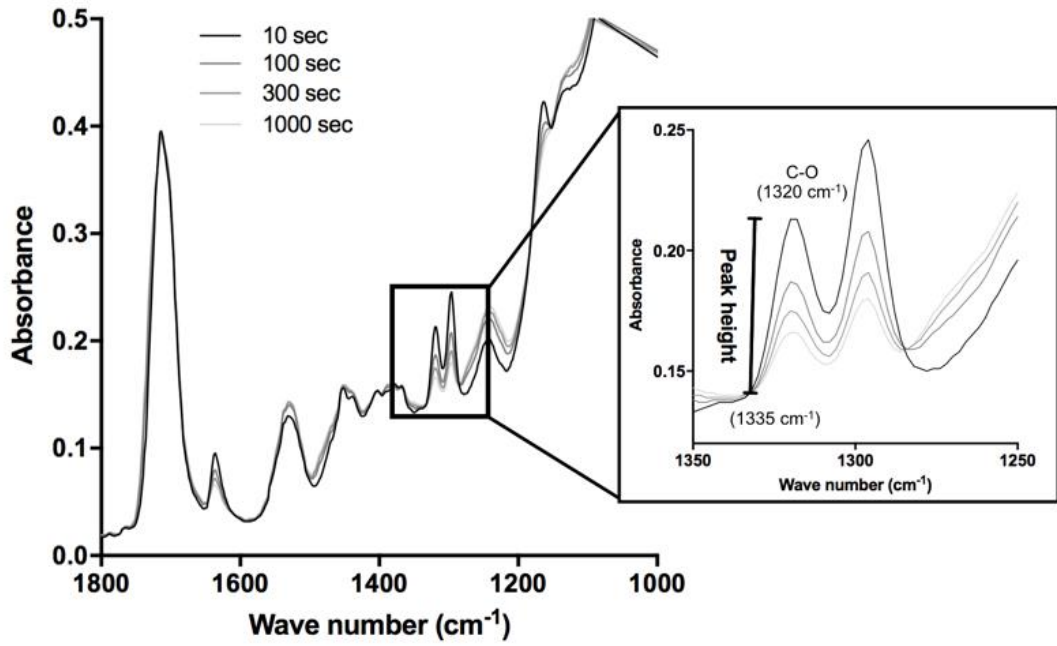


Fig 2-4 FTIR spectra upon polymerisation obtained from the bottom of composites.

In this study, monomer conversion ( $D_c$ ) (Fig 2-5 A) was obtained using equation 2-12 (Aljabo et al., 2015).

$$D_c (\%) = \frac{100(\Delta B_0 - \Delta B_t)}{\Delta B_0} \quad \text{Equation 2-12}$$

Where  $\Delta B_0$  and  $\Delta B_t$  were the absorbance of the C-O peak ( $1320 \text{ cm}^{-1}$ ) above background level at  $1335 \text{ cm}^{-1}$  initially and after time  $t$ . Final peak height and degree of monomer conversion were calculated by linear extrapolation of the data versus inverse time to zero. Additionally, rate of polymerisation ( $R_p$ ,  $\% \cdot \text{s}^{-1}$ ) was calculated using equation 2-13.

$$R_p = \frac{dD_c}{dt} \quad \text{Equation 2-13}$$

Where  $\Delta D_c$  is the change of monomer conversion over time  $t$  (13 data points). The maximum rate of polymerisation ( $R_p^{\max}$ ) was recorded (Fig 2-5 B).

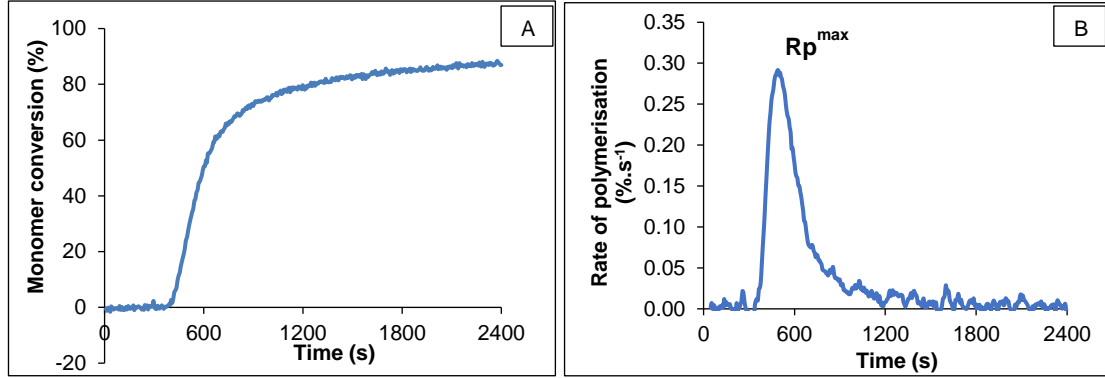


Fig 2-5 A) Example monomer conversion and B) rate of polymerisation versus time of an experimental bone composite.

#### 2.3.4.2 Calculated polymerisation shrinkage and heat generation

One mole of polymerising C=C groups typically gives volumetric shrinkage of 23 cm<sup>3</sup>/mol and generates 57 kJ of heat (Dewaele et al., 2006). Total percentage volume shrinkage ( $\varphi$ ) (%) and heat generation ( $\epsilon$ ) (kJ/cc) due to the polymerisation process can be calculated using the following equations (Main, 2013).

$$\varphi = 23(M_f)D_c\rho\sum_i\frac{n_ix_i}{W_i}100 \quad \text{Equation 2-14}$$

$$\epsilon = 57(M_f)\left(\frac{D_c}{100}\right)\rho\sum_i\frac{n_ix_i}{W_i} \quad \text{Equation 2-15}$$

where  $M_f$ , monomer fraction;  $D_c$ , monomer conversion (%);  $\rho$ , composite density (g/cm<sup>3</sup>);  $n_i$ ; the number of C=C bonds per molecule;  $W_i$ , molecular weight (g/mol) of each monomer;  $x_i$ , mass fraction of monomer.

### 2.3.5 Mass and volume change

To assess mass and volume changes due to water sorption of composites, disc specimens were prepared using metal circlips (1 mm in thickness and 10 mm in diameter) as a mould (Fig 2-6). The sample was covered with an acetate sheet on top and bottom surfaces. The composites were cured either by light (dental composites) or chemical activation (bone composites). The disc was left for 24 hr to allow completion of polymerisation. Then, it was carefully removed and any excess trimmed.



**Fig 2-6 Disc sample of dental and bone composite**

Disc specimens were subsequently weighed and immersed in a tube containing 10 mL of deionised water or SBF. The tubes were incubated at 37 °C for up to 9 weeks. At various time points, the samples were removed and carefully blot dried. Their mass and volume were subsequently measured using a four-figure balance with a density kit (Mettler Toledo, Greenfield, Royston, UK) (Leung et al., 2005). Samples were subsequently placed back into the original storage solution. The percentage mass and volume change,  $\Delta M$  and  $\Delta V$ , were determined from equation 2-16 and 2-17 respectively (Mehdawi et al., 2013).

$$\Delta M (\%) = \frac{100[M_t - M_0]}{M_0} \quad \text{Equation 2-16}$$

$$\Delta V (\%) = \frac{100[V_t - V_0]}{V_0} \quad \text{Equation 2-17}$$

where  $M_0$  and  $V_0$  is initial mass and volume, whilst  $M_t$  and  $V_t$  are mass and volume at time  $t$  after immersion.



### 2.3.6 Polylysine release

Polylysine (PLS) release of experimental dental and bone composites were assessed using UV spectrometry and high-performance liquid chromatography (HPLC) respectively.

#### 2.3.6.1 Ultraviolet (UV) spectrometry

Disc specimen was stored in a tube containing 10 mL of deionised water. They were stored in an incubator at 37 °C for up to 7 weeks. At each time point (1, 6 and 24 hr, 1, 2, 3, 4, 5, and 6 weeks), the storage solution was removed for analysis and replaced with a fresh solution. A Trypan Blue (TB, Sigma Aldrich, Gillingham, UK) assay was modified to enable analysis of the PLS concentration (Grotzky et al., 2010). Briefly, 80 ppm of TB in 0.02 MES (4-Morpholineethanesulfonic acid, Sigma Aldrich, Gillingham, UK) / 0.03 NaCl (Sigma Aldrich, Gillingham, UK) was mixed with equal volume of sample storage solution. Then, the resultant mix was stored at 37 °C for 1 hr to enable a precipitation reaction between TB and the PLS. They were then allowed to cool to room temperature for 20 min.

The mixture was centrifuged at 13000 rpm for 20 min using a centrifuge with a maximum capacity of 4x750 ml (Sorvall Legend RT, ThermoFisher Scientific, MA, USA). The remaining supernatant was carefully pipetted and analysed using an ultraviolet / visible (UV) spectrometer (Unicam UV 500, Thermospectronic, Cambridge, UK). Absorbance between 300 and 800 nm due to unreacted TB was recorded (Fig 2-7 A). This enabled generation of a calibration curve of absorbance at 580 nm versus PLS concentration (2<sup>nd</sup> batch) (Fig 2-7 B). The cumulative amount of PLS release (%) at time  $t$  was then calculated using equation 2-18.

$$\% \text{ PLS release} = \frac{100[\sum_0^t P_t]}{w_{PLS}}$$

**Equation 2-18**

Where  $w_{PLS}$  is the amount of PLS (g) incorporated in the specimen,  $P_t$  is the amount of PLS released into each storage solution (g) collected at time  $t$ .

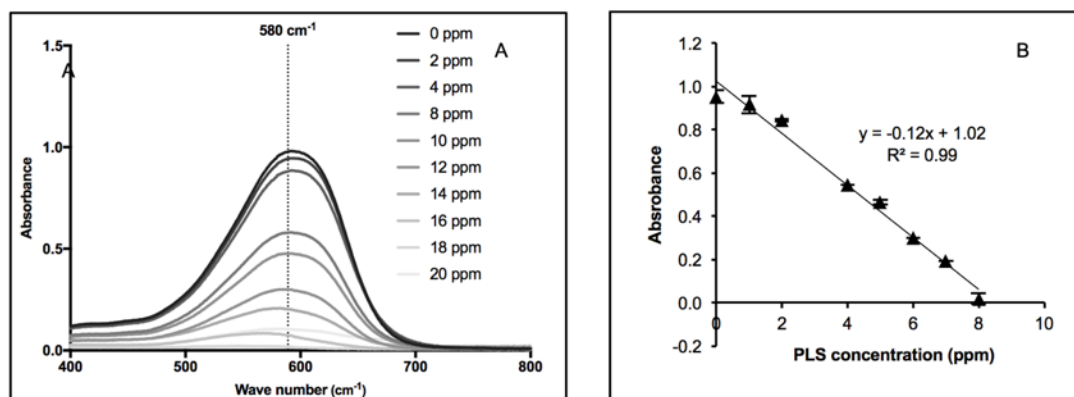


Fig 2-7 A) UV spectra of the standard PLS solutions and B) PLS concentration calibration curve of absorbance versus PLS concentration.

### 2.3.6.2 High performance liquid chromatography (HPLC)

Disc specimens were immersed in 1 mL of deionised water and incubated at 37 °C for 1, 6, 24, 48, 120 hr, then 1, 2, 3, 4, and 5 weeks. At each time point, the storage solution was removed and replaced with a fresh solution. Chromatographic separation of the storage solution was performed using Shimadzu HPLC systems (Shimadzu corporation, Kyoto, Japan) in hydrophilic interaction liquid chromatography (HILIC) mode.

HILIC mode is a powerful HPLC technique to analyse polar compounds, charged substances, carbohydrate, and peptides. This mode employed traditional polar stationary phase such as silica, whilst acetonitrile (ACN) is a commonly mobile phase (Venkatasami and Sowa, 2010). Benefits of using ACN include miscibility with water, low absorbance at short wavelength (< 280 nm), low pressure apply to column, and high elution strength. The separation mechanism of an analyte in HILIC mode is not yet concluded but the separation could be governed by a partition between ACN-rich mobile

phase and water-enriched layer adsorbed onto the hydrophilic stationary phase (Buszewski and Noga, 2012).

Stationary phase used in the current study was a Luna® NH<sub>2</sub> Column (250 x 4.6 mm, particle size of 5 µm, Phenomenax, Torrance, CA, USA). The column temperature was controlled at 30 °C. Mobile phase was a mixture of solvent A (acetonitrile with 0.1 vol% phosphoric acid) and solvent B (deionised water with 0.1 vol% phosphoric acid). Phosphoric acid was added to enhance retention of polylysine, ( $pK_b = 5$ ), and improve separation of the analyte. The separation was carried out with flow rate of 1 mL/min for the mobile phase. The solvent gradient (vol%) of mobile phase is presented in Table 2-6.

**Table 2-6 Concentration of mobile phases. Solvent A and B were acetonitrile with 0.1 vol% phosphoric acid and deionised water with 0.1 vol% phosphoric acid respectively.**

Time (min)	Concentration of mobile phase (vol%)	
	Solvent A	Solvent B
0 - 5	15	85
5 - 30	95	5
30 - 34	15	85

Injection volume of the sample was 200 µL. Absorbance at 210 nm was recorded. Retention time for PLS was found to be at 19 - 27 min (Fig 2-8). The retention time of PLS obtained from the 2<sup>nd</sup> batch (used in Chapter 3 to 7) and 3<sup>rd</sup> batch (used in Chapter 8) was broader than that of the 1<sup>st</sup> batch. This may indicate a variability of molecular weight of PLS supplied from the manufacturer. The plots of concentration of PLS versus the area under the curve between 19-27 min was used to generate a PLS calibration curve (Fig 2-9).

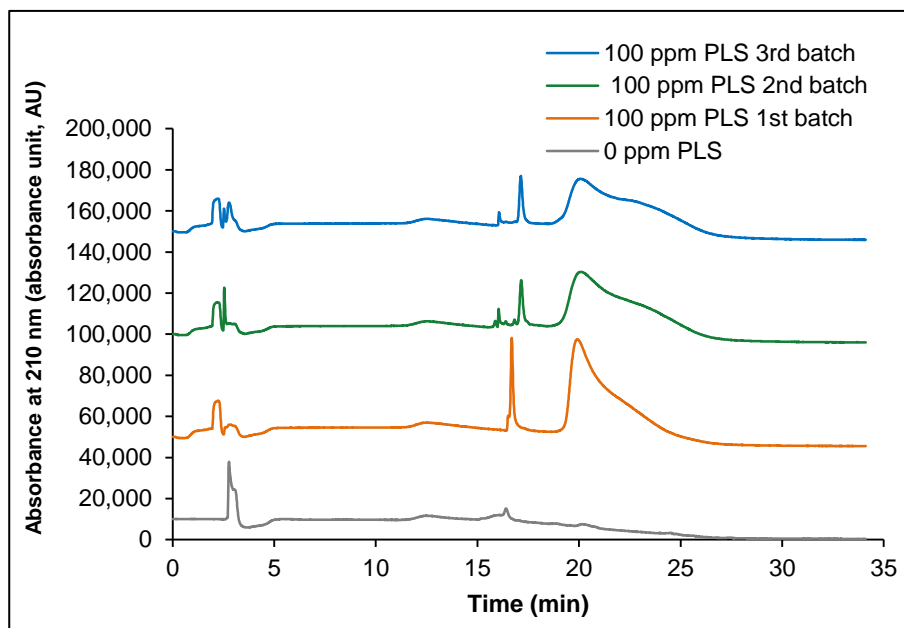


**Fig 2-8 Chromatograms of PLS from different batches. Retention time of PLS from 2<sup>nd</sup> and 3<sup>rd</sup> batch was broader than that of 1<sup>st</sup> batch.**

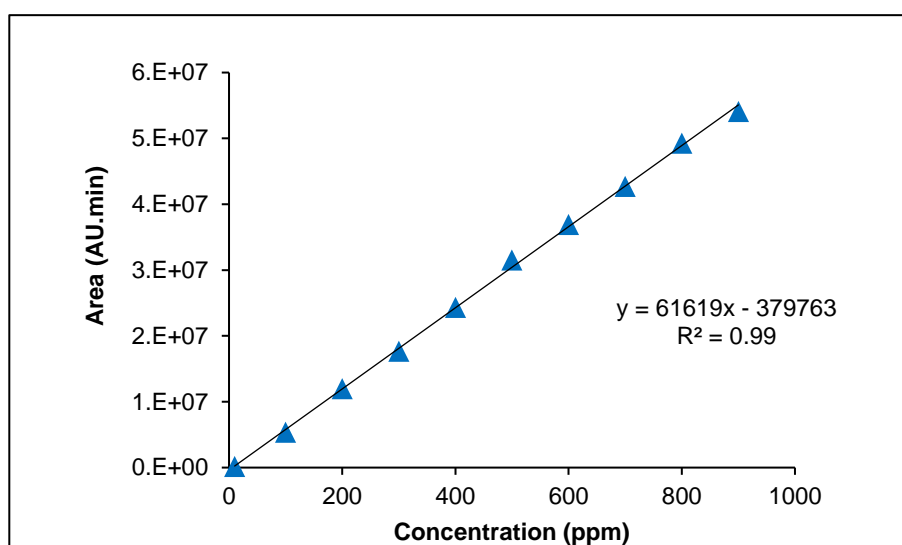


**Fig 2-9 Plot of area under the curve of PLS retention time (19 – 27 min) versus concentration of PLS (3<sup>rd</sup> batch).**

The cumulative amount of PLS release (%) at time  $t$  was then calculated using equation 2-18. The release of PLS was expected to follow a diffusion-controlled process and be proportional to the square root of time. In plotting PLS release versus square root of time (Fig 2-10), straight lines with a negative intercept on the y axis were observed due to a delay before any release from the composite.

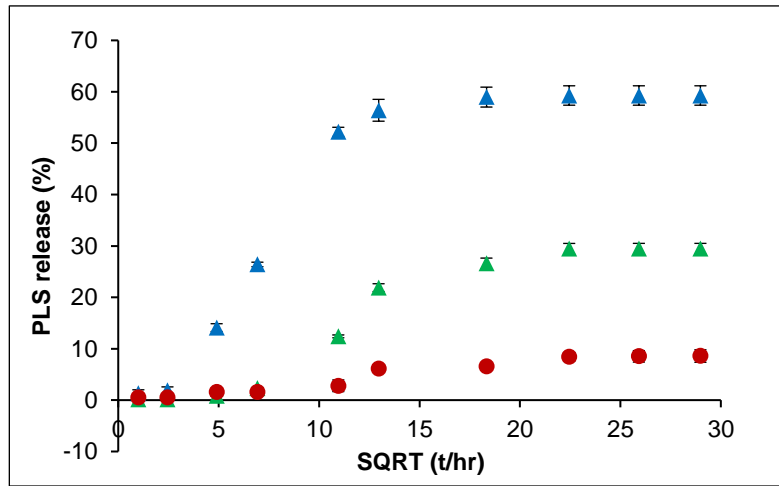


Fig 2-10 Example of PLS release profiles from experimental bone composites.

Time at which the PLS was first released (delay time,  $t_d$ ) was obtained from intercepts on the x axis of the linear regression lines. A modified Fick's equation (equation 2-19) was then employed to calculate a diffusion coefficient ( $D$ ,  $\text{cm}^2\text{s}^{-1}$ ).

$$\Delta PLS_t = (\Delta PLS_{t \rightarrow \infty}) 2 \sqrt{\frac{D}{\pi d^2}} (t^{0.5} - t_d^{0.5}) \quad \text{Equation 2-19}$$

Where  $\Delta PLS_t$  and  $\Delta PLS_{t \rightarrow \infty}$  are cumulative release (%) at time  $t$  and maximum release at time infinity,  $d$  is sample thickness (m), and  $t_d$  is delay time.

### 2.3.7 Strontium release

To analyse  $\text{Sr}^{2+}$  release from experimental bone composites, disc specimens were prepared and immersed in a tube containing 10 mL of deionised water. The specimens were then incubated at 37 °C for 4 weeks. The storage solution was collected for analysis and replaced with a fresh solution at 24 hr, 1, 2, 3, and 4 weeks. The collected solution was mixed with 2% nitric acid.  $\text{Sr}^{2+}$  calibration standards were prepared using the ICP-multi element standard solution XVI (Certipur Reference Materials, Merck KGaA, Germany) (Fig 2-11). The standards contained  $\text{Sr}^{2+}$  concentrations of 1 ppm, 250 ppb, 100 ppb, 25 ppb, 10 ppb, 2.5 ppb, and 1 ppb. Interference ions for  $\text{Sr}^{2+}$  are alkali ions such as sodium, potassium, and rubidium (Ying, 2015). The accumulative amount of  $\text{Sr}^{2+}$  release from the sample was calculated using the equation 2-20.

$$\% \text{ Sr release} = \frac{100[\sum_0^t S_t]}{w_{\text{Sr}}} \quad \text{Equation 2-20}$$

where  $w_{\text{Sr}}$  is the initial amount of  $\text{Sr}^{2+}$  in the sample (g),  $S_t$  is the amount of  $\text{Sr}^{2+}$  released into storage solution (g) collected at time  $t$  (hr).

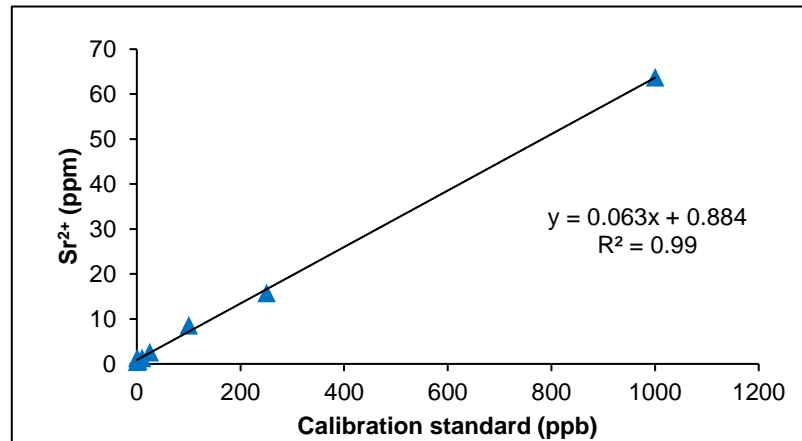


Fig 2-11 Calibration curve for  $\text{Sr}^{2+}$  release

## 2.3.8 Surface apatite formation

### 2.3.8.1 Raman microscopy

Raman microscopy (Horiba Jobin Yvon, Paris, France) was employed to assess the apatite formation on the composite surface. Disc specimens were immersed in tube containing 10 mL of SBF and stored in an incubator at 37 °C for 24 hr, 1 week or 4 weeks. At each time point, specimens were removed, blot dried and secured on glass microscope slides. The specimens were excited by He-Ne laser of 633 nm through a microscope of 50x objective. Surface point spectra were obtained in the region of 800-1700  $\text{cm}^{-1}$  using a confocal hole of 300  $\mu\text{m}$ , giving an approximate spatial resolution of 5  $\mu\text{m}$  in x, y and z directions. For single point spectra, the average of 20 spectra each of 10 s acquisition time was generated.

To obtain Raman maps, point spectra were obtained every 4  $\mu\text{m}$  over an area of 40x50  $\mu\text{m}^2$ . After baseline subtraction, spectra were normalised over the full spectral range and chemical maps generated using LabSpec 5 software. Using the full spectra of pure components, this program enables chemical maps to be generated even when, as with different phosphates, main peaks are partially overlapping. In the maps, different colours indicate which chemical component is the dominant phase at a given point on the material surface (Fig 2-12). The phosphate P-O stretch ( $\nu_1\text{PO}_4$ ) gives intense peaks which are shown in Fig 2-13.

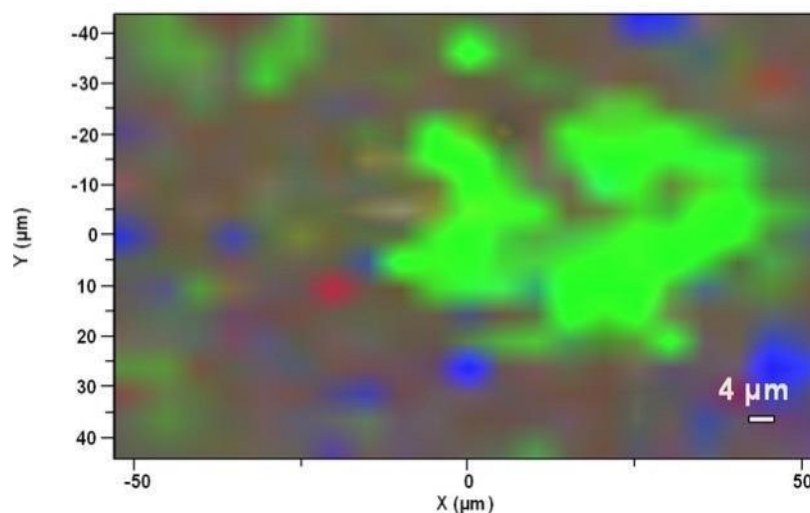


**Fig 2-12 Example Raman mapping.** Blue and green areas represent the polymer plus glass regions versus an apatite coating respectively. Yellow and red areas represent regions of brushite and TSrP.

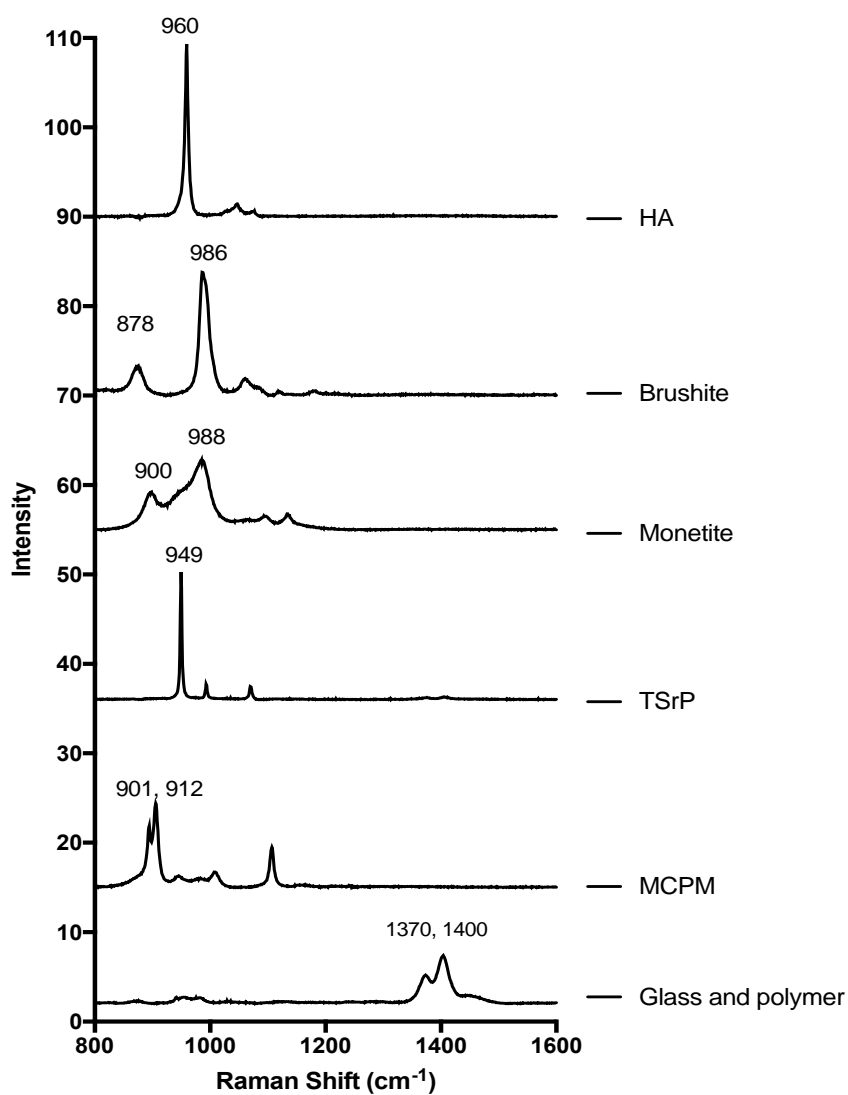


**Fig 2-13 Raman spectra of each pure chemical** (Young et al., 2008; Mehdawi et al., 2009).



### 2.3.8.2 Scanning electron microscope (SEM) and energy-dispersive X-ray micro-analysis (EDX)

Disc samples were sputtered with gold-palladium using a coating machine (Polaron E5000, East Sussex, UK) for 90 s at 20 mA. The sample was then examined under SEM (Phillip XL-30, Eindhoven, The Netherlands) operating with primary beam energy of 5 kV and a current of approximately 200 pA. Elemental composition of the specimen's surface was undertaken using energy-dispersive X-ray micro-analysis (EDX) (Inca X-Sight 6650 detector, Oxford Instrument, UK) with a beam energy of 20 kV. The ratio of Ca/Si and Ca/P were recorded from three representative areas (20 x 20 µm) on the surface of the samples (Aljabo et al., 2016).

### 2.3.9 Mechanical properties

Both bone and dental composite biaxial flexural strength and modulus of elasticity were determined. Compressive strength and fatigue biaxial flexural strength testing were additionally undertaken with the experimental bone composites.

#### 2.3.9.1 Compressive strength

Bone composites were injected into a cylindrical stainless steel mould (6 mm in length and 4 mm in diameter). They were covered with acetate sheets and left for 24 hr. Then, specimens were removed, trimmed, and immersed in a tube containing 10 mL of SBF and stored in an incubator at 37 °C for 24 hr prior to compression strength testing. The test was performed using a universal testing machine (Intron 4502, Wycombe, UK) with a 5 kN load cell at a cross head speed of 1 mm/min. Compressive strength ( $C_s$ , Pa) was calculated using the following equation (Tan et al., 2016).

$$C_s = \frac{F}{\pi l^2}$$

Equation 2-21

Where  $F$  is load at failure (N),  $l$  is radius of specimen (m).

### 2.3.9.2 Biaxial flexural strength (BFS)

Prior to testing, disc specimens were immersed in a tube containing 10 mL of SBF then stored in an incubator at 37 °C for up to 4 weeks. A “Ball on ring” jig (Higgs et al., 2001) (Fig 2-14A) was used with a computer-controlled universal testing machine (Shimadzu AGSX, Kyoto, Japan) equipped with 2 kN load cell. The specimens’ thickness was recorded using a digital vernier calliper (Moore & Wright, West Yorkshire, UK). The sample was placed on a ring support (8 mm in diameter) (Fig 2-14). The load was applied using a 4 mm diameter spherical ball indenter at 1 mm.min<sup>-1</sup> crosshead speed.

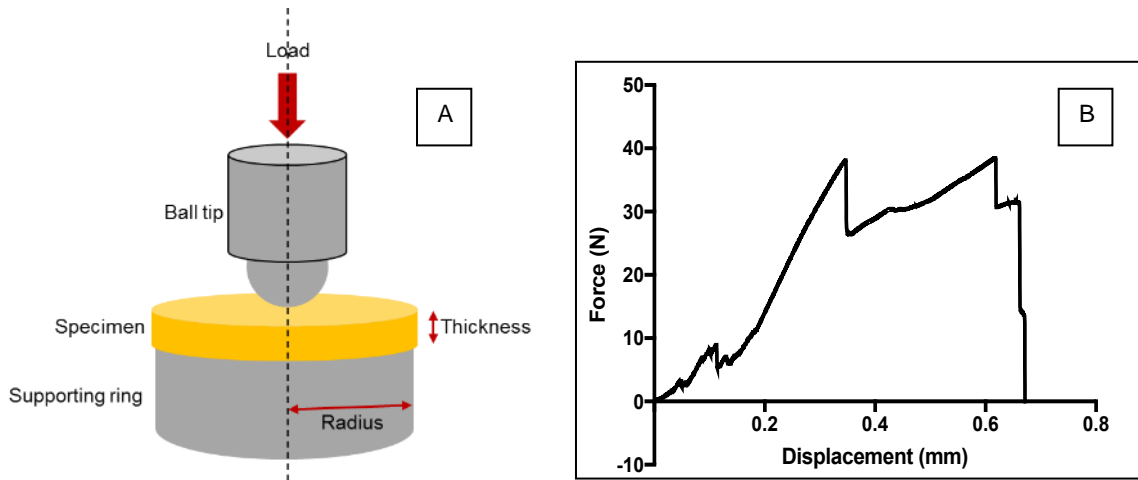


**Fig 2-14 A) schematic of ball on ring test, B) example of force versus displacement diagram from BFS testing.**

The failure stress was recorded in N and the biaxial flexural strength ( $S$ ; Pa) was calculated using the following equation:

$$S = \frac{F}{d^2} \left\{ (1 + \nu) \left[ 0.485 \ln \left( \frac{r}{d} \right) + 0.52 \right] + 0.48 \right\} \quad \text{Equation 2-22}$$

Where  $F$  is the load at failure (N),  $d$  is the specimens thickness (m),  $r$  is the radius of circular support (m), and  $\nu$  is Poison's ratio (0.3).

Then, the force versus displacement graph (Fig 2-14 B) was also used to calculate the biaxial modulus of elasticity using equation 2-23 (Higgs et al., 2001).

$$E = \left( \frac{\Delta H}{\Delta W_c} \right) \times \left( \frac{\beta_c d^2}{q^3} \right) \quad \text{Equation 2-23}$$

Where  $E$  is modulus of elasticity of the specimen (Pa),  $\frac{\Delta H}{\Delta W_c}$  is rate of change of load with regards to central deflection or gradient of force versus displacement curve (N/m),  $\beta_c$  is centre deflection function and centre deflection junction (0.5024)(Higgs et al., 2001),  $q$  is ratio of support radius to the radius of disc, and  $\nu$  is Poison's ratio (0.3).

### 2.3.9.3 Fracture toughness ( $K_{IC}$ )

Fracture toughness testing protocol for bone composites was performed according to the BS ISO 13586:2000, Plastics-Determination of fracture toughness ( $G_{IC}$  and  $K_{IC}$ )- Linear elastic fracture mechanics (LEFM) approach (British Standard, 2016). Beam specimens were prepared by injecting the bone composites into a putty silicone mould, then covered with an acetate sheet and left for 24 hr. They were removed and trimmed using a silicon carbide paper (grit size 250-500). Crack was created using a diamond disc (Ilie et al., 2012).

Dimension of the specimen (Fig 2-15) was verified using a digital Vernier calliper under a stereomicroscope. Specimens were immersed in a tube containing 10 mL of SBF and stored in an incubator at 37 °C for 24 hr. Testing was conducted using a three-point bending testing jig with the universal testing machine (Shimadzu AGSX, Japan) equipped with 2 kN load cell using a crosshead speed of 10 mm/min. The fracture toughness ( $K_{IC}$ , Pa.m<sup>1/2</sup>) was calculated using equation 2-24.

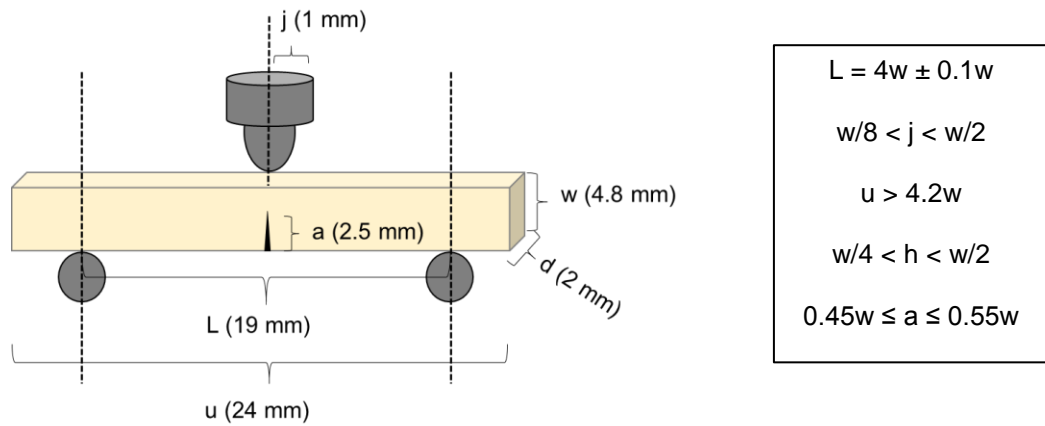


**Fig 2-15 Schematic of fracture toughness testing and required dimensions of specimen according to BS ISO 13586:2000+A1:2003, Plastics-Determination of fracture toughness ( $G_{IC}$  and  $K_{IC}$ )-Linear elastic fracture mechanics (LEFM) approach.**

$$K_{IC} = f(\alpha) \frac{F}{d\sqrt{w}}$$

**Equation 2-24**

Where  $d$  is the specimen thickness (m),  $w$  is the specimen width (m),  $F$  is load at failure (N),  $b$  is crack length (m),  $\alpha$  is  $\frac{b}{d}$ , and  $f(\alpha)$  is the geometry calibration factor calculated by using the following equation (British Standard, 2016).

$$f = 6\alpha^{1/2} \frac{1.99 - \alpha(1-\alpha)(2.15 - 3.93\alpha + 2.7\alpha^2)}{(1+2\alpha)(1-\alpha)^{3/2}}$$

**Equation 2-25**

#### 2.3.9.4 Biaxial flexural fatigue testing

The fatigue testing protocol was modified from BS ISO 16402:2008, Implants for surgery- Acrylic resin cement-Flexural fatigue testing of acrylic resin cements used in orthopaedics (British Standard, 2008). Specimens were immersed in a tube containing 10 mL of SBF, then stored in an incubator at 37 °C for 4 weeks prior the test. The testing was performed in a glass container with circulated SBF at the controlled temperature of  $37 \pm 1$  °C (Fig 2-16).

Five specimens were subjected to biaxial flexural strength testing using Zwick HC10 servo hydraulic testing frame (Zwick Testing Machine Ltd., Herefordshire, UK) equipped with a 1 kN load cell using a crosshead speed of 1 mm/min (Pittayachawan et al., 2007). BFS of the composites were calculated using equation 2-22. Then, a sinusoidal load of 5 Hz (Harmata et al., 2015) was applied to specimens using 80%, 70%, 60%, and 50% of mean BFS (five specimens per each level of stress) (n=20).

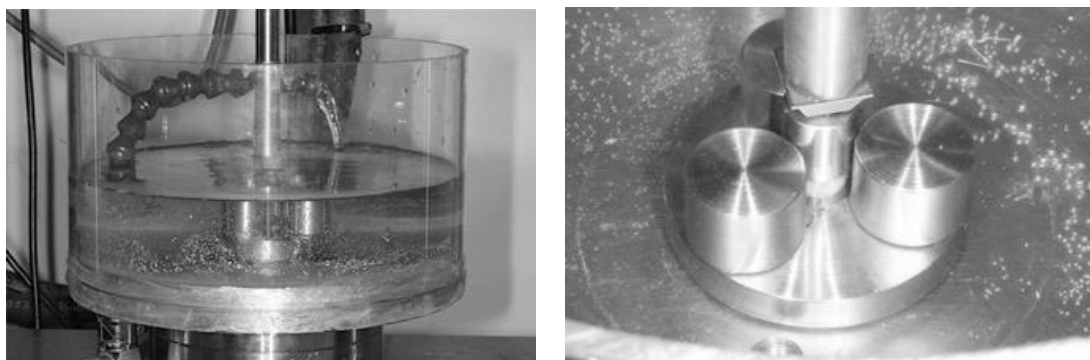


**Fig 2-16 Testing performed under circulated SBF at the controlled temperature of  $37 \pm 1$  °C**

The tests were continued until fracture occurred or the requisite number of load cycles (100,000 cycles) had been applied. BFS was plotted against cycles of failure to generate classical stress-number of cycle curve (S/N curve) (Fig 2-17). Failure cycle from 1<sup>st</sup> to 5<sup>th</sup> samples were plotted against BFS which therefore gave five S/N curves. Mean of gradient from the plots of 80 to 50 % of mean BFS versus failure cycles was obtained (n=5) and used to compare fatigue performance (Koster et al., 2013). Furthermore,

failure cycle at stress level of 10 MPa was obtained by extrapolating the regression line. This value represents fatigue life (log cycle) of materials upon applying low stress that may generate during normal movements such as flexion, lateral bending, or walking (Rohlmann et al., 2010).

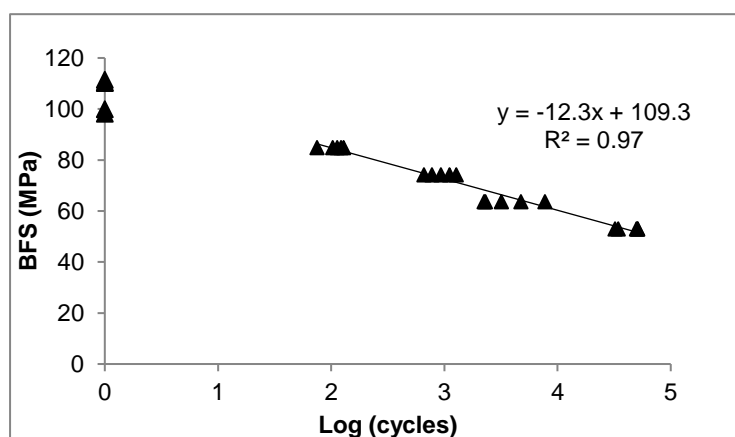


**Fig 2-17** Example of plot between stresses versus number of log (cycles) from biaxial flexural fatigue testing to generate S/N curve.

### 2.3.10 Cytocompatibility test using MTS assay

Cytocompatibility of bone composites using bone marrow mesenchymal stem cells (MSCs; obtained from a donor from Institute for Regenerative Medicine, Texas A&M Health Science Center College of Medicine) were assed using MTS assay. This test was performed by Dr Caitriona O'Rourke. Bone marrow mesenchymal stem cells (MSCs) were cultured under standard conditions (37 °C, 95% air, 5% CO<sub>2</sub>, 95% relative humidity) in minimum essential medium (MEM, Gibco, Life Technologies, Paisley) supplemented with penicillin and streptomycin (100 U/mL and 100 mg/mL, respectively; Sigma Aldrich, Gillingham, UK) and 10 vol% foetal calf serum (Sigma Aldrich, Gillingham, UK) in standard cell culture flasks. Passage numbers 3-6 were used for studies.

Disc samples were sterilised using UV light. They were incubated in 600 µL of cell culture media for 24 hr under standard conditions (controlled temperature of 37 °C, 95% air, 5%

CO<sub>2</sub>, and 95% relative humidity). MSCS were seeded at a density of 30,000 cells/cm<sup>2</sup> in a 96 well plate (n=5). After 24 hr, cell culture medium was replaced with conditioned medium in which the disc specimens were immersed and incubated for 24 hours.

Cell metabolic activity was assessed using 3-(4,5-dimethylthiazol-2-yl)-5-(3-carboxymethoxyphenyl)-2-(4-sulfophenyl)-2H-tetrazolium MTS assay (CellTiter 96® AQueous One Solution Cell Proliferation Assay, Promega, Southampton, UK). CellTiter (20 µL) was added to each well containing cells immersed in 100 µL of conditioned culture medium. Following 90 min incubation under standard conditions, absorbance was measured at 490 nm using Infinite M200 plate reader (Tecan, Männedorf, Switzerland). In all cases, controls that incorporated cells cultured on standard tissue culture plastic was included.

### 2.3.11 Statistical analysis

All values and errors reported throughout this thesis were mean with 95% confidence intervals (95% CI) respectively. SPSS Statistics version 24 for Window (IBM, USA) was used for statistical analysis. Homogeneity of variance was assessed using Levene's test. When variances were equal, data were analysed using one-way analysis of variance (ANOVA) followed by post-hoc Tukey's test for multiple comparisons. Alternatively, the Kruskal-Wallis test followed by multiple comparison using Dunnett's T3 tests was used if their variances were not equal (Hatamleh and Watts, 2010; Ender et al., 2016; Hyun and Ferracane, 2016). The significance value was set at  $p = 0.05$ . Line fitting for regression analysis was undertaken using the Linest function in Microsoft Office Excel 2016 for Window.

Factorial analysis was used to assess the effect of variables on properties of composites. A full factorial equation for two (equation 2-26) and three variables (equation 2-27) each at high and low levels can be fitted using the following equations respectively (Mehdawi et al., 2013).

$$\ln P = \langle \ln P \rangle \pm a_1 \pm a_2 \pm a_{1,2} \quad \text{Equation 2-26}$$

$$\ln P = \langle \ln P \rangle \pm a_1 \pm a_2 \pm a_3 \pm a_{1,2} \pm a_{1,3} \pm a_{2,3} \pm a_{1,2,3} \quad \text{Equation 2-27}$$

Where  $a_1$ ,  $a_2$ , and  $a_3$  were the effect of each variable on the property  $P$  of the composites,  $\langle \ln P \rangle$  is the average value of  $\ln P$ . The  $a_{1,2}$ ,  $a_{1,3}$ ,  $a_{2,3}$ , and  $a_{1,2,3}$  are interaction effects. The percentage effect of each variable,  $Q$ , can be calculated using the following equation (Panpisut et al., 2016).

$$Q(\%) = 100 \left( 1 - \frac{G_H}{G_0} \right) = 100(1 - \exp(2a_i)) \quad \text{Equation 2-28}$$

$G_H$  and  $G_0$  are the geometric average property for the samples with the variable at its high versus low value respectively. The effect of variable change was considered significant if the magnitude of  $a_i$  was greater than both its calculate 95% CI and interaction terms.



## Chaper 3 UDMA / TEGDMA Dental Composites containing Calcium / Strontium Phosphate and Polylysine

N.B. : This chapter is the subject of this publication “Panpisut P, Liaqat S, Zacharaki E, Xia W, Petridis H, Young AM (2016) Dental Composites with Calcium / Strontium Phosphates and Polylysine. PLoS ONE 11(10): e0164653. doi:10.1371/journal.pone.0164653 ”.

### 3.1 Abstract

**Purpose:** The study aim was to produce remineralising (MCPM, TSrP) and antibacterial (PLS) agent - containing dental composites that promote water sorption induced volume expansion, surface apatite formation, and PLS release. High monomer conversion and strength are also required.

**Materials and Methods:** Light curable monomers containing UDMA and TEGDMA were mixed with powder using PLR of 4:1. Powder phase consisted of a dental glass (7  $\mu\text{m}$ ) with /or without remineralising agents (10 wt% MCPM and 15 wt% TSrP) and /or PLS (2.5 wt%). Monomer conversion was assessed using FTIR. Gravimetric study was performed in water and SBF. Surface apatite formation of the composites after immersion in SBF for up to 4 weeks were analysed using Raman spectroscopy and SEM. PLS release in deionised water was measured using UV-spectroscopy. Additionally, biaxial flexural strength was assessed after immersion in SBF for 24 hr. A commercial composite (Z250) was used for comparison.

**Results:** The additives decreased monomer conversion from 76 to 64 % but was always higher than with Z250 (54%). The addition of these phosphates increased hygroscopic expansion of the composites from 2 to 4 vol%. The higher of these was comparable to

the calculated polymerisation shrinkage of (~ 3.4 vol%). These phosphates promoted surface apatite formation after immersion in SBF. Thickness of these apatite layers after 4 weeks increased from ~ 10 to 20  $\mu\text{m}$  upon the addition of PLS. Burst release of PLS (3.7 %) was observed irrespective of phosphate addition. Although these additives reduced strength of the experimental composites (from 154 to 104 MPa) they were all still stronger than that required from ISO 4049 (>80 MPa after 24 hours immersion).

**Conclusion:** MCPM and TSrP promoted volume expansion and surface apatite precipitation. These are expected to help compensate inevitable polymerisation shrinkage and remineralise demineralised dentine. Composites also showed release of PLS at early time which may help to kill any residual bacteria.

## 3.2 Introduction

As previously mentioned in Chapter 1, dental amalgam will be gradually phased down as a consequence the 2013 Minamata agreement on mercury (Austin et al., 2016). Dental composites will eventually become the only suitable direct restorative materials for posterior restorations. The main problem of the composites is high risk of secondary caries due to bacterial microleakage, which is enhanced by polymerisation shrinkage and lack of antibacterial action. To address these issues, remineralising and antibacterial agents have been incorporated in dental composites.

High monomer conversion of dental composites is required to ensure high mechanical properties and low risk of toxic monomers leaching. Studies showed that composites containing UDMA as the base monomer exhibited higher monomer conversion and biaxial flexural strength than composites containing Bis-GMA (Walters et al., 2016). This could be due primarily to the lower glass transition temperature of UDMA compared with Bis-GMA (Sideridou et al., 2002). High monomer conversion, however, associates with high polymerisation shrinkage.

Remineralising agents such as calcium phosphates previously promoted water sorption enhanced volume expansion which may compensate the polymerisation shrinkage of experimental dental composites (Aljabo et al., 2015). These compounds also enabled calcium and phosphate ions release and surface apatite precipitation (Mehdawi et al., 2013; Aljabo et al., 2016). These may help to remineralise the demineralised dentine (Gandolfi et al., 2011) and fill gaps formed due to the shrinkage respectively. Additionally, strontium has been used in glass ionomer cements and bioactive glass for orthopaedic applications (Lippert and Hara, 2013; Shahid et al., 2014). It enhanced radiopacity of the cements and apatite precipitation on the bioactive glass. Furthermore,

it was found that strontium provided a synergistic antibacterial effect with fluoride (Lippert and Hara, 2013). The addition of phosphate compounds, however, reduced final monomer conversion and strength of dental composites (Aljabo et al., 2015). This may result in an increased risk of toxic monomer leaching and potential failure of the restoration respectively.

Polylysine (PLS) is an FDA approved preservative and widely used in preserved package food in Japan and South Korea. It has strong antimicrobial activity, high thermal stability and safety (Bo et al., 2016; Shi et al., 2016). Hence, this compound may be beneficial as an antibacterial agent for dental composites which could help to kill residual bacteria and reduce bacterial microleakage.

### **3.3 Hypotheses**

According to the literature described above, dental composites that can promote remineralisation and antibacterial actions could potentially reduce bacterial microleakage. It was expected that remineralising and antibacterial agents - containing dental composites can be produced by incorporation of MCPM, TSrP, and PLS. Previous studies showed that dental composites containing UDMA as base monomer exhibited higher conversion than dental composites containing Bis-GMA (Walters et al., 2016). It was therefore anticipated that monomer conversion of UDMA/TEGDMA experimental dental composites would be higher than that of a commercial material containing Bis-GMA as the base monomer.

Phosphates (MCPM with TCP) from 10 to 40 wt% were incorporated to enable remineralising properties of UDMA/TEGDMA experimental composites in previously published studies (Aljabo et al., 2015; Aljabo et al., 2016). The increase of these phosphates reduced monomer conversion and increased hygroscopic expansion,

chlorhexidine release, and surface apatite formation of the composites. High level of phosphates (40 wt%), however, led to a reduction of composite's strength. Composites containing intermediate level of phosphate (20 wt%) in the previous studies exhibited hygroscopic expansion comparable with polymerisation shrinkage without detrimentally reduced monomer conversion and mechanical properties. Experimental composites in this chapter will therefore contain 25 wt% of phosphates (PO; 10 wt% of MCPM and 15 wt% of TSrP). Hence, it was anticipated that the addition of 25 wt% PO will promote hygroscopic expansion and surface apatite precipitation for experimental bone composites without detrimentally reduced monomer conversion and mechanical properties of the composites.

An alternative antibacterial agent is required due to concerns of developing antibiotic resistance and severe allergic reaction of patients to chlorhexidine. Polylysine (PLS), which is used as a food preservative that can provide antimicrobial actions, will be added into the following experimental dental composites. It was hypothesized that the addition of 2.5 wt% PLS will promote antibacterial agent release for the experimental composites. PLS is hydrophilic homopolymer, hence, low level of this compound (2.5 wt%) will be used to reduce possible detrimental effects on mechanical properties of the composites.

### **3.4 Aims and objectives**

The aim of this chapter was to develop novel PLS - releasing dental composites with added remineralising agents (MCPM, TSrP) that promote water sorption induced volume expansion and surface apatite formation. The objectives of this study were to assess:

- 1) Monomer conversion and calculated polymerisation shrinkage;
- 2) Water sorption induced mass and volume change;
- 3) Material induced surface apatite precipitation;
- 4) PLS release;
- 5) Biaxial flexural strength and modulus of elasticity of the experimental dental composites.

Four formulations with and without 25 wt% phosphates (PO) and / or 2.5 wt% polylysine (PLS) added to the powder phase were examined. A commercial dental composite (Z250 shade B3, 3M, USA) was used for comparison.

### 3.5 Materials and Methods

Experimental dental composites were prepared using a powder to liquid ratio of 4:1 (weight ratio). The liquid phase contained 70 wt% UDMA, 25 wt% TEGDMA, 1 wt% CQ, and 1 wt% DMPT. The powder phase of each formulation is presented in Table 3-1. The powder and liquid were weighed and mixed using a planetary centrifugal mixer at 3500 rpm for 10 s followed by 2000 rpm for 2 min. The resultant-mixture had consistency similar to a commercial packable composite.

**Table 3-1 Composition of powder phase of experimental composites.**

Formulations	7 $\mu$ m glass (wt%)	MCPM (wt%)	TSrP (wt%)	PLS (wt%)
<b>PO<sub>25</sub>PLS<sub>2.5</sub></b>	72.5	10	15	2.5
<b>PO<sub>25</sub>PLS<sub>0</sub></b>	75	10	15	0
<b>PO<sub>0</sub>PLS<sub>2.5</sub></b>	97.5	0	0	2.5
<b>PO<sub>0</sub>PLS<sub>0</sub></b>	100	0	0	0

Monomer conversion was assessed using FTIR-ATR (n=5) at a controlled temperature of 25 °C. Mass and volume changes in water (n=3) and SBF (n=3) were measured using a density kit, surface apatite formation after immersion in SBF (n=1) was assessed using Raman spectroscopy and SEM, PLS release in deionised water using UV-spectroscopy (n=3), and biaxial flexural strength tests after immersion in SBF for 24 hr (n=8) were performed. All testing protocols were described in Chapter 2. Additionally, photographs of post-cured disc specimens were taken to compare their translucencies. A commercial dental composite (Z250 shade B3, 3M, USA) was used for comparison.

### 3.6 Statistical analysis

Data were analysed using one way ANOVA and multiple comparison using Tukey's test or Kruskal-Wallis test followed by Dunnett's T3 test ( $p = 0.05$ ). Furthermore, two-variable factorial analysis with low and high level of variables (equations 2-26,28) was used to assess effect of phosphates (0 wt% versus 25 wt%) and polylysine (0 wt% versus 2.5 wt%) on monomer conversion, calculated polymerisation shrinkage, and biaxial flexural strength of the experimental dental composites.

### 3.7 Results

#### 3.7.1 Monomer conversion and calculated polymerisation shrinkage

Conversion of monomer in all materials rapidly increased to over 50% after exposure to the curing light (Fig 3-1 A). The experimental composites exhibited significantly higher monomer conversion (64 – 76 %) than Z250 ( $54 \pm 3$  %) (Fig 3-1 B). The conversions of  $\text{PO}_0\text{PLS}_{2.5}$  ( $74 \pm 1$  %) and  $\text{PO}_0\text{PLS}_0$  ( $74 \pm 1$  %) were significantly higher than that of  $\text{PO}_{25}\text{PLS}_{2.5}$  ( $65 \pm 1$  %) and  $\text{PO}_{25}\text{PLS}_0$  ( $67 \pm 1$  %). The conversion of  $\text{PO}_{25}\text{PLS}_{2.5}$  was comparable to  $\text{PO}_{25}\text{PLS}_0$ . Additionally,  $\text{PO}_0\text{PLS}_0$  had translucency similar to Z250 (Fig 3-1 C). Translucency of the cured experimental composites from highest to lowest were  $\text{PO}_0\text{PLS}_0$ ,  $\text{PO}_0\text{PLS}_{2.5}$ ,  $\text{PO}_{25}\text{PLS}_0$ , and  $\text{PO}_{25}\text{PLS}_{2.5}$  respectively.

Monomer conversion produced calculated polymerisation shrinkage of  $3.1 (\pm 0.1)$ ,  $3.2 (\pm 0.1)$ ,  $3.5 (\pm 0.1)$ , and  $3.5 (\pm 0.1)$  vol% for  $\text{PO}_{25}\text{PLS}_{2.5}$ ,  $\text{PO}_{25}\text{PLS}_0$ ,  $\text{PO}_0\text{PLS}_{2.5}$ , and  $\text{PO}_0\text{PLS}_0$  respectively (Fig 3-1 D). The shrinkages of  $\text{PO}_{25}\text{PLS}_{2.5}$  and  $\text{PO}_{25}\text{PLS}_0$  were significantly lower than that of  $\text{PO}_0\text{PLS}_{2.5}$  and  $\text{PO}_0\text{PLS}_0$ . Manufacturer did not supply the exact composition of Z250, therefore, the shrinkage could not be calculated. Factorial analysis (equations 2-26,28) indicated that final monomer conversion and calculated



polymerisation shrinkage of the composites increased by  $11 \pm 2$  % upon removal of PO whilst the effect of PLS was negligible.

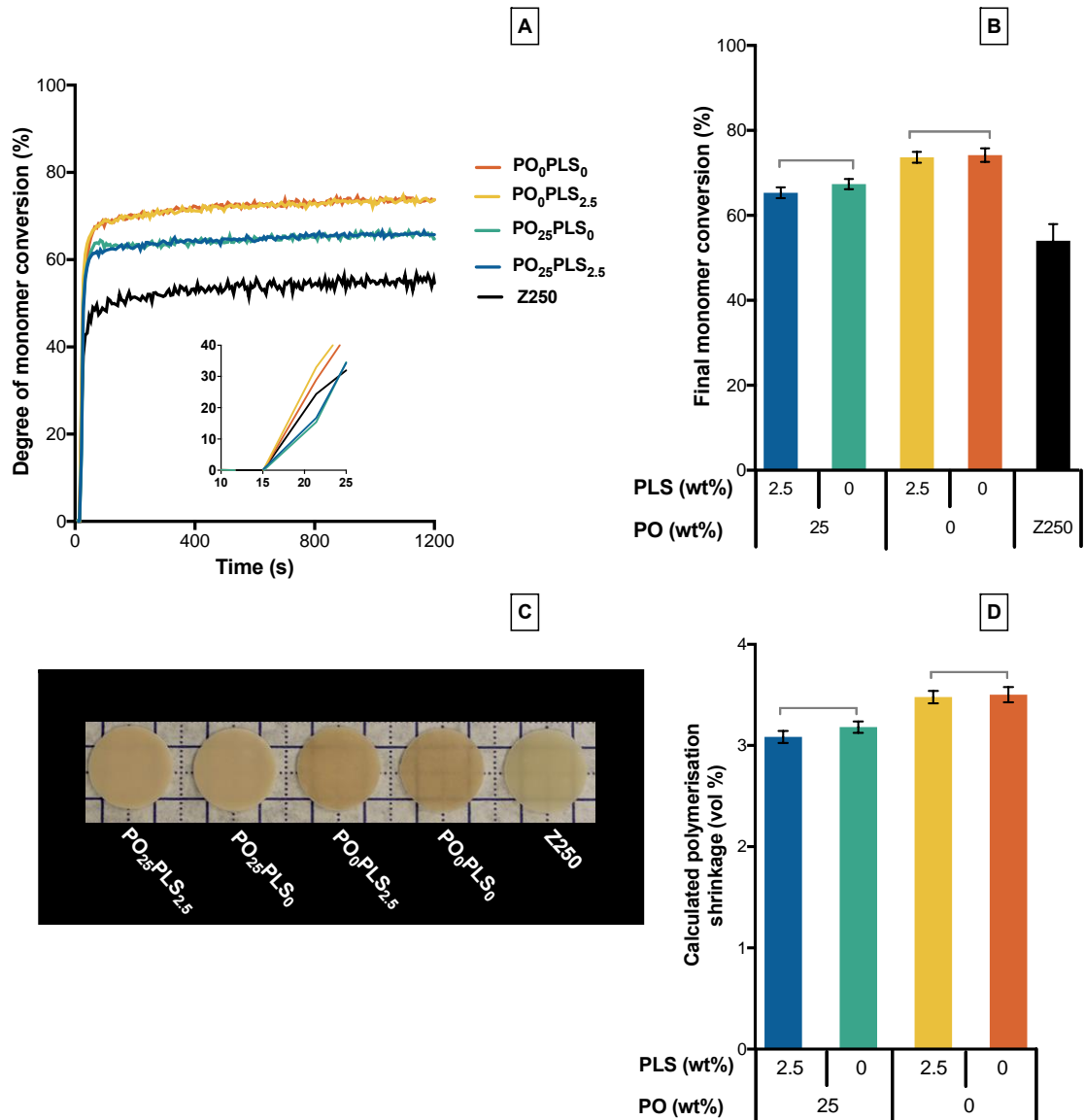


**Fig 3-1 (A) Monomer conversion versus time (light turned on at 10 s and cured for 40 s), (B) final monomer conversion of each material, (C) light cured composite discs showing different translucencies and (D) calculated polymerisation shrinkage. Lines indicate no significant difference ( $p > 0.05$ ). Error bars are 95% CI ( $n=5$ ). Adapted from Panpisut P, Liaqat S, Zacharaki E, Xia W, Petridis H, Young AM (2016) *Dental Composites with Calcium / Strontium Phosphates and Polylysine*. PLoS ONE 11(10): e0164653. doi:10.1371/journal.pone.0164653.g001.**

### 3.7.2 Mass and volume changes upon water sorption

Mass change of  $\text{PO}_0\text{PLS}_0$  began to level off at 2 weeks, then reached final values of  $1.4 \pm 0.1$  and  $1.0 \pm 0.1$  wt% in water and SBF respectively (Fig 3-2). Upon addition of PLS ( $\text{PO}_0\text{PLS}_{2.5}$ ), mass continued to increase, then reached final values of  $2.0 \pm 0.1$  wt% and  $1.7 \pm 0.2$  wt% in water versus SBF respectively. Upon addition of phosphates, the final mass changes at 9 weeks in water and SBF were  $0.0 \pm 0.2$  wt% and  $1.5 \pm 0.3$  wt% for  $\text{PO}_{25}\text{PLS}_0$ , and  $-0.6 \pm 0.4$  wt% and  $2.0 \pm 0.1$  wt% for  $\text{PO}_{25}\text{PLS}_{2.5}$ . Difference in mass change of  $\text{PO}_{25}\text{PLS}_0$  and  $\text{PO}_{25}\text{PLS}_{2.5}$  in SBF versus in water were plotted. This gave gradients of  $0.039 (\pm 0.002)$  and  $0.075 (\pm 0.005)$  wt%.hr<sup>-0.5</sup> for  $\text{PO}_{25}\text{PLS}_0$  and  $\text{PO}_{25}\text{PLS}_{2.5}$  respectively.

Conversely, volume changes of the composites in both solutions reached maxima and then levelled off at late time (Fig 3-2). The final volume change of  $\text{PO}_{25}\text{PLS}_{2.5}$ ,  $\text{PO}_{25}\text{PLS}_0$ ,  $\text{PO}_0\text{PLS}_{2.5}$  and  $\text{PO}_0\text{PLS}_0$  were  $(4.5 \pm 0.2)$ ,  $(3.7 \pm 0.1)$ ,  $(2.2 \pm 0.2)$ ,  $(2.1 \pm 0.1)$  vol% in water, and  $(5.2 \pm 0.1)$ ,  $(4.6 \pm 0.1)$ ,  $(1.9 \pm 0.1)$ ,  $(1.9 \pm 0.1)$  vol% in SBF respectively. Differences in final values in water versus SBF of  $\text{PO}_{25}\text{PLS}_{2.5}$ ,  $\text{PO}_{25}\text{PLS}_0$ ,  $\text{PO}_0\text{PLS}_{2.5}$ , and  $\text{PO}_0\text{PLS}_0$  were  $(0.7 \pm 0.1)$ ,  $(0.9 \pm 0.2)$ ,  $(-0.4 \pm 0.1)$ ,  $(-0.1 \pm 0.0)$  vol% respectively.

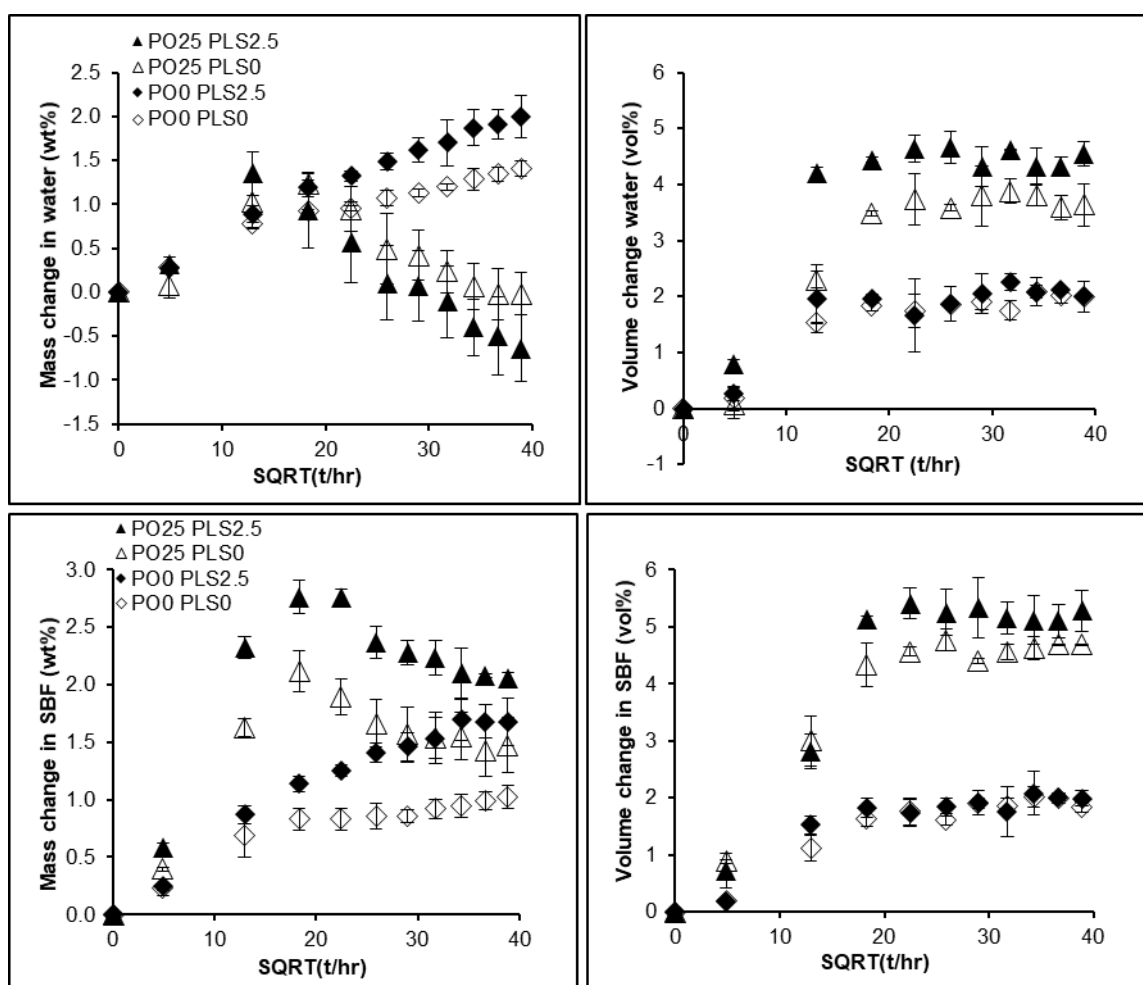


**Fig 3-2** Changes of composite's mass and volume upon immersion in SBF or deionised water as a function of square root of hour. Error bars are 95% CI (n=3). Adapted from Panpisut P, Liaqat S, Zacharaki E, Xia W, Petridis H, Young AM (2016) *Dental Composites with Calcium / Strontium Phosphates and Polylysine*. PLoS ONE 11(10): e0164653. doi:10.1371/journal.pone.0164653.g002.

### 3.7.3 Apatite formation

At all immersion time points, only peaks attributed to glass and polymers were observed from Raman spectra of  $\text{PO}_0\text{PLS}_{2.5}$  and  $\text{PO}_0\text{PLS}_0$  (data not presented). After one day immersion in SBF, Raman spectra of  $\text{PO}_{25}\text{PLS}_{2.5}$  and  $\text{PO}_{25}\text{PLS}_0$  were dominated by peaks for glass, polymer, and TSP (Fig 3-3). The surface MCPM would have fully dissolved so its peak was not visible. Raman maps at this time point of  $\text{PO}_{25}\text{PLS}_{2.5}$  and  $\text{PO}_{25}\text{PLS}_0$  showed areas of apatite formation (green areas) (Fig 3-3). Additionally, brushite (orange regions) were observed with  $\text{PO}_{25}\text{PLS}_{2.5}$ . The increase in intensity of average Raman apatite peaks ( $960\text{ cm}^{-1}$ ) was more evident with  $\text{PO}_{25}\text{PLS}_{2.5}$  than  $\text{PO}_{25}\text{PLS}_0$ . At 1 week, an apatite layer ( $> 1\text{ }\mu\text{m}$ ) was fully covering the underlying  $\text{PO}_{25}\text{PLS}_{2.5}$  composite. This, however, did not occur until 4 weeks with  $\text{PO}_{25}\text{PLS}_0$ .

No surface apatite formation was observed on the SEM images of  $\text{PO}_0\text{PLS}_{2.5}$  and  $\text{PO}_0\text{PLS}_0$ . A thin layer of surface apatite was detected on  $\text{PO}_{25}\text{PLS}_{2.5}$  and  $\text{PO}_{25}\text{PLS}_0$  samples at all timepoints of immersion (Fig 3-4). The apatite layer contained globules which revealed a porous structure at higher magnification. Size of globules and dimension of cracks were used to estimate the thickness of the apatite layers. The thickness of the layers on  $\text{PO}_{25}\text{PLS}_0$  were approximately 1, 5 and  $10\text{ }\mu\text{m}$  after 1 day, 1, and 4 weeks respectively. At these time periods, the approximate thickness of the layers on  $\text{PO}_{25}\text{PLS}_{2.5}$  were 2, 10, and  $20\text{ }\mu\text{m}$ .

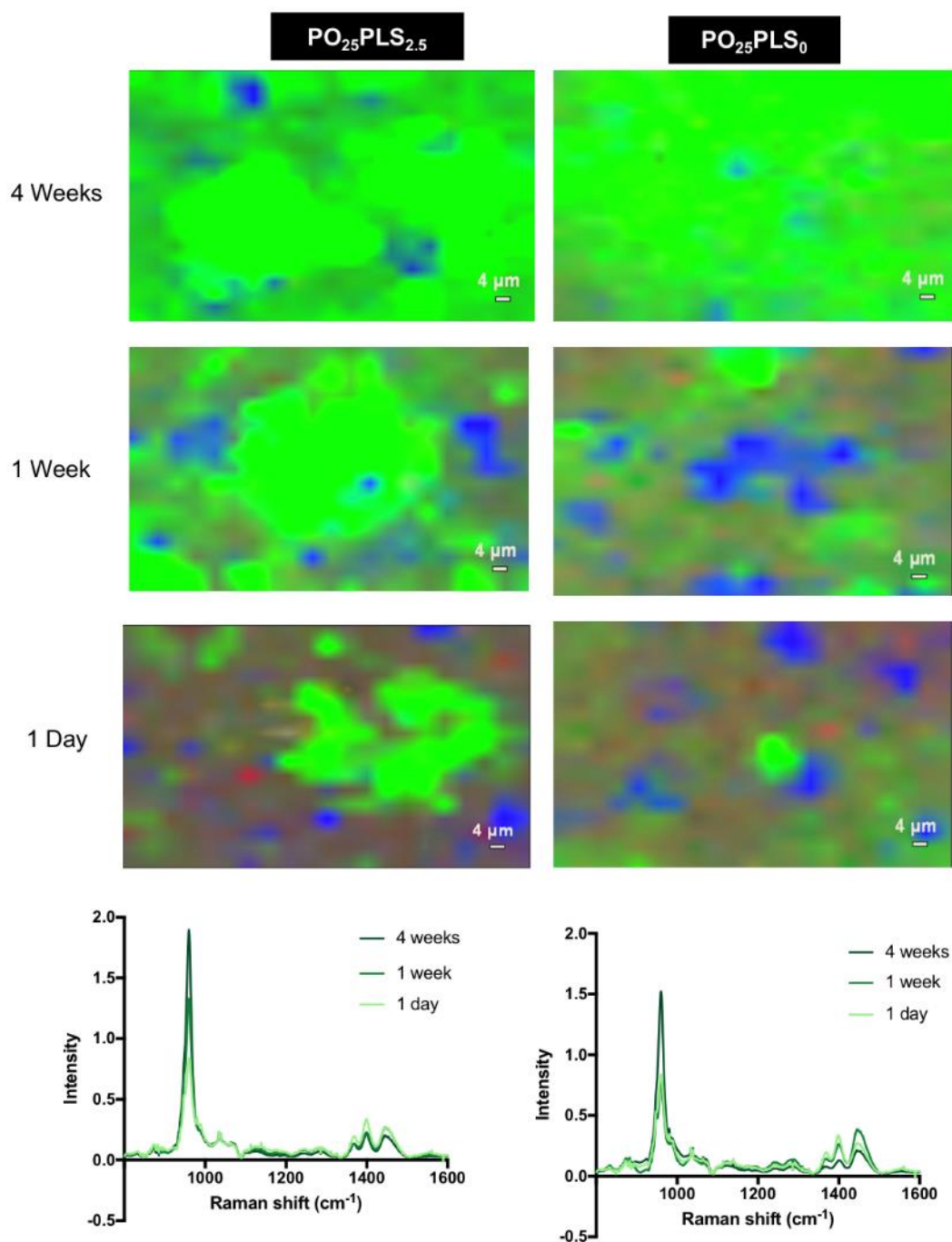


**Fig 3-3** Acquired average Raman spectra and Raman maps from surfaces of  $\text{PO}_{25}\text{PLS}_{2.5}$  and  $\text{PO}_{25}\text{PLS}_0$  after immersion in SBF for 1 day, 1 week, and 4 weeks. Polymer plus glass regions and apatite are represented by blue and green areas. Brushite and TSrP are represented by yellow and red areas. MCPM was not observed in the mapping process. In both formulations, blues areas indicate polymer and glass peaks between 1300 and 1500  $\text{cm}^{-1}$  are dominant in point spectra. A substantial increase in the apatite scattering peak is observed with  $\text{PO}_{25}\text{PLS}_{2.5}$  at 1 week, but this can be seen for both formulations at 4 weeks. Adapted from Panpisut P, Liaqat S, Zacharaki E, Xia W, Petridis H, Young AM (2016) *Dental Composites with Calcium / Strontium Phosphates and Polylysine*. PLoS ONE 11(10): e0164653. doi:10.1371/journal.pone.0164653.g00.

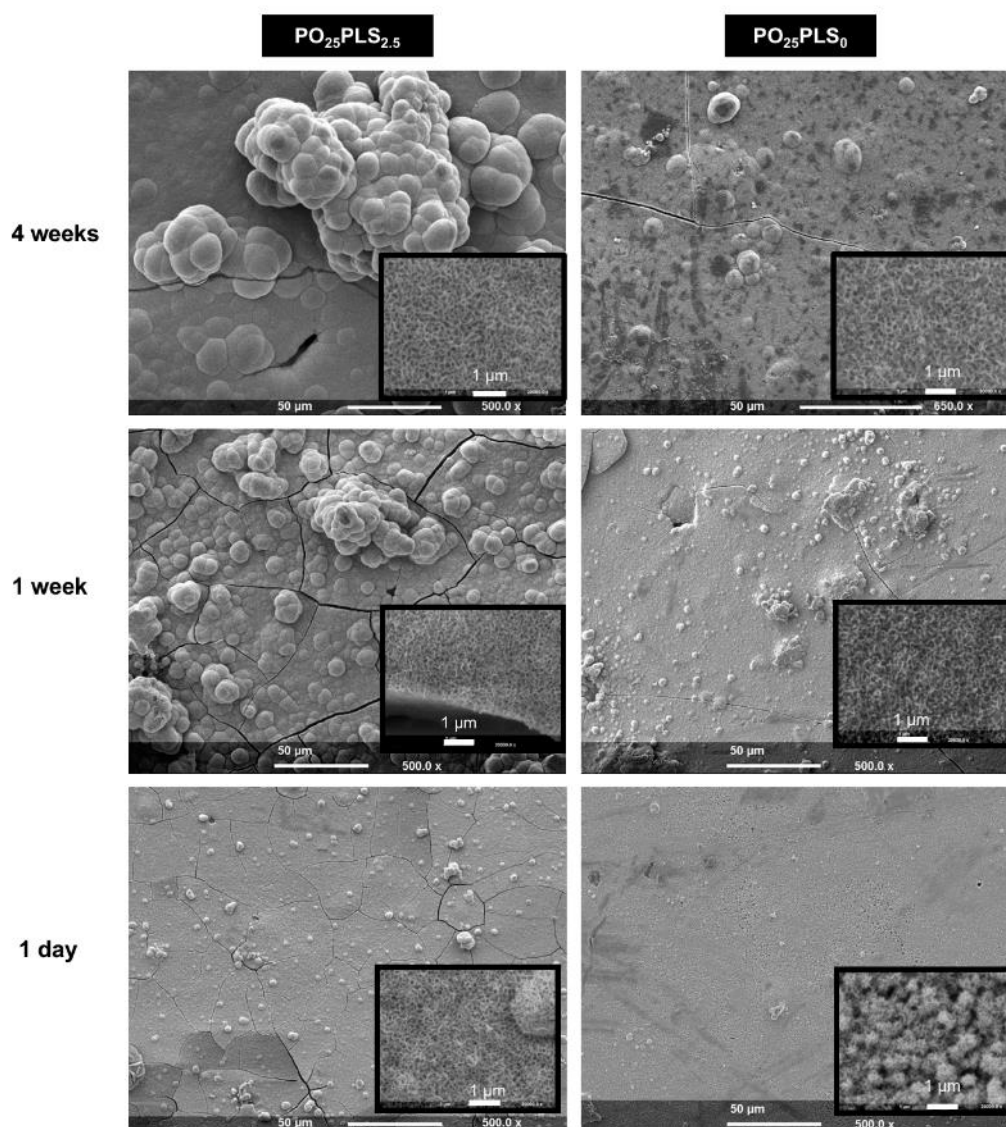


**Fig 3-4 SEM images of  $PO_{25}PLS_{2.5}$  and  $PO_{25}PLS_0$  composite surfaces after immersion in SBF for 1 day, 1 week or 4 weeks.** Adapted from Panpisut P, Liaqat S, Zacharaki E, Xia W, Petridis H, Young AM (2016) *Dental Composites with Calcium / Strontium Phosphates and Polylysine*. PLoS ONE 11(10): e0164653. doi:10.1371/journal.pone.0164653.g004.

### 3.7.4 Polylysine release

PLS release of PO<sub>25</sub>PLS<sub>2.5</sub> and PO<sub>0</sub>PLS<sub>2.5</sub> were not significantly different (Fig 3-5). A burst release of polylysine at 6 hr was observed with PO<sub>25</sub>PLS<sub>2.5</sub> ( $25 \pm 2$  ppm,  $3.4 \pm 1.0$  %) and PO<sub>0</sub>PLS<sub>2.5</sub> ( $23 \pm 2$  ppm,  $4.0 \pm 0.8$  %). The gradients of PLS release versus square root of hour after this burst were  $0.26 \pm 0.06$  %·hr<sup>-0.5</sup> and  $0.23 \pm 0.04$  %·hr<sup>-0.5</sup> for PO<sub>25</sub>PLS<sub>2.5</sub> and PO<sub>0</sub>PLS<sub>2.5</sub> respectively ( $R^2 > 0.95$ ).

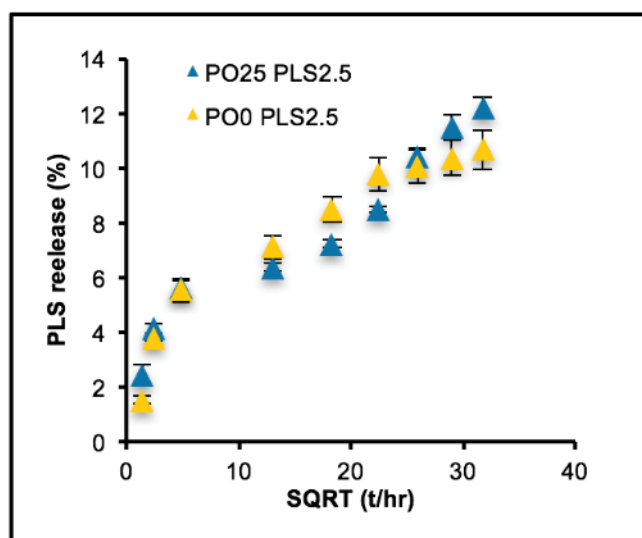


**Fig 3-5 Cumulative PLS release from the composite discs immersed in deionised water for up to 6 weeks. Error bars are 95% CI (n=3).** Adapted from Panpisut P, Liaqat S, Zacharaki E, Xia W, Petridis H, Young AM (2016) *Dental Composites with Calcium / Strontium Phosphates and Polylysine*. PLoS ONE 11(10): e0164653. doi:10.1371/journal.pone.0164653.g004.

### 3.7.5 Biaxial flexural strength (BFS) and modulus of elasticity

Z250 ( $217 \pm 22$  MPa) and PO<sub>25</sub>PLS<sub>2.5</sub> ( $104 \pm 3$  MPa) exhibited highest and lowest BFS respectively (Fig 3-6 A). BFS of PO<sub>25</sub>PLS<sub>0</sub> ( $125 \pm 4$  MPa) and PO<sub>0</sub>PLS<sub>2.5</sub> ( $127 \pm 6$  MPa) were comparable but both were significantly lower than that of PO<sub>0</sub>PLS<sub>0</sub> ( $154 \pm 6$  MPa). The highest modulus of elasticity was obtained from Z250 ( $6.2 \pm 0.4$  GPa) but this was comparable to PO<sub>0</sub>PLS<sub>0</sub> ( $5.7 \pm 0.3$  GPa) (Fig 3-6 B). PO<sub>25</sub>PLS<sub>2.5</sub> ( $5.0 \pm 0.1$  GPa) showed the lowest modulus which was comparable to that for PO<sub>25</sub>PLS<sub>0</sub> ( $5.5 \pm 0.4$  GPa) and PO<sub>0</sub>PLS<sub>2.5</sub> ( $5.5 \pm 0.3$  GPa).

Factorial analysis (equations 2-26,28) indicated that BFS of experimental composites was increased by  $23 \pm 5$  % and  $20 \pm 4$  % upon removal of PO and PLS respectively. Conversely, these additives had insignificant effect on modulus of elasticity of the experimental composites.

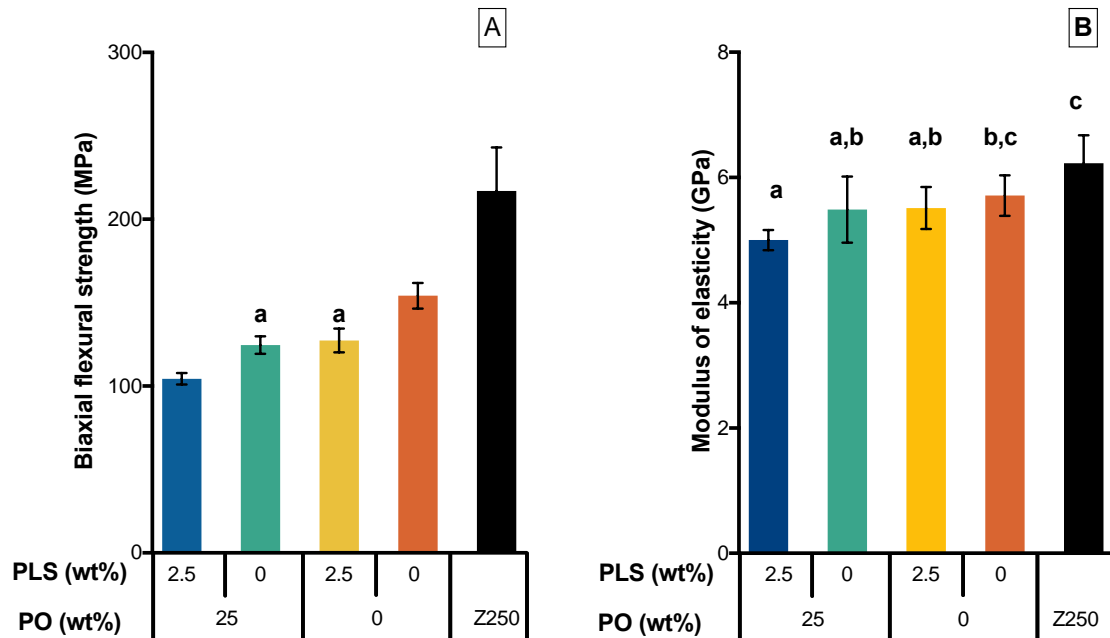


**Fig 3-6 A) Biaxial flexural strength and B) modulus of elasticity of composites. Same letters indicate no significant difference ( $p > 0.05$ ). Error bars are 95% CI ( $n=8$ ). Adapted from Panpisut P, Liaqat S, Zacharaki E, Xia W, Petridis H, Young AM (2016) *Dental Composites with Calcium / Strontium Phosphates and Polylysine*. PLoS ONE 11(10): e0164653. doi:10.1371/journal.pone.0164653.g006.**



### 3.8 Discussion

The chapter developed novel dental composites containing remineralising (Ca / Sr phosphates) and antibacterial (polylysine) agents. Monomer conversion with calculated polymerisation shrinkage, mass and volume changes upon water sorption, polylysine release, surface apatite formation, and early mechanical properties of the composites were assessed.

#### 3.8.1 Monomer conversion

The release of unreacted monomers due to insufficient monomer conversion of dental composites may cause toxicity, allergic reaction, and shift the ecology of dental biofilm toward high cariogenicity (Gupta et al., 2012; Esteban Florez et al., 2016; Nedeljkovic et al., 2016b). The eluted monomers were significantly reduced when the final conversion of dental composites was greater than ~ 50 % (Durner et al., 2012; Lempel et al., 2014). The conversions of the experimental composites in the current study were greater than this critical level and in accordance with that of light cured commercial dental composites (50 – 70 %) reported in published studies (Marovic et al., 2015; Yu et al., 2017). Furthermore, the conversion of Z250 in this study was consistent with that obtained from published studies using a similar technique (de Oliveira et al., 2015; Zorzin et al., 2015).

Monomer composition plays an essential role in determining final monomer conversion of dental composites. Monomer conversion of UDMA/TEGDMA dental composites in the current studies was higher than that of Z250 (which contains Bis-GMA as primary base monomer). Generally, high monomer conversion is obtained from polymers containing flexible and low glass transition temperature ( $T_g$ ) monomers.  $T_g$  of TEGDMA, UDMA, and Bis-GMA monomer reported by Sideridou et al. (2002) were -83, -35, and -8 °C respectively. The same study reported final conversions at room temperature of

76%, 67%, and 39% for TEGDMA, UDMA, and Bis-GMA homopolymers respectively. The ranges of these final conversions are consistent with the conversions observed from the experimental composites and Z250.

Monomer conversions in this thesis were obtained with specimen thickness of 1 mm. Studies have demonstrated that the conversion of Z250 was decreased significantly when the thickness was > 1 mm (Lempel et al., 2014; Aljabo et al., 2015). Conversion of greater than 50% with a thickness up to 4 mm was observed, however, with composites using a similar monomer composition (Aljabo et al., 2015) to this present study. This result may facilitate the bulk placement of experimental composites, in contrast to the control commercial material which needs to be placed incrementally to ensure sufficient monomer conversion. Such a layering process may increase the risk of voids entrapment affecting clinical outcomes of the restoration (Abbas et al., 2003).

The addition of phosphates and PLS negatively affected monomer conversion of experimental composites. This might be the result of enhanced light scattering due to the mismatch of refractive indices between monomer and fillers in the composites. The refractive index of the UDMA/TEGDMA mixture, glass, TSrP, MCPM, and PLS were approximately 1.47, 1.46, 1.65, 1.54, and 1.42 respectively (Antonucci et al., 1991; Richert et al., 2004; Fujita et al., 2005; Yang et al., 2006). Any monomer / filler mismatch of refractive indices may decrease the light transmission, thereby reducing monomer conversion (Howard et al., 2010). This subsequently reduced calculated polymerisation shrinkage in formulations with phosphates addition ( $\text{PO}_{25}\text{PLS}_{2.5}$  and  $\text{PO}_{25}\text{PLS}_0$ ).

A previous study (Aljabo et al., 2015) has demonstrated good agreement between calculated and experimental polymerisation shrinkage. The shrinkage of experimental composites in this chapter are comparable to previous studies with composites of similar

composition (Walters et al., 2016). The calculated shrinkage of the experimental composites was slightly higher than that of ~ 2 vol% observed previously with Z250 (Nagem Filho et al., 2007; Boaro et al., 2013). The shrinkage of experimental composites, however, fell within the range of polymerisation shrinkage observed with other commercial dental composites (2- 4 vol%) (Yu et al., 2017).

### 3.8.2 Mass and volume changes

Under a clinical environment, a dental composite restoration is continuously exposed to various oral fluids leading to water sorption. The water-plasticised and expanded polymer network results in reduction in mechanical and physical properties (Ferracane, 2006; Sideridou et al., 2007). This water is, however, required to enable the release of remineralising and antibacterial components (Mehdawi et al., 2013; Zhang et al., 2016a). Mass changes upon water sorption of a dental composite is usually a diffusion-controlled process (Wei et al., 2011). Therefore, the results in the above study were plotted versus the square root of time.

Water sorption increased the composite mass and dissolved the components enabling their release. The dissolution of MCPM produces phosphoric acid and dicalcium phosphate. The latter can precipitate as lower density brushite that binds with water. The phosphoric acid can be released from the composite to etch and aid tooth bonding or react with tristrontium phosphate forming distrontium phosphate

Mass changes observed with  $\text{PO}_0\text{PLS}_{2.5}$  and  $\text{PO}_0\text{PLS}_0$  in this study were not influenced by the storage solution. Mass changes of these composites were also comparable to those observed with commercial composites (Wei et al., 2013). In contrast, the mass change of phosphates-containing composites ( $\text{PO}_{25}\text{PLS}_{2.5}$  and  $\text{PO}_{25}\text{PLS}_0$ ) were strongly influenced by the storage solution. The net mass loss of composites in deionised water

could be the result of imbalance between components loss and mass gain due to water sorption. Surface apatite precipitation may help to counteract the mass loss of  $\text{PO}_{25}\text{PLS}_{2.5}$  and  $\text{PO}_{25}\text{PLS}_0$  in SBF. The difference in mass change in water versus SBF of  $\text{PO}_{25}\text{PLS}_{2.5}$  was higher than that of  $\text{PO}_{25}\text{PLS}_0$ . This may imply that PLS enhanced apatite precipitation for the composites.

The addition of phosphates showed a significant effect on volume changes. The possible explanation for this might be the formation of low density brushite inside the composite. Previous suggestions are that this may lead to expansion of the surrounding polymer matrix (Mehdawi et al., 2009; Mehdawi et al., 2013). Furthermore, the 1% difference in volume change observed at late time with  $\text{PO}_{25}\text{PLS}_{2.5}$  and  $\text{PO}_{25}\text{PLS}_0$  in water versus in SBF would be consistent with a 10  $\mu\text{m}$  layer of apatite. This would be expected to help remineralisation of >10  $\mu\text{m}$  depth of surrounding acid affected dentine.

The final volume expansion of experimental composites with phosphates was comparable to the calculated polymerisation shrinkage. The expansion could potentially help to balance the shrinkage and to relieve shrinkage stress (Meriwether et al., 2013; Park and Ferracane, 2014), thereby reducing marginal gaps and adhesion failure.

### 3.8.3 Apatite formation

The apatite precipitation on the composite surface was expected to help seal gaps at the tooth-restoration interface and remineralise any demineralised dentine. Blood plasma diluted with water has been used as a simulated dentinal fluid for various *in vitro* studies (Ozok et al., 2002; Qin et al., 2006; Qin et al., 2011). Furthermore, SBF has similar ions concentration to blood plasma and has commonly been used to assess the apatite forming ability of materials (Yan et al., 2011; Brauer, 2015).

The addition of PO promoted surface apatite formation for experimental dental composites. Additionally, replacement of TCP and CHX in a previous study (Aljabo et al., 2016) by TSrP and PLS did not remove apatite forming ability of the new composites in this chapter. The benefit of TSrP and PLS compared with the original additives would be the enhanced radiopacity and eukaryotic cell compatibility for the composites respectively (Hidalgo and Dominguez, 2001; Fischer et al., 2003; Shahid et al., 2014).

The addition of PLS was found to promote the precipitation of surface apatite. The positively charged lysine from PLS in addition to water sorption may have encouraged the mineral release and could have attracted a negatively charged pro-nucleation cluster. This may have increased the nucleation sites and subsequently enhanced apatite precipitation (Nudelman et al., 2010). The rapid formation of apatite would be expected to enable immediate remineralising of any residual demineralised dentine and help to minimise gap formation at the tooth-restoration interface. The thicknesses of apatite layers in the above study were  $\sim 10\text{ }\mu\text{m}$ . This is comparable to gaps previously observed due to polymerisation shrinkage (Benetti et al., 2015).

#### **3.8.4 Polylysine release**

Chlorhexidine has been added in dental materials to reduce bacterial accumulation or prevent enzymatic degradation of hybrid layers at the resin-dentine interface (Frassetto et al., 2016; André et al., 2017). An increase of antibiotic resistance, and severe allergic reactions to this agent have been reported in recent studies (Kulik et al., 2015; Pemberton, 2016; Saleem et al., 2016). Additionally, studies have demonstrated that high release of CHX was obtained only when calcium phosphate or a hydrophilic monomer was added (Mehdawi et al., 2013; Aljabo et al., 2016).

The addition of PLS enabled PLS release from experimental composites. The release of PLS in this study was not dependant on the level of PO addition. This might be due to the fact that PLS itself was able to promote water sorption due to its high water solubility compared to CHX. Furthermore, PLS is a polyelectrolyte (Lubbert et al., 2005). Upon exposure to aqueous solutions, the polymer chains of polylysine will become positively charged and generate repulsive forces between the monomer units. This may lead to polymer chain extension and movement of PLS chain from dental composites into the surrounding liquid. The release of PLS in the current study can be explained using equation 3-1 which was modified from equation 2-19.

$$\Delta PLS = \Delta PLS_0 + \Delta PLS_{\infty} \sqrt{\frac{2Dt}{\pi d^2}} \quad \text{Equation 3-1}$$

Where  $\Delta PLS$ ; the change in cumulative PLS in the solution,  $\Delta PLS_0$ ; early burst release,  $\Delta PLS_{\infty}$ ; maximum change in the solution,  $D$ ; PLS diffusion coefficient,  $t$ ; time,  $d$ ; sample thickness. PLS on the surface of composite may dissolve leading to early burst release. In the 10 mL of storage solution this gave 23 – 25 ppm which in one study was greater than minimum inhibitory concentration (20 ppm) of PLS for *Streptococcus mutans*, which is one of the cariogenic bacteria (Badaoui Najjar et al., 2009). Although bacterial killing is more difficult on surfaces where bacteria form biofilms. The limited level of water in dentinal tubules could lead to much higher PLS concentrations. This early PLS release therefore has potential to reduce the growth of residual cariogenic bacteria in a cavity.

### 3.8.5 Biaxial flexural strength and modulus of elasticity

Sufficient strength of a dental composite is required to ensure successful restoration. The commonly used standard, BS ISO 4049, requires a mean minimum three point flexural strength of 80 MPa from specimens stored in water for 24 hr (British Standard,

2009). It has been shown that the flexural strength from biaxial flexural test was more consistent and comparable to that of three-point bending test (Pick et al., 2010). Hence, the results from experimental composites in this study should pass the standard.

Mean BFS values of experimental composites (104 – 154 MPa) were in the range of that obtained from commercial materials in other studies (80 – 160 MPa) (Randolph et al., 2016). Furthermore, the mean BFS values were comparable or higher than those reported for calcium phosphates-containing composites in other published works (20 – 33 MPa) (Marovic et al., 2014), (70 MPa) (Cheng et al., 2016), (60 – 90 MPa) (Zhang et al., 2016a). The addition of PO and PLS decreased the BFS of the experimental composites. This could be due to the combination of the decrease in monomer conversion, the increase in water sorption, and the lack of adequate chemical bond between these additives and the polymer matrix (Ferracane, 2006).

A strong interfacial bond between the inorganic filler and polymer matrix is usually obtained through the use of a silane coupling agent such as methacryloxypropyltrimethoxysilane (Sideridou and Vouvoudi, 2015). The additives in the current study were not silane treated to enable their reaction and release. A chemical bond between PO / PLS and polymer matrix may develop through the bifunctional monomer (4-META). This chemical bond may, however, not suffice to provide significant benefit to mechanical properties. Additionally, the releasing of components and higher water sorption may affect the long-term mechanical properties of the composites. With the provided level of PO, a previous study suggested that the degree of reduction in strength was no more than that observed with Z250 (Aljabo et al., 2015). This could be due to the formation of high-density dicalcium phosphates in the pores left after the release of reactive fillers (Mehdawi et al., 2013).

### **3.9 Conclusions**

This study developed light cured Ca/Sr phosphates - and polylysine - containing dental composites. The addition of phosphates induced hygroscopic expansion that was comparable to the calculated polymerisation shrinkage. The additives also promoted apatite formation, which may help to reseal any restoration gaps in addition with the potential to remineralise any demineralised dentine. Furthermore, the burst release of polylysine may help to kill any residual bacteria. Although addition of these fillers decreased the final monomer conversion and strength of the composites, these properties were still within an acceptable range.



## **Chaper 4 Effect of Powder to Liquid Ratio, Polypropylene Glycol Dimethacrylate (PPGDMA) level, and Glass Particle Size on Rheological Properties and Physical Stability of Novel Bone Composites**

### **4.1 Abstract**

**Purpose:** This study modified dental composite formulations to develop Ca/Sr phosphate (MCPM, TSrP) and antibacterial polylysine (PLS) - containing injectable bone composites for vertebroplasty. The composites should exhibit rheological properties such as shear-thinning to facilitate ease of injection. Additionally, the composites should become a solid-like fluid at rest to ensure no phase separation upon long-term storage. Variables most likely to strongly affect rheological properties of the pre-cured bone composites such as powder to liquid ratio (PLR), PPGDMA diluent level, and glass filler size were examined.

**Materials and Methods:** Experimental bone composites with varying PLR (3:1, 2.6:1, 2.3:1), diluent monomer (PPGDMA) (75, 50, 25 wt%), and glass filler size (7  $\mu\text{m}$ , 0.7  $\mu\text{m}$ , and equal masses of 7 and 0.7  $\mu\text{m}$ ) but no initiator or activator were added. Dynamic strain and frequency sweep measurements using an oscillatory strain-controlled rheometer were performed to assess viscoelastic properties of the composite pastes. Then, a steady flow curve was undertaken to assess changes of composite's viscosities upon increasing shear rate. A commercial bone composite (Cortoss) was used for comparison.

**Results:** The pre-cured bone composites exhibited solid-like behaviour when low strain and frequencies were applied. At low strain, storage modulus of experimental bone

composites containing high PLR and small glass filler size was comparable to Cortoss. Greater liquid like behaviour was observed upon increasing the strain or frequency above a critical value. Increasing PLR and decreasing glass particle size increased storage modulus and critical strain of the composites respectively. Viscosities of all materials decreased upon increasing shear rate (shear-thinning). Viscosity of all experimental bone composites were lower than that of Cortoss. Raising PLR and decreasing PPGDMA level increased viscosity of experimental bone composites.

**Conclusion:** The experimental bone composites were viscoelastic fluids. Increase of PLR and decrease of glass filler size enhanced solid-like behaviour of the composites. This may ensure long-term paste stability. Viscosity of the composites was mainly affected by PLR and level of PPGDMA. Furthermore, the composites exhibited shear-thinning behaviour which is desirable for an injectable material.

## 4.2 Introduction

Vertebroplasty and kyphoplasty procedures involve injection of a bone cement through a fine cannula into the collapsed vertebra. It has been shown that viscosity of a bone cement affects bone-composite interdigitation, cement distribution, injected volume, and risk of cement extravasation (Nieuwenhuijse et al., 2010). Lewis (2011) suggested that viscosity of the cements should be sufficiently low to allow penetration of the cement through a cannula and the cancellous bone but not too low to permit extravasation.

A concern of currently used PPMA cements is the rapid changing of viscosity after mixing. The cements exhibit low viscosity initially but this was rapidly increased with time (Farrar and Rose, 2001; Baroud et al., 2006). The limited time of suitable viscosity for PMMA cements may therefore complicate clinical application. This could lead to poor cement distribution or cement leakage (Baroud et al., 2006).

A major advantage of recently developed bone composites is a better controlled rheology compared to PMMA cements. Bone composites are a suspension of inorganic particles in organic matrix. Hence, long-term paste stability is of concern as fillers in composite pastes could sediment under various conditions such as changes of temperature or stress induced by vibration during shipment (Tadros, 2004).

The combination of inorganic fillers and monomers enables optimisation of composites viscoelastic properties (Alenezi et al., 2017), which is required for injectable materials. Such composites exhibit rheological behaviour between that of elastic (solid) and viscous (liquid) materials (Al-Ahdal et al., 2014). The mixtures of properties lead to complex behaviours such as shear-thinning (viscosity decreases upon increasing shear rate), thixotropy (viscosity depends on time), or yield stress (flow is not initiated if the applied the stress is insufficient)(Mari et al., 2014). The response characteristic to external force

or frequency of viscoelastic materials mainly depends on the absolute value and ratio of elastic and viscous behaviour. These properties are complex and may be difficult to control. Studies assessed rheological properties of such materials using several methods. Oscillatory rheological test is one commonly used methods for assessing solid and viscous behaviour of injectable composites (Al-Ahdal et al., 2014; Borhan et al., 2016).

Rheological properties of composites are complex and governed by multiple factors. Examples of these factors are monomer compositions, filler compositions, and the interactions between filler particles and resin matrix. Ellakwa et al. (2007) demonstrated that increase of diluent monomer (TEGDMA) decreased viscosity of flowable (injectable) composites. The increase of this diluent monomer, however, is also associated with an increased polymerisation shrinkage. Previous studies revealed that replacing PPGDMA with TEGDMA increased final monomer conversion and reduced polymerisation shrinkage of experimental composites (Main, 2013; Khan, 2015; Walters et al., 2016). This was primarily due to the higher molecular weight and lower density of methacrylate groups of PPGDMA compared with TEGDMA.

The viscosity of flowable composites was also increased by an increase of filler content, the addition of irregular surfaces, or the incorporation of glass fibres (Lee et al., 2008). Furthermore, Beun et al. (2009) revealed that an increase of weight fraction of microfiller (diameter of 0.1  $\mu\text{m}$ ) to macrofiller (diameter of 1  $\mu\text{m}$ ) increased viscosity of flowable composites. The authors explained that high surface area of small particle attributed to the increase of viscosity of the composites.

### 4.3 Hypotheses

It was expected that injectable bone composites can be developed by modifying dental composite formulations. Powder to liquid ratio of the bone composites in this chapter was reduced from 4:1, which was used in dental composites in previous chapter, to 3:1, 2.6:1, or 2.3:1 (mass ratio). These ratios were a range that enabled adequate flow through a syringe with relatively narrow tips (diameter of ~ 2 mm). Diluent monomer used in the bone composites was PPGDMA due to the benefits described above. Glass particle size was also decreased from 7 to 0.7  $\mu\text{m}$  to improve physical stability (reduce particle sedimentation) of bone composite pastes.

According to literature, flowable dental composites showed viscoelastic properties. It was therefore anticipated that bone composites will also exhibit viscoelastic properties. High physical stability of the paste at rest (i.e. when composites are exposed to minimum strain/frequency) is required to prevent sedimentation of powder phase and ensure long shelf-life of the bone composites. Hence, bone composites should exhibit more solid-like behaviour upon applied low strain or frequency. During injection, however, the composites should be transformed from a solid-like to liquid-like fluid to facilitate the injection of materials. This may additionally improve the infiltration of the composites into the porous bone which could subsequently enhance bone integration.

According to literature, factors that could affect rheological properties of bone composites include powder to liquid ratio (PLR), diluent monomer PPGDMA level, and glass particle size. It was, therefore, expected that increasing PLR, decreasing PPGDMA diluent level and glass filler size would enhance solid-like behaviour of the composites. The consequence of these changes would be an increased viscosity of the bone composites. Hence, the bone composite pastes should exhibit shear-thinning

behaviour so that their viscosity could be decreased upon increasing shear rate to facilitate ease of injection.

#### **4.4 Objectives**

The aim of this study was to develop injectable bone composites that exhibit long-term paste stability (no sedimentation) and viscosity that is suitable for injection. The objectives were to assess the effects of composite powder to liquid ratio (PLR), diluent PPGDMA level, and glass filler sizes on rheological properties of the bone composites. The level of MCPM and TSrP in the filler phase are as in Chapter 3 but the level of PLS has been doubled to counteract the effect of using lower total powder contents to control flow. A commercial bone composite (Cortoss, Stryker, Newbury, Berkshire, UK) was used for comparison.

## 4.5 Materials and Methods

### 4.5.1 Material preparation

Powder to liquid ratios (mass ratio) were 3:1, 2.6:1, or 2.3:1. These PLR were lower than with the dental composites to enable production of more fluid and readily injectable pastes. The liquid phases, before mixing with the powder phase, contained varying weight ratios of UDMA: PPGDMA (70:25, 45:50, 20:75 wt:wt%) with a fixed level of HEMA (5 wt%)(Table 4-1). HEMA was added to improve surface wettability (Sellenet et al., 2007). In the bone composites HEMA was used instead of 4-META due to interactions between 4-META and the bone composite activator (observed after mixing) causing monomer instability (precipitation). Initiator and activator were not added at this stage to prevent possible solidification in the rheometer but are expected to have little effect on rheology due to their low levels.

Powder phases contained 70 wt% glass filler (0.7, 7  $\mu\text{m}$ , or equal mass of 0.7 and 7  $\mu\text{m}$ ) with the remainder a fixed level of MCPM (10 wt%), TSrP (15 wt%), and PLS (5 wt%). The liquid and powder were weighed using a four-figure balance. The composites were mixed using a planetary mixer (SpeedMixer, DAC 150.1 FVZ, Hauschild Engineering, Germany) at 2000 rpm for 2 min. An apparent viscosity of the mixed composite pastes was recorded.

**Table 4-1 Formulations of experimental bone composites for rheological test. Liquid phase contained fixed level of HEMA (5 wt%). Powder phase contained fixed level of active fillers (10 wt% MCPM, 15 wt% TSrP, and 5 wt% PLS).**

Formulations	Powder to liquid (R)	PPGDMA (P)	UDMA (U)	Glass filler (G)	
	Mass ratio	wt% of monomers in liquid phases		particle size and wt% in powder phase	
				0.7 $\mu\text{m}$	7 $\mu\text{m}$
<b>R<sub>3</sub>P<sub>75</sub>G<sub>7</sub></b>	3:1	75	20	0	70
<b>R<sub>3</sub>P<sub>75</sub>G<sub>0.7</sub></b>	3:1	75	20	70	0
<b>R<sub>3</sub>P<sub>25</sub>G<sub>7</sub></b>	3:1	25	70	0	70
<b>R<sub>3</sub>P<sub>25</sub>G<sub>0.7</sub></b>	3:1	25	70	70	0
<b>R<sub>2.6</sub>P<sub>50</sub>G<sub>7/0.7</sub></b>	2.6:1	50	45	35	35
<b>R<sub>2.3</sub>P<sub>75</sub>G<sub>7</sub></b>	2.3:1	75	20	0	70
<b>R<sub>2.3</sub>P<sub>75</sub>G<sub>0.7</sub></b>	2.3:1	75	20	70	0
<b>R<sub>2.3</sub>P<sub>25</sub>G<sub>7</sub></b>	2.3:1	25	70	0	70
<b>R<sub>2.3</sub>P<sub>25</sub>G<sub>0.7</sub></b>	2.3:1	25	70	70	0

#### 4.5.2 Rheological testing

Rheological properties of the experimental bone composites were measured using a strain-controlled oscillatory rheometer (ARES, TA instruments, DE, USA) with parallel plate geometry (25 mm in diameters). Composite pastes (n=2) were placed at the centre of the geometry. The distance between plates was set at  $1.0 \pm 0.2$  mm. After loading, the pastes were allowed to rest for 30 min before the test was started to ensure dissipation of any preshearing due to manipulation and loading of the pastes.

Dynamic strain and frequency sweep measurements were performed to assess viscoelastic properties of the composite pastes. For the strain sweep measurement, applied strain was increased from 0.008 % to 10 % while the oscillating frequency was fixed at 6.28 rad/s (Serra-Gómez et al., 2016). The frequency sweep measurement was performed by increasing angular frequencies from 0.05 to 100 rad.s<sup>-1</sup> with the strain fixed at 0.05 %. Storage and loss modulus (G' and G''), tangent of phase angle ( $\tan\delta$ ;  $\delta$  is ratio



of  $G''$  over  $G'$ ) (equations 2-1 to 2-6) and critical strain (strain when  $G'$  is declined) were measured. Finally, a continuous shear experiment (flow curve measurement) was undertaken to assess viscosity (equation 2-7) of the composite pastes with the shear rate ranging from 0.001 to 1  $s^{-1}$  for 90 s and from 1 to 100  $s^{-1}$  for 60 s. All tests were performed at a controlled temperature of 30 °C.

Storage modulus ( $G'$ ) represents the ability of materials to store energy without a phase difference between stress and strain.  $G'$  represents elastic component or the solid-like behaviour of fluids whereas  $G''$  represents viscous component or liquid-like behaviour.  $G'$  higher than  $G''$  indicates that materials are solid-like fluids. This can be additionally described using  $\tan\delta$  which is the tangent of phase angle ( $\tan\delta = G'' / G'$ ). Strong interaction between filler and resin matrix is observed with solid-like fluids (i.e. well-structured fluid). Dropping of  $G'$  at certain strain level (critical strain) indicates the disruption of fluid structure or physical / chemical bonds between fillers and resin matrix. High  $G'$  and critical strain therefore indicates more solid-like materials. Beyond this critical strain,  $G'$  drops more than  $G''$  leading to an increase of  $\tan\delta$  and the materials become more liquid-like.

## 4.6 Statistical analysis

Three variables with two levels factorial design (equations 2- 27,28) were employed to assess the effect of PLR (3:1, 2.3:1), PPGDMA level (75, 25 wt%), glass particle size (7, 0.7  $\mu m$ ) on storage modulus and critical strain from strain/frequency sweep measurements in addition to viscosity from flow curve measurement.

## 4.7 Results

### 4.7.1 Apparent viscosity

Simple visual inspection and manipulation of pastes enabled a crude estimation of relative paste viscosity and stability to sedimentation. Apparent viscosity of  $R_3P_{25}G_{0.7}$  was comparable with that of Cortoss (Table 4-2).  $R_3P_{75}G_{0.7}$ ,  $R_3P_{25}G_7$ , and  $R_{2.3}P_{25}G_{0.7}$  were of intermediate viscosity obviously higher in viscosity than all other composites. On average, the experimental composites containing 25 wt% of PPGDMA had higher apparent viscosity than the composites containing a higher level of this low viscosity diluent monomer. Furthermore, using small glass filler (0.7  $\mu\text{m}$ ) increased the apparent viscosity of the composite pastes.

Poor wetting was observed with  $R_3P_{25}G_{0.7}$  resulting in a very dry and crumbling paste. Conversely, high fluidity, large particle size and lack of sufficient paste structure with  $R_{2.3}P_{75}G_7$  and  $R_{2.3}P_{25}G_7$  enabled sedimentation of powder phases after storage at 4 °C for 24 hr.

**Table 4-2 Apparent viscosity and stability of the mixed composite pastes. Light, medium, and dark shades represent low, medium, and high apparent values respectively. Stars indicate sedimentation of the composite paste after storage in a fridge for 24 hr.**

Variables	PLR (mass ratio)	3:1				2.6:1	2.3 :1				Cortoss
	PPGDMA (wt%)	75		25		50	75		25		
	Glass filler (µm)	7	0.7	7	0.7	7+0.7	7	0.7	7	0.7	
Viscosity							*		*		

#### **4.7.2 Strain sweep measurement**

The strain-sweep curve of composites indicated that storage modulus ( $G'$ ) and loss modulus ( $G''$ ) remained unchanged (i.e. exhibited a linear viscoelastic region) at low strain but declined above a critical strain (Fig 4-1). When reaching these critical strains,  $G'$  of the composites dropped more than  $G''$  leading to an increase in  $\tan\delta$  above 1. This was particularly evident with sediment formulations ( $R_{2.3}P_{75}G_7$  and  $R_{2.3}P_{25}G_7$ ). This rise of  $\tan\delta$  upon increasing of strain was however not evident with Cortoss.

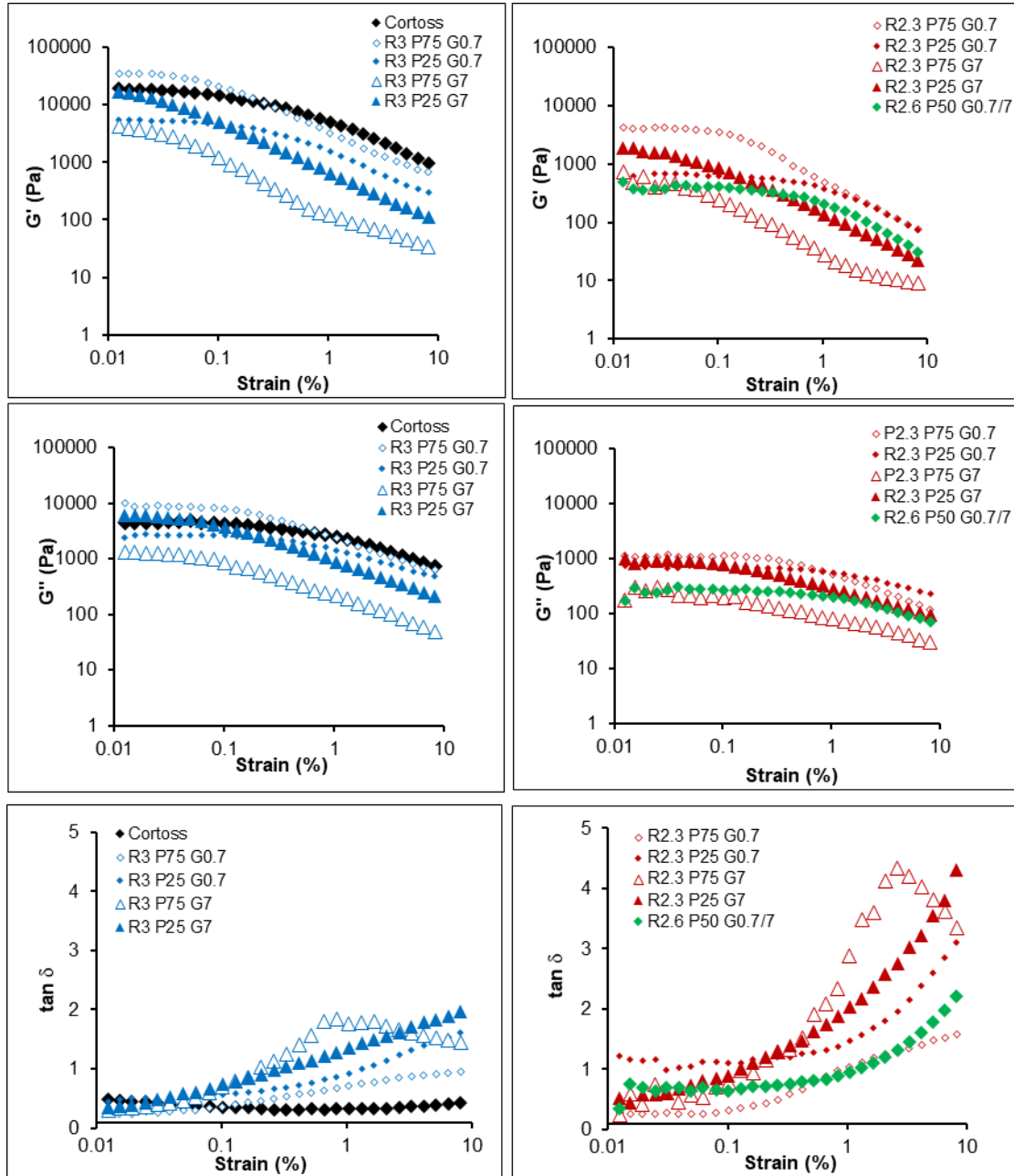
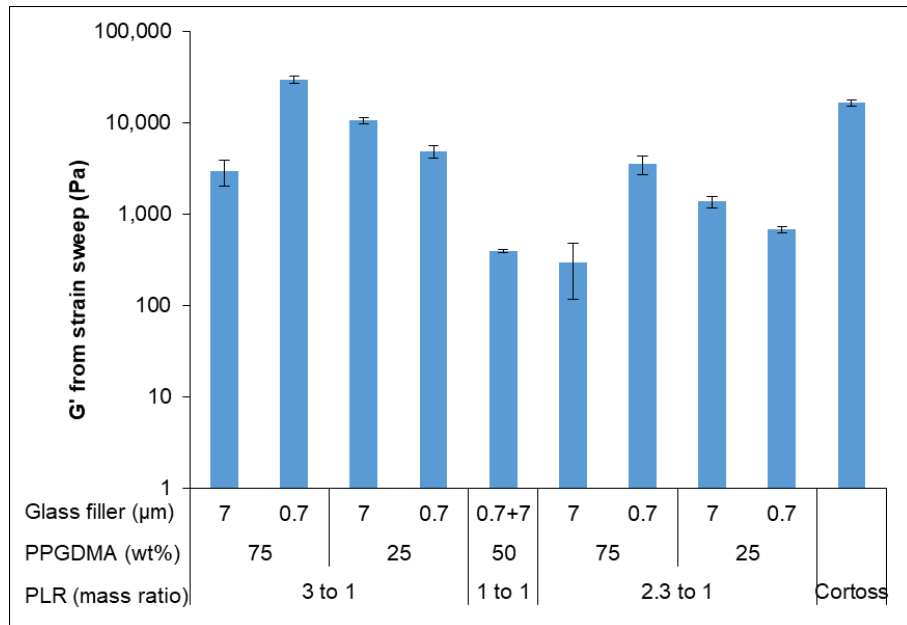


Fig 4-1 Storage modulus ( $G'$ ), loss modulus ( $G''$ ), and tangent of phase angle ( $\tan \delta$ ) plotted on log-log scales from strain sweep measurement of experimental bone composites and Cortoss. The frequency was fixed at 6.28 rad/s.

#### 4.7.2.1 Storage modulus ( $G'$ )

Average  $G'$  at strain between 0.01 – 0.1 % of experimental bone composites and Cortoss are presented in Fig 4-2. Experimental bone composites prepared with high PLR exhibited higher  $G'$  than the composites prepared with low PLR. Highest and lowest  $G'$  were obtained from  $R_3P_{75}G_{0.7}$  (29,550 Pa) and  $R_{2.3}P_{75}G_7$  (297 Pa) respectively. The  $G'$  of  $R_3P_{75}G_{0.7}$  was also higher than that of Cortoss (16,443 Pa). The average  $G'$  of the intermediate formulation ( $R_{2.6}P_{50}G_{0.7/7}$ , 395 Pa) was lower than the average  $G'$  of experimental bone composites (6719 Pa).

Factorial analysis indicated that  $G'$  of experimental bone composites was strongly affected by PLR (Fig 4-3).  $G'$  of the composites increased by  $735 \pm 135$  % upon increasing PLR. A strong interaction effect between PPGDMA level and glass particle size was also observed. This indicated that  $G'$  of the composites could either increase or decrease upon changing particle size depending on PPGDMA level. For example, when PPGDMA level was high,  $G'$  of the composites was increased by  $134 \pm 60$  % upon decreasing glass particle size. This effect, was, however, reversed when PPGDMA level was low.



**Fig 4-2** An average of  $G'$  (plotted on log scale) at strain between 0.01 to 0.1 % from strain sweep measurement. Error bars are 95 %CI (n=2).

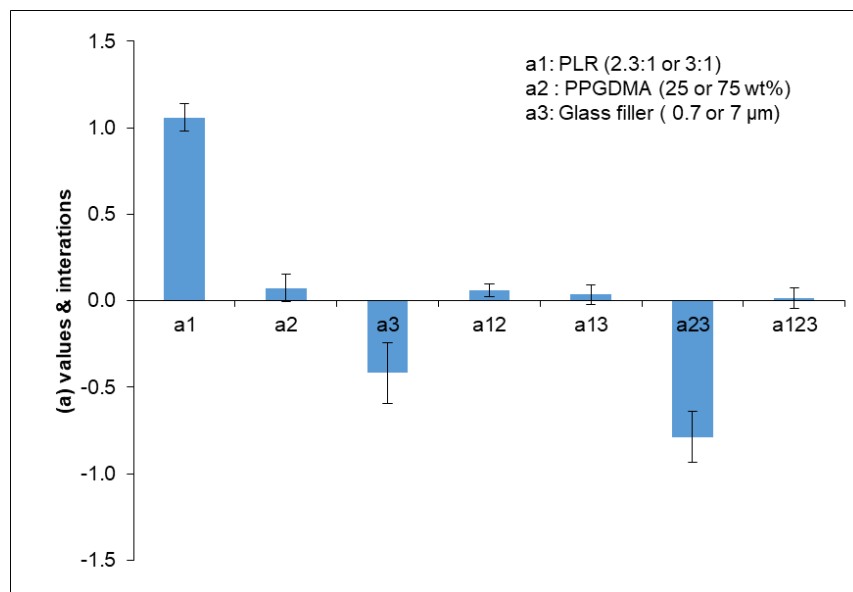


**Fig 4-3** Factorial analysis describing effect of PLR, PPGDMA, glass particle size, and their interaction effects on  $G'$  of experimental bone composites. Error bars are 95 %CI (n=2).

#### 4.7.2.2 Critical strain

A constant or independence of  $G'$  upon increasing strain indicates an intact structure of composites pastes and therefore solid-like behaviour. Beyond certain strain levels (critical strain),  $G'$  can decline, indicating a disruption of the fluid structure. The highest critical strain was observed with  $R_{2.3}P_{25}G_{0.7}$  (0.42 %) and  $R_{2.6}P_{50}G_{7/0.7}$  (0.42 %), which were higher than that of Cortoss (0.33 %) (Fig 4-4). Additionally, the critical strain of experimental bone composites containing 0.7  $\mu\text{m}$  glass filler were higher than that of the composites containing only 7  $\mu\text{m}$  glass filler. The average critical strain of the intermediate formulation ( $R_{2.6}P_{50}G_{0.7/7}$ , 0.42 %) was higher than the average  $G'$  of experimental bone composites (0.09 %).

Factorial analysis revealed that the primary factor affecting critical strain of the experimental bone composites was glass particle size (Fig 4-5). Critical strain of the composites was increased by  $643 \pm 1$  % upon decreasing glass particle size. The effect of PLR and PPGDMA were small and comparable with interaction effects. Factorial analysis was not employed for  $\tan\delta$  due to the lack of any trends from results.

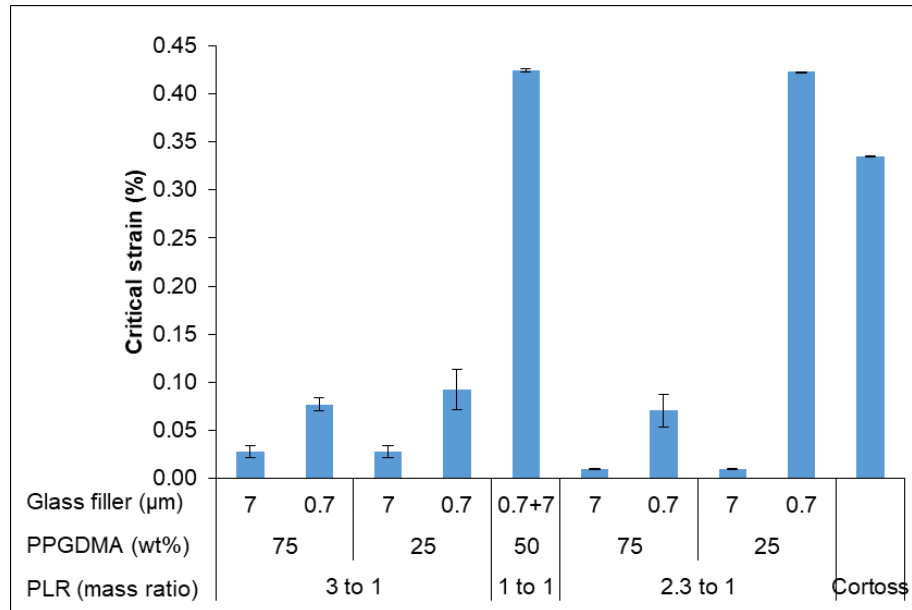


Fig 4-4 Critical strain (i.e. strain level where storage modulus drops) of all materials.

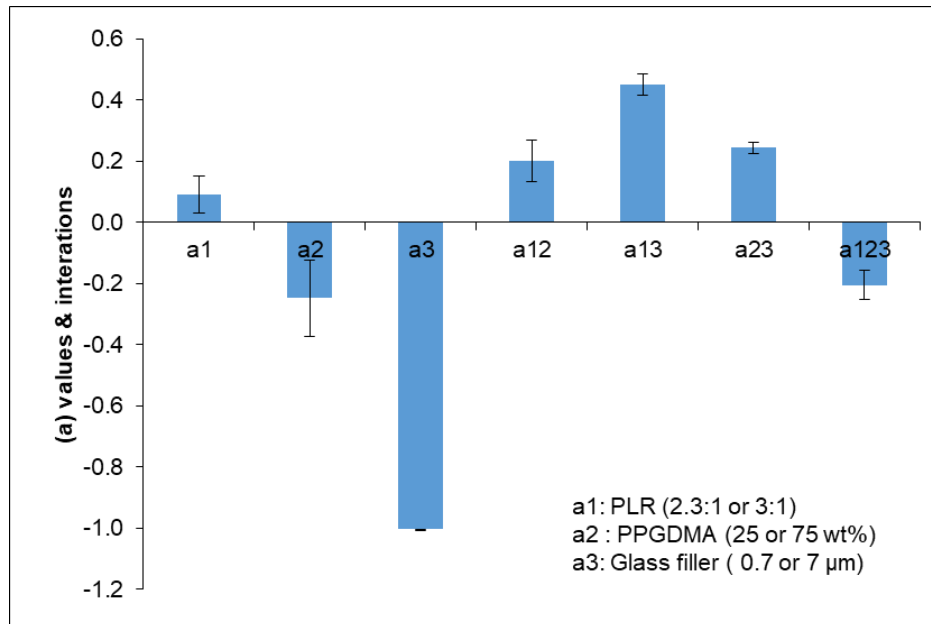


Fig 4-5 Factorial analysis describing effect of PLR, PPGDMA, glass particle size, and their interaction effects on critical strain of experimental composites.



### 4.7.3 Frequency sweep measurement

The independence of  $G'$  upon changing frequency indicated solid-like behaviour of composite pastes. This was largely observed with all materials except for  $R_{2.3}P_{75}G_7$  and  $R_{2.3}P_{25}G_7$  which showed a strong dependence of  $G'$  upon changing frequency (Fig 4-6).

Storage modulus ( $G'$ ) of composites prepared with PLR of 2.3 and 2.6 were lower than that of the composites prepared with PLR of 3:1.  $G'$  of Cortoss and the experimental bone composites prepared with PLR of 3:1 slightly decreased upon decreasing frequency (Fig 4-6). At high frequency loss modulus ( $G''$ ) of three composites ( $R_3P_{25}G_{0.7}$ ,  $R_{2.3}P_{25}G_{0.7}$ , and  $R_{2.6}P_{75}G_{0.7/7}$ ) exceeded their  $G'$  leading to the increase of  $\tan\delta$ .

Average of  $G'$  at frequency between 0.1 and 1  $\text{rad.s}^{-1}$  are presented in Fig 4-7. Highest and lowest  $G'$  were obtained from  $R_3P_{75}G_{0.7}$  (12,789 Pa) and  $R_{2.6}P_{70}G_{0.7/7}$  (68 Pa). The average  $G'$  of the intermediate formulation ( $R_{2.6}P_{70}G_{0.7/7}$ ) was lower than that of experimental bone composites (2750 Pa)

Factorial analysis indicated that primary factor influencing  $G'$  of experimental composites was PLR (Fig 4-8).  $G'$  of the composites was increased by  $951 \pm 238$  % upon raising PLR. Strong interaction effect between PPGDMA level and glass particle size was observed. This suggested that changing glass particle size increased or decreased  $G'$  of the composites depending on level of PPGDMA. Factorial analysis was not employed for  $\tan\delta$  due to the lack of trend from the results.

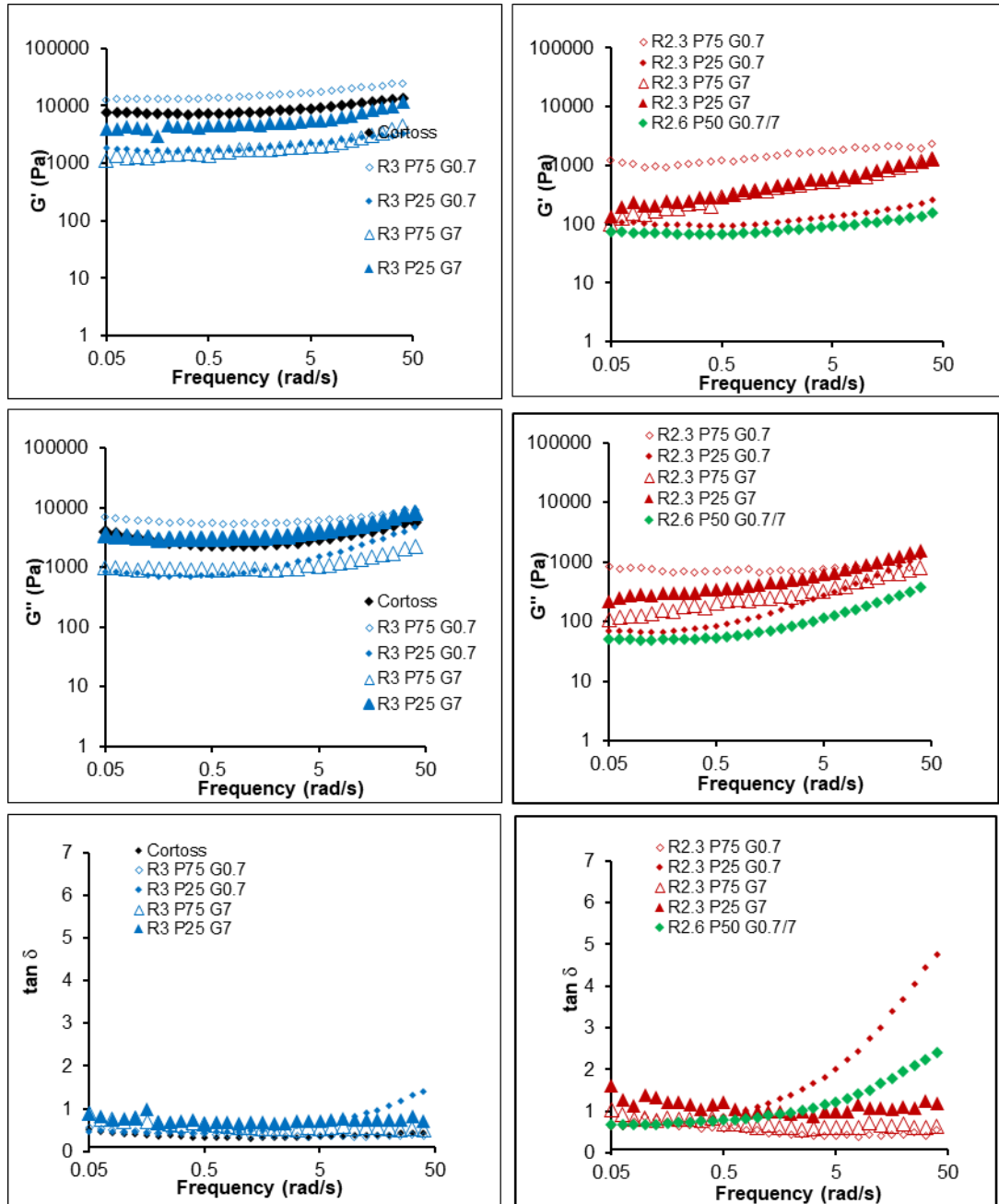
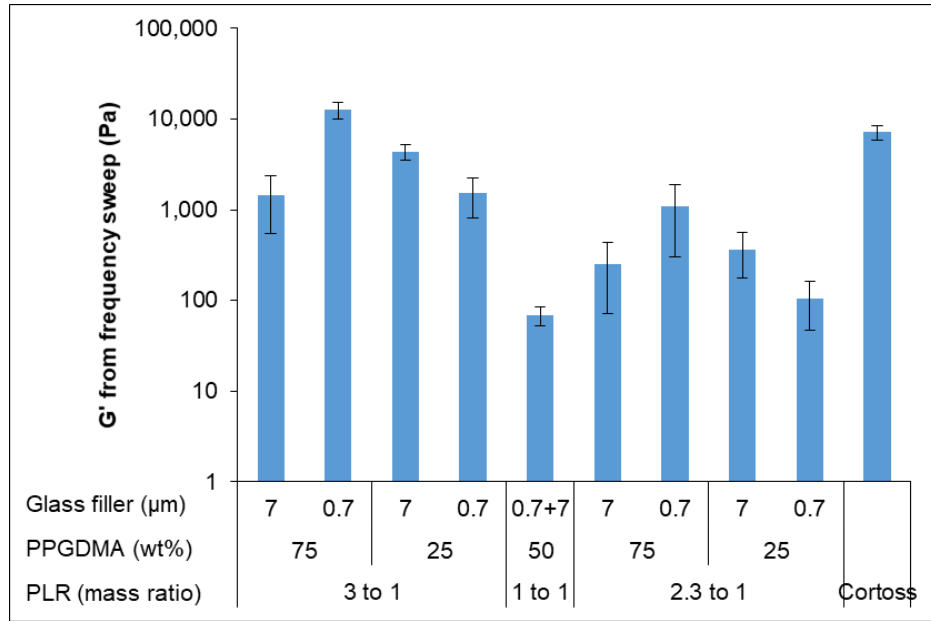
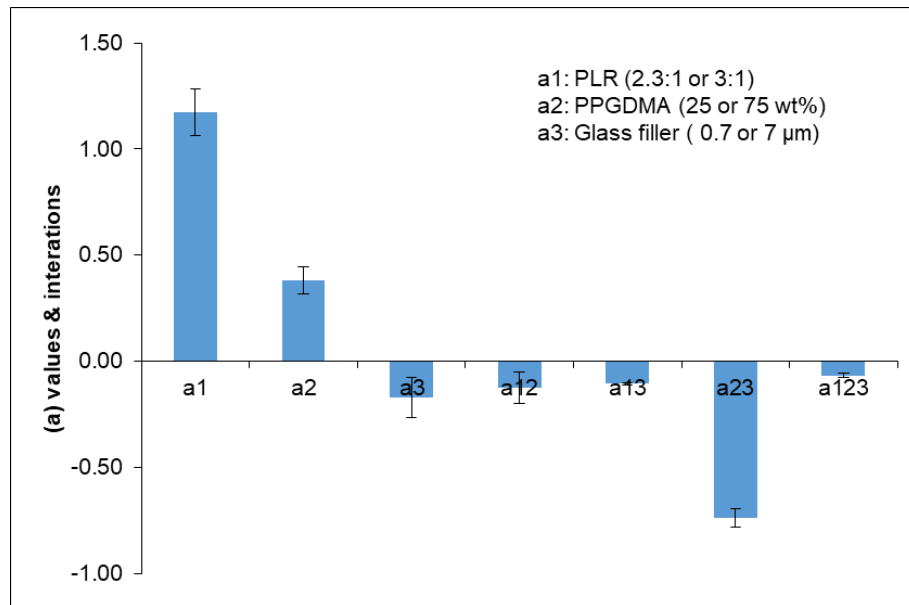


Fig 4-6 Storage modulus ( $G'$ ), loss modulus ( $G''$ ), and tangent of phase angle ( $\tan \delta$ ) plotted on log-log scales from frequency measurement of experimental bone composites and Cortoss. The strain was fixed at 0.05 %.



**Fig 4-7 Average of G' (plotted on log scale) at frequency between 0.1 to 1 rad.s<sup>-1</sup> from strain sweep measurement. Error bars are 95 %CI (n=2).**



**Fig 4-8 Factorial analysis describing effect of PLR, PPGDMA, glass particle size, and their interaction effects on G' of experimental composites from frequency sweep measurement.**

#### 4.7.4 Flow curve measurement

Viscosities of all materials decreased upon increasing shear rate indicating a shear-thinning behaviour (Fig 4-9). Average viscosities at shear rate between 0.1 to 1  $\text{s}^{-1}$  are presented in Fig 4-10. Highest and lowest viscosity were observed with Cortoss (2677 Pa.s) and  $\text{R}_{2.3}\text{P}_{75}\text{G}_7$  (89 Pa.s). Highest viscosities among experimental bone composites were obtained from  $\text{R}_3\text{P}_{25}\text{G}_{0.7}$  (2092 Pa.s) and  $\text{R}_3\text{P}_{25}\text{G}_7$  (2002 Pa.s). The average viscosity of experimental bone composites (720 Pa.s) was higher than that of the intermediate formulation (98 Pa.s).

From factorial analysis, main factors that affected viscosity of experimental composites were PLR and level of PPGDMA (Fig 4-11). Viscosity of the composites increased by  $386 \pm 70 \%$  and  $305 \pm 33 \%$  upon increasing PLR and decreasing PPGDMA level respectively. Effect from glass particle size was comparable to interaction effects.

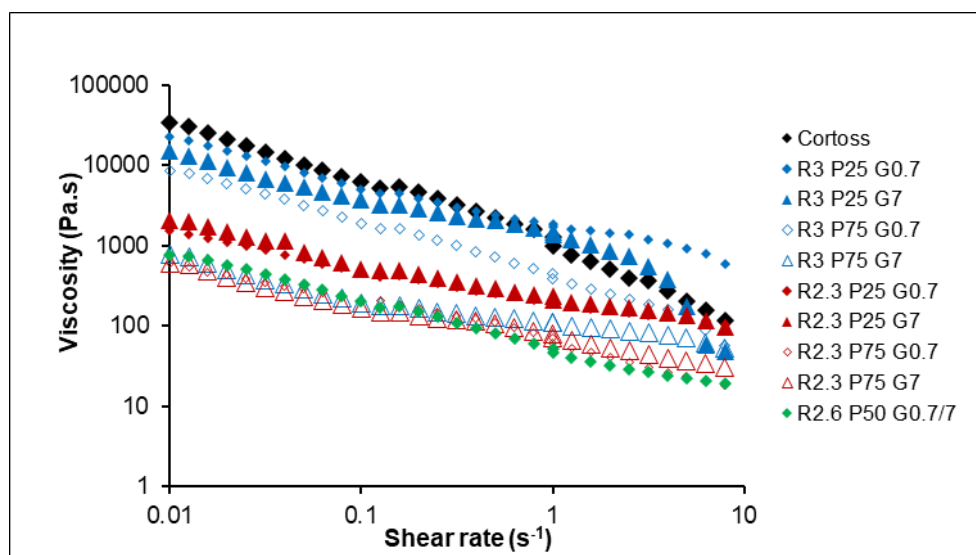
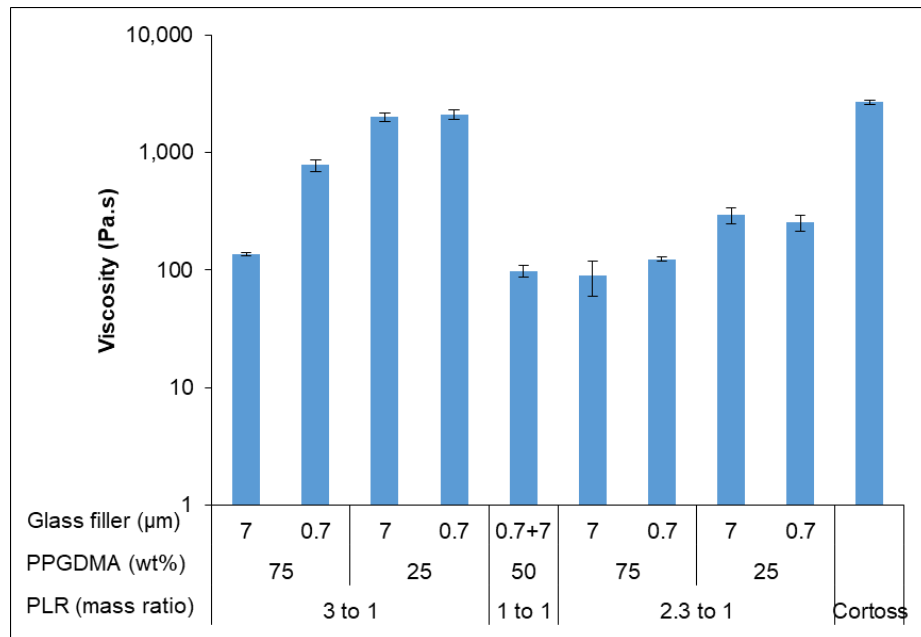
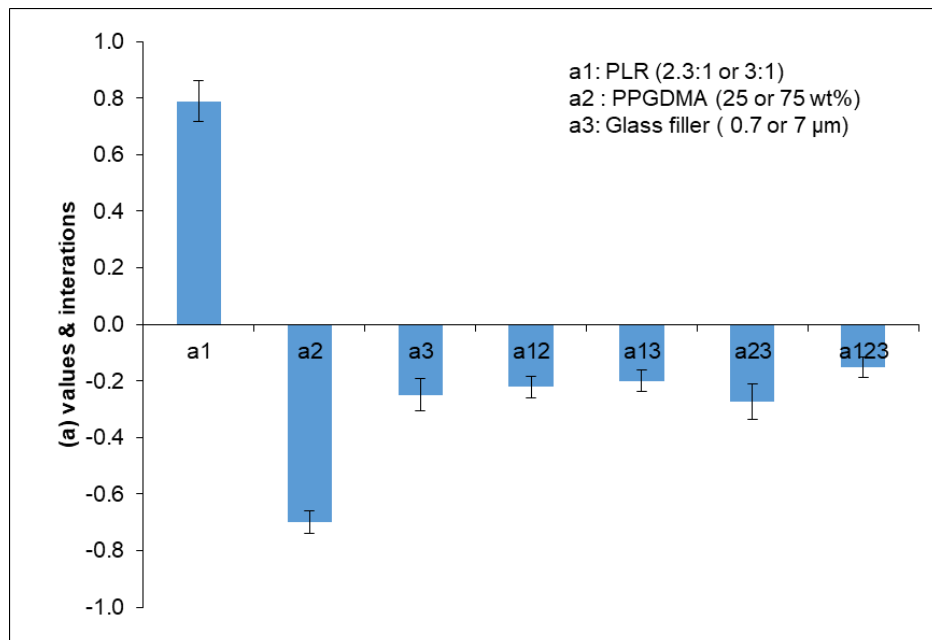


Fig 4-9 Viscosity versus shear rate ( $\text{s}^{-1}$ ) plotted on log-log scales of each material. All material showed a reduction of viscosity upon increasing shear rate.



**Fig 4-10 Average of viscosities (plotted on log scale) at shear rate between 0.1 and 1 s<sup>-1</sup>. Error bars are 95 % CI (n=2).**



**Fig 4-11 Factorial analysis describing effects of PLR, PPGDMA, glass particle size, and their interactions on viscosity of experimental bone composites. Error bars are 95 % CI (n=2).**

## 4.8 Discussion

This study assessed the effect of powder to liquid ratio, PPGDMA level, and glass particle sizes on rheological properties of the experimental bone composites.

As mentioned earlier, an ideal injectable bone composite should exhibit solid-like behaviour when exposed to low strain or frequency during storage or shipment. This may help to prevent sedimentation of the composite paste inside a double-barrel syringe. During injection, however, the structure of the paste should be easily disrupted enabling liquid-like behaviour. This may facilitate injection and flow of materials through small cracks and porosities of the fractured vertebra, which could ensure a good bone-composite adaptation/integration. Viscosity of the experimental bone composites should preferably increase again after the applied force is removed (thixotropic) to prevent cement leakage.

### 4.8.1 Apparent viscosities

Apparent viscosities of the experimental bone composites prepared with PLR of 2.3:1 were lower than that previously observed with experimental dental composites, which were prepared with PLR of 4:1, in Chapter 3. The reduced viscosity of bone composites would allow loading of the materials into a double-barrel syringe, which can be injected through an automatic mixing tip. Cortoss showed higher apparent viscosity than majority of experimental bone composites. Manufacturer of this commercial composite therefore supplies this material with a larger mixing tip (diameter of 5 mm) compared with the mixing tip (diameter of 2 mm) of experimental bone composites. High apparent viscosity observed with  $R_3P_{25}G_{0.7}$  suggests this formulation may not be suitable for use with syringe and mixing tip of the current study.

#### 4.8.2 Strain sweep measurement

Pastes of experiment bone composites showed viscoelastic properties. Solid-like behaviour was observed at low strain whilst more liquid-like behaviour was obtained at high strain. The increase of PLR increased storage modulus of experimental bone composites as was expected. Interaction effect between PPGDMA level and glass particle size, however, complicated the effect of each variable. Decreasing glass particle size increased storage modulus of the composites only when the PPGDMA level was high. This could be due to the fact that high level of diluent monomer compromised fluid structure of the composite pastes. Large surface area of small glass filler may mitigate the effect from high level diluent monomer by enabling strong interaction between monomers and silane coated on the surface of filler (Lee et al., 2006; Song et al., 2015). This effect from decreasing glass filler size reversed when PPGDMA level was low. High surface area may consequently lead to poor wetting of the small glass filler by monomers thereby compromising the fluid structure of composite pastes.

The decline of storage modulus ( $G'$ ) upon increasing strain (critical strain) indicates the disruption of fluid structure. Higher critical strain indicates a longer linear viscoelastic region and more solid-like of fluids. It suggests strong interaction between monomers and powder of the composite pastes. High surface area of small glass filler may therefore enable strong interaction between fillers and monomers. Hence, the primary effect on critical strain was glass particle size.

Tangent of phase angle ( $\tan\delta$ ) represents the ratio of liquid-like component ( $G''$ ) over solid-like component ( $G'$ ) of materials. The rising of  $\tan\delta$  observed with  $R_{2.3}P_{75}G_7$  and  $R_{2.3}P_{25}G_7$  upon increasing strain (Fig 4-1) indicated that the composites became more

liquid-like. This strong liquid-like behaviour may, however, increase the risk of sedimentation at rest which was observed with these formulations.

Sedimentation results from gravitational pull exceeding Brownian diffusion which is a random motion due to a collision of particles. Sedimentation is common when particle radius is greater than 1  $\mu\text{m}$  and the density difference between filler and medium exceeds 0.1 g/cc (Tadros, 2004). Additionally, sedimentation rate for more dilute dispersions is inversely proportional to viscosity of the medium. Raising diluent monomer level may therefore increase the risk of sedimentation.

#### **4.8.3 Frequency sweep measurement**

Composites that exhibited solid-like behaviour showed  $G'$  that are independence from angular frequency. It can be seen that  $G'$  of  $R_{2.3}P_{75}G_7$  and  $R_{2.3}P_{25}G_7$  was increased upon raising applied frequency (Fig 4-6). This may represent strong liquid-like behaviour of these formulations which is in agreement with the result from strain sweep measurement. The factor that most strongly affected  $G'$  of composites in frequency sweep measurements was powder to liquid ratio, which was in agreement with the strain sweep measurements.

#### **4.8.4 Flow curve measurement**

Flow curve measurement provided viscosity versus shear rate of experimental bone composites. This may mimic the flow of materials during injection in vertebroplasty. All materials in this chapter exhibited shear-thinning behaviour as their viscosities decreased upon increasing shear rate. This may allow easy injection during clinical application. The increase of powder content and decrease of diluent monomer level increased viscosity of the composite pastes. This was in agreement with previous



published studies (Ellakwa et al., 2007; Al-Ahdal et al., 2014). Changing glass particle size, however, showed minimal effect on the viscosity.

Limitation of this study was that initiator nor activator were incorporated into the experimental bone composites in order to enable material removal from the rheometer. Time sweep measurement of the composite should be tested in future studies to assess whether the viscosity of the composite pastes can be returned when the applied force is removed, which may help to prevent cement extravasation.

It has to be pointed out that results of the intermediate formulation of experimental bone composites did not exhibit intermediate results as would be expected for study designs without complex interaction effects between variables. This may be due to the complexity of composite rheological properties and interactions between monomer and filler phases.

In summary, increasing PLR from 2.3:1 to 3:1 enhanced solid-like behaviour which may improve paste stability. Increasing PLR also led to an increase of viscosity that may compromise handling properties and the manipulation of the pastes. The increase of PPGDMA from 25 to 75 wt% reduced viscosity of the composite pastes. Increasing ratio of diluent monomer to bulk monomer may increase heat generation and polymerisation shrinkage of the composites. This will be assessed in Chapter 8. Reducing glass filler size from 7 to 0.7  $\mu\text{m}$  enhanced solid-like behaviour and increased critical strain due possibly to the increase of filler-monomer interaction. Additionally, decreasing glass filler size showed no significant average effect on viscosity. Close to optimal physical stability and rheological properties, are observed with PLR of 2.3:1, 25 wt% PPGDMA, and 0.7  $\mu\text{m}$  glass filler.

This chapter analysed physical paste stability and flow characteristics of bone composites (without initiator/activator) upon applied strain, frequency, and shear rate.

Chemical stability and shelf life of composite pastes containing initiator and activator will be demonstrated in the next chapter.

## **4.9 Conclusions**

This study investigated the effect of powder to liquid ratio, PPGDMA level, and glass particle size on rheological properties of experimental bone composites. Within the limitations of this study, the following conclusions could be drawn.

- 1) The pre-cured experimental bone composite pastes exhibited viscoelastic properties. The composites showed solid-like behaviour when low frequency and strain were applied. Increasing the frequency and strain enabled liquid-like behaviour of the materials.
- 2) Increasing PLR and the use of small glass filler enhanced solid-like behaviour of the composites.
- 3) The increase of PLR and decrease of PPGDMA level increased viscosity of the composites. Furthermore, the composites exhibited shear-thinning behaviour as their viscosities reduced upon increasing shear rate.

## **Chaper 5 Assessment of High Temperature Aging on Concentrated Active Ingredient Dispersions and Bone Composite Pastes to Aid Prediction of Long-Term Chemical Stabilities of New Component Mixtures.**

### **5.1 Abstract**

**Purpose:** The objective was to assess chemical stability of monomers containing concentrated reactive components (MCPM, TSrP, PLS) and initiator pastes containing PPGDMA instead of TEGDMA upon high temperature accelerated ageing. Monomer conversion of the composite pastes after long term ageing at different storage temperatures was also examined.

**Materials and Methods:** Equal masses of MCPM, TSrP and PPGDMA, or PLS and UDMA or PPGDMA were mixed. FTIR spectra of the mixtures were obtained at elevated temperature (80 °C) for 1 hr. Initial, final, and difference spectra (difference between initial and final spectra) were recorded. FTIR spectra of the initiator composite pastes containing either PPGDMA or TEGDMA were recorded at elevated temperatures (50, 60, 70, and 80 °C). A predicted solidification time of the paste at low temperatures (4, 23, 37 °C) was obtained using Arrhenius equation. Additionally, the composites were aged at storage temperatures of 4, 23, 37 °C for up to 12 months. At various time points (1 day, 1, 3, 9, and 12 months), solidification of initiator paste and monomer conversion of the composites were examined.

**Results:** No spectral changes attributable to formation of new products or indicating reaction between phosphates or PLS with monomers were detected. The observed and predicted solidification time of initiator paste of PPGDMA based composite was longer than that of TEGDMA based composite. The PPGDMA based bone composite showed

higher monomer conversion than the TEGDMA based composite. Ageing the composites showed minimal effect on final monomer conversion. No solidification of initiator pastes for up to 12 months was observed with composites stored at 4 °C.

**Conclusion:** This study produced chemical activated bone composites pastes that are chemically stable upon high temperature ageing. Replacing TEGDMA by PPGDMA and storing experimental bone composites at 4 °C improved stability of initiator paste.

## 5.2 Introduction

Monocalcium and tricalcium phosphates were incorporated into dental composites or bone cements to promote mineralising properties for the materials (Han et al., 2009; Sa et al., 2015; Aljabo et al., 2016). Solubility of calcium phosphate compounds is determined by their Ca/P ratio. Low Ca/P ratio phosphates such as monocalcium phosphate can dissolve and release calcium and phosphate ions upon exposure to water. This subsequently enabled dicalcium phosphates precipitation (Tamimi et al., 2012). It has been shown that dicalcium phosphates can be detected after mixing powder of monocalcium phosphate with tricalcium phosphate at an ambient temperature (22 °C) without mixing with water (Gbureck et al., 2005). The study assumed that the condensed humidity could act as the reacting medium facilitating the precipitation of dicalcium phosphates. This could reduce shelf life of the cements.

A concern of chemical activated bone composite is their susceptibility to thermal initiated polymerisation due to the decomposition of benzoyl peroxide in initiator paste (Shim et al., 2005). Benzoyl peroxide (BP) can slowly dissociate even at low temperature. Therefore, manufacturers usually recommend to store chemical activated pastes below 4 °C (Cardoso et al., 2014). This ideal storage condition may, however, be difficult to achieve in some circumstances. For example, medical products shipping to tropical regions were exposed to an approximate temperature of - 4 to 42 °C and 10 to 40 °C during air and marine transport respectively (Nakamura et al., 2013).

The fluctuation in storage temperature may affect the stability and curing characteristics of the bone composites. The effect of temperature on stability or shelf life of materials can be assessed using accelerated aging method (Main, 2013). The method simulates real time aging by storing samples at an elevated temperature in reduced amount of time

(American Society for Testing and Materials, 2013). Main (2013) employed Arrhenius equation to assess the effect of initiator and activator levels on predicted shelf life of UDMA/TEGDMA experimental bone composites upon accelerated temperature ageing. Main also revealed that decreasing level of initiator increased inhibition time and predicted shelf-life without detrimental effect on final monomer conversion of the composites. Khan (2015) and Walters et al. (2016) assessed the effect of replacing lower molecular weight TEGDMA by higher molecular weight PPGDMA. The studies showed that PPGDMA increased inhibition time, reduced polymerisation shrinkage, and monomer conversion of bone and dental composites. However, effect of different diluent monomers (TEGDMA and PPGDMA) on stability of experimental bone composites has not as yet been investigated.

### **5.3 Hypotheses**

Previous chapter has demonstrated effects of powder to liquid ratio, diluent monomer level, and glass particle sizes on rheological properties and the risk of powder sedimentation that could potentially reduce shelf life of pre-cured bone composite pastes. This chapter will focus on the stability of active ingredients (MCPM, TSrP, and PLS) and effect of type of diluent monomer on long term stability of experimental bone composites containing initiator and activator.

Reactions between chemicals in the precured composite pastes that are accelerated by high temperature ageing can be monitored by obtaining FTIR spectra before and after the temperature ageing. Additionally, FTIR spectra can be compared with expected spectra. Any unexpected FTIR spectra may indicate the formation of new products and therefore poor stability of active ingredients. It was, therefore, anticipated that

unpredicted or new FTIR spectra will not be observed from of the concentrated mixtures of active ingredients in monomers upon accelerated temperature ageing.

It is known that raising temperature will increase rate of polymerisation. The relationship between rate of polymerisation and temperature also follows Arrhenius type equation, which can be used to predict shelf life of bone composites (Main, 2013). Using the Arrhenius equation in Main's study demonstrated that the predicted shelf life of UDMA/TEGDMA composites decreased linearly with the increase of initiator and activator concentrations. The effect of different diluent monomers, however, has not yet been investigated. It was expected that the Arrhenius method can be used to assess the stability of initiator and activator pastes of experimental bone composites containing different diluent monomers (TEGDMA or PPGDMA).

According to the literature described above, replacing lower molecular weight diluent monomer (TEGDMA) by higher molecular weight monomer (PPGDMA) increased inhibition time, reaction rate, and final monomer conversion of experimental bone composites. It was anticipated that replacing TEGDMA by PPGDMA will not affect stability of the initiator or activator pastes. It was also expected that monomer conversion of the UDMA/PPGDMA experimental bone composites will be higher than that of UDMA/TEGDMA base composite as was observed with previous studies. In addition, monomer conversion of the composites should remain unchanged upon paste pre-ageing at different temperatures to ensure long shelf-life of the composites.

## 5.4 Objectives

The aim of this study was to develop chemically activated bone composites that have long-term chemical stability. The objectives of this study were to assess:

- 1) Stability of reactive ingredients (MCPM, TSrP, and PLS) in monomers;
- 2) Stability of initiator and activator pastes of experimental bone composites containing PPGDMA versus TEGDMA upon accelerated temperature ageing;
- 3) The effect of paste aging at fridge temperature (4 °C), room temperature (23 °C), and body temperature (37 °C) on subsequent monomer conversion for composites containing PPGDMA versus TEGDMA.

## 5.5 Materials and method

### 5.5.1 Stability of active ingredients in monomers

MCPM and TSrP were mixed with monomers (Table 5-1) to assess the stability of mixed phosphate components in the experimental bone composites. Furthermore, PLS was mixed with bulk (UDMA) or diluent monomer (PPGDMA) to ensure the stability of PLS in the composite paste. High levels of powder phase were used to accelerate any possible reactions and aid ease of detection by FTIR.

**Table 5-1 Formulations of the composites for chemical stability test.**

<b>Formulation/component</b>	<b>UDMA (g)</b>	<b>PPGDMA (g)</b>	<b>MCPM (g)</b>	<b>TSrP (g)</b>	<b>PLS (g)</b>
Formulation 1	0	1	1	1	0
Formulation 2	1	0	0	0	1
Formulation 3	0	1	0	0	1



Powder and monomer were weighed using a four-figure balance and mixed using a planetary mixer (SpeedMixer, DAC 150.1 FVZ, Hauschild Engineering, Germany) at 2000 rpm for 2 min. FTIR spectra of the mixtures held at a controlled temperature of 80 °C were measured for 1 hr. Initial and final spectra of the mixtures, in addition to the difference between initial and final spectra (residual), were recorded. The spectra were then compared with expected spectra obtained from FTIR of pure components at 23 °C (Table 5-2) using the modified Beer-Lambert-Bonguer 's equation (equation 2-9). New or unpredicted peaks obtained from the test may indicate the formation of new products due to reaction between components.

**Table 5-2 FTIR peaks powder and liquid phase. Reported positions were obtained from published studies (Young et al., 2004; Rozenberg and Shoham, 2007; Young et al., 2008; Shukla and Rai, 2013; Azam et al., 2015).**

Peak wave number (cm <sup>-1</sup> )		Assignments	Intensity	Components
Observed positions	Reported positions			
Powder phase				
952	-		m	TSrP
956	955	PO sym stretch	s	MCPM
984	984	PO sym stretch	s	Brushite
988	992	PO sym stretch	s	Monetite
1006	-		s	TSrP
1048	1060	PO asym stretch	s	Brushite
1066	1064	PO asym stretch	s	Monetite
1086	1075	PO asym stretch	s	MCPM
1110	1132	PO asym stretch	s	Brushite
1114	-		w	TSrP
1122	1128	PO asym stretch	s	Monetite
1508	1504	Protonated $\text{NH}_3^+$ side chain groups	s	PLS
1558	1537 - 1566	C-N (amide II) stretch	s	PLS
1660	1650 -1670	C=O (amide I) stretch	s	PLS
2866	2871	CH <sub>2</sub> stretch	w	PLS
2918	2937	CH <sub>2</sub> stretch	w	PLS
3236	3240	Amide A	w	PLS
3382	3378	NH stretch	w	PLS
Liquid phase				
1136	1120, 1114	C-O-C asym stretch	s	UDMA, PPGDMA
1168	1168	C=C stretch	s	PPGDMA, UDMA
1244	1240	N-H deformation	s	UDMA
1290,1320	1300,1320	C-O stretch	m	UDMA, PPGDMA
1378	1370	C-H bend	w	PPGDMA
1448	1453	C-H scissor	m	UDMA, PPGDMA
1512	1525	N-H deformation	s	UDMA
1638	1635	C=C stretch	w	UDMA, PPGDMA
1714	1720	C=O stretch	s	UDMA, PPGDMA
2882	2890	C-H stretch	w	PPGDMA
2964	2960	C-H stretch	w	UDMA
2976	2960	C-H stretch	w	PPGDMA
3334	3295-3460	N-H stretch	w	UDMA

Intensity of the peaks: w: weak; m: medium; s: strong.

### 5.5.2 Stability of experimental bone composites

Experimental bone composites were prepared using a powder to liquid ratio (weight ratio) of 2.3:1 to enable injection of the composites through a fine bore needle. The liquid phase (Table 5-3) contained 70 wt% UDMA, 25 wt% of PPGDMA or TEGDMA, and 5 wt% of HEMA. To this was added either BP (3 wt% of total liquid phase) for the initiator liquid or NTGGMA (2 wt%) for the activator liquid. Khan (2015) revealed that setting kinetic and mechanical properties of experimental bone composites were strongly affected by concentrations of BP and NTGGMA. The level of BP and NTGGMA for experimental bone composites after mixing in this thesis were 1.5 wt% and 1 wt% which was expected to enable high final monomer conversion of the composites. These levels of BP and NTGGMA were fixed in all formulations throughout this thesis to prevent any effects from level of initiator and activator variation.

**Table 5-3 Components of liquid phases before mixing with the powder phase.**

Liquid phase / components	UDMA	PPGDMA / TEGMA	HEMA	BP	NTGGMA
	wt% of monomers	wt% of monomers	wt% of monomers	wt% of liquid	wt% of liquid
<b>Initiator liquid</b>	70	25	5	3	0
<b>Activator liquid</b>	70	25	5	0	2

N.B. Upon mixing the composite BP and NTGGMA concentrations will become 1.5 and 1 wt% respectively

Powder phase (Table 5-4) contained mono calcium phosphate (MCPM) (10 wt% of filler after mixing), glass fibre (20 wt% of filler), tristrontium phosphate (7.5 wt% of filler after paste mixing), and polylysine (5 wt% of filler).

**Table 5-4** The powder phase of each formulation was mixed with PPGDMA (PPG) or TEGDMA (TEG) liquid phases presented in Table 5-3.

Formulations		0.7 $\mu$ m glass fillers (wt%)	Glass fibres (wt%)	MCPM (wt%)	TSrP (wt%)	PLS (wt%)
<b>M<sub>10</sub>PPG / M<sub>10</sub>TEG</b>	Initiator paste	55	20	20	0	5
	Activator paste	60	20	0	15	5

N.B. MCPM in filler is halved after mixing initiator and activator paste. TSrP and PLS are half and double that in the dental composite respectively.

Powder and monomer were weighed and mixed using the same method described earlier in Chapter 2 (section 2.1). Monomer conversion versus time of initiator and activator pastes of the experimental bone composites were measured at control temperatures of 80, 70, 60, and 50 °C. Solidification time (time when monomer conversion reached 50%) were recorded. Predicted solidification time of initiator paste solidification at low temperatures (4, 23, and 37 °C) of the experimental bone composites were obtained assuming an Arrhenius type equation (equations 2-14,15). Additionally, the composites were stored at 4, 23, and 37 °C. At various time points (1 day, 1, 3, 9, and 12 months), the composites were removed and checked for any solidification of the initiator paste. At time points and temperatures where solidification had not occurred, composites were mixed and their inhibition time, maximum rate of polymerisation (equation 2-13), and final monomer conversion (equation 2-12) were reassessed.

## 5.6 Results

### 5.6.1 Stability of active ingredients in monomers

Formulation 1 containing equal masses of MCPM, TSrP, and PPGDMA was prepared to assess if dicalcium phosphates can be formed due to MCPM reacting with TSrP in monomer upon high temperature ageing. Absorbance remained largely unchanged upon aging except for an increase in peaks at 948, 1006, and 1088  $\text{cm}^{-1}$  (Fig 5-1 A). A residual spectrum, obtained from the difference in final and initial spectra, is compared with spectra of pure chemicals in Fig 5-1 B. The residual spectrum had strong peaks at 954, 1016, and 1046  $\text{cm}^{-1}$  consistent with TSrP (948, 1006, and 1046  $\text{cm}^{-1}$ ). It is possible that a strontium equivalent of monetite or brushite is being formed although the positions of the peaks suggest sedimentation is a more likely explanation of spectral changes. The increased absorbance of the TSrP peaks could occur upon sedimentation of particles and their better contact with the ATR diamond. The smaller size of TSrP (10 micron) compared with that of MCPM (50 micron) will facilitate this increased diamond contact.

PLS was mixed with an equal mass of monomers to assess stability of PLS in UDMA (formulation 2) or PPGDMA (formulation 3) upon accelerated high temperature aging. The similarities in initial, final and predicted spectra indicate good stability (Figs 5-2 A, 5-3 A). The residual spectra are consistent with an increase in PLS contact with the diamond possibly due to sedimentation or melting of the PLS particles (Figs 5-2 B, 5-3 B). The residual spectrum was stronger using PPGDMA presumably due to its lower viscosity enabling greater sedimentation.

## Formulation 1: PPGDMA+TSrP+MCPM

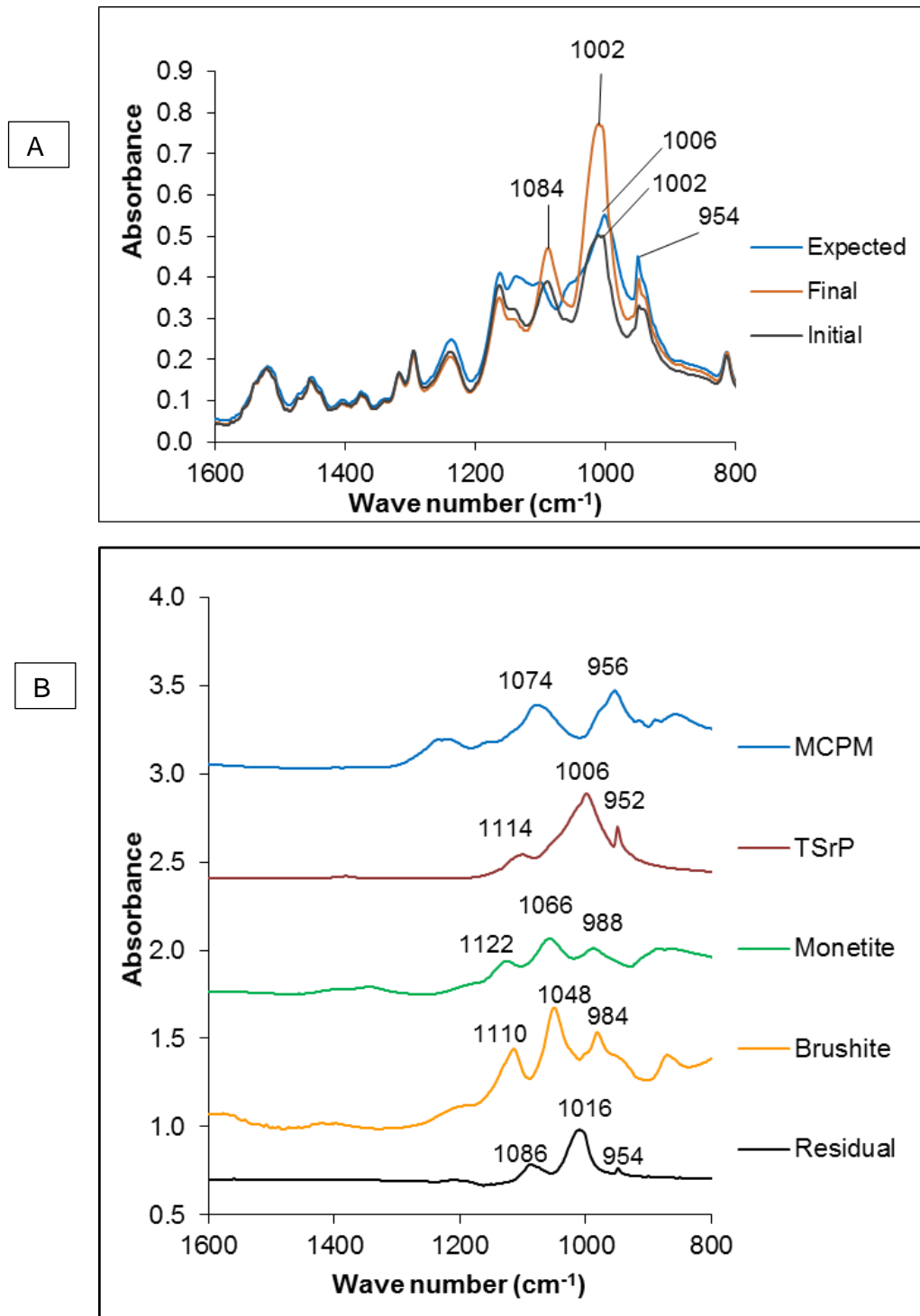


Fig 5-1 A) Initial, 1 hour 80 °C stored, and expected FTIR spectra of a mixture of equal masses of MCPM, TSrP, and PPGDMA. B) Spectra of pure phosphates and Residual spectrum (difference between final and initial spectra). Labels indicate phosphate peaks ( $\text{PO}_4$ ).

## Formulation 2: UDMA + PLS

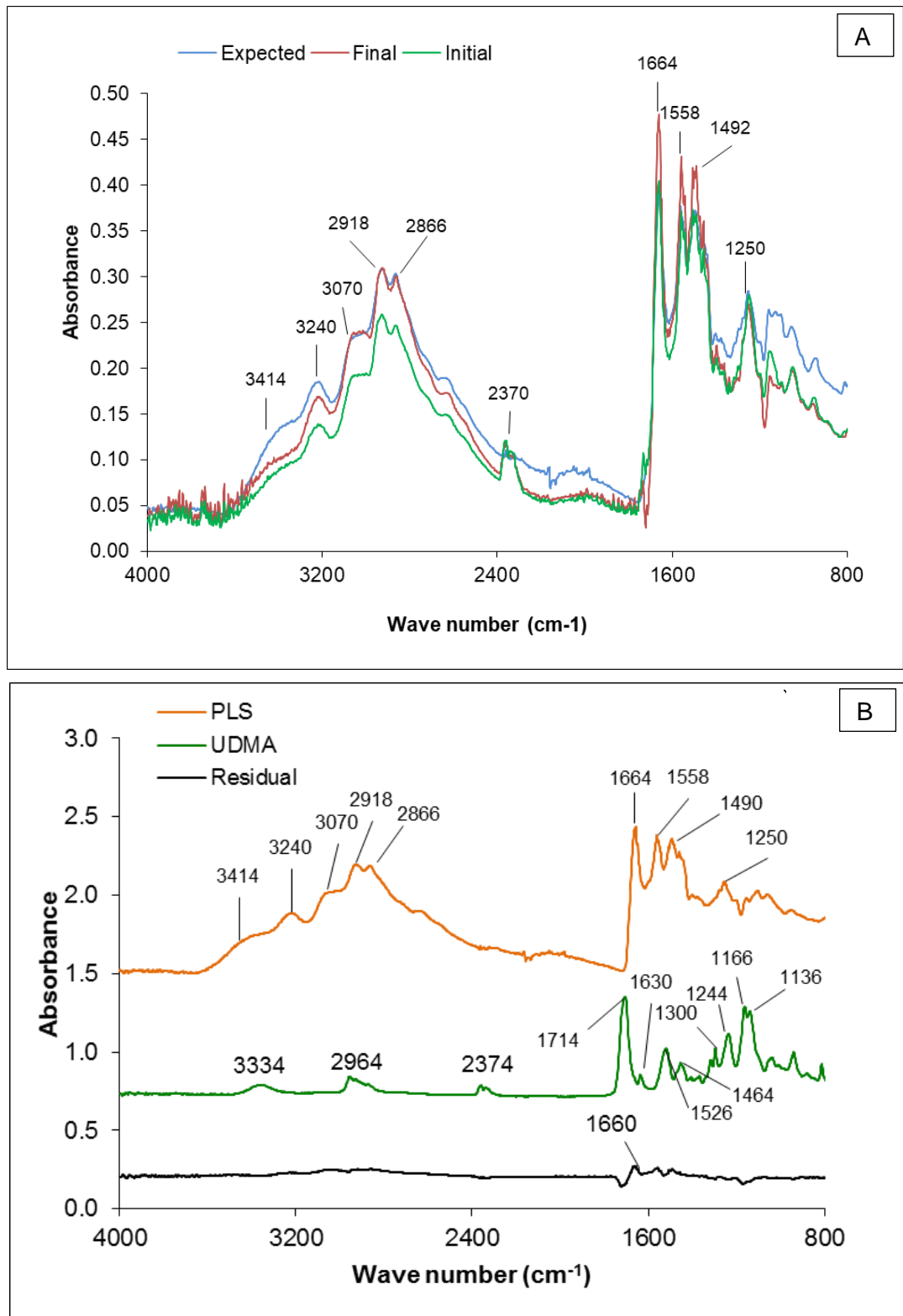


Fig 5-2 A) Initial, 1 hour 80 °C stored, and expected FTIR spectra of a mixture of equal masses of PLS and UDMA. B) Spectra of pure components and Residual spectrum (difference between final and initial spectra).

## Formulation 3: PPGDMA + PLS

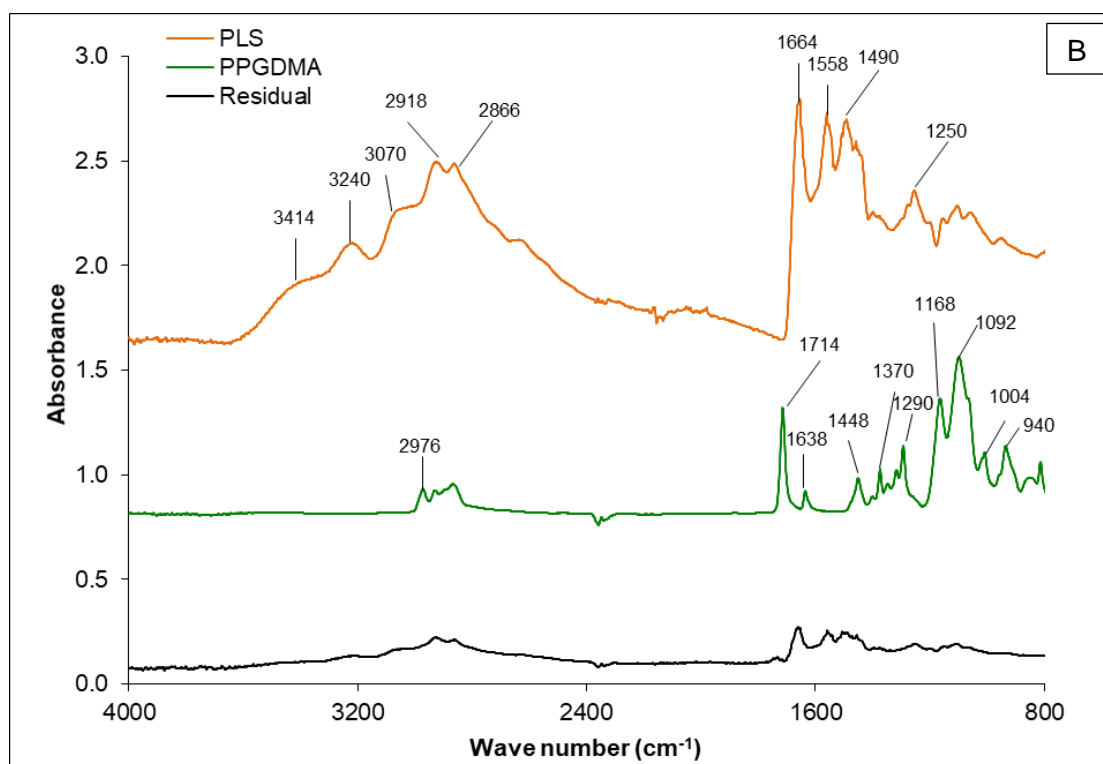
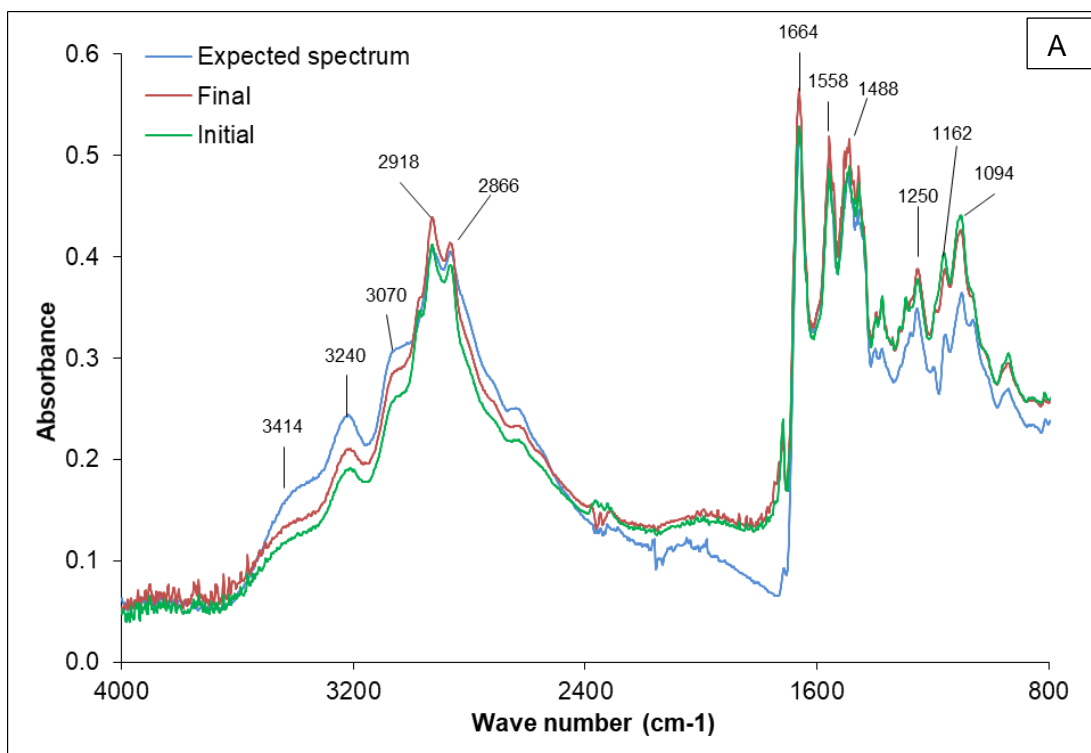


Fig 5-3 A) Initial, 1 hour 80 °C stored, and expected FTIR spectra of a mixture of equal masses of PLS and PPGDMA. B) Spectra of pure components and Residual spectrum (difference between final and initial spectra).



## 5.6.2 Stability of initiator and activator pastes

### 5.6.2.1 Predicted paste stability

Plots of monomer conversion of initiator and activator pastes of  $M_{10}$ PPG tested at 80 °C versus time are shown in Fig 5-4. The initiator paste exhibited rapid increase of monomer conversion. Conversion of 50 % in the initiator paste was obtained at 5 min ( $t_{50}$ ). In contrast, monomer conversion of the activator paste was barely changed (< 5%) over 1 hour at 80 °C.

As the initiator pastes were more susceptible to thermal-initiated polymerisation initiator pastes of  $M_{10}$ PPG and  $M_{10}$ TEG were used to quantify time of solidification at high temperature and predict that at low temperature (shelf life) by employing Arrhenius equations. Monomer conversion of the composites measured at elevated temperatures (50 – 80 °C) are given in Fig 5-5. In this study,  $t_{50}$  was the time when monomer conversion reached 50% which was used to indicate the time at which self-initiated polymerisation or solidification would occur.

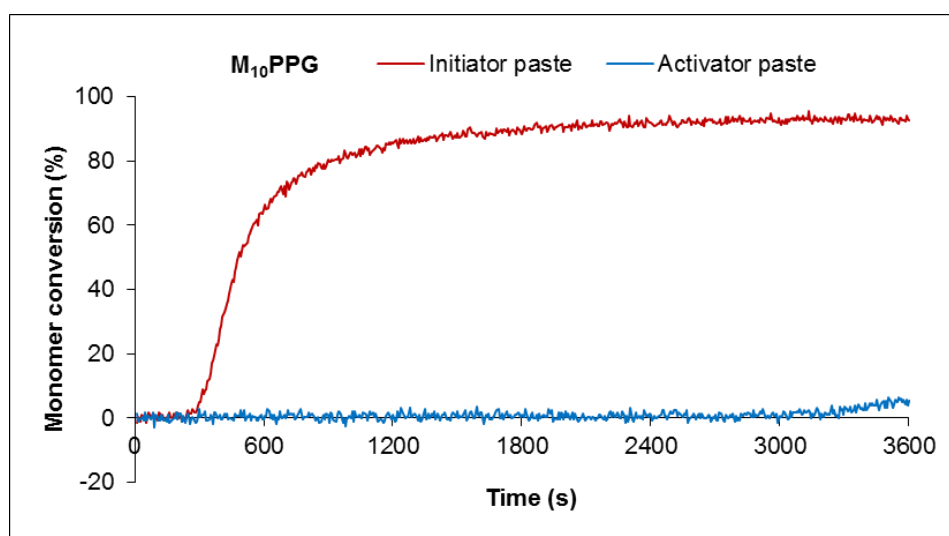


**Fig 5-4 Example polymerisation profiles for initiator and activator pastes of  $M_{10}$ PPG at 80 °C. After 5 min, the initiator paste showed rapid monomer conversion levelling off at >90% after 20 min. In contrast, the conversion of the activator paste was negligible even after 1 hour at 80 °C.**

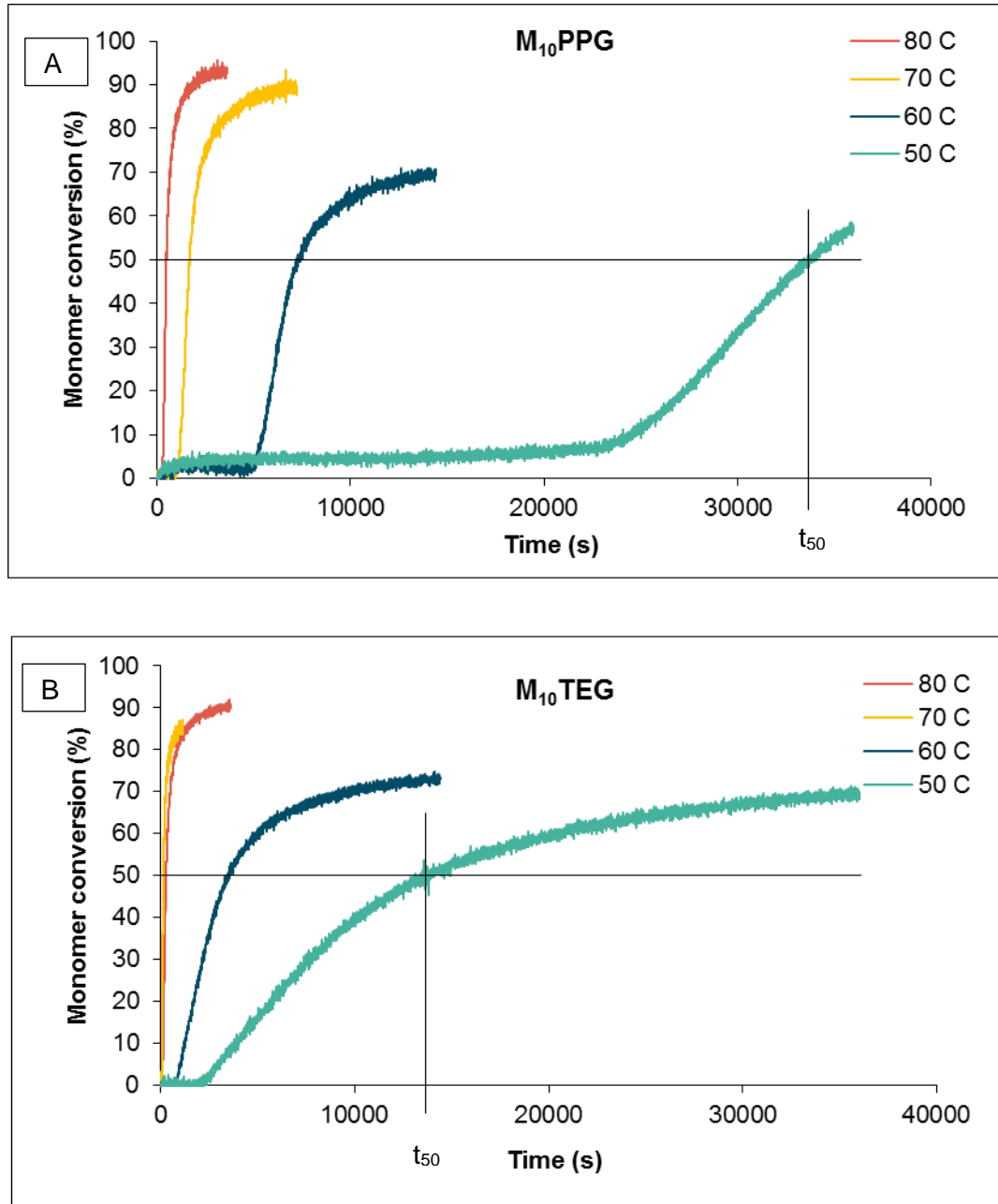


**Fig 5-5** Polymerisation profiles of A) M<sub>10</sub>PPG and B) M<sub>10</sub>TEG initiator pastes at different temperatures. Time when monomer conversion reached 50% ( $t_{50}$ ) was used in the Arrhenius plots.

Plots of  $\ln(1/t_{50})$  versus inverse temperature (Kelvin) (Fig 5-6) demonstrated a good linear relationship ( $R^2 = 0.99$ ) as expected from the Arrhenius equation (equations 2-7,8).  $t_{50}$  of the experimental bone composites at low temperatures (4, 25, and 37 °C) was extrapolated from regression lines (Table 5-5). It can be seen that  $t_{50}$  of M<sub>10</sub>TEG was shorter than M<sub>10</sub>PPG at all tested temperatures. The predicted  $t_{50}$  of M<sub>10</sub>PPG was longer than M<sub>10</sub>TEG at all temperatures. These predicted  $t_{50}$  were compared with the observed solidification time of initiator paste stored at 4, 23, and 37 °C in the next section.

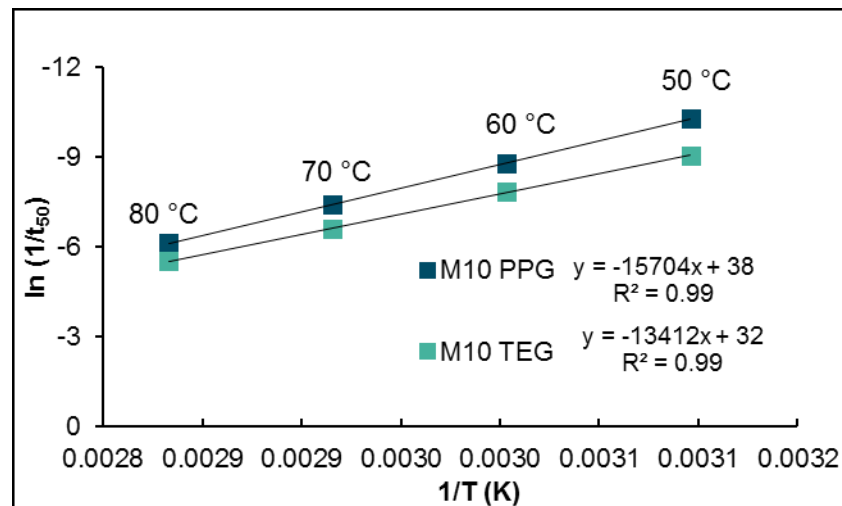


Fig 5-6 Arrhenius plots of  $\ln 1/t_{50}$  versus inverse temperature (T) in Kelvin.

### 5.6.2.2 Observed initiator paste stabilities

M<sub>10</sub>PPG and M<sub>10</sub>TEG were stored at 4, 23, and 37 °C and inspected after 1 day, and 1, 3, 9 and 12 months. Over 12 months all activator pastes remained fluid irrespective of temperature. At 1 month, however, initiator pastes of both M<sub>10</sub>PPG and M<sub>10</sub>TEG had solidified in the syringe stored at 37 °C (Table 5-5). Initiator pastes stored at 23 °C were solidified between 1 and 3 months for M<sub>10</sub>TEG but between 3 and 9 months for M<sub>10</sub>PPG. No solidification of initiator pastes was observed for composites stored at 4 °C. The observed solidification time of the initiator pastes showed similar trends but generally were longer than those predicted from the Arrhenius plots.

**Table 5-5 Predicted  $t_{50}$  at 4, 23, and 37 °C obtained using Arrhenius method and observed times of solidification of initiator pastes.**

Temperature (°C)	M <sub>10</sub> PPG		M <sub>10</sub> TEG	
	$t_{50}$	Time of solidification	$t_{50}$	Time of solidification
37 °C	3 days	< 1 month	1 day	< 1 month
23 °C	30 days	3-9 months	4 days	1-3 months
4 °C	40 months	> 12 months	2 months	> 12 months

### **5.6.3 Effect of ageing on monomer conversion of the experimental bone composites**

M<sub>10</sub>PPG and M<sub>10</sub>TEG were kept at storage temperatures of 37, 23, and 4 °C. At time points and temperatures where solidification had not occurred, the composites were mixed and their monomer conversion kinetics were reassessed. Initiator pastes of both formulations kept at 37 and 23 °C were solidified before 9 months. Therefore, monomer conversion of the composites stored for longer time (9 -12 months) was assessed only from the composites kept at the storage temperature of 4 °C.

### 5.6.3.1 Inhibition time

The inhibition times of M<sub>10</sub>PPG pastes stored at 37, 23, and 4 °C measured after relatively short storage times (1 day – 3 months) were all comparable (54 – 64 s) (Fig 5-7). The average inhibition time of the composite kept at 4 °C for a longer storage time (9 -12 months) was slightly increased to  $76 \pm 18$  s. For M<sub>10</sub>TEG, the inhibition times of composite pastes kept at 37, 23, and 4 °C for up to 3 months were 45 – 50 s. Longer term storage at 4 °C increased this time to  $97 \pm 15$  s.

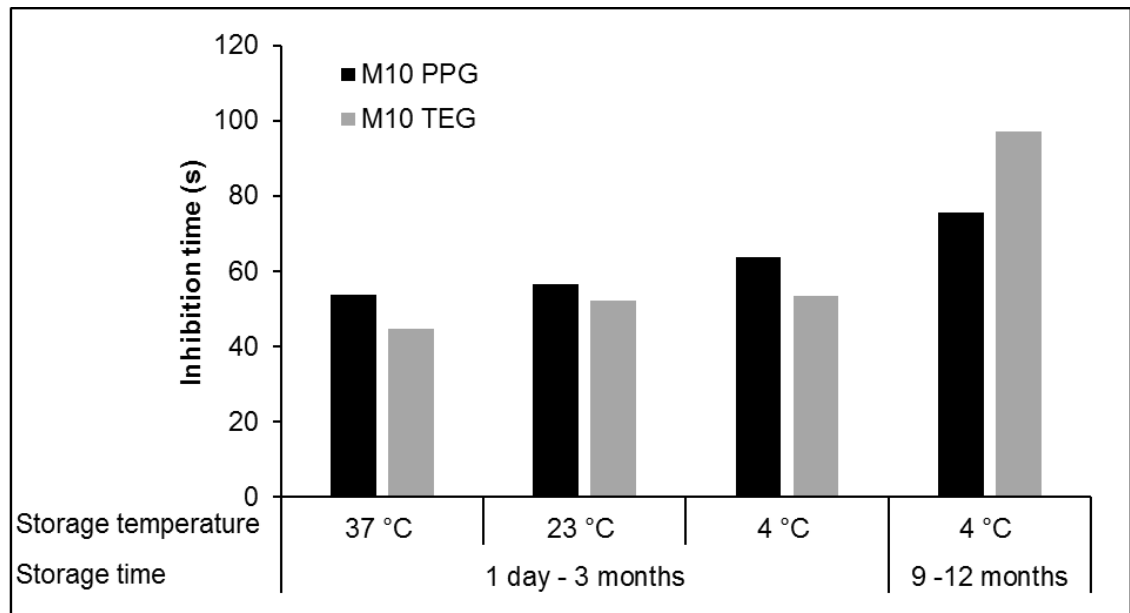


**Fig 5-7** An average of inhibition time of the experimental bone composites kept at different storage temperature measured at early time (1 day – 3 months) and late time (9-12 months).

### 5.6.3.2 Rate of polymerisation

With shorter storage periods, average maximum rates of polymerisation ( $R_p^{\max}$ , equation 2-10) of M<sub>10</sub>PPG composites ( $0.5 \text{ \%}\cdot\text{s}^{-1}$ ) were higher than those of M<sub>10</sub>TEG ( $0.3 \text{ \%}\cdot\text{s}^{-1}$ ) (Fig 5-8). For longer stored pastes (9 – 12 months at  $4 \text{ }^{\circ}\text{C}$ ),  $R_p^{\max}$  of both M<sub>10</sub>PPG and M<sub>10</sub>TEG were slightly reduced ( $0.4 \pm 0.1$  and  $0.2 \pm 0.0 \text{ \%}\cdot\text{s}^{-1}$  respectively).

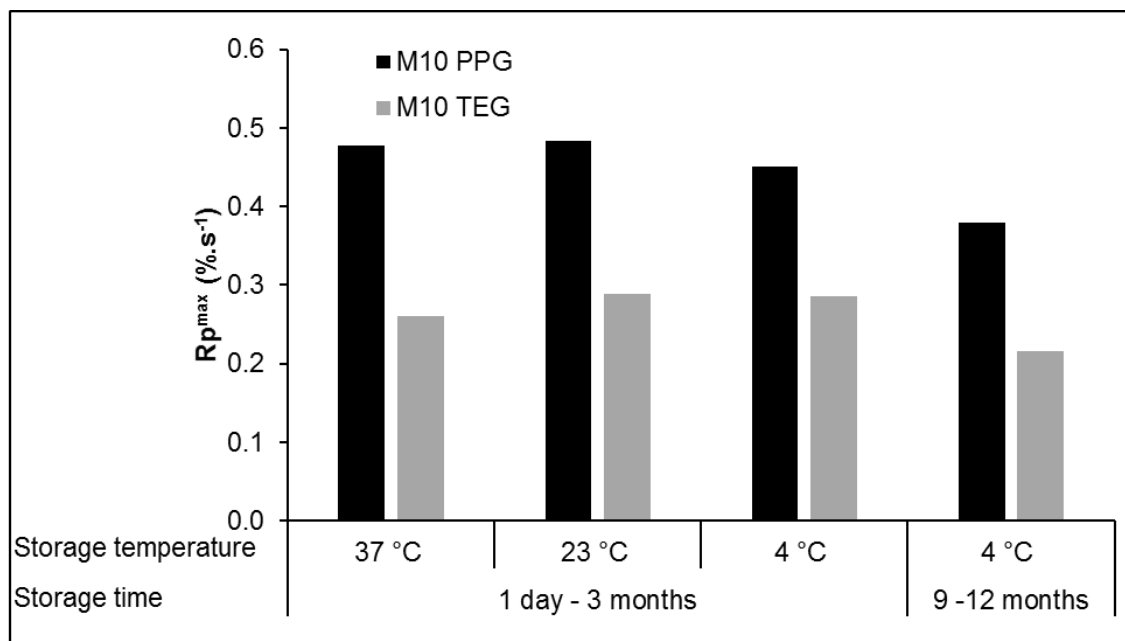


**Fig 5-8** Average maximum rate of polymerisation ( $R_p^{\max}$ ) of the experimental bone composites kept at different storage temperatures for either short (1 day – 3 months) or longer (9-12 months) time periods.

### 5.6.3.3 Final monomer conversion

M<sub>10</sub>PPG exhibited higher final monomer conversion than M<sub>10</sub>TEG at all time points and storage temperatures (Fig 5-9). Effects of storage time / temperature on final monomer conversion were small.

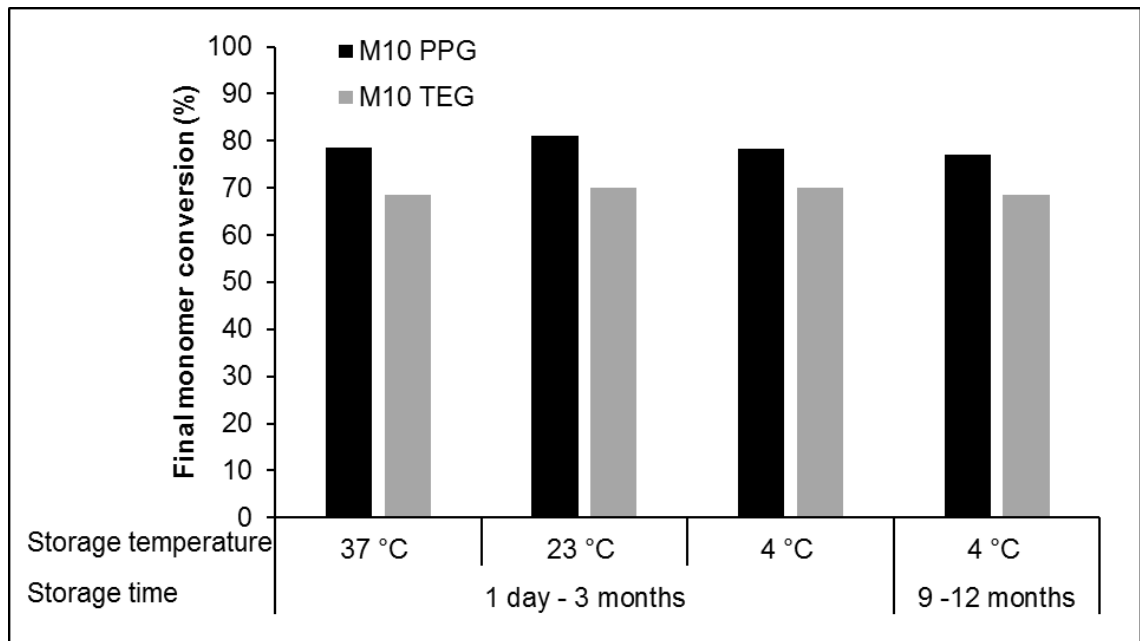


**Fig 5-9** Average final monomer conversion of the experimental bone composites kept at different storage temperature for either short (1 day – 3 months) or longer time periods (9-12 months).



## 5.7 Discussion

This study assessed the stability of active ingredients in monomers upon accelerated high temperature ageing. Predicted and observed solidification times of the initiator pastes in addition to monomer conversion of the experimental bone composites containing lower and higher molecular weight monomers (TEGDMA or PPGDMA) were measured. Additionally, the effect of ageing, at different storage temperatures, on subsequent monomer conversion kinetics of the composites was examined.

An ideal bone composite should exhibit high chemical stability, i.e. no reaction occurring between active ingredients, to maintain mineralising and antibacterial properties of the composites. Additionally, initiator and activator pastes should not be susceptible to storage temperatures to avoid premature or thermal initiated polymerisation during storage or shipment

### 5.7.1 Stability of chemical components

Upon exposure to water or humidity, monocalcium phosphates can dissolve or react with tricalcium phosphate and subsequently transform to dicalcium phosphates (brushite or monetite) as products. Due to the lower solubility of dicalcium phosphates compared to monocalcium phosphate, the formation of these dicalcium phosphates in composite pastes may hamper the mineralising properties of the experimental bone composites.

FTIR spectra of neither brushite nor monetite were detected with the concentrated suspension of phosphate particles upon high temperature ageing. The final FTIR spectrum of the mixture showed an increase of peaks attributable to TSrP which is likely simply due to the sedimentation of this small diameter filler. This sedimentation was likely to be due to the decrease of viscosity of monomer upon heating. Similarly, changes

in spectra upon the application of heat to mixtures of PLS with bulk and diluent monomers was suggestive primarily of sedimentation or melting rather than any chemical reaction of PLS.

Observed spectra were compared with expected spectra obtained from the FTIR spectra of pure chemicals which were measured at 25 °C. Hence, the expected spectra were slightly different from the observed spectra but still in good agreement with the measured spectra.

### **5.7.2 Stability of initiator paste**

Stability of initiator or activator in composites is crucial to avoid premature or thermal initiated polymerisation during storage or shipment. This may lead to solidification of composite pastes and reduce shelf life of materials. The Arrhenius method employed in the current chapter enabling prediction of solidification time of initiator pastes upon storing at low temperature, which may relate with shelf life of experimental bone composites.

The effect of different diluent monomers on solidification time at elevated temperatures of experimental bone composites followed Arrhenius equation. The observed solidification time of experimental bone composites at high temperatures and the predicted solidification time at low temperatures of initiator paste containing PPGDMA was longer than that of initiator paste containing TEGDMA. This could be due to the greater mobility of free radicals with lower molecular TEGDMA polymerising mixtures compared to that of higher molecular weight PPGDMA polymerising mixtures. Furthermore, inhibitor systems used in the supplied TEGDMA monomer was 200 mmol MEHQ (4-Methoxyphenol), whilst that of PPGDMA monomer was the mixture of 100 mmol MEHQ and 100 mmol BHT (butylated hydroxytoluene). A study has demonstrated

that the addition of BHT enhanced stabilisation effect of MEHQ (Belbakra et al., 2014). The combination of the inhibitors may additionally improve stability of the initiator in PPGDMA composite.

The solidification time at low temperatures extrapolated from Arrhenius equation of both composites were underpredicted (i.e. shorter than the observed solidification). The reason for this might be that polymerisation kinetic of the composites at low temperatures may deviate from Arrhenius behaviour (temperature dependence). This may imply that the actual shelf life of the composite would be longer than the predicted shelf life which is desirable.

### **5.7.3 Effect of aging on monomer conversion of the experimental bone composites containing PPGDMA or TEGDMA**

At all storage temperatures and time points, the experimental bone composite containing PPGDMA exhibited higher monomer conversion than the composite containing TEGDMA. This finding is in good agreement with results from previous studies (Khan, 2015; Walters et al., 2016). The possible explanation might be that monomer chain of PPGDMA was longer than that of TEGDMA. Long monomer chain with low cross-linking density may lower steric hindrance in polymerising mixtures of PPGDMA-based composites. This condition therefore facilitated the mobility of the radical chains, thereby increasing monomer conversion (Goncalves et al., 2008).

Inhibition time of polymerisation of the experimental bone composites slightly increased upon ageing especially with the TEGDMA based formulation. This could be due to the loss of initiator or activator due to ageing. This, however, had negligible effect on final monomer conversion in both composite formulations. A possible explanation might be that the final monomer conversion was mainly governed by properties of consisting

monomers such as chemical structure, molecular weight, or glass transition temperature (Sideridou et al., 2006). Another explanation for this could be that the final monomer conversion of composites is affected less by initiator than reaction rate and inhibition time. Khan (2015) has demonstrated that final monomer conversion of bone composites decreased linearly with the inverse square root of initiator and activator concentration.

In summary, active ingredients contained in experimental bone composites were stable upon ageing at high temperature. This may ensure that mineralising or antibacterial actions of the composites will not be compromised by fluctuation in temperatures or long-term storage. Furthermore, replacing diluent TEGDMA by PPGDMA improved stability of the initiator paste. Therefore, PPGDMA will be used as primary diluent monomer in experimental bone composite formulations in the following chapters.

## 5.8 Conclusions

Within the limitations of this study, the following conclusions could be drawn.

- 1) Reactive ingredients appeared chemically stable in monomers upon high temperature ageing although enhanced particle sedimentation could occur.
- 2) Initiator paste of composite containing PPGDMA was more stable than initiator paste of composite containing TEGDMA.
- 3) Paste ageing can increase inhibition times and reduce reaction rates but has less of an effect on final monomer conversions.

## Chaper 6 Effect Glass Filler Size / Shape, MCPM, and Level of PPGDMA on Mechanical Properties of Injectable Bone Composites

### 6.1 Abstract

**Purpose:** The objectives were to assess the effect of glass filler size, fibres, and MCPM level on biaxial flexural strength (BFS) and fracture toughness ( $K_{IC}$ ) of the composites. Additionally, the effect of increasing diluent monomer (PPGDMA) on BFS and modulus of elasticity of the composites were also examined.

**Materials and Methods:** Experimental bone composites were prepared using PLR of 2.3:1. In the first study, a fixed chemical activated liquid phase containing UDMA (70 wt%), PPGDMA (25 wt%), and HEMA (5 wt%) was used. Powder phase after mixing the initiator paste with activator paste contained glass filler (0.7 or 7  $\mu\text{m}$ ), fibres (0 or 20 wt%), MCPM (5 or 10 wt%), with fixed TSrP (7.5 wt%). Specimens were made and immersed in SBF for 24 hr.  $K_{IC}$  was obtained from single-edge notched beam specimens using three-point bending testing jig. For the second study, composites with varying level of PPGDMA (25, 50, 75, and 95 wt%) were prepared with fixed glass filler (0.7  $\mu\text{m}$ ), 20 wt% fibres, 10 wt% MCPM, 7.5 wt% TSrP, and 5 wt% PLS. Biaxial flexural strength (BFS) and modulus of elasticity were measured using a ball-on-ring jig and disc shape specimens. Commercial bone composite (Cortoss) and PMMA cement (Simplex) were used as comparisons.

**Results:** Average BFS (113 MPa) and  $K_{IC}$  (1.6 MPa.m<sup>1/2</sup>) of the experimental bone composites with fixed monomer phase were higher than those of Cortoss (101 MPa, 1.3 MPa.m<sup>1/2</sup>). The use of small glass particle (0.7  $\mu\text{m}$ ) increased BFS by 25 % whilst the

effect of MCPM and fibres were negligible. The addition of fibre increased  $K_{IC}$  by 30 % whilst the effect of glass filler size and MCPM level were minimal. Raising PPGDMA level from 25 to 95 wt% significantly reduced BFS (from 114 to 37 MPa) and modulus of elasticity (from 2.3 to 0.4 GPa) of the experimental bone composites.

**Conclusion:** This study developed bone composites that have flexural strength greater than 50 MPa required from ISO 5833 while exhibiting a stiffness comparable with cancellous bone. Using small glass filler and the addition of fibres improved BFS and  $K_{IC}$  of the experimental bone composites respectively. MCPM level had minimal effect on mechanical properties. The increase of PPGDMA reduced modulus of elasticity to levels comparable with cancellous bone (< 0.7 GPa) but this also decreased BFS of the composites.

## 6.2 Introduction

Vertebroplasty and kyphoplasty are generally performed as a day case procedure (Lee et al., 2009; Wardlaw et al., 2009). Hence, patients can usually walk or do normal activities soon after the procedure. Early strength of the injected bone cement is therefore considerably important to ensure the stabilisation of fractured vertebra and therefore pain relief for the patients.

It is known that mechanical properties of composite materials are affected by composition of filler phase (Ilie and Hickel, 2009). The addition of hydrophilic calcium phosphates into bone cements can promote surface apatite precipitation which is known to promote *in vivo* bone bonding (Tanaka et al., 2016). These compounds, however, reduced strength of the material (Aljabo et al., 2015) due primarily to the enhanced water sorption.

Common mechanism of composites failure is crack propagation. Cracks may originate from flaws or inhomogeneities containing within the materials. It has been shown that the addition of fibres retarded crack propagation by reflecting propagated cracks or bridging the cracks (Zhou et al., 2009; Quinn and Quinn, 2010). Furthermore, Khan (2015) revealed that the addition of fibre enabled ductile fracture behaviour for experimental bone composites. This behaviour could potentially allow the composites to deform without fracture which is desirable. Poor dispersion or agglomeration of fibres may, however, reduce strength of the composites (Drummond, 2008).

Glass particle size has significant effect on strength of composites (Juhasz et al., 2004; Fu et al., 2008). Previous studies demonstrated that strength of the composites is generally increased with decreasing particle size. The addition of glass fibres or fillers increased strength but also increased stiffness of composites (Randolph et al., 2016).

It is proposed that a possible mechanism of developing adjacent vertebral fracture after vertebroplasty is the mechanical mismatch between high stiffness bone cement and low stiffness cancellous bone (Schröder et al., 2016). Studies have shown that the stiffness of bone cements was significantly decreased by the addition of hyaluronic acid, blood plasma, castor oils, or normal saline (Boger et al., 2008; Ahn et al., 2009; Lopez et al., 2011; Carlsson et al., 2015; Schröder et al., 2016). These compounds, however, negatively affected polymerisation, handling, and mechanical properties of the materials. Main (2013) revealed that the increase of high molecular weight and flexible diluent monomer (PPGDMA) reduced modulus of elasticity of the composites. The composites in Main's study contained only glass filler (particle size was unknown) and glass fibres. The additional benefits of increasing PPGDMA would have been increased monomer conversion and reduced polymerisation shrinkage (Walters et al., 2016).



### 6.3 Hypotheses

High early strength of bone composites is required to stabilise collapsed vertebra which may allow patients to do daily activities soon after vertebroplasty. According to literature and results from Chapter 3, it is known that the addition of hydrophilic fillers will reduce mechanical properties of experimental bone composites due primarily to the increase in water sorption. Optimal levels of MCPM are expected to be between 5 and 10 wt% of powder (Aljabo et al., 2015). MCPM level in the current study will be either 5 or 10 wt% with fixed level of TSrP (7.5 wt%). It was expected that using low level of MCPM and TSrP will not detrimentally affect mechanical properties of experimental bone composites in this chapter.

It is known that fibres will increase ability of materials to slow down crack propagation or help to bridge cracks. Previous studies by Khan (2015) revealed that the addition of fibres by 10 or 20 wt% also enabled ductile fracture behaviour for experimental bone composites without causing detrimental effect on monomer conversion of the materials. However, fracture toughness, which is the ability of materials to resist crack propagation, was not assessed in Khan's study. It was, therefore, expected that the addition of fibres (20 wt%) will increase fracture toughness of the experimental bone composites in this chapter.

Chapter 4 demonstrates that decreasing glass particle size from 7 to 0.7  $\mu\text{m}$  enhanced solid-like behaviour of the composites. According to the literature described above, decreasing glass particle size also increases mechanical properties of materials. It was, therefore, anticipated that decreasing glass filler size from 7 to 0.7  $\mu\text{m}$  will increase mechanical properties of experimental bone composites in the current study.

It is proposed that using low stiffness bone cements could potentially reduce adjacent vertebral fractures after vertebroplasty. Main (2013) demonstrated that level of flexible diluent PPGDMA in resin matrix affected the modulus of elasticity of experimental bone composites. It was, therefore, expected that increasing ratio of higher flexible diluent monomer (PPGDMA) to more viscous bulk monomer (UDMA) will reduce modulus of elasticity of the experimental bone composites.

## **6.4 Objectives**

The aim of this chapter was to develop high early strength injectable bone composites that provide modulus of elasticity comparable with cancellous bone. The objectives were to assess the effects of:

- 1) MCPM level, fibre addition, and glass particle size on biaxial flexural strength and fracture toughness of experimental bone composites;
- 2) PPGDMA level on biaxial flexural strength and modulus of elasticity of the experimental bone composites.

Commercial injectable bone composite (Cortoss; Stryker, Newbury, Berkshire, UK) and PMMA (Simplex; Stryker, Newbury, Berkshire, UK) cement were used for comparison.

## 6.5 Material preparation

### 6.5.1 Formulations containing different levels of MCPM, fibres, and glass particle size

In the first part of this chapter, the liquid phase contained 70 wt% UDMA, 25 wt% of PPGDMA, and 5 wt% of HEMA. To this was added either BP (3 wt% of total liquid phase) for the initiator liquid or NTGGMA (2 wt% of total liquid phase) for the activator liquid (Table 6-1).

Table 6-1 Components of liquid phases before mixing with the powder phase.

Liquid phase / components	UDMA	PPGDMA	HEMA	BP	NTGGMA
	wt% of monomers	wt% of monomers	wt% of monomers	wt% of liquid	wt% of liquid
<b>Initiator liquid</b>	70	25	5	3	0
<b>Activator liquid</b>	70	25	5	0	2

NB Upon mixing the composite BP and NTGGMA concentrations will become 1.5 and 1 wt% respectively

The first part of this chapter investigated the effect of MCPM, in addition to glass particle size and fibre removal, on biaxial flexural strength and fracture toughness of experimental bone composites after immersion in SBF for 24 hr. Formulations of these composites are presented in Table 6-2. All testing protocols are described in Chapter 2.

**Table 6-2 Formulations with varying glass particle sizes, MCPM, and fibre level. Powder phases were mixed with PPGDMA-liquid phase presented in Table 4-1. Activator paste glass sizes were the same as in the initiator pastes.**

Formulations	Glass filler size (µm)	Glass filler (wt%)	Glass fibre (wt%)	MCPM (wt%)	TSrP (wt%)	PLS (wt%)
<b>M<sub>5</sub>F<sub>20</sub>G<sub>0.7</sub></b>	<b>0.7</b>	65	<b>20</b>	<b>10</b>	<b>0</b>	5
<b>M<sub>5</sub>F<sub>20</sub>G<sub>7</sub></b>	<b>7</b>	65	<b>20</b>	<b>10</b>	<b>0</b>	5
<b>M<sub>10</sub>F<sub>20</sub>G<sub>0.7</sub></b>	<b>0.7</b>	55	<b>20</b>	<b>20</b>	<b>0</b>	5
<b>M<sub>10</sub>F<sub>20</sub>G<sub>7</sub></b>	<b>7</b>	55	<b>20</b>	<b>20</b>	<b>0</b>	5
Activator paste	<b>0.7 or 7*</b>	60	<b>20</b>	<b>0</b>	<b>15</b>	5
<b>M<sub>5</sub>F<sub>0</sub>G<sub>0.7</sub></b>	<b>0.7</b>	85	<b>0</b>	<b>10</b>	<b>0</b>	5
<b>M<sub>10</sub>F<sub>0</sub>G<sub>0.7</sub></b>	<b>0.7</b>	75	<b>0</b>	<b>20</b>	<b>0</b>	5
Activator paste	<b>0.7 or 7*</b>	80	<b>0</b>	<b>0</b>	<b>15</b>	5

\* Glass filler size in the initiator paste was the same as the activator paste.

### 6.5.2 Formulations containing varying level of PPGDMA diluent monomer

Formulations of experimental bone composites examined in the second part of this chapter were prepared according to Table 6-3. For these formulations, the powder was fixed as in M<sub>10</sub>F<sub>20</sub>G<sub>0.7</sub> but the level of PPGDMA and UDMA were varied. Biaxial flexural strength and modulus of elasticity of experimental bone composites and commercial materials after being immersed in SBF for 24 hr (n=8) were assessed. All testing protocols are described in Chapter 2.

**Table 6-3 Formulations with varying level of PPGDMA. Liquid phases of each formulation were mixed with powder phases of M<sub>10</sub>F<sub>20</sub>G<sub>0.7</sub>.**

Formulations		UDMA	PPGDMA	HEMA	BP	NTGGMA
		wt% of monomers	wt% of monomers	wt% of monomers	wt% of total liquid phase	wt% of total liquid phase
<b>25 PPG</b>	Initiator liquid	<b>70</b>	<b>25</b>	5	3	0
	Activator liquid	<b>70</b>	<b>25</b>	5	0	2
<b>50 PPG</b>	Initiator liquid	<b>45</b>	<b>50</b>	5	3	0
	Activator liquid	<b>45</b>	<b>50</b>	5	0	2
<b>75 PPG</b>	Initiator liquid	<b>20</b>	<b>75</b>	5	3	0
	Activator liquid	<b>20</b>	<b>75</b>	5	0	2
<b>90 PPG</b>	Initiator liquid	<b>5</b>	<b>90</b>	5	3	0
	Activator liquid	<b>5</b>	<b>90</b>	5	0	2

## 6.6 Statistical analysis

Data in first and second studies were analysed using one-way ANOVA followed by multiple comparisons using Tukey's test or Kruskal-Wallis test with Dunnett's T3 test ( $p = 0.05$ ). Factorial analysis was additionally employed to analyse the data of first study. BFS and fracture toughness data was assessed assuming equations for two levels factorial design experiments each with high and low level of two variables (equations 2-26, 2-28). This enabled determination of the effect of MCPM (10 versus 5 wt%) and glass fibre addition (20 versus 0 wt%) with glass filler size fixed (0.7  $\mu\text{m}$ ) or of MCPM (10 versus 5 wt%) and filler size (7 versus 0.7  $\mu\text{m}$ ) with fixed level of fibre (20 wt%).

## 6.7 Results

### 6.7.1 Effect of MCPM level, fibre addition, and glass particle size

#### 6.7.1.1 Biaxial flexural strength

Highest and the lowest BFS were obtained from Simplex ( $131 \pm 1$  MPa) and  $M_{10}F_{20}G_7$  ( $96 \pm 7$  MPa) respectively (Fig 6-1). BFS of  $M_{10}F_{20}G_{0.7}$  ( $126 \pm 6$  MPa),  $M_5F_{20}G_{0.7}$  ( $118 \pm 6$  MPa), and  $M_5F_0G_{0.7}$  ( $122 \pm 6$  MPa) were comparable to that of Simplex but were significantly higher than that of Cortoss ( $101 \pm 5$  MPa). Factorial analysis indicated that the effect of MCPM and fibre on BFS of experimental bone composites were negligible (Figs 6-2 A,B). BFS of the composites was, however, increased by  $25 \pm 8$  % upon decreasing glass filler size from 7 to  $0.7 \mu\text{m}$  (Fig 6-2 B).

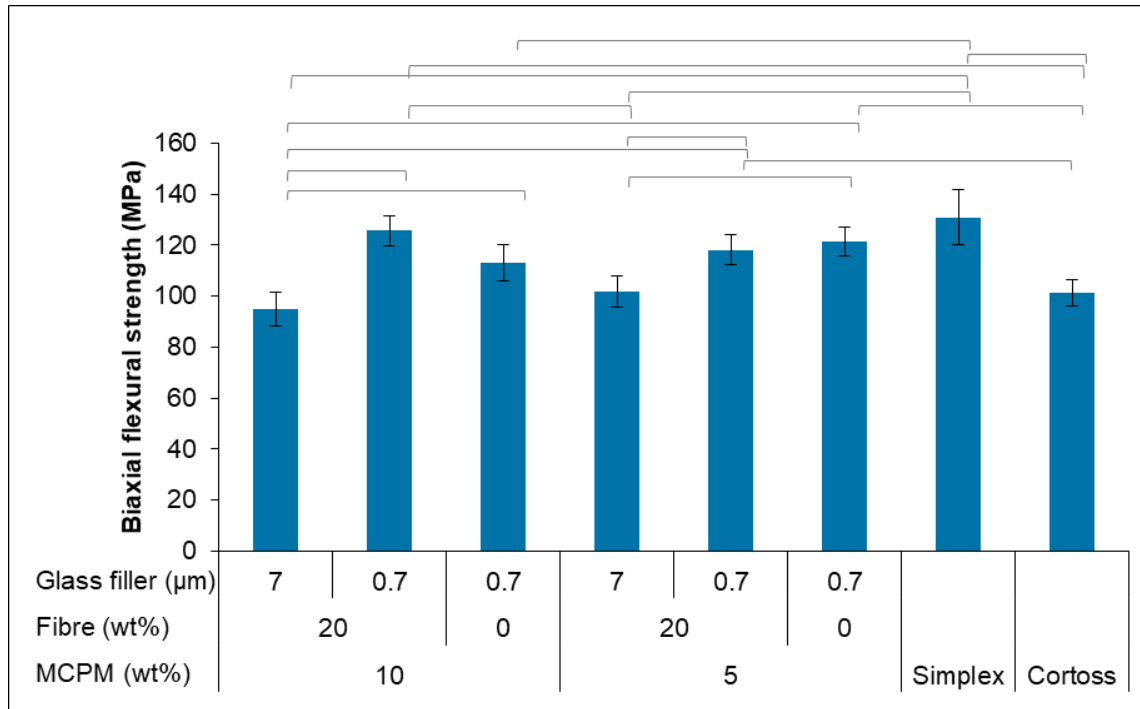


Fig 6-1 Biaxial flexural strength after immersion in SBF for 24 hr. Error bars are 95% CI (n=8). Lines indicate significant difference ( $p < 0.05$ ).

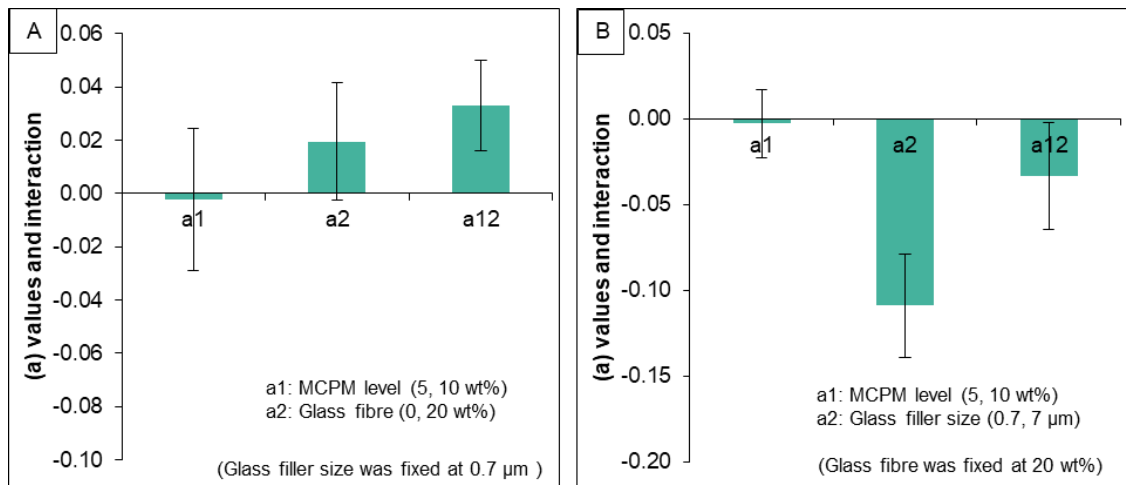


Fig 6-2 Factorial analysis describing the effect of MCPM level, glass fibre, glass filler size, and interaction effects on BFS of experimental bone composites. Error bars are 95 %CI (n =8).

#### 6.7.1.2 Fracture toughness ( $K_{IC}$ )

The highest and lowest  $K_{IC}$  were obtained from  $M_5F_{20}G_{0.7}$  ( $1.9 \pm 0.1 \text{ MPa.m}^{1/2}$ ) and Cortoss ( $1.3 \pm 0.1 \text{ MPa.m}^{1/2}$ ) respectively (Fig 6-3).  $K_{IC}$  of  $M_5F_{20}G_{0.7}$  was also significantly higher than that of Simplex ( $1.5 \pm 0.1 \text{ MPa.m}^{1/2}$ ) and Cortoss. Factorial analysis indicated that primary effect influencing  $K_{IC}$  was the addition of fibre (Fig 6-4 A).  $K_{IC}$  of the composites was increased by  $30 \pm 10 \%$  upon the addition of fibre

Fracture surface of tested specimens were examined by SEM (Fig 6-5). Cortoss exhibited a smooth fracture surface compared to other materials. Multiple porosities ( $\sim 1 \mu\text{m}$ ) embedded with radiopacifier particles were seen on the fracture surface of Simplex. The fracture surface of experimental bone composites containing either 5 or 10 wt% of MCPM revealed brushite precipitation (Fig 6-6). In addition, holes of pulled-out fibres and different orientation of fibres were seen on the fracture surface.



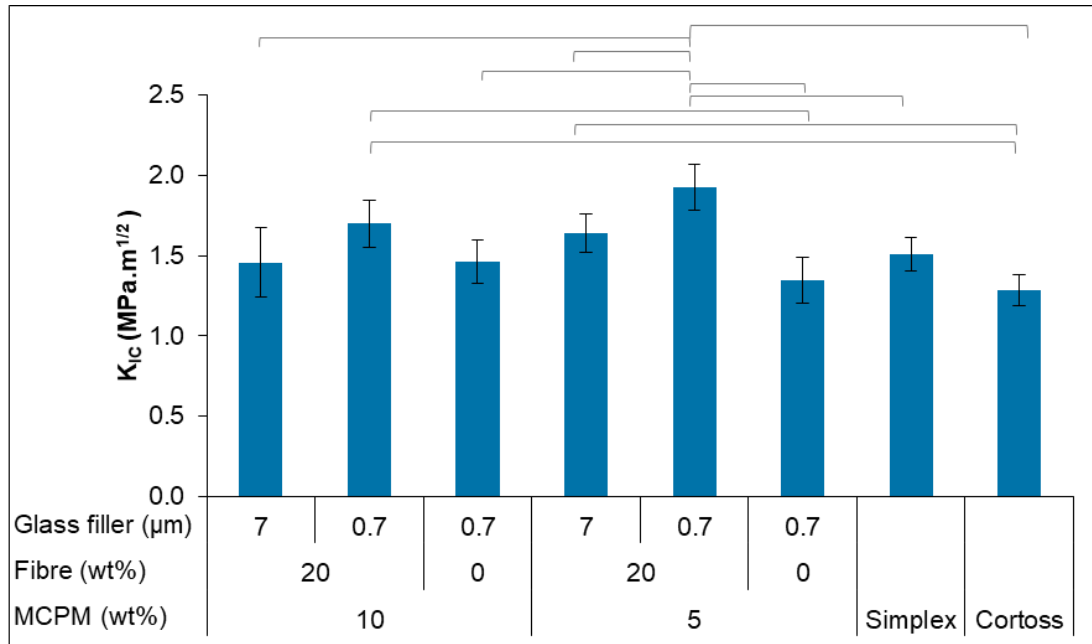


Fig 6-3 Fracture toughness of all materials after immersion in SBF for 24 hr. Error bars are 95% CI (n=8). Lines indicate significant difference ( $p < 0.05$ ).

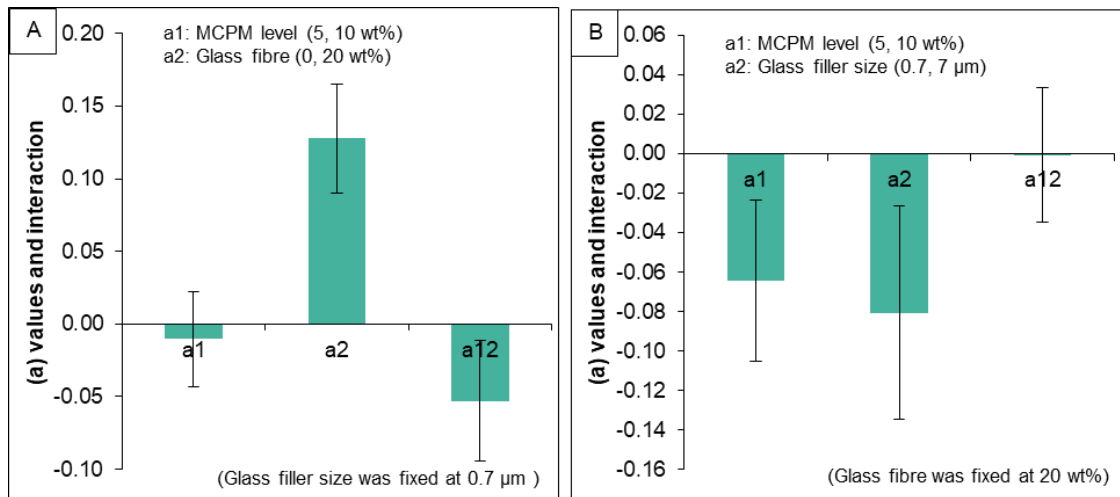
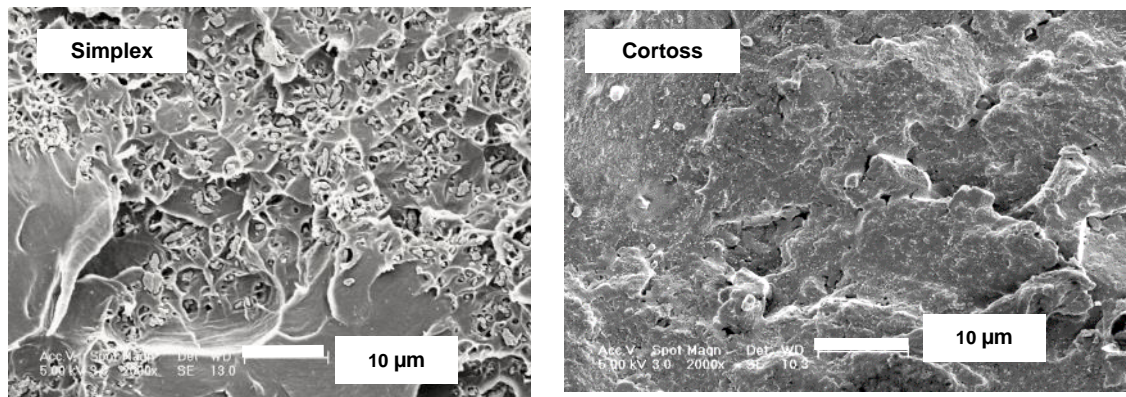
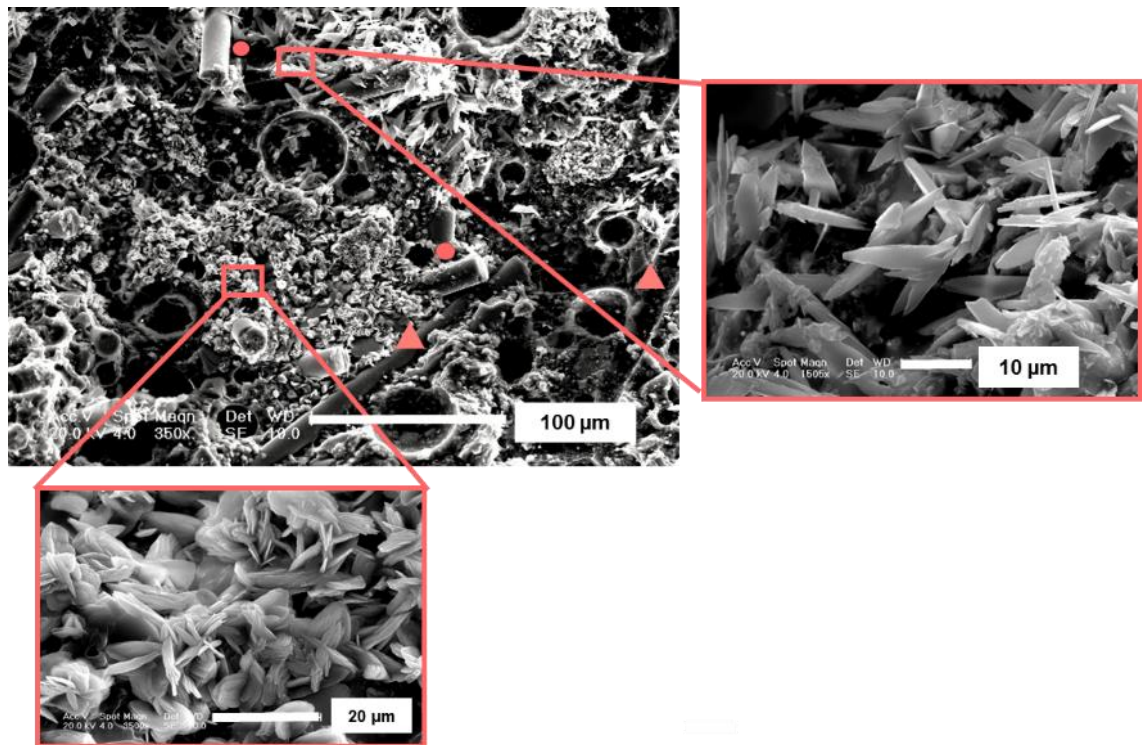


Fig 6-4 Factorial analysis describing the effect of MCPM level, glass fibre, glass filler size and interaction effects on fracture toughness of the experimental bone composites. Error bars are 95% CI (n = 8).



**Fig 6-5 Representative fracture surface of commercial materials. Multiple porosities with small particles were seen with Simplex.**



**Fig 6-6 Representative fracture surface of the experimental composite from fracture toughness test. Circles and triangle represent fibre that oriented perpendicular and parallel to the fracture surface respectively. Squares represent areas of brushite precipitation.**

### **6.7.2 Effect of PPGDMA level on biaxial flexural strength and modulus of elasticity**

BFS and modulus of elasticity of experimental bone composites were significantly decreased upon the increase of PPGDMA (Figs 6-7). The highest and lowest of both BFS and modulus among the experimental composites were observed with 25PPG ( $117 \pm 6$  MPa,  $2.7 \pm 0.3$  GPa) and 95PPG ( $37 \pm 2$  MPa,  $0.4 \pm 0.0$  GPa) respectively (Figs 6-7 A). BFS of Cortoss ( $85 \pm 6$  MPa) was not significantly different to that of 50PPG ( $88 \pm 5$  MPa) (Fig 6-7 A). 50PPG ( $1.51 \pm 0.13$  GPa) also exhibited comparable modulus of elasticity to Simplex ( $1.52 \pm 0.06$  GPa) (Fig 6-7 B). Additionally, Cortoss ( $2.3 \pm 0.2$  GPa) showed comparable modulus of elasticity to 25PPG ( $2.7 \pm 0.3$  GPa).

The changing in modulus of elasticity upon increasing PPGDMA was decreased as PPGDMA level was raised (Fig 6-8). The changing in strength was, however, constant upon increasing PPGDMA level.

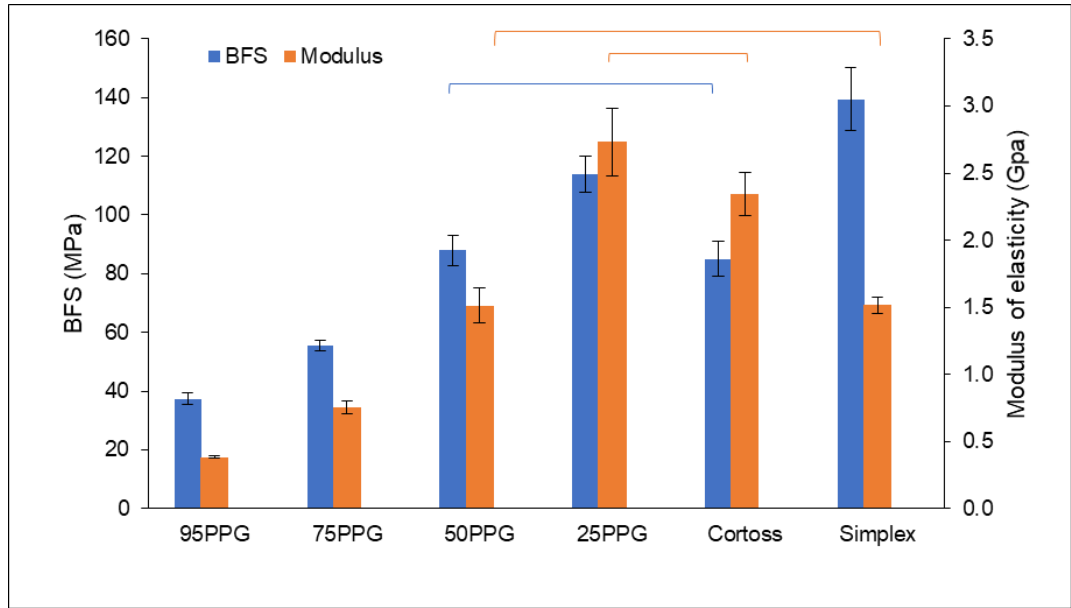


Fig 6-7 Biaxial flexural strength and modulus of elasticity of the experimental bone composites and Cortoss after immersion in SBF for 24 hr. Error bars are 95 %CI (n=8). Solid lines indicate no significant difference ( $p > 0.05$ ).

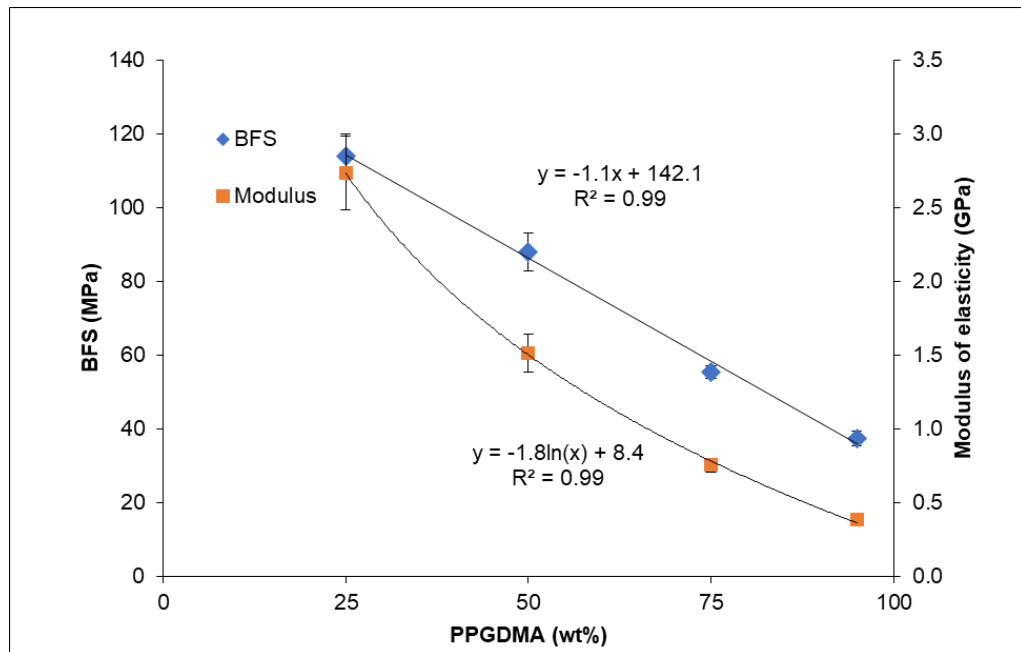


Fig 6-8 Biaxial flexural strength and modulus of elasticity of the experimental bone composites versus level of PPGDMA. Error bars are 95 %CI (n=8).

## 6.8 Discussion

Mechanical properties of bone composites at early time were assessed and compared with commercial materials. An ideal bone composite should exhibit early high strength to ensure the stabilisation of collapsed vertebra. This could relieve pain and facilitate daily movements for patients soon after vertebroplasty. Modulus of elasticity of the composites should, however, decrease with time to allow an efficient load transfer from adjacent vertebra. This could potentially help to reduce the adjacent vertebral fracture which is one of the common complications of vertebroplasty.

This chapter investigated the early strength of experimental bone composites. Additionally, an effect of filler compositions including MCPM level, glass particle size, and the addition of glass fibre on strength of the composites were assessed. Furthermore, strength and modulus of elasticity of experimental bone composites containing different levels of PPGDMA was also examined.

### 6.8.1 Effect of MCPM level, fibre addition, and glass particle size and on biaxial flexural strength (BFS) and fracture toughness ( $K_{IC}$ )

The incorporation of MCPM (5 to 10 wt%) in experimental bone composites showed no detrimental effect on mechanical properties of the composites. These values, however, could be decreased upon an increase in aging time (Aljabo et al., 2015).

The addition of fibre significantly improved fracture toughness ( $K_{IC}$ ) of the experimental bone composites. The addition of fibre, however, did not advantageously increase biaxial flexural strength of the composites. This similar finding was also reported by Bocalon et al. (2016). The authors of that study explained that  $K_{IC}$  is governed by the microstructure of composites, whilst the strength was more influenced by susceptible areas such as

matrix-filler interfaces. The addition of fibre increased  $K_{IC}$  by bridging the fracture surfaces, thus more energy was required at the propagating crack to break the material (Peterlik et al., 2006). However, the addition of fibre also introduced susceptible fibre-matrix interfaces that may lower strength of the materials.

The fibre orientation also plays an important role on strength of composites (Khan et al., 2015). SEM images revealed that the glass fibres in the experimental bone composites were randomly orientated (Fig 6-6). The fibres that were oriented parallel to the fracture plane or the applied load do not reinforce the composite effectively (Khan et al., 2015; Bocalon et al., 2016). Another issue with the addition of fibre was the increase of cement's viscosity which could hinder the injection of the materials (Kane et al., 2010).

The use of small glass filler increased BFS and  $K_{IC}$  of the composites. This may be explained by the fact that at the given filler loading, smaller particle filler exhibited higher surface area. This may have provided more active sites for polymer/filler interaction, thus encouraging more efficient stress transfer between resin matrix and fillers (Fu et al., 2008). Additionally, sedimentation of 7  $\mu\text{m}$  glass filler that may occur in the paste could reduce homogeneity of composite specimens and thereby compromise their strength.

BFS and modulus of elasticity values of Cortoss and Simplex were comparable with values reported in a previously published study (96 MPa and 131 MPa for Cortoss and Simplex) (Boyd et al., 2008; Main, 2013). Additionally, fracture toughness of Simplex in the current study ( $1.5 \text{ MPa}\cdot\text{m}^{1/2}$ ) is consistent with that obtained from a previously published study ( $1.6 \text{ MPa}\cdot\text{m}^{1/2}$ ) (Hasenwinkel et al., 2002). The radiopacifier (barium sulphate) in the PMMA cements does not bond with the surrounding matrix. Thus, particles were agglomerated and formed voids inside the cement. This feature also observed in studies of Main (2013) and Khan (2015). These inhomogeneities may act

as crack initiators / facilitators, thereby decreasing fracture toughness of the cement (Baleani et al., 2003; Sinnett-Jones et al., 2009).

### 6.8.2 Effect of PPGDMA level on biaxial flexural strength and modulus of elasticity

The amount of diluent monomer in experimental dental and bone composites produced at the UCL Eastman Dental Institute have usually been fixed at 25 wt% (Main, 2013; Aljabo et al., 2015; Khan, 2015; Aljabo et al., 2016). The experimental bone composites using this level of diluent monomer may have exhibited high mean BFS values, however, their modulus of elasticity would be much higher than that of cancellous bone (0.1 – 0.7 GPa) (Banse et al., 2002). The result from this chapter indicated that increasing PPGDMA reduced modulus of elasticity of the composites. The composites that exhibited modulus of elasticity comparable to cancellous bone were formulations containing 75 wt% (0.8 GPa) and 95 wt% (0.4 GPa) of PPGDMA.

The conventional rule of mixture (equation 6-1) (Lee et al., 2014) suggests that modulus of elasticity of materials is proportional to modulus of elasticity of resin matrix.

$$E_{composite} = V_{filler}E_{filler} + (1 - V_{filler}) E_{matrix} \quad \text{Equation 6-1}$$

Where  $E_{composite}$ ,  $E_{filler}$ ,  $E_{matrix}$  are modulus of elasticity of composite, filler, and resin matrix respectively,  $V_{filler}$  is volume fraction of filler.

Previous work of Main (2013) demonstrated that the modulus of bone composites depend on the stiffness of their constituents (fillers and polymers) which can be predicted using the Voight-Reuss models (equation 6-1). Main's results indicated that modulus of the composites was mainly governed by levels of PPGDMA. This was in good agreement with the results from this chapter. Furthermore, relationship of BFS and modulus of

elasticity (E) and PPGDMA level of experimental bone composites in this chapter can be explained using equations 6-2 and 6-3 respectively.

$$\text{BFS} = c - kv \quad \text{Equation 6-2}$$

$$E = c - k \ln(v) \quad \text{Equation 6-3}$$

Where  $c$  is intercept of  $x$  axis,  $k$  is constant,  $e$  is exponential function, and  $v$  is mass fraction of PPGDMA. This suggests that level of change of modulus and strength is different upon increasing PPGDMA. It is preferable that the composites exhibit sufficient strength to stabilise the fractured vertebra in addition to reduced stiffness that may be more comparable with that of surrounding bone.

In summary, early strength of the experimental bone composites was not detrimentally affected by using 5 or 10 wt% of MCPM. The addition of fibre also improved fracture toughness of the composites. Furthermore, reducing glass filler diameter from 7 to 0.7  $\mu\text{m}$  not only enhanced solid-like behaviour of composite pastes but also increased biaxial flexural strength of the materials. A longer-term mechanical strength study of the composites is now required. This will be covered in Chapter 7.

Increasing PPGDMA level decreased the modulus of elasticity; yet, this also decreased the strength of the composite. However, the effect on strength was less than the effect on modulus of elasticity of the composites. Concerns of increasing diluent monomer may include high polymerisation shrinkage and long-term strength. This will be assessed in Chapter 8.



## 6.9 Conclusions

Within the limitation of this study, the following conclusions could be drawn

- 1) Using 5 or 10 wt% of MCPM showed no detrimental effect on early strength of the experimental bone composites. Furthermore, the addition of fibre (20 wt%) and decreasing glass filler diameter from 7 to 0.7  $\mu\text{m}$  increased fracture toughness and biaxial flexural strength of the experimental bone composites respectively.
- 2) Increasing PPGDMA reduced modulus of elasticity of the experimental bone composites but this also decreased their strength.

## Chaper 7 Effect of Diluent Monomer and MCPM level on Monomer Conversion, Volumetric stability, Strontium release, Apatite formation, and Fatigue Resistance of Bone Composites

### 7.1 Abstract

**Purpose:** The objectives of this chapter were to assess monomer conversion - induced shrinkage versus water sorption - promoting volumetric expansion, strontium release, surface apatite formation, and mechanical properties of experimental bone composites as a function of diluent monomer (TEGDMA vs PPGDMA) and MCPM level.

**Materials and methods:** Experimental bone composites were prepared using PLR of 2.3:1. Chemically activated dimethacrylate monomers contained either 25 wt% of TEGDMA or PPGDMA. Powder phase after mixing consisted of 0.7  $\mu\text{m}$  glass fillers, 7.5 wt% TSrP, 5 wt% PLS, and varying levels of MCPM (0, 5, or 10 wt%). Monomer conversion was assessed using FTIR-ATR. Mass and volume changes in SBF were measured using gravimetric studies. Surface apatite formation after immersion in SBF for 1 week was examined using SEM.  $\text{Sr}^{2+}$  release in deionised water for up to 4 weeks was assessed using ICP-MS. Biaxial flexural strength and fatigue after immersion in SBF for 4 weeks were tested. Then stress versus number of failure cycles (S-N curves) were plotted. Commercial PMMA (Simplex) and bone composite (Cortoss) were used for comparison.

**Results:** Experimental bone composites exhibited higher monomer conversion (74 – 82 %) than Cortoss (64 %). Replacing TEGDMA with PPGDMA increased monomer conversion by 5 %. Conversely, replacing PPGDMA by TEGDMA increased polymerisation shrinkage by 22 %. The use of PPGDMA and increasing MCPM enhanced water sorption induced volume expansion and  $\text{Sr}^{2+}$  release. Composites containing 10 wt% of MCPM level promoted surface apatite precipitation. The increase of MCPM decreased strength and gradient of S/N curve. The gradients for experimental composites containing MCPM (6-7 MPa/log cycle) were comparable

to that of Cortoss (6 MPa/log cycle) but advantageously were much reduced when compared with that of Simplex (18 MPa/log cycle). Additionally, the experimental composites showed comparable predicted fatigue life (~ 8 log cycle) to commercial materials.

**Conclusion:** This study produced bone composites with high monomer conversion to ensure sufficient long-term strength / fatigue resistance to support fractured bone. Furthermore, the composites provided water sorption induced expansion and Ca/Sr phosphate release. These could potentially compensate polymerisation shrinkage and enhance bone integration / repair.

## 7.2 Introduction

As mentioned in Chapter 1, limitations of the current commercially available PMMA bone cement include high polymerisation shrinkage, heat generation, and toxic monomers release. These damages the surrounding tissue and may subsequently impair bone-cement integration (Wegener et al., 2012). The development of bone composites has partially solved these issues but some limitations remained. For example, bulk (Bis-GMA) and diluent (TEGDMA) monomers contained in the commercial composites were associated with decreased monomer conversion and increased polymerisation shrinkage of dental composites respectively (Cornelio et al., 2014; Al Sunbul et al., 2016). The low conversion may enable the release of unreacted monomer and the more commonly employed highly cytotoxic amine activator (di(hydroxyethyl)-*p*-toluidine) (Bakopoulou et al., 2009).

It can be assumed that inhibition time, i.e. time before monomers are converted to polymer, may approximately equal working time of bone composites. Lewis (2006) suggested that working time (i.e. time after mixing that materials can be manipulated) of bone cement that are supplied as powder and liquid phases for vertebroplasty should be ~ 6-10 min. This recommended working time may include approximately 2 min required for mixing of powder and liquid and transfer of mixed cement into a syringe. Hence, the working time for bone composites that are supplied as a two-paste preloaded syringe, which can be injected directly to a cannula, can be assumed to be approximately 4 to 8 min. Khan (2015) demonstrated that inhibition time of experimental bone composites is inversely proportional to concentration of initiator (BP) and activator (NTGGMA). Reducing these components increased inhibition time allowing longer working time of the materials but reduced rate of polymerisation, final monomer conversion, and mechanical properties of the composites.

Cement washout by physiological fluids after injection is of concern for slow setting cements such as calcium phosphate cements. This could lead to cement embolisms and cause serious complications. Rate of polymerisation of bone composites determine setting characteristics of bone composites. Main (2013) and Khan (2015) previously developed experimental bone composites that exhibit high polymerisation rate. After inhibition time passed, monomer conversion of the composites reach their final monomer conversion rapidly (snap setting). This snap setting of composites may help prevent cement dissolution or wash out from the threatened vertebra.

It has been shown that increasing monomer conversion of composites could potentially reduce toxic monomers elution (Zhang et al., 2016b). Khan (2015) also demonstrated that replacing DMPT by NTGGMA increased monomer conversion of experimental bone composites. High monomer conversion, however, inevitably leads to high polymerisation shrinkage and heat generation resulting in gap formation or fibrous capsulation (Orr et al., 2003; Race et al., 2004; Kinzl et al., 2012b). Walters et al. (2016) recently confirmed that replacing TEGDMA with a longer chain, higher molecular weight but lower crosslinking density polypropylene glycol dimethacrylate (PPGDMA) enhanced monomer conversion, reduced polymerisation shrinkage, and improved cytocompatibility of dental composites. Additionally, Khan et al. (2014) proposed that using NTGGMA as activator enhanced cytocompatibility of experimental composites compared with DMPT. This could be due to NTGGMA containing a methacrylate group that can polymerise with the polymer network. This may reduce the leaching of this activator. Additionally, monomer conversion could be enhanced.

Calcium phosphates have been incorporated into bone cements to promote *in vivo* bone-cement integration through surface apatite precipitates (Sa et al., 2015). An additional benefit from the incorporation of phosphates was the enhanced volume expansion due

to water sorption to compensate polymerisation shrinkage (Aljabo et al., 2015). Optimal levels of MCPM are expected to be between 5 and 10 wt% of powder (Aljabo et al., 2015). Furthermore, studies have shown that incorporation of Sr substituted calcium phosphate apatite into bone cement promoted osteoblast functions whilst inhibited osteoclast functions (Luo et al., 2015; Schumacher et al., 2016). Khan (2015) revealed that raising level of hydrophilic compounds such as phosphates and polylysine increased the release of  $\text{Sr}^{2+}$  from experimental bone composites due probably to an enhanced water sorption. Increasing hydrophilic fillers, however, reduced mechanical properties of the composites.

Mechanical properties of materials are usually assessed under a uniformly increase in load (static loading). This involves a resistance to fracture (strength, fracture toughness) or stiffness (modulus of elasticity) of materials at a point of time. However, failure of materials can be due to crack propagation induced by repetitive subcritical loads (fatigue failure). A study indicated that high strength under static loading was not directly related to high fatigue resistance (Belli et al., 2014). It is known that water sorption reduces mechanical properties of materials. The absorbed water, however, acts as a plasticiser of resin matrix. This plasticised or expanded resin matrix could help blunting and generating compressive stress at the tip of fatigue cracks, thereby improving fatigue resistance of the cements (May-Pat et al., 2012).

Fatigue performance of materials can be assessed by obtaining the gradient from stress versus failure cycle curve (S/N curve). Low gradient may represent high fatigue performance of materials. Materials with low gradient will exhibit larger extension of failure cycles than that of composites with high gradient (Koster et al., 2013). Additionally, fatigue life (i.e. failure cycle at low stress level) can be extrapolated from the regression line of S/N curve.

### 7.3 Hypotheses

Chapter 5 demonstrated that replacing TEGDMA by PPGDMA increased monomer conversion and stability of initiator paste of experimental bone composites. Khan (2015) indicated that mechanical properties between UDMA/PPGDMA and UDMA/TEGDMA base experimental bone composites were comparable. The study also revealed that inhibition time, rate of polymerisation, final monomer conversion, polymerisation shrinkage, and strength of the composites decreased linearly upon raising level of phosphates (MCPM with tricalcium phosphate or tristrontium phosphate). Furthermore, Khan showed that raising level of both MCPM and TSrP increased level of  $\text{Sr}^{2+}$  release. The following work assessed whether the findings in Khan's study could be validated.

Monomer systems of experimental bone composites used in the current study were UDMA/TEGDMA or UDMA/PPGDMA. According to the benefits of PPGDMA described in the literature and results from Chapter 5, it was expected the inhibition time, rate of polymerisation, and final monomer conversion of PPGDMA base experimental bone composites will be higher than those of TEGDMA base composites. Furthermore, Inhibition of the experimental bone composites should be preferably at ~ 4 to 8 min. It was anticipated that composites containing PPGDMA, as a consequence of its higher molecular weight, will exhibit lower calculated polymerisation shrinkage than the composites containing TEGDMA.

Phosphates in the current study are MCPM (0, 5, 10 wt%) with fixed level of TSrP (7.5 wt%). Whilst these components can reduce monomer conversions, it was anticipated from results of Chapter 6 that these relatively low levels should have minimal detrimental effect on polymerisation of the composites.

It was expected that hygroscopic expansion of experimental bone composites is affected by flexibility of resin matrix and the level of hydrophilic MCPM. It was therefore anticipated that the composites containing PPGDMA and/or higher level of MCPM will promote greater mass increase and volume expansion than the composites containing TEGDMA and/or lower level of MCPM. Through optimisation of composition, this may enable matching with calculated polymerisation shrinkage. Additionally, the higher flexibility of PPGDMA compared with TEGDMA in addition to increase water sorption of MCPM may enhance surface apatite formation and  $\text{Sr}^{2+}$  release.

Chapter 6 demonstrates that increasing MCPM from 5 to 10 wt% did not detrimentally reduce early strength of the experimental bone composites. It was anticipated that the increase water sorption upon long-term ageing will affect mechanical properties of the composites. Mechanical properties of experimental bone composites from previous works by Main (2013) and Khan (2015) were mainly tested in single/continuous load. Literature described above, however, suggests that failure of materials could be due to fatigue failure induced by repetitive subcritical loads. Additionally, water plasticisation of resin matrix may reduce crack propagation from repetitive loads during fatigue testing. It was, therefore, expected that replacing TEGDMA with PPGDMA and increasing MCPM may improve fatigue properties of the experimental composites in this chapter.



## 7.4 Objectives

The aim of this study was to develop Ca/Sr containing novel injectable bone composites.

The objectives were to assess:

- 1) Inhibition time, rate of polymerisation, final monomer conversion and calculated polymerisation shrinkage / heat generation at a controlled temperature of 25 °C;
- 2) Mass and volume changes in SBF;
- 3) Surface apatite formation in SBF;
- 4) Strontium release in deionised water;
- 5) Strength and fatigue of the experimental bone composites after immersion in SBF for 4 weeks and tested in SBF at a controlled temperature of 37 °C.

The effect of diluent monomer (PPGDMA versus TEGDMA) and MCPM level (0, 5, and 10 wt%) were also investigated. Commercial PMMA cement (Simplex, Stryker, Newbury, Berkshire, UK) and bone composite (Cortoss, Newbury, Berkshire, UK) were used for comparison.

## 7.5 Materials and Methods

Experimental bone composites were prepared using powder to liquid ratio of 2.3:1. The liquid phase contained 70 wt% UDMA, 25 wt% of PPGDMA or TEGDMA, and 5 wt% of HEMA. To this was added either BP (3 wt% of total liquid phase) for the initiator liquid or NTGGMA (2 wt% of total liquid phase) for the activator liquid (Table 7-1).

**Table 7-1 Components of liquid phases before mixing with the powder phase.**

Liquid phase / components	UDMA	PPGDMA / TEGDMA	HEMA	BP	NTGGMA
	wt% of monomers	wt% of monomers	wt% of monomers	wt% of liquid	wt% of liquid
<b>Initiator liquid</b>	70	25	5	3	0
<b>Activator liquid</b>	70	25	5	0	2

N.B. Upon mixing the composite BP and NTGGMA concentrations will become 1.5 and 1 wt% respectively.

Powder phase contained glass filler (0.7  $\mu$ m), mono calcium phosphate (MCPM)(0,5,10 wt% after paste mixing), glass fibre (20 wt% of filler), tristrontium phosphate (7.5 wt% of filler after paste mixing) and polylysine (5 wt% of filler) (Table 7-2).

**Table 7-2 Formulations with varying level MCPM\* (0, 5, 10 wt%) and types of diluent monomer (PPGDMA, TEGDMA). The powder phase of each formulation was mixed with PPGDMA (PPG) or TEGDMA (TEG) liquid phases presented in Table 7-1. Other particle sizes are given in Table 2-2.**

Formulations		0.7 $\mu$ m glass fillers (wt%)	Glass fibres (wt%)	MCPM (wt%)	TSrP (wt%)	PLS (wt%)
<b>M<sub>0</sub>PPG / M<sub>0</sub>TEG</b>		75	20	<b>0</b>	0	5
<b>M<sub>5</sub>PPG / M<sub>5</sub>TEG</b>	Initiator paste	65	20	<b>10</b>	0	5
<b>M<sub>10</sub>PPG / M<sub>10</sub>TEG</b>		55	20	<b>20</b>	0	5
<b>All formulations</b>	Activator paste	60	20	0	15	5

N.B. MCPM in filler is halved after mixing initiator and activator paste.

Monomer conversion at 25 °C was assessed using FTIR-ATR (n=3), mass and volume changes in SBF were measured using a density kit (n=3) and surface apatite formation after immersion in SBF for 1 week was assessed using SEM (n=1). Furthermore,  $\text{Sr}^{2+}$  released into deionised water obtained using ICP-MS (n=3) and biaxial flexural strength (n=5) and fatigue at 4 weeks (n=20) were also examined. All testing protocols were described in Chapter 2.

## 7.6 Statistical analysis

Data were analysed using one-way ANOVA followed by multiple comparison using Tukey's test or Kruskal-Wallis test followed by Dunnett's T3 test ( $p = 0.05$ ). Two variables factorial design with low and high level of variables (equations 2-26,28) was employed to assess any effect of MCPM level (0 versus 5 wt%, 5 versus 10 wt%) and diluent monomer (TEGDMA versus PPGDMA) on monomer conversion, mass and volume changes, strontium release, and mechanical properties of the experimental bone composites.

## 7.7 Results

### 7.7.1 Monomer conversion

#### 7.7.1.1 Inhibition time

Examples of polymerisation profiles are presented in Fig 7-1. The longest and shortest inhibition time were obtained from Simplex ( $403 \pm 2$  s) and M<sub>10</sub>TEG ( $28 \pm 7$  s) respectively (Fig 7-2). The inhibition time of the experimental bone composites, except for M<sub>0</sub>PPG ( $150 \pm 5$  s), was significantly shorter than that of Cortoss ( $155 \pm 5$  s).

Factorial analysis indicated that the primary factor affecting inhibition time of experimental bone composites was type of diluent monomer (Fig 7-3). Replacing TEGDMA by PPGDMA increased inhibition time on average by two folds (209 %). The inhibition time was increased on average by 60 % upon decreasing MCPM level from 5 to 0 wt% but this is primarily observed with PPGDMA rather than with TEGDMA. The effect of increasing MCPM from 5 to 10 wt% on inhibition time was negligible (Fig 7-3 B).

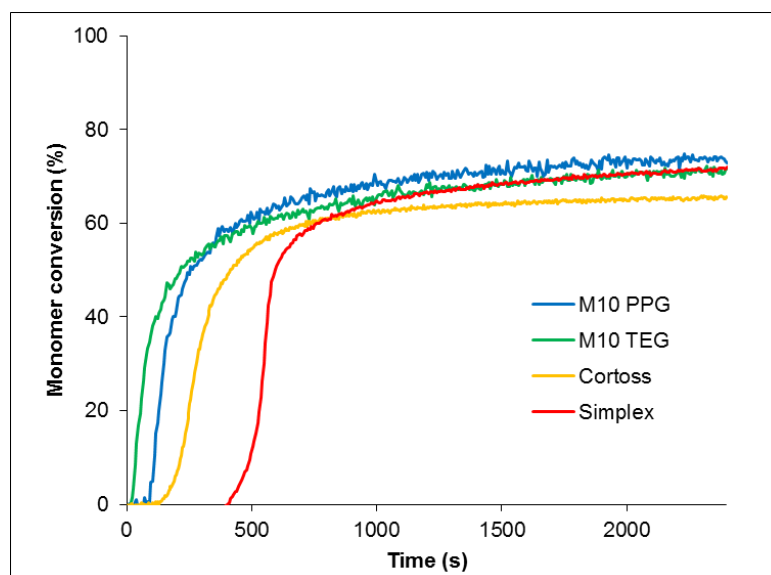


Fig 7-1 Example polymerisation profiles of experimental bone composites measured at controlled temperature of 25 °C.

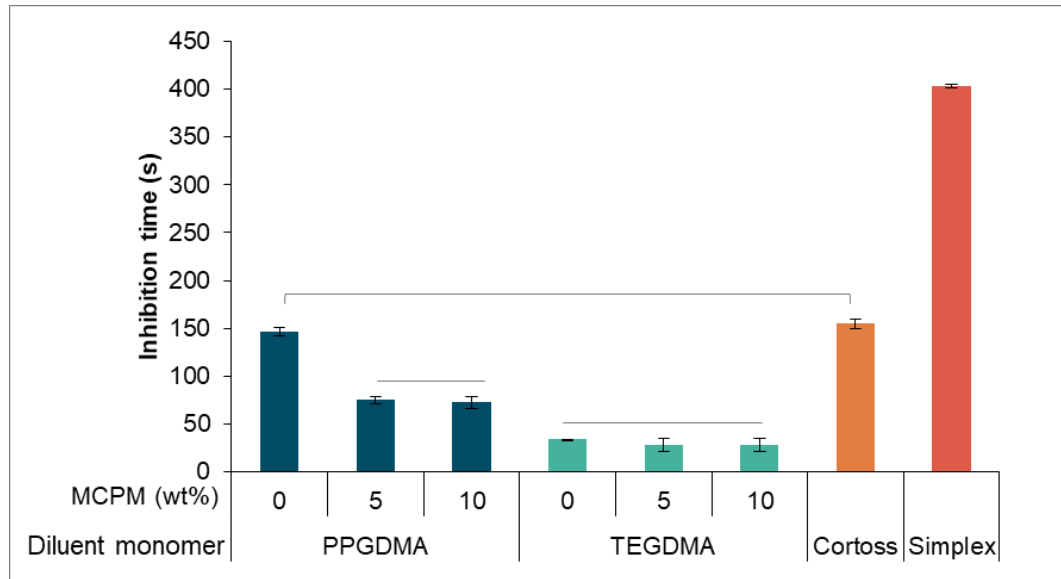


Fig 7-2 Inhibition time of experimental bone composites. Lines indicate no significant difference ( $p > 0.05$ ). Error bars are 95 %CI ( $n = 3$ ).

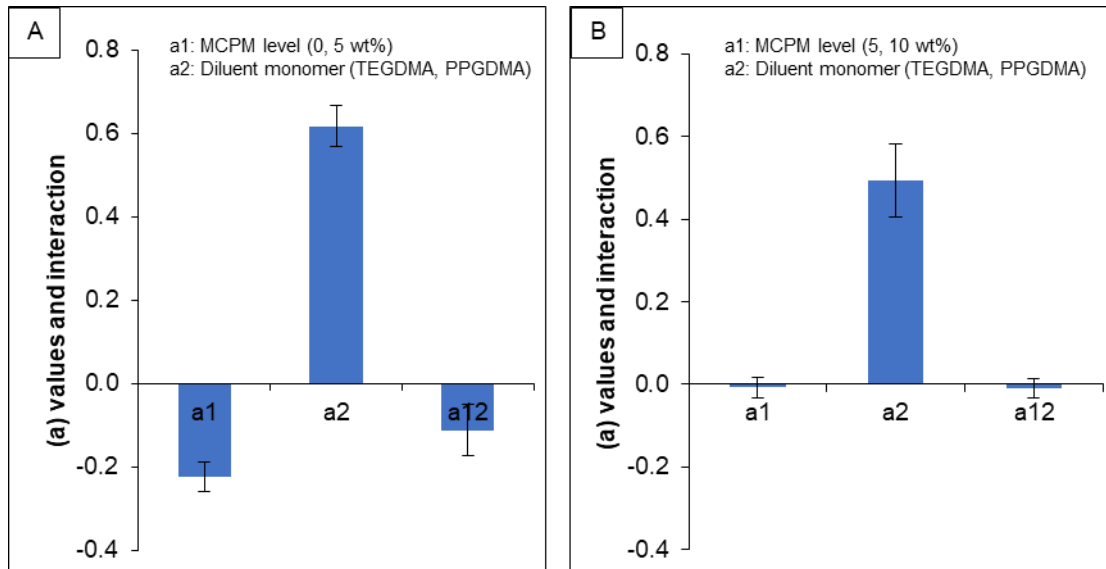
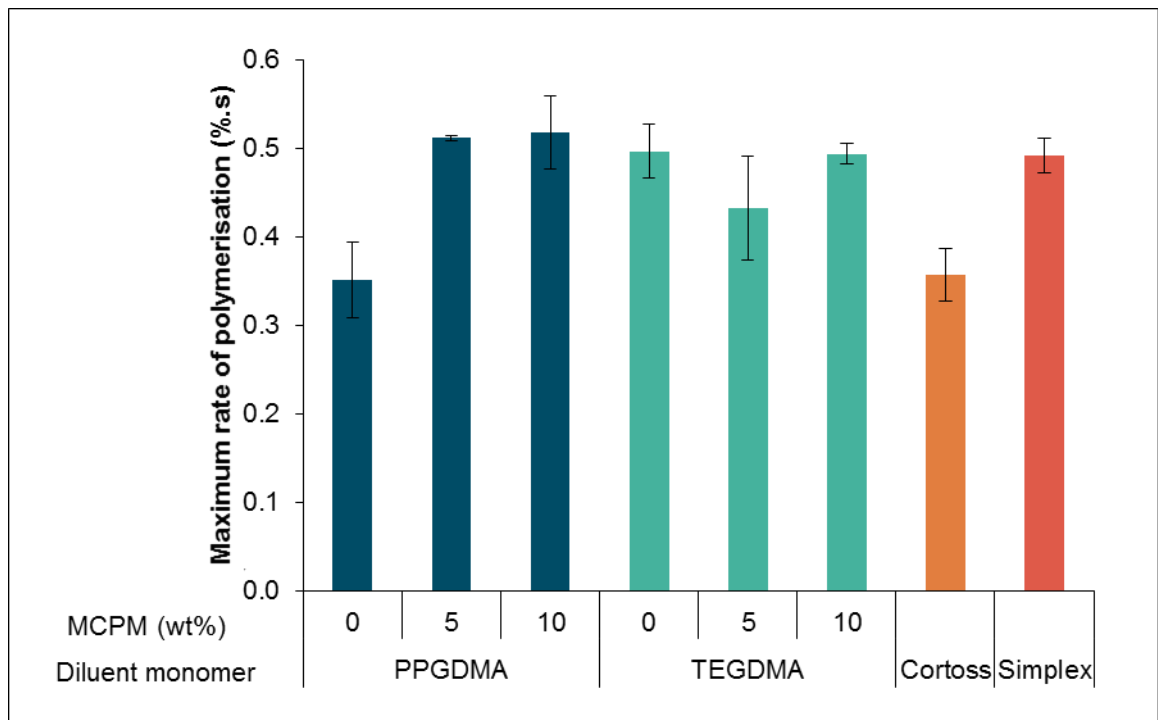


Fig 7-3 Factorial analysis describing the effect of MCPM level, diluent monomers, and their interaction effects on inhibition time. Error bars are 95 %CI ( $n = 3$ ).

### 7.7.1.2 Rate of polymerisation

Highest maximum rate of polymerisation ( $R_p^{\max}$ ,  $\% \cdot s^{-1}$ ) was obtained from  $M_{10}$ PPG ( $0.52 \pm 0.04 \ \% \cdot s^{-1}$ ) (Fig 7-4). No significant difference in  $R_p^{\max}$  amongst materials was obtained. The average effects of increasing MCPM level and type of diluent monomer on  $R_p^{\max}$  were negligible (Fig 7-5).



**Fig 7-4** Maximum rate of polymerisation ( $R_p^{\max}$ ) of experimental bone composites. Error bars are 95 %CI (n =3).

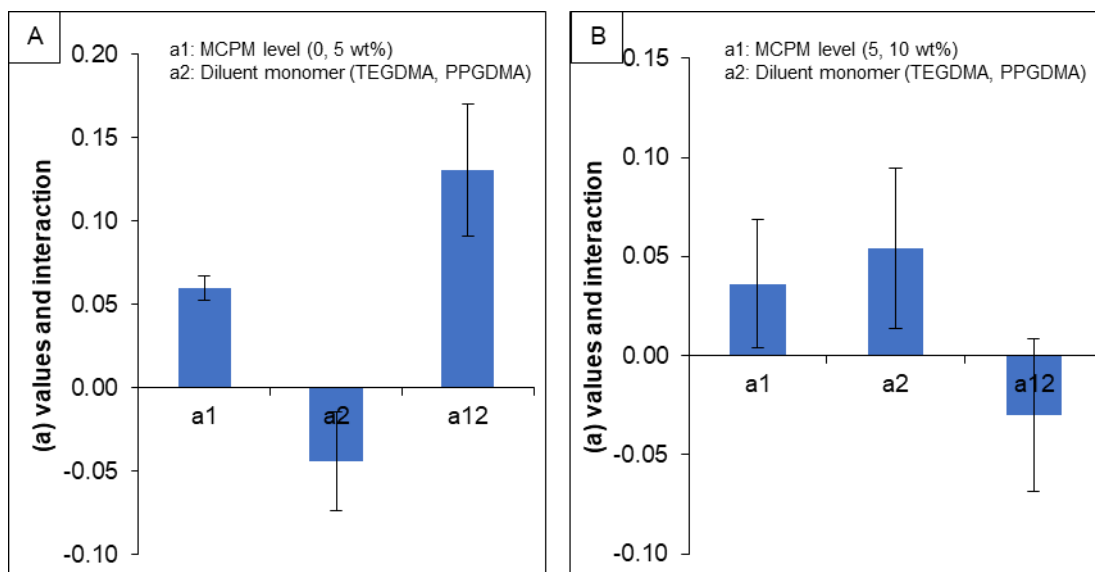


Fig 7-5 Factorial analysis describing the effect of MCPM level, diluent monomers, and their interaction effects on  $R_p^{\max}$ . Error bars are 95 %CI (n =3).

### 7.7.1.3 Final monomer conversion

All experimental bone composites exhibited higher monomer conversion (75 – 82 %) than Cortoss ( $64 \pm 1$  %) (Fig 7-6).  $M_{10}$ PPG ( $82 \pm 1$  %) showed significantly higher final monomer conversion than Simplex ( $78 \pm 1$  %). Monomer conversion of PPGDMA-based bone composites (~ 80%) was higher than that of TEGDMA-based composites (~ 76 %). Factorial analysis indicated that monomer conversion was affected by MCPM level and diluent monomers (Fig 7-7). Replacing TEGDMA with PPGDMA increased monomer conversion on average by 5 %. The effect of MCPM on monomer conversion was dependent upon level of MCPM. Monomer conversion was increased by 5 % upon increasing MCPM from 0 to 5 wt% or decreasing MCPM from 10 to 5 wt%.

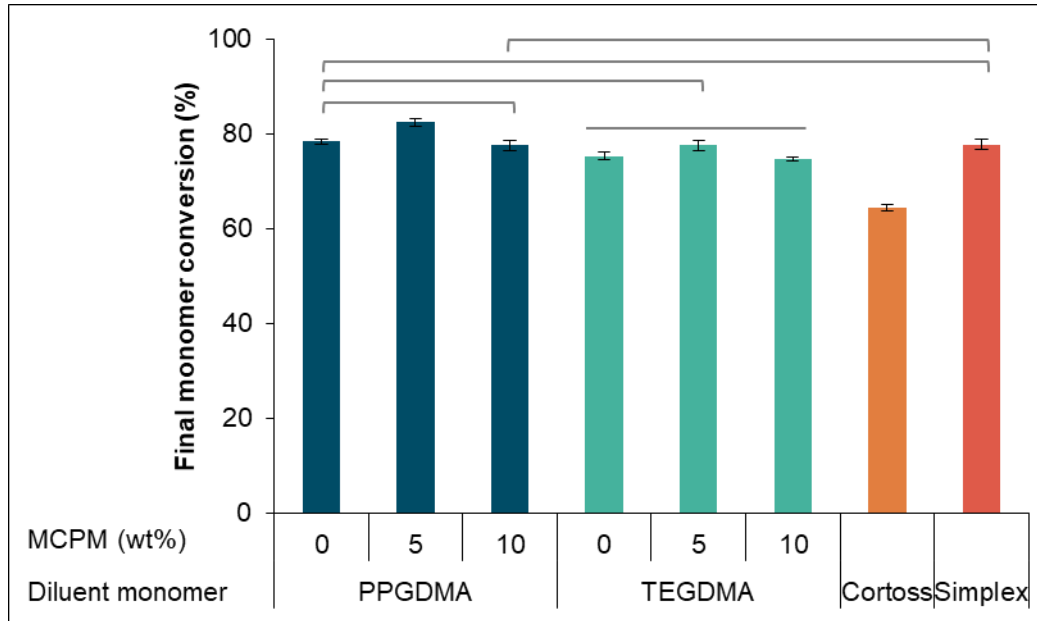


Fig 7-6 Final monomer conversion of experimental bone composites. Lines indicate no significant difference ( $p > 0.05$ ). Error bars are 95 %CI (n = 3).

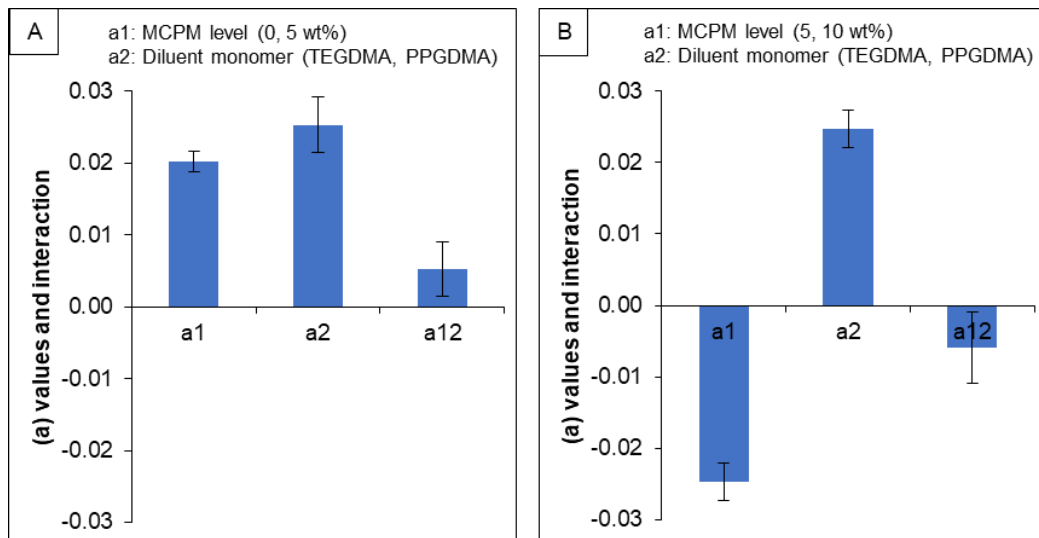


Fig 7-7 Factorial analysis describing the effect of MCPM level, diluent monomers, and their interaction effects on monomer conversion. Error bars are 95 %CI (n = 3).



#### **7.7.1.4 Calculated polymerisation shrinkage and heat generation**

Calculated polymerisation shrinkage and heat generation of TEGDMA-based formulations (5.1 vol% and 0.127 kJ/cc) were higher than those of PPGDMA-based formulations (4.2 vol% and 0.104 kJ/cc) (Fig 7-8). Factorial analysis indicated that the primary factor affecting shrinkage and heat generation was diluent monomers (Fig 7-9). The shrinkage and heat generation were increased on average by 22% upon replacing PPGDMA by TEGDMA. The average effect of MCPM was negligible.

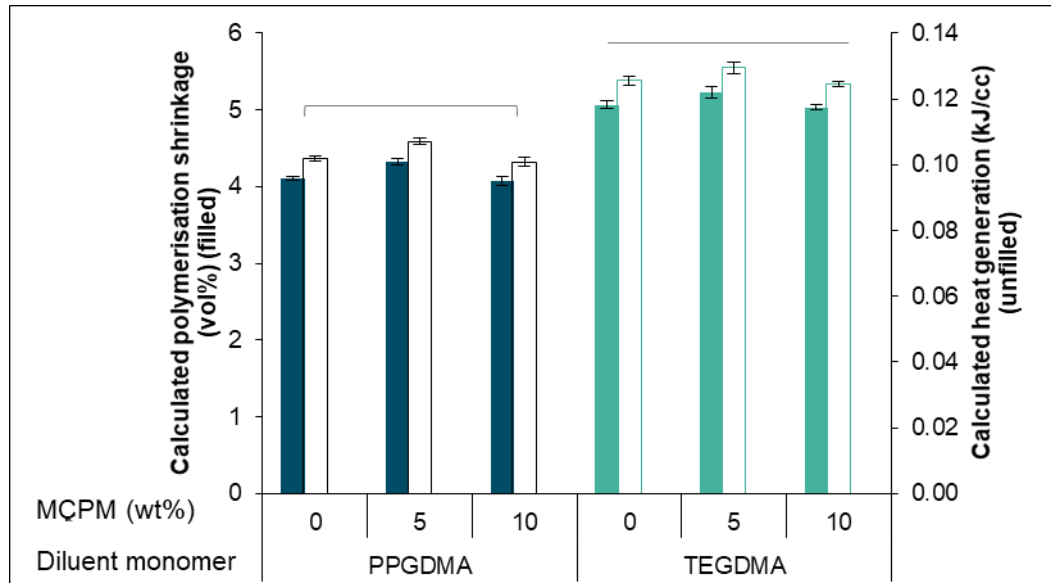


Fig 7-8 Calculated polymerisation shrinkage and heat generation. Lines indicate no significant difference ( $p > 0.05$ ). Error bars are 95 %CI (n =3).

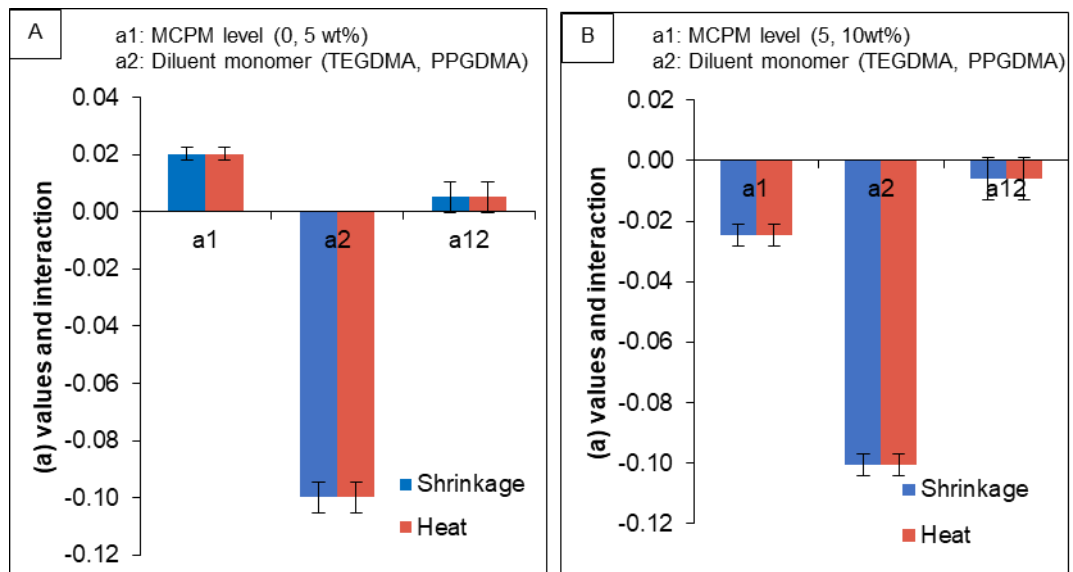


Fig 7-9 Factorial analysis describing the effect of MCPM level, diluent monomers, and their interaction effects on calculated polymerisation shrinkage/heat generation. Error bars are 95 %CI (n =3).

### 7.7.2 Mass and volume changes

Early mass changes of all materials increased linearly with square root of time (Fig 7-10). At 1 week, mass change of Simplex, Cortoss, M<sub>0</sub>TEG and M<sub>0</sub>PPG reached final values of (1.6 ± 0.1), (3.0 ± 0.1), (2.7 ± 0.1), and (3.0 ± 0.1) wt% respectively. These mass changes then levelled off. Upon increasing MCPM, mass of the composites continued to increase and reached final values of 3.4 ± 0.1 wt% (M<sub>5</sub>TEG), 4.0 ± 0.2 wt% (M<sub>5</sub>PPG), 4.3 ± 0.1 wt% (M<sub>10</sub>TEG), and 5.8 ± 0.0 wt% (M<sub>10</sub>PPG) at 4 weeks.

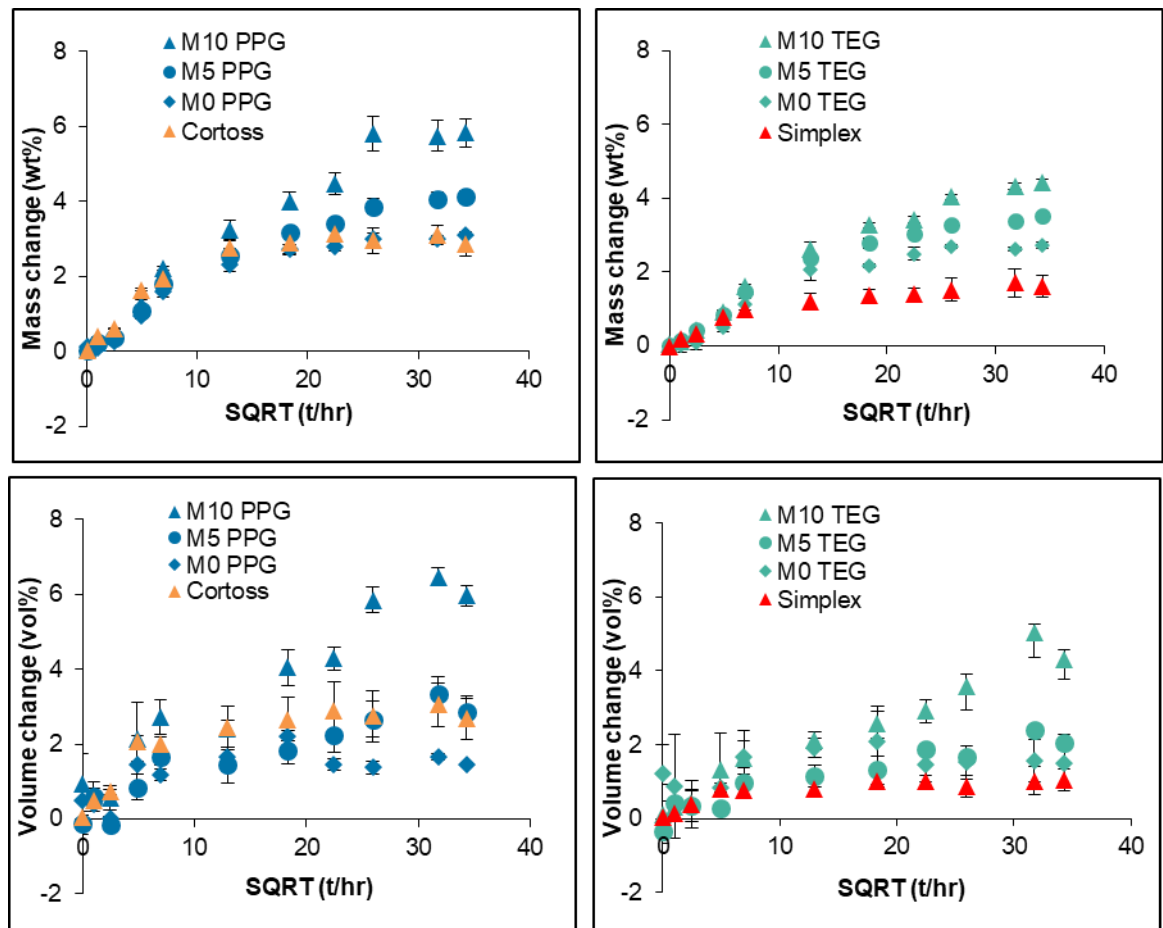


Fig 7-10 Mass and volume changes versus square root of time (hr) of all materials immersed in SBF up to 7 weeks. Error bars are 95% CI (n=3).

Volume change of Simplex, Cortoss, M<sub>0</sub>TEG, M<sub>0</sub>PPG, M<sub>5</sub>TEG, and M<sub>5</sub>PPG reached maximum values at 1 week of (1.0 ± 0.1), (2.8 ± 0.2), (1.5 ± 0.2), (1.5 ± 0.2), (2.1 ± 0.4), and (3.0 ± 0.4) vol% respectively. For M<sub>10</sub>TEG and M<sub>10</sub>PPG, volume changes continued to increase for longer, reaching average values after 4 weeks of (4.3 ± 0.9) and (6.1 ± 0.4) vol% respectively.

Initial gradients of mass and volume change versus square root of time are presented in Table 7-2. These were (0.19 – 0.24) vol%.hr<sup>-0.5</sup> and (0.13 – 0.22) vol%.hr<sup>-0.5</sup> for PPGDMA based composites, (0.17 – 0.19) wt%.hr<sup>-0.5</sup> and (0.16 – 0.18) vol%.hr<sup>-0.5</sup> for TEGDMA based composites. The highest gradients were obtained from M<sub>10</sub>PPG ((0.24 ± 0.01) wt%.hr<sup>-0.5</sup> and (0.22 ± 0.01) vol%.hr<sup>-0.5</sup>). Rate of mass and volume increase were (0.15 ± 0.01) wt%.hr<sup>-0.5</sup> and (0.16 ± 0.02) vol%.hr<sup>-0.5</sup> for Simplex and (0.22 ± 0.01) vol%.hr<sup>-0.5</sup> and (0.37 ± 0.07) vol%.hr<sup>-0.5</sup> for Cortoss.

**Table 7-2 Results from mass and volume changes of each material. Errors are 95 %CI (n=3).**

Formulations	Rate of mass increase (wt%.hr <sup>-0.5</sup> )	Mass change at late time (wt%)	Rate of volume increase (vol%.hr <sup>-0.5</sup> )	Volume change at late time (vol%)
<b>M<sub>0</sub>PPG</b>	0.19 ± 0.02 <sup>b</sup>	3.0 ± 0.1	0.13 ± 0.02 <sup>b</sup>	1.5 ± 0.2
<b>M<sub>5</sub>PPG</b>	0.19 ± 0.01 <sup>b</sup>	4.0 ± 0.2	0.10 ± 0.02 <sup>c</sup>	3.0 ± 0.4
<b>M<sub>10</sub>PPG</b>	0.24 ± 0.01 <sup>c</sup>	5.8 ± 0.0	0.22 ± 0.03 <sup>c</sup>	6.1 ± 0.4
<b>M<sub>0</sub>TEG</b>	0.17 ± 0.02 <sup>b</sup>	2.7 ± 0.1	0.16 ± 0.03 <sup>b</sup>	1.5 ± 0.2
<b>M<sub>5</sub>TEG</b>	0.19 ± 0.01 <sup>b</sup>	3.4 ± 0.1	0.08 ± 0.00 <sup>c</sup>	2.1 ± 0.4
<b>M<sub>10</sub>TEG</b>	0.19 ± 0.00 <sup>c</sup>	4.3 ± 0.2	0.15 ± 0.02 <sup>c</sup>	4.3 ± 0.9
<b>Cortoss</b>	0.22 ± 0.01 <sup>b</sup>	3.0 ± 0.1	0.37 ± 0.07 <sup>a</sup>	2.8 ± 0.2
<b>Simplex</b>	0.15 ± 0.01 <sup>b</sup>	1.6 ± 0.1	0.16 ± 0.02 <sup>a</sup>	1.0 ± 0.1

Data were calculated up to 1 day (<sup>a</sup>), 2 weeks (<sup>b</sup>), and 5 weeks (<sup>c</sup>)

### 7.7.3 Surface apatite formation

At 1 week, no precipitates were observed on surfaces of M<sub>0</sub>TEG, M<sub>0</sub>PPG, M<sub>5</sub>TEG, Simplex, and Cortoss (Fig 7-11). Thin surface apatite (~ 1 µm) layers partially covered surfaces of M<sub>10</sub>TEG and M<sub>10</sub>PPG but patchy crystals more consistent with brushite were observed on some areas of M<sub>5</sub>PPG.

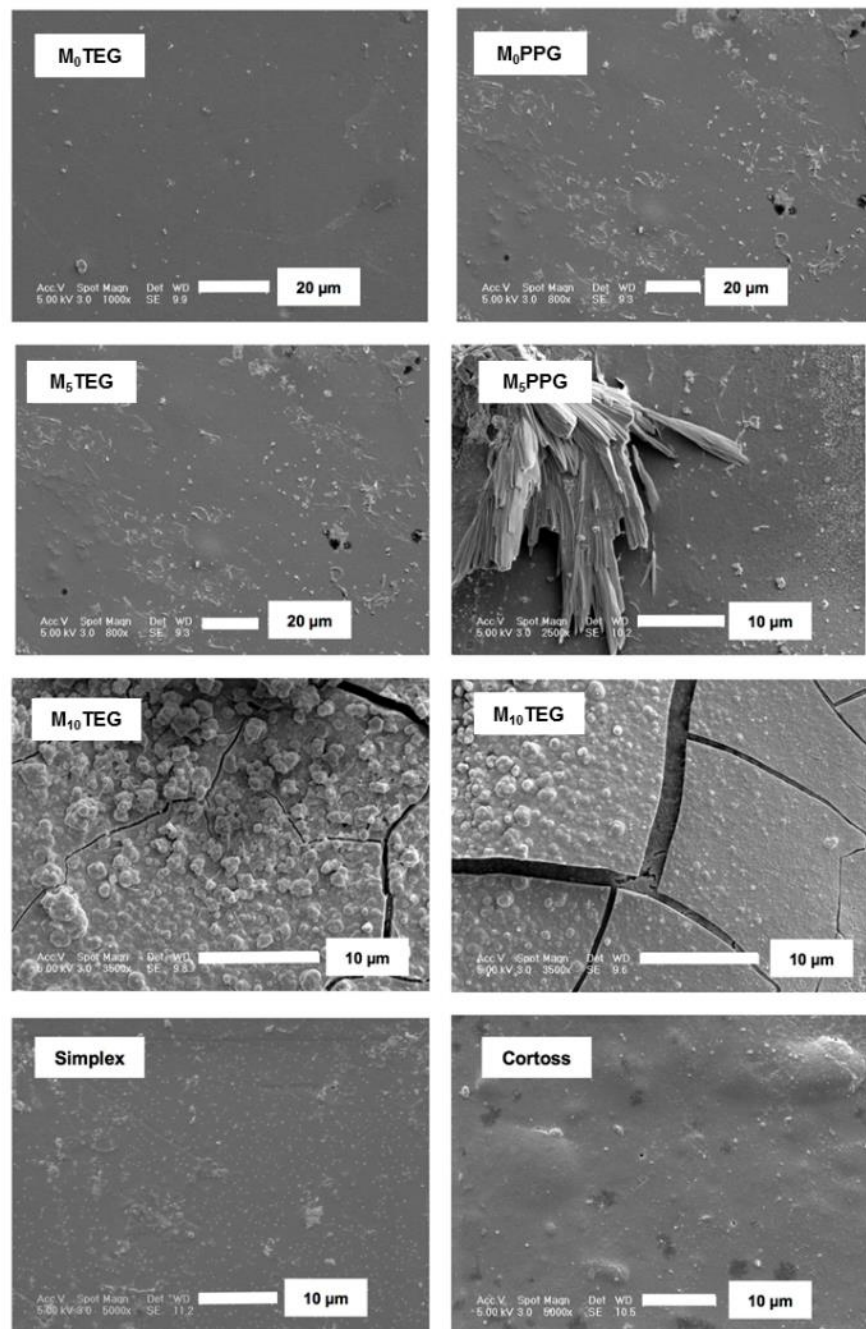


Fig 7-11 Representative SEM images for each material after 1 week immersion in SBF.

#### 7.7.4 Strontium ( $\text{Sr}^{2+}$ ) release

The cumulative release of  $\text{Sr}^{2+}$  was linear with time (Fig 7-12). Highest and lowest rate of  $\text{Sr}^{2+}$  release was  $0.0015 \text{ \%}.\text{hr}^{-1}$  and  $0.0002 \pm 0.01 \text{ \%}.\text{hr}^{-1}$  observed with  $\text{M}_{10}\text{PPG}$  and  $\text{M}_0\text{PPG}$  respectively.  $\text{M}_{10}\text{PPG}$  exhibited the highest  $\text{Sr}^{2+}$  release at 4 weeks ( $1.12 \pm 0.02 \text{ \%}$ ). Factorial analysis indicated that level of MCPM and diluent monomers both affected the release of  $\text{Sr}^{2+}$  (Fig 7-13). The effect of diluent monomers was, however, dependent upon level of MCPM. The cumulative release of  $\text{Sr}^{2+}$  at 4 weeks was increased on average by 126 % upon increasing MCPM from 0 to 5 wt% or 5 to 10 wt%. Additionally, the release was increased by  $111 \pm 34 \text{ \%}$  upon replacing TEGDMA by PPGDMA when MCPM was increased from 5 to 10 wt%.

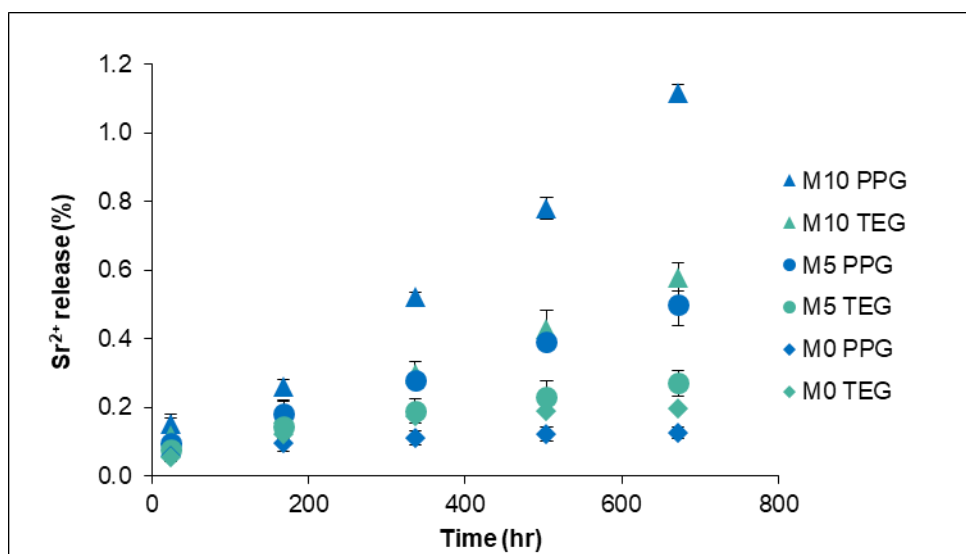
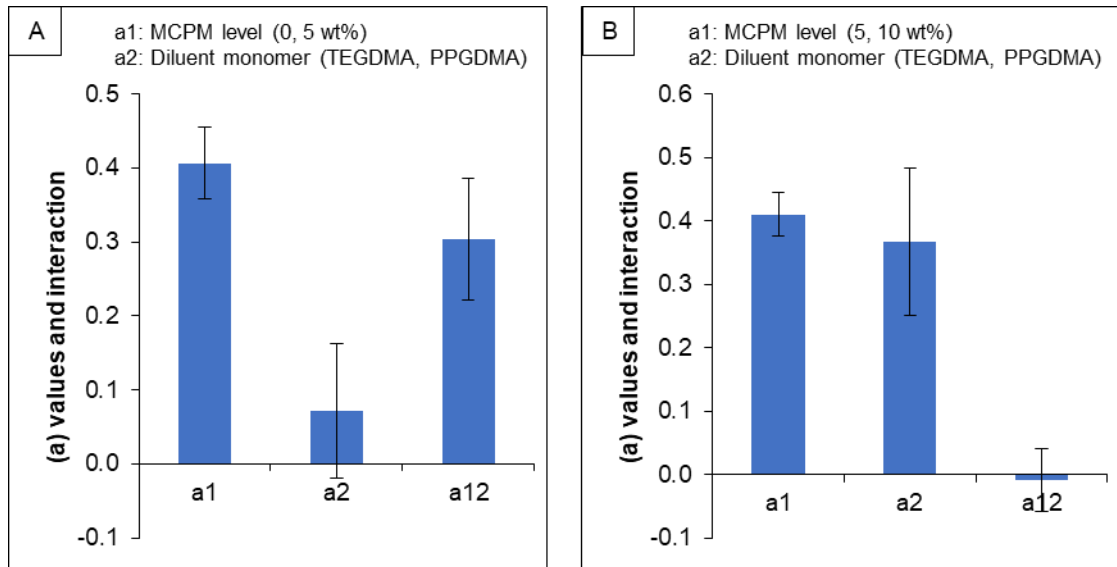


Fig 7-12 Cumulative  $\text{Sr}^{2+}$  release versus hr from bone composites immersed in deionised water up to 4 weeks. Error bars are 95% CI (n=3).



**Fig 7-13** Factorial analysis describing the effect of MCPM level, diluent monomers, and their interaction effects on the cumulative  $\text{Sr}^{2+}$  release at 4 weeks. Error bars are 95 %CI (n =3). Stars indicate negative effect from variables.

## 7.7.5 Biaxial flexural fatigue

### 7.7.5.1 Biaxial flexural strength tested at 37 °C

The highest BFS of materials tested in SBF at controlled temperature of 37 °C was obtained from Simplex ( $137 \pm 4$  MPa) (Fig 7-14).  $M_5\text{PPG}$  had a comparable BFS ( $63 \pm 2$  MPa) to  $M_5\text{TEG}$  ( $65 \pm 3$  MPa). The BFS of both  $M_5\text{PPG}$  and  $M_5\text{TEG}$  were significantly higher than that of  $M_{10}\text{PPG}$  ( $54 \pm 3$  MPa),  $M_{10}\text{TEG}$  ( $57 \pm 2$  MPa), and Cortoss ( $58 \pm 2$  MPa).

Factorial analysis revealed the strong effect of MCPM level on BFS (Fig 7-15 A). BFS was increased by  $73 \pm 9$  % and  $18 \pm 4$  % upon decreasing of MCPM level from 5 to 0 wt% and 10 to 5 wt% respectively. The effect of using different diluent monomer was negligible.

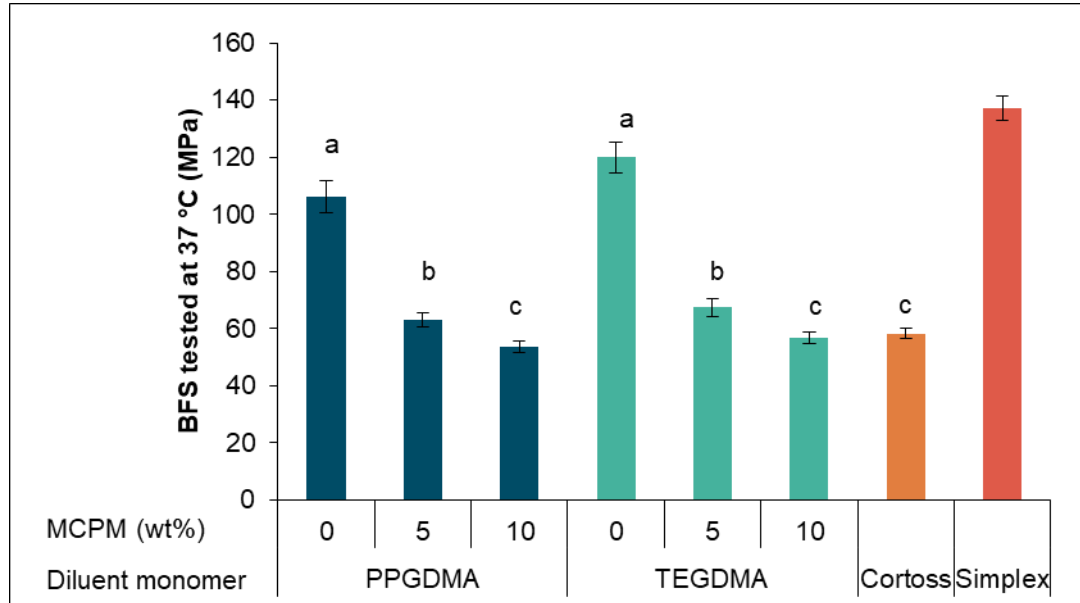


Fig 7-14 BFS of all materials after immersion in SBF for 4 weeks tested in wet condition at 37 °C. Error bars are 95% CI (n=5). Same letters indicate no significant difference ( $p > 0.05$ )

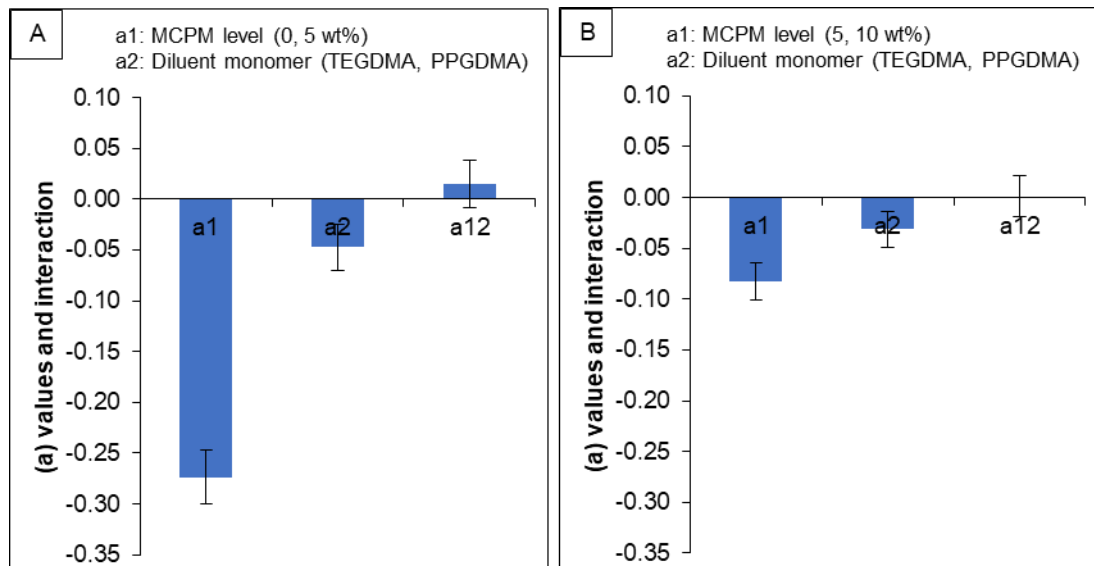


Fig 7-15 Factorial analysis describing the effect of MCPM level, diluent monomers, and interaction effects on BFS at 4 weeks. Error bars are 95 %CI (n =5).



#### 7.7.5.2 Gradient of S/N curve

Plots of biaxial flexural strength versus logarithm of failure cycle (S/N curve) are presented in Fig 7-16. Logarithm of failure cycles increased upon the decrease of applied stress. Highest gradient of the S/N curve was observed among M<sub>0</sub>PPG ( $12 \pm 1$  MPa/log cycle), M<sub>0</sub>TEG ( $16 \pm 2$  MPa/log cycle), and Simplex ( $18 \pm 2$  MPa/log cycle) (Fig 7-17). The gradient of the S/N curve among M<sub>5</sub>PPG ( $7 \pm 1$  MPa/log cycle), M<sub>10</sub>PPG ( $6 \pm 1$  MPa/log cycle), M<sub>5</sub>TEG ( $6 \pm 1$  MPa/log cycle), M<sub>10</sub>TEG ( $6 \pm 1$  MPa/log cycle) and Cortoss ( $6 \pm 1$  MPa/log cycle) were comparable.

Factorial analysis revealed the strong effect of MCPM level on the gradient of experimental composites (Fig 7-18 A). Gradient of S/N curve of the composites increased by  $126 \pm 30$  % upon decreasing MCPM from 5 to 0 wt%. The effect of decreasing MCPM from 10 to 5 wt% and using different diluent monomers were negligible.

#### 7.7.5.3 Fatigue life upon BFS of 10 MPa

Failure cycle of all materials upon applying stress of 10 MPa (fatigue life) was obtained by extrapolating the regression lines from S/N plots (Fig 7-19). The predicted fatigue life (log cycle) at an applied stress of 10 MPa for the experimental composites (7.5 – 8.2 log cycle) was not significantly different from that for the commercial products (7.8 – 7.9 log cycle). Additionally, factorial analysis showed that MCPM level and diluent monomer had no significant effect on the fatigue life (Fig 7-20).

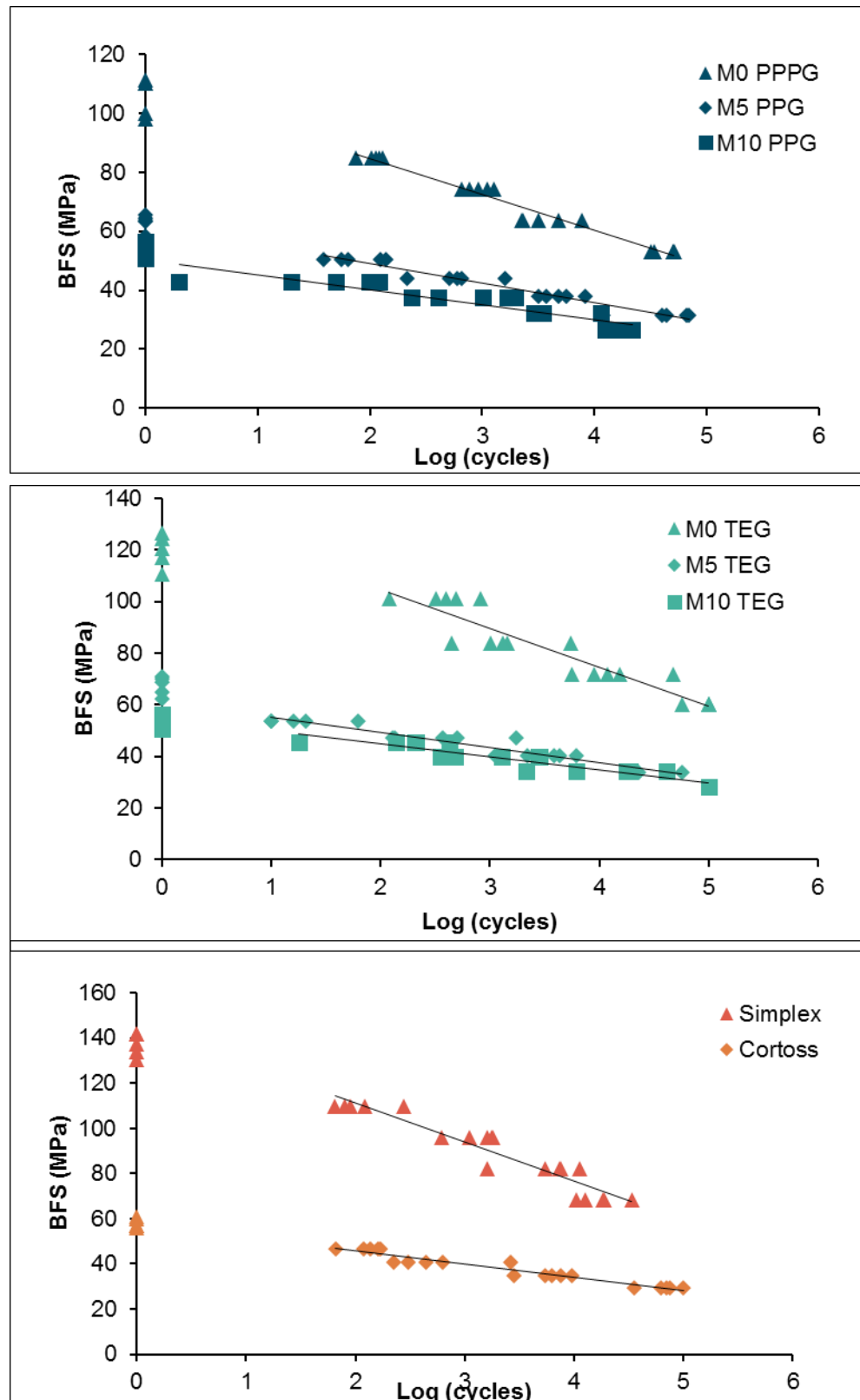


Fig 7-16 Plots of BFS versus log (cycle) (n=20). Gradients of regression lines (S/N curve) were used to compare fatigue performances.

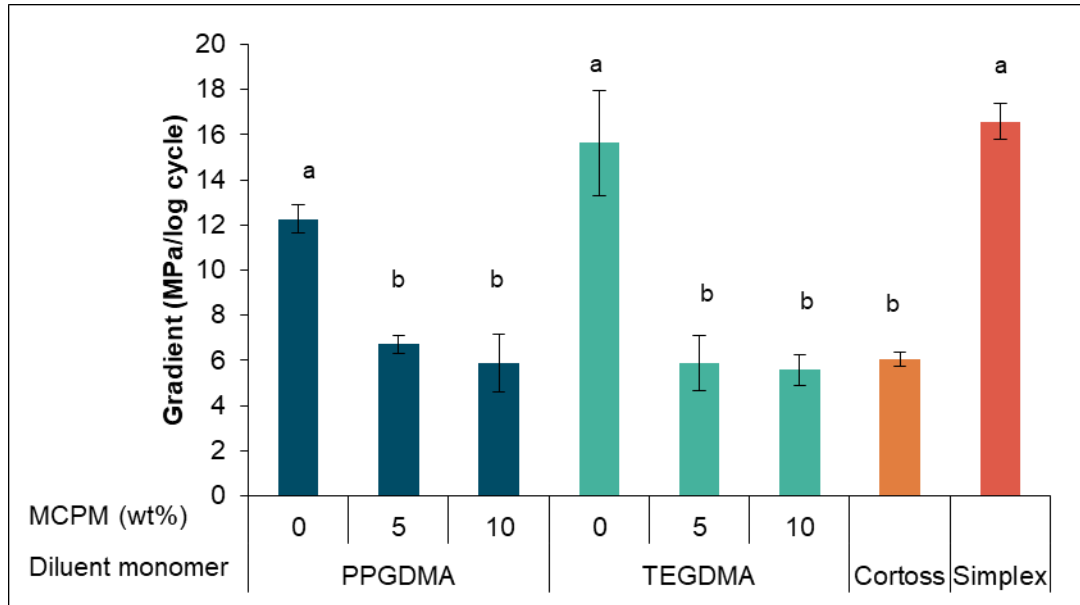


Fig 7-17 Gradient of *S-N* curves. Error bars are 95% CI (n=5). Same letters indicate no significant difference ( $p > 0.05$ ).

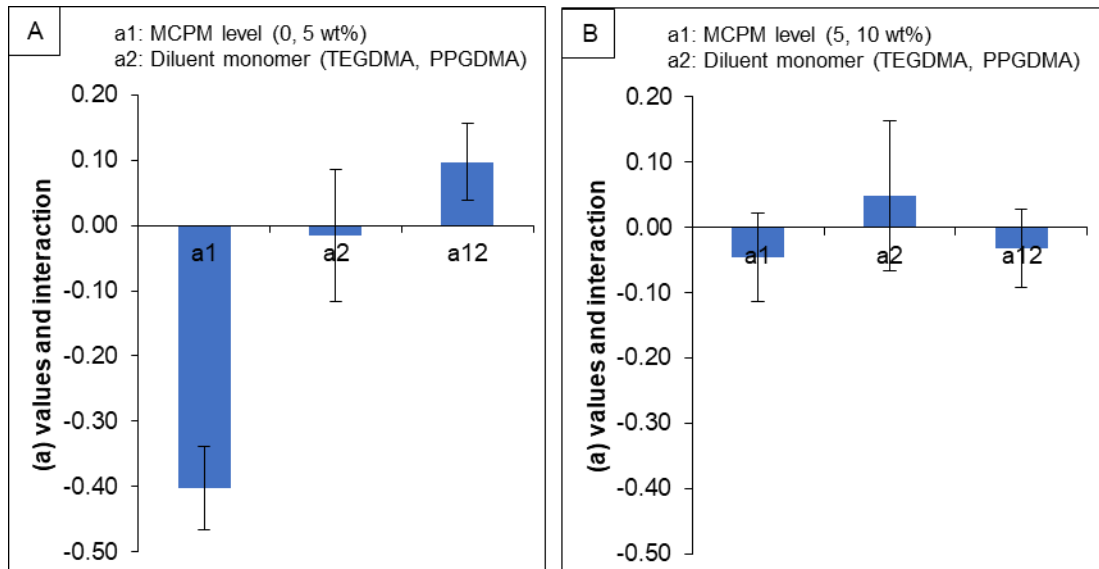


Fig 7-18 Factorial analysis describing the effect of MCPM level, diluent monomers, and their interaction effects gradient of *S/N* curve. Error bars are 95% CI (n=5).

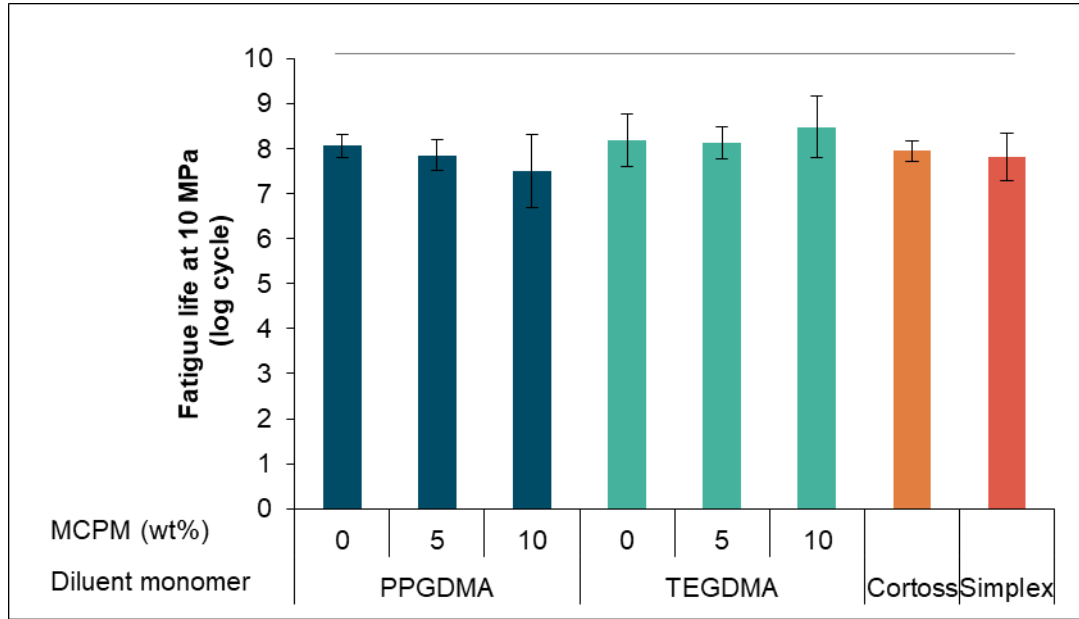


Fig 7-19 Fatigue life upon applied stress of 10 MPa of the experimental composites and commercial products. Error bars are 95% CI (n=5). Line indicates no significant difference ( $p > 0.05$ ).

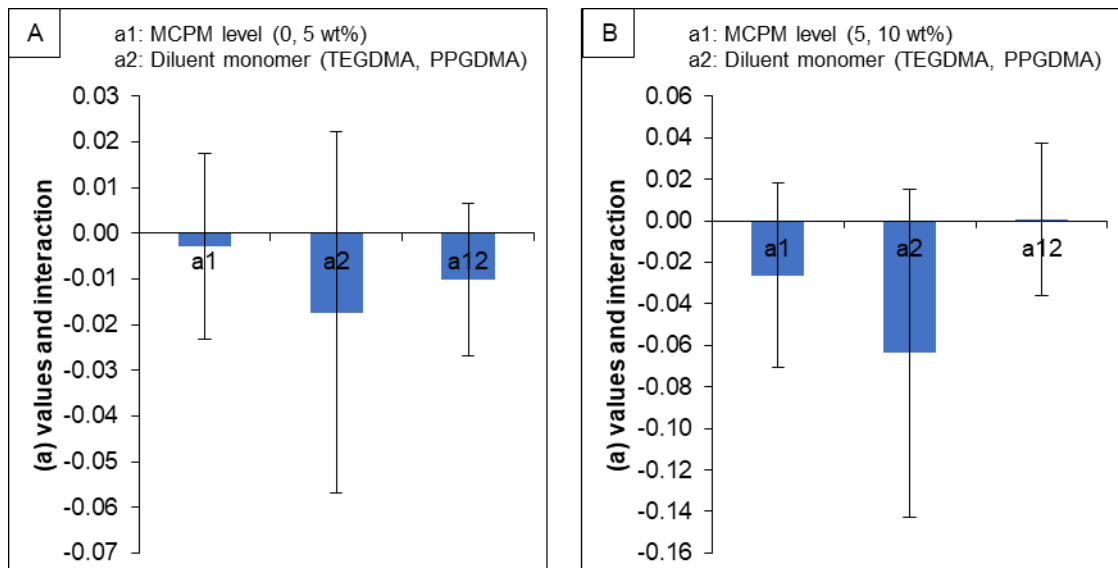


Fig 7-20 Factorial analysis describing the effect of MCPM level, diluent monomers, and their interaction effects on fatigue life. Error bars are 95 %CI (n =5). Stars indicate negative effect from variables.

## 7.8 Discussion

The aim of this study was to develop novel Ca/Sr containing bone composites for vertebroplasty. Monomer conversion, mass and volume changes, surface apatite precipitation,  $\text{Sr}^{2+}$  release, and biaxial flexural fatigue were assessed. The effect of MCPM levels (0, 5, and 10 wt%) and diluent monomer (TEGDMA and PPGDMA) were also examined.

### 7.8.1 Monomer conversion

An ideal bone composite should exhibit sufficient working time for the clinician preferably 4 – 8 min. High rate of polymerisation is required to prevent the composites being washed out by physiologic fluid after injection. Additionally, high monomer conversion is required to reduce risk of toxic monomers leaching and ensure good strength. Furthermore, low shrinkage / heat generation is needed to ensure bone-composite integration. The results from this chapter are partially in agreement with Khan (2015). Replacing TEGDMA by PPGDMA increased inhibition time and final monomer conversion but decreased calculated polymerisation shrinkage. Raising MCPM level decreased inhibition time. However, its effect on rate of polymerisation, final monomer conversion, and calculated polymerisation shrinkage were complex.

#### 7.8.1.1 Inhibition time

It is assumed that setting time and handling properties of the experimental bone composite might be governed by the inhibition time of the materials. Lewis (2006) proposed that working time of PMMA cements in vertebroplasty, which require mixing of powder with liquid components and transfer to a syringe, should be approximately 6 – 10 min. This proposed working time is also in accordance with that required by BS ISO 5833:2002 Implants for surgery-Acrylic resin cements (British Standard, 2002). Mixing

time (47 s) plus inhibition time (403 s) of Simplex from the current study (~ 8 min in total) fell within this recommendation. Furthermore, it can be assumed that working time of two-paste and preloaded bone composites can be shortened by ~ 2 min as the mixing of powder with liquid and a transfer of mixed paste to a syringe are not required. The inhibition time of Cortoss in the current study was ~ 3 min which was slightly shorter than expected desired working time for bone composites (4 - 8 min).

Average inhibition time of experimental bone composites in the current study was ~ 1 min, which may be too short. This can be regarded as a drawback of these materials as clinicians may have limited working period for injection of the experimental bone composites. This will be due an overly high level of initiator and activator which should be reduced in future work.

The inhibition time of the PPGDMA-based composites decreased when MCPM was added. This may be the result of the improved wettability as a consequence of reduced small glass filler in powder phases below a critical point known as the glass wet point. Being sufficiently optimised powder content may minimise the amount of O<sub>2</sub> containing air bubbles that increase inhibition time. This effect was not evident in TEGDMA-based formulations. This may be a consequence of low molecular weight of TEGDMA which can improve wetting of the powder phase in the composite pastes.

PPGDMA-based composites showed longer inhibition time compared with TEGDMA-based composites as was expected. This could be due to that lower molecular weight TEGDMA facilitating the movement of free radicals that will initiate the polymerisation. This result is in agreement with results from Main (2013) and Khan (2015).

#### **7.8.1.2 Rate of polymerisation**

Bone composites with high rate of polymerisation are preferable as the composites should ideally be polymerised immediately after they are delivered to the affected site. This could reduce risk of cement leakage from the application site or wash out by physiological fluid (Yu et al., 2013). The rapid reduction in strength due to cement washout is a major limitation for slow setting cements such as calcium phosphate cements (Chen et al., 2015). This cement being washed out could also lead to serious complications such as pulmonary cement embolism. Although PPGDMA-based composites exhibited longer inhibition time, these composites subsequently polymerised at a similar rate to the TEGDMA-based composites. Furthermore, no significant effect of MCPM on rate of polymerisation was obtained due probably to the level of MCPM used in this chapter was low.

#### **7.8.1.3 Final monomer conversion**

Monomer conversion of Simplex (80 %) in the current study is in a good agreement with that obtained from published studies (Vallo, 2002; Ali et al., 2015). It should be noted that methylmethacrylate (MMA) monomer in Simplex contains only one methacrylate group to undergo polymerisation (Fig 7-21). Hence, all MMA monomers need to be polymerised completely, e.g. 100% conversion, to prevent the leaching of unreacted monomers. Since the conversion of Simplex was ~ 80 %, this may imply that a certain amount of unbounded MMA monomer can be released. On the contrary, dimethacrylate monomers contain two methacrylate groups, thereby the polymerisation of 50% of methacrylate groups may be sufficient to prevent leaching out of monomers.

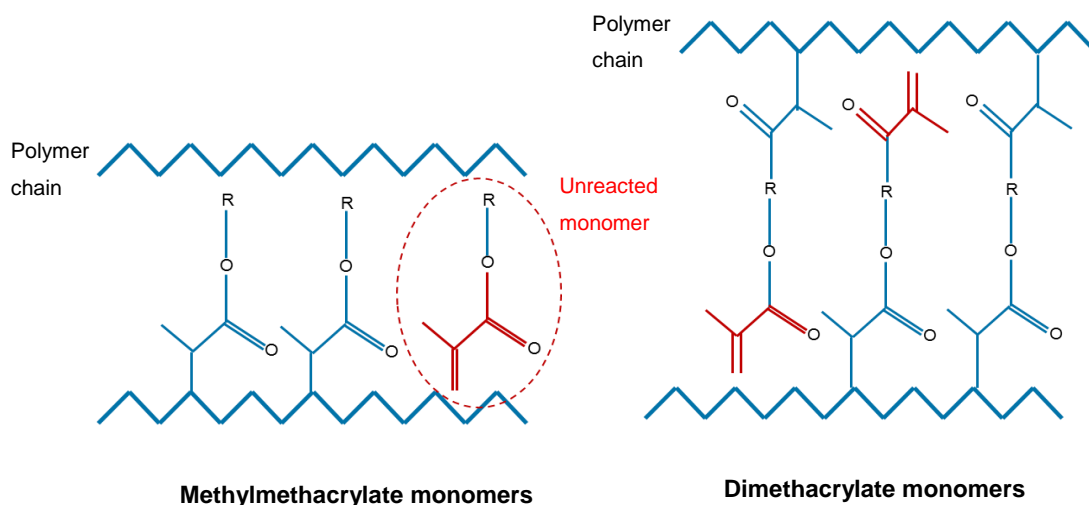


**Fig 7-21 Schematics representing the polymerisation of methylmethacrylate (MMA) and dimethacrylate monomers. The methacrylate group of all MMA monomers have to be polymerised to prevent the release of unreacted monomers. In contrast, polymerisation of 50 % of methacrylate groups in dimethacrylate monomers may be sufficient to prevent leaching of the monomers.**

The conversion of Cortoss in the current study was lower than that (80%) reported by Pomrink et al. (2003). This inconsistency may be due to the use of differential scanning calorimeter (DSC) instead of FTIR in the earlier published study. A number of studies have demonstrated that DSC tends to give higher final conversion than FTIR (Esposito Corcione et al., 2008; Esposito Corcione et al., 2009). DSC measures the monomer conversion by calculating molar heat generated upon polymerisation. This calculation is based on an assumption that the heat generation due to the conversion of C=C is the same for all monomers. Results, however, can vary due to the presence of lower molecular weight monomers or unsaturated impurities in the polymerising mixture that may generate higher heat (Imazato et al., 2001; Suh et al., 2003).

The experimental bone composites exhibited higher final monomer conversion compared to Cortoss. As mentioned earlier in Chapter 3, high glass transition



temperature ( $T_g$ ) monomers generally give low final monomer conversion. The lower conversion of commercial composite may be attributed to the high  $T_g$  of monomer (Bis-GMA) that was used as primary base monomer in the composite.

Low molecular weight TEGDMA with a high crosslinking density may restrict the movement of radical chains in the polymerising mixture, thus reducing final monomer conversion of TEGDMA-based composites (Martim et al., 2017). Hence, replacing TEGDMA by higher molecular weight and lower cross-linking density PPGDMA increased monomer conversion of the composites. This was in agreement with previous studies (Main, 2013; Khan, 2015; Walters et al., 2016). However, the effect of MCPM on final monomer conversion was complex.

#### **7.8.1.4 Calculated polymerisation shrinkage**

The lower concentration of double bonds per mole with PPGDMA contributed to the lower calculated polymerisation shrinkage and heat generation of PPGDMA-based composites compared to the TEGDMA-based composites. This was in agreement with previous studies (Main, 2013; Khan, 2015; Walters et al., 2016). Calculated polymerisation shrinkage of experimental bone composites in the current study was comparable to that of Cortoss (4 vol%) (Main, 2013) but lower than the shrinkage observed from PMMA bone cement (6 – 7 vol%) (Kuehn et al., 2005).

It is proposed that gaps at cement-bone interfaces could be the consequence of thermal damage due to exothermic polymerisation reaction, especially with PMMA cements (Saleh et al., 2016). The calculated heat generation of the experimental bone composites in the current study (~ 0.1 kJ/cc). The low heat generation of the experimental bone composites may help to decrease the risk of tissue damage, thereby improving bone-cement integration.

### 7.8.2 Mass and volume changes

Mass increase due to water sorption of Simplex reached maximum values within 2 days. This is consistent with that obtained from a published study (Ayre et al., 2014). Cortoss exhibited greater mass increase compared to Simplex due probably to the lower monomer conversion, higher flexibility of polymer network, and hydrophilicity of bioactive glass contained in Cortoss (Bae et al., 2010).

For experimental bone composites, their mass and volume changes were governed primarily by MCPM level and type of diluent monomer. Raising MCPM level enhanced water uptake leading to the increase of mass and volume as was previously observed in novel dental composites in the previous chapter and published studies (Mehdawi et al., 2013; Aljabo et al., 2015). Low crosslinking density and high flexibility of PPGDMA polymer may promote water diffusion, thereby increasing the mass and volume changes of the PPGDMA-based composite

An increase of volume expansion due to the increase of MCPM level and using PPGDMA are expected to compensate an unavoidable polymerisation shrinkage (Kuehn et al., 2005). The volume increase of PMMA bone cement in the current study (~ 2 vol %) was lower than the shrinkage reported from a published study (6 - 7 vol%) (Kuehn et al., 2005). This mismatch between shrinkage-expansion may lead to gap formation around this cement and subsequently affect bone-cement integration (Yimin et al., 2013). Cortoss and the experimental bone composites with 10 wt% MCPM exhibited volume expansion comparable to their polymerisation shrinkage. This may help to relieve shrinkage stress and minimise gaps at composite-bone interface. This may enhance composite-bone integration.

### 7.8.3 Surface apatite formation

The formation of apatite layer may provide biological benefits such as a chemical bond with bone (Huang et al., 2017). The result from this study suggests that the addition of 10 wt% of MCPM encouraged the precipitation of surface apatite after immersion in SBF for 1 week. Replacing TEGDMA by PPGDMA, however, provided no advantageous effect on surface apatite precipitation. Furthermore, the amount of precipitates was less than that observed with the novel experimental dental composites in the previous chapter due presumably to the lower PLR and therefore phosphates in the experimental bone composites.

Cortoss contained bioactive glass aimed to provide mineralisation enabling chemical bond with bone (Boyd et al., 2008). This commercial composite, however, failed to promote precipitation of surface apatite after immersion in SBF for 1 week. This could be due to the slow degradation of its calcium phosphate glass (combeite) (Lieberman et al., 2005). The apatite-forming ability in SBF is a feasible method for the determination of the bone bonding potential in biomaterials prior to the animal testing which requires large expenses and resources. It should be noted that the major limitation of SBF is the lack of proteins which could act *in vivo* as nucleation inhibitors (Pan et al., 2010).

### 7.8.4 Sr<sup>2+</sup> release

Strontium is of interest in new materials for orthopaedic applications due to its beneficial effects such as the promotion of osteoblastic whilst reducing osteoclastic activities (Liu et al., 2016; Schumacher et al., 2016). Local delivery of Sr<sup>2+</sup> to the surrounding osteoporotic vertebra may help to increase bone mass and improve mechanical properties of the osteoporotic vertebra. This, in turn, could potentially reduce adjacent vertebral fracture (Chen and Lin, 2016).

The addition of TSrP in the experimental bone composites in this study enabled  $\text{Sr}^{2+}$  release.  $\text{Sr}^{2+}$  has potential to substitute the cation in calcium phosphate biominerals (Frasnelli et al., 2017). This ionic substitution, however, may hamper  $\text{Sr}^{2+}$  release to the surrounding environment. The increase of MCPM level enhanced the  $\text{Sr}^{2+}$  release due possibly to the increase in water sorption. This is in accordance with a previous study (Khan, 2015). The lower crosslinking density and greater free volume of PPGDMA compared to TEGDMA also additionally increased the  $\text{Sr}^{2+}$  release of the composites. The effect of  $\text{Sr}^{2+}$  released from the bone composites on the osteoblast and osteoclast response needs to be assessed in future studies.

## **7.8.5 Biaxial flexural fatigue**

### **7.8.5.1 Biaxial flexural strength (BFS)**

BFS of composites containing MCPM ( $\text{M}_5\text{PPG}$ ,  $\text{M}_{10}\text{PPG}$ ) after long-term ageing (53, 63 MPa) was lower than that of the same formulations obtained at early time (118, 125 MPa) in Chapter 6 as was expected. This could be due to the increase of water sorption causing plasticisation of the resin matrix, thereby reducing the strength of the composites (Ferracane, 2006). The composites containing 5 or 10 wt% MCPM showed comparable BFS. This is desirable as increasing MCPM promoted hygroscopic expansion to compensate polymerisation shrinkage, enhanced surface apatite formation, and increased polylysine release. Furthermore, replacing TEGDMA by PPGDMA reduced strength of the composites but this was not highly significant. This is in accordance with results from Khan (2015).

#### **7.8.5.2 Biaxial flexural fatigue**

Injected bone composites should be able to withstand the fluctuating and repetitive loads during physical activities (Wilke et al., 2006). Stress versus number of cycles until failure (*S-N* curve) was previously used to assess fatigue properties of various different materials (Jeffers et al., 2005; Pittayachawan et al., 2007; Harmata et al., 2015). The gradient of the *S-N* curve can be used to predict failure cycle number when the applied stress is reduced. At a given applied stress, the steep gradient of *S-N* curve was associated with a significant reduction in failure cycles (Shah et al., 2013). Therefore, a low gradient rather than high gradient was preferable in terms of fatigue performance (Koster et al., 2013).

Factors that may affect the fatigue properties of bone cement include specimen shape and sizes, chemical structure, testing protocol, and testing environment (Kurtz et al., 2005). Standard fatigue testing protocols have included four-point-bending with beam samples, pure tensile test with tapered samples, and uniaxial tension/compression test with cylindrical tapered samples (Dean et al., 2005). The biaxial flexural fatigue test used in this study was efficient for the testing of multiple batches but did not facilitate comparison with other published studies.

The highest gradient of *S-N* curve was observed from Simplex. This could be due to the lack of reinforcing glass fillers or glass fibre, and pores contained inside the cement (Kurtz et al., 2005). The addition of MCPM promoted water sorption which is known to negatively affect the strength of experimental bone composites (Ferracane, 2006). Water sorption plasticised matrix, however, it may help to reduce the generated residual compressive stresses at the tip of fatigue cracks, thus retarding crack propagation (Schmitt et al., 2004; Takeshige et al., 2007; May-Pat et al., 2012). Additionally, fibres could help to bridge the voids in the composites that may act as points of initiation of

cracks during fatigue (Kane et al., 2010). These phenomena may therefore partly explain the lower gradient of *S-N* curves in the experimental bone composites containing MCPM. Replacing TEGDMA by PPGDMA may enhance water sorption but this was not advantageous on fatigue properties of the experimental bone composites.

In the body, bone cements are subjected to complex stresses. A finite element analysis demonstrated that the maximum stresses generated in the injected cement after vertebroplasty may range from 5 to 10 MPa (Rohlmann et al., 2010). A stress of 10 MPa was, therefore, used to assess failure cycles (fatigue life) from regression lines. The extrapolated fatigue life from regression line suggested that the experimental composites provided comparable fatigue life to commercial products. This may ensure a long-term mechanical performance of experimental bone composites.

The major limitations of the composites in the current study was that inhibition time of the experimental bone composites was far too short. This was primarily due to the attempt to develop bone composites with high monomer conversion, thus high level of initiator and activator were used (1.5 wt% BP and 1 wt% NTGGMA after mixing). All composites in this thesis contained the same level of these components to fix the effect from initiator / activator and allow assessment of other variables. Level of initiator/activator will be optimised in future works.

## 7.9 Conclusions

Within the limitations of this study, the following conclusions could be drawn.

- 1) The addition of MCPM decreased inhibition of the experimental bone composites. Replacing TEGDMA diluent monomer with PPGDMA increased inhibition time and monomer conversion of the experimental bone composites. The use of PPGDMA decreased calculated polymerisation shrinkage / heat generation for the experimental bone composites.
- 2) Increasing MCPM level and replacing TEGDMA by PPGDMA promoted water sorption-induced expansion. This hygroscopic expansion was comparable with the calculated polymerisation shrinkage.
- 3) Increasing the level of MCPM promoted surface apatite formation. Replacing TEGDMA by PPGDMA did not advantageously enhance surface apatite formation.
- 4) Increasing the level of MCPM and the use of PPGDMA enhanced  $\text{Sr}^{2+}$  release.
- 5) The increase of MCPM level reduced the BFS of the composites but showed no detrimental effect on fatigue properties of the composites. Replacing TEGDMA by PPGDMA slightly affected mechanical properties of the experimental bone composites.

## Chaper 8 Development of Low Stiffness, Polylysine Releasing, and Mineralising Injectable Bone Composites for Vertebroplasty

### 8.1 Abstract

**Purpose:** The aim of this study was to assess the effects of PPGDMA, MCPM plus TSrP (PO), and PLS on injectability, monomer conversion, mass and volume changes, PLS release, surface apatite formation, and mechanical properties in addition to cytocompatibility were examined.

**Materials and Methods:** Chemically activated experimental bone composites were prepared using PLR of 2.3:1. Composites with PLR of 3:1 were additionally prepared for the injectability test. Liquid phase contained varying level of PPGDMA:UDMA (25:70, 50:45, and 75:20 wt:wt) with fixed 5 wt% HEMA. Powder phase after mixing initiator with activator pastes contained glass filler, PO (12.5, 25, and 50 wt%), and PLS (2.5, 5, and 10 wt%). Injectability of the composite pastes was performed using a universal testing machine. Monomer conversion was assessed using FTIR-ATR. Mass and volume changes of composites in SBF were measured using a density kit. PLS release in deionised water was analysed using HPLC. Surface apatite formation was assessed using SEM-EDX. Compressive strength at 24 hr in addition to biaxial flexural strength/fatigue for up to 4 weeks were also examined. Cytocompatibility of experimental bone composites to bone marrow mesenchymal stem cells (MSCS) was assessed using MTS assay. Commercial PMMA (Simplex) and composite (Cortoss) bone cements were used for comparison.



**Results:** Decrease of PLR and increase of PPGDMA lowered required injection force. Increasing PPGDMA from low to high monomer fraction increased inhibition time on average from 1 min to 5 min. The increase of PPGDMA slightly decreased rate of polymerisation on average from 0.51 to 0.36 %·s<sup>-1</sup>. This also increased final monomer conversion on average from 84 to 97 % but raised polymerisation shrinkage and heat generation by only 6 % due to its high molecular weight. The increase of PPGDMA and MCPM also enhanced volume expansion, PLS release, and surface apatite formation. Increasing all variables decreased strength, fatigue, and modulus of elasticity. The maximum effect of each variable on modulus of elasticity was greater than on strength by ~ 20%. Furthermore, the modulus at late time of the experimental composites containing high PPGDMA was less than 1 GPa. Increasing PPGDMA and PO reduced metabolic activity relatively to control of MSCS by 59 % and 258 % respectively.

**Conclusion:** This study produced composites that exhibited low stiffness, high PLS - releasing, and apatite – forming. To prevent adjacent vertebral fracture, formulations with high PPGDMA would be beneficial. Additionally, increasing PPGDMA improved injectability and monomer conversion of the experimental bone composites. The increase of PO and PPGDMA enhanced surface apatite formation and PLS release but reduced cytocompatibility. Increasing these variables, however, reduced mechanical properties but provided modulus of elasticity more comparable with cancellous bone.

## 8.2 Introduction

Cement leakage is a common complication of vertebroplasty. Most leakage is asymptomatic but some serious complications have been reported (Janssen et al., 2017). Studies suggested that using high viscosity cements reduced the risk of cement leakage (Baroud et al., 2006; Zhan et al., 2017). The forces required for the delivery of such cements may however exceed the human physical limit (Habib et al., 2010). Hence, manufacturers have provided injection devices that can generate pressure and force to aid injection of highly viscous cements. Most clinicians, however, prefer to use simple syringes, which allow good tactile feeling and force feedback during injection (Boger and Wheeler, 2011). High viscosity reduced cement infiltration volume in bone (Hsu et al., 2014), which may affect bone-cement integration.

According to Chapter 4, the viscosity of experimental bone composites can be reduced by increasing level of PPGDMA or decreasing powder to liquid ratio. Additionally, Chapter 6 demonstrated that increasing PPGDMA level also reduced modulus of elasticity of experimental bone composites to a level that is comparable with cancellous bone. Furthermore, replacing TEGDMA by PPGDMA in Chapter 7 increased monomer conversion of experimental bone composites.

Generally, high monomer conversion is associated with high polymerisation shrinkage and shrinkage stress. The shrinkage and stress could be potentially balanced by hygroscopic expansion of composites (Park and Ferracane, 2014). This expansion could be promoted by the addition of phosphate compounds (Aljabo et al., 2015). The addition of phosphates encouraged surface apatite formation (Aljabo et al., 2016) which is known to promote *in vivo* bone bonding.

Post-operative infection after vertebroplasty is a rare complication but is usually associated with high mortality rates (Abdelrahman et al., 2013). Therefore, antibiotic-loaded bone cements are often employed to prevent this complication. In general, only 10 % of the total amount of antibiotic incorporated in the PMMA bone cement can be released (Anagnostakos and Kelm, 2009; Miola et al., 2013). This could be due to the rigidity of PMMA resin matrix that may impair the diffusion of drugs (Slane et al., 2014). Furthermore, the slow and sustained release of an antibiotic from PMMA cement has raised a concern of developing antibiotic resistance to the commonly used antibiotics such as vancomycin or gentamycin.

Inert soluble porogens were incorporated in bone cements to generate pores that could facilitate the diffusion and release of antibiotics (Slane et al., 2014). Matos et al. (2014) showed that the addition of lactose enabled total release of minocycline from a PMMA cement. Likewise, Wu et al. (2016b) have demonstrated that the addition of gelatine sponges increased the gentamycin release by 4 to 6 folds. The addition of these porogens, however, inevitably reduced the mechanical properties of the cements.

Adjacent vertebral fracture is a common complication after vertebroplasty. A proposed aetiology for the adjacent vertebral fracture was the mechanical mismatch between the low stiffness vertebral cancellous bone and the high stiffness bone cement (Wang et al., 2012). Studies demonstrated that the stiffness of bone cements was significantly decreased by the addition of hyaluronic acid, blood plasma, castor oils, or normal saline (Boger et al., 2008; Ahn et al., 2009; Lopez et al., 2011; Carlsson et al., 2015; Schröder et al., 2016). These additives, however, affected handling properties and polymerisation of the materials.

When materials are implanted into human tissues, host responses such as inflammation, wound healing, or foreign body reactions could occur at the tissue-material interface. A cytocompatible bone composite is required to ensure bone-integration and reduce fibrous encapsulation which is commonly observed with PMMA cement (Ooms et al., 2003). Toxicity of composites may be due to leaching of uncured monomers or leachable substances, such as drugs or ions at high level. Studies showed that dimethacrylate monomers in composites were toxic to human cells (Schweikl et al., 2006; Chang et al., 2014). For example, HEMA reduced viability of human lung epithelial cells due to the interruption of cell cycle, increased apoptosis, and decreased cell proliferation (Morisbak et al., 2015). Additionally, a study showed UDMA increased proinflammatory cytokine production and enhanced oxidative stress in dental pulp cells (Chang et al., 2014). Furthermore, the addition of highly soluble calcium phosphates such as MCPM may also be toxic to eukaryotic cells as it produces acid after reacting with water (Dorozhkin, 2011). Additionally, excess calcium ions affected oxidative mechanisms, metabolic activities, and induced apoptosis of eukaryotic cells (Mansfield et al., 2003; Orrenius et al., 2003).

### 8.3 Hypotheses

Experimental bone composites that require high injection force may compromise handling properties of the materials. Chapter 4 demonstrated that the viscosity of experimental bone composites could be decreased by reducing powder to liquid ratio or increasing PPGDMA level. The injection force required for the dispersal of the experimental bone composites, however, has not yet been investigated. According to the rheological results in Chapter 4, it was expected that the required injection force of the composites would be reduced upon reducing PLR or increasing PPGDMA level of the composites. Chapter 4 also indicated that increasing glass filler particle size from 0.7 to 7 had no significant effect on viscosity of experimental bone composites. It was anticipated that increasing level of large particle size fillers including MCPM (diameter of 53  $\mu\text{m}$ ), TSrP (diameter of 10  $\mu\text{m}$ ), and PLS (diameter of 20-50  $\mu\text{m}$ ) would reduce the required injection force of the composites in this chapter.

According to previous chapters, replacing TEGDMA by PPGDMA improved stability of the initiator paste, inhibition time, and monomer conversion of experimental bone composites. An average inhibition time of the PPGDMA based composites in Chapter 7 (1 min) was far too short compared with the expected required inhibition time (4 – 8 min). As composites containing PPGDMA instead of TEGDMA gave greater inhibition times and monomer conversions with the comparable rate of reaction, higher PPGDMA might further increase these properties. Due to the high molecular weight of PPGDMA, it was expected that increasing monomer conversion will not have detrimental effect on calculated polymerisation shrinkage and heat generation.

Replacing TEGDMA by PPGDMA and raising hydrophilic MCPM increased water sorption and strontium release of experimental bone composites in Chapter 7. It was

anticipated that increasing PPGDMA, PO (MCPM plus TSrP), and PLS would enhance hygroscopic expansion making it more comparable with calculated polymerisation shrinkage. The increase in water sorption by raising PPGDMA, PO, and PLS was also expected to promote PLS release and surface apatite formation.

Raising PPGDMA, PO, and PLS may consequently reduce mechanical properties of experimental bone composites. Although, a requirement of strength of bone composites has not yet been established, the BS ISO 5833 (implants for surgery-acrylic resin cements) can be used as a provisional requirement. To pass requirements of the standard, mechanical properties of experimental composites should be higher than 70 MPa for compressive strength, 50 MPa for flexural strength, and 1.8 GPa for flexural modulus after immersion in a liquid for 24 hr. Additionally, it was expected that increasing flexible PPGDMA and hydrophilic fillers (PO and PLS) would reduce modulus of elasticity of the composites upon ageing to match with that of cancellous bone (0.1 – 0.7 GPa). Furthermore, it was anticipated that the increase of these components would not detrimentally affect fatigue of the materials.

High flexibility of resin matrix and increased water sorption of composites may enable rapid release of components that could negatively affect the surrounding bone cells. This is undesirable as it could impair bone-composite integration. Cytocompatibility of experimental bone composites was tested by measuring metabolic activity of bone marrow mesenchymal stem cells (MSCS) cultured in conditioned medium. This medium had composites previously immersed in it for 24 hr (Chapter 2, section 2.3.10). It is anticipated that through control of PPGDMA, PO, PLS any detrimental effects on metabolic activity of MSCS can be minimised.

## 8.4 Aim and objectives

The aim of this chapter was to develop low stiffness, polylysine - releasing, and apatite - forming bone composites that are easy to inject. The objectives of this study were to assess:

- 1) Injection forces required to expel different composite pastes through a syringe with an outlet diameter of 1.8 mm;
- 2) Inhibition time, maximum rate of polymerisation, final monomer conversion, and calculated polymerisation shrinkage and heat generation from final monomer conversions;
- 3) Mass and volume change after immersion in SBF for 4 weeks;
- 4) Polylysine release in deionised water for 4 weeks;
- 5) Apatite formation after immersion in SBF for 4 weeks;
- 6) Strength, modulus and fatigue of bone composites after immersion in SBF for 4 weeks;
- 7) Metabolic activity of mesenchymal stem cells cultured in solutions previously immersed by composite discs;

The effect of PPGDMA, PO, and PLS were examined. Commercial PMMA cement (Simplex; Stryker, Newbury, Berkshire, UK) and bone composite (Cortoss; Stryker, Newbury, Berkshire, UK) were used for comparison.

## 8.5 Materials and Methods

Powder to liquid ratio (weight ratio) of composites in this study were 2.3:1. To demonstrate the effect of PLR on injection, however, formulations with high PLR (3:1) were additionally prepared.

The liquid phase before mixing with the powder phase contained UDMA and PPGDMA with fixed level of 5 wt% HEMA. To this was added either BP (3 wt% of total liquid phase) for the initiator liquid or NTGGMA (2 wt% of total liquid phase) for the activator liquid. After mixing, level of BP and NTGGMA were halved (1.5 and 1 wt% respectively).

The powder phase contained glass filler (0.7  $\mu\text{m}$ ) and PLS (Table 8-1). To this was added either MCPM for the initiator powder or TSrP for the activator powder. MCPM:TSrP was 1:1.5 by weight which is approximately equimolar. Total amount of MCPM and TSrP (PO) in powder phase will be halved after mixing with liquid phase. Fibre was not used in this study as it caused a blockage in the mixing tip when high level of PPGDMA (75 wt%) was used. Additionally, high level of active ingredients was used in this study to enable easy visualisation of property trends upon increased level of additives.



**Table 8-1 Formulations of experimental bone composites.** HEMA was fixed at 5 wt%. BP and NTGGMA after mixing were fixed at 1.5 wt% and 1 wt%. Total amount of MCPM and TSrP (PO) in powder phase will be halved after mixing with liquid phase.

Formulations	PPGDMA (P)	UDMA (U)	MCPM (PO)	TSrP	Polylysine (PLS)
	wt% of monomers in liquid phase		wt% in powder phase before mixing with liquid phase		
			Initiator powder	Activator powder	Each powder
<b>P<sub>75</sub>PO<sub>50</sub>PLS<sub>10</sub></b>	75	20	40	60	10
<b>P<sub>75</sub>PO<sub>50</sub>PLS<sub>2.5</sub></b>	75	20	40	60	2.5
<b>P<sub>75</sub>PO<sub>12.5</sub>PLS<sub>10</sub></b>	75	20	10	15	10
<b>P<sub>75</sub>PO<sub>12.5</sub>PLS<sub>2.5</sub></b>	75	20	10	15	2.5
<b>P<sub>50</sub>PO<sub>25</sub>PLS<sub>5</sub></b>	50	45	20	30	5
<b>P<sub>25</sub>PO<sub>50</sub>PLS<sub>10</sub></b>	25	70	40	60	10
<b>P<sub>25</sub>PO<sub>70</sub>PLS<sub>2.5</sub></b>	25	70	40	60	2.5
<b>P<sub>25</sub>PO<sub>12.5</sub>PLS<sub>10</sub></b>	25	70	10	15	10
<b>P<sub>25</sub>PO<sub>12.5</sub>PLS<sub>2.5</sub></b>	25	70	10	15	2.5

Injectability of the composite pastes (n=3) were assessed using a universal testing machine, monomer conversion was measured using FTIR-ATR (n=3). Additionally, mass and volume changes in SBF were assessed using gravimetric studies (n=3), PLS release in deionised water was analysed using HPLC (n=3), Ca/P and Ca/ Si ratio of surface apatite layers were assessed using SEM-EDX (n=3). Furthermore, compressive strength after immersion in SBF for 24 hr (n=5), biaxial flexural strength and modulus of elasticity (n=5) in addition to biaxial flexural fatigue testing after immersion in SBF for 4 weeks (n=25) were also examined. The metabolic activity of MSCs using MTT assay (n=5), which was performed by Dr Catriona O'Rourke, was also examined. All testing protocols are previously described in Chapter 2.

## 8.6 Statistical analysis

Data were analysed using one-way ANOVA or Kruskal-Wallis test followed by multiple comparison using Tukey's test or Dunnett's T3 test ( $p = 0.05$ ) respectively. Three-level factorial design with low and high level of variables (equations 2-27,28) was employed to assess the effect of PPGDMA (25 or 75 wt%), PO (12.5 or 50 wt%), and PLS (2.5 or 10 wt%) on injection force, inhibition time, rate of polymerisation, final monomer conversion, mass and volume changes, PLS release, Ca/P or Ca/Si ratio of surface apatite, mechanical properties of experimental bone composites in addition to metabolic activity of MSCS.

## 8.7 Results

### 8.7.1 Injectability

All experimental bone composites prepared with PLR of 3:1 or 2.3:1 and Cortoss exhibited injectability of greater than 90 % except for  $P_{25}PO_{12.5}PLS_{2.5}$  that prepared with PLR of 3:1 ( $14 \pm 3$  %). The injection force required for all experimental composites increased upon raising PLR from 2.3:1 to 3:1 (Fig 8-1). For experimental bone composites prepared with PLR of 2.3:1, highest and lowest injection force were obtained from  $P_{25}PO_{12.5}PLS_{10}$  ( $23 \pm 4$  N) and  $P_{75}PO_{12.5}PLS_{10}$  ( $4 \pm 0$  N) respectively. The injection force of experimental composites prepared with PLR of 2.3:1 except for  $P_{25}PO_{12.5}PLS_{10}$  and  $P_{25}PO_{12.5}PLS_{2.5}$  ( $21 \pm 2$  N) was significantly lower than that of Cortoss ( $20 \pm 2$  N).

For the composites prepared with PLR of 3:1, the highest and lowest injection force were obtained from  $P_{25}PO_{12.5}PLS_{2.5}$  ( $100 \pm 0$  N) and  $P_{75}PO_{50}PLS_{10}$  ( $7 \pm 2$  N) respectively. Injection force of  $P_{25}PO_{12.5}PLS_{2.5}$  and  $P_{25}PO_{12.5}PLS_{10}$  ( $92 \pm 2$ ) was significantly higher than that of Cortoss. In contrast,  $P_{75}PO_{50}PLS_{10}$  and  $P_{75}PO_{12.5}PLS_{2.5}$  required significantly lower injection forces than Cortoss.

Factorial analysis indicated primary factors affecting the required injection force for experimental bone composites prepared with PLR of 2.3:1 was PPGDMA level. The primary factor of composites prepared with PLR 3:1 was PPGDMA, PO, PLS (Fig 8-2). The required injection force was increased by  $173 \pm 21$  % and  $241 \pm 28$  % upon decreasing PPGDMA level for the composites prepared with PLR of 2.3:1 and 3:1 respectively. Additionally, the injection force was increased by  $240 \pm 24$  % and  $40 \pm 5$  % upon decreasing PO and PLS for the composites prepared with PLR of 3:1.

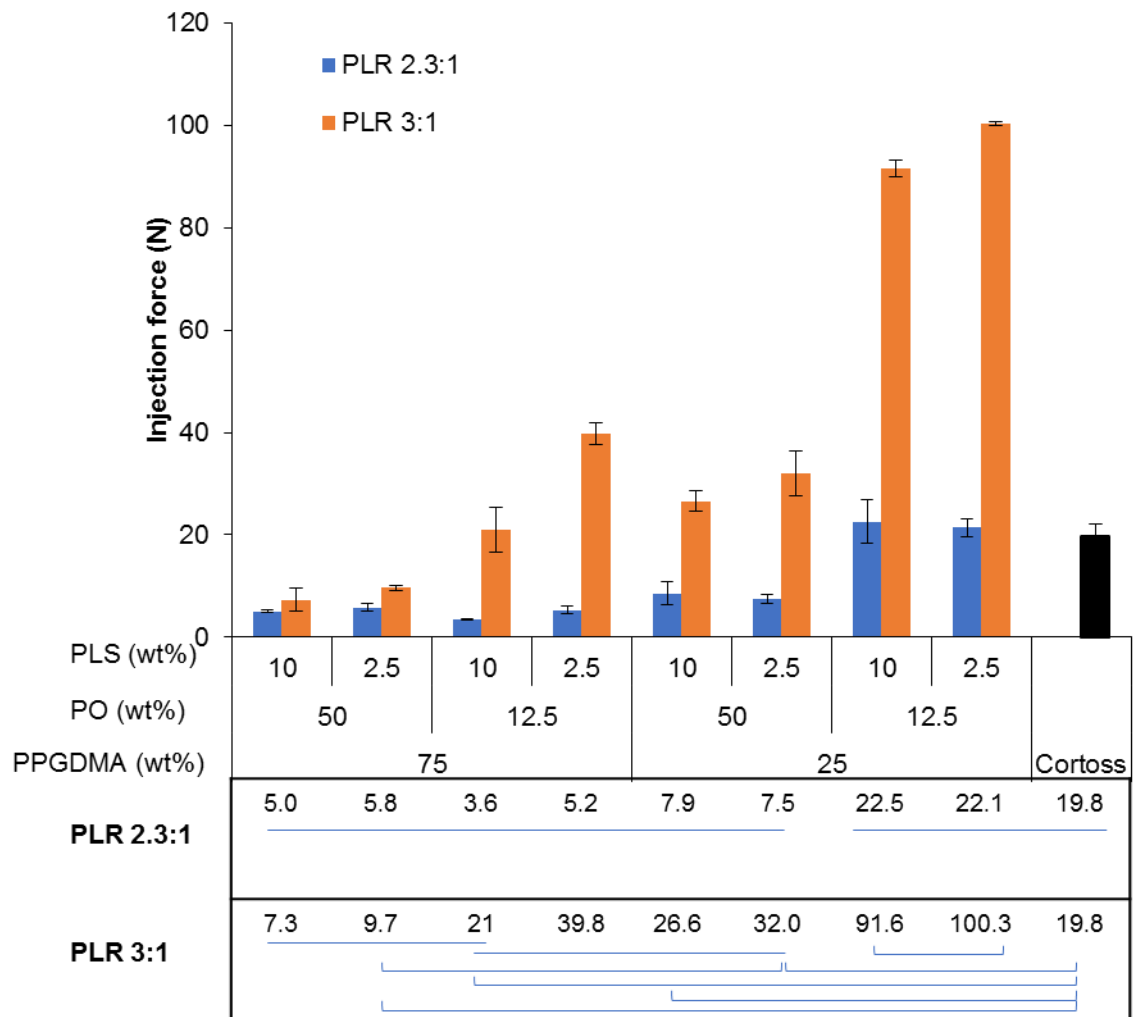
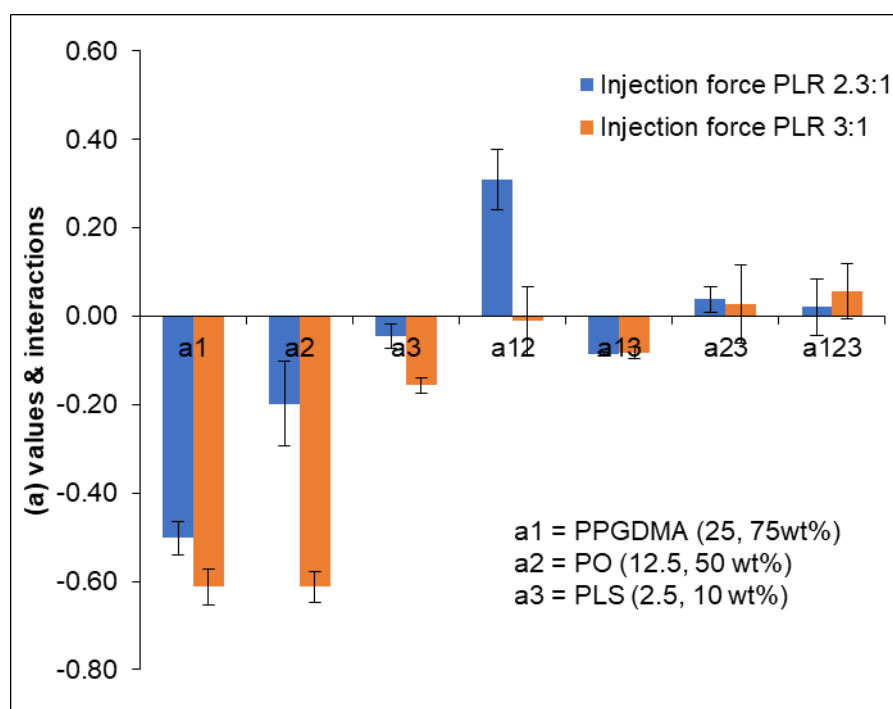


Fig 8-1 Injection force required for experimental bone composites. Lines indicate no significant difference ( $p > 0.05$ ). Error bars are 95% CI ( $n=3$ ).



**Fig 8-2** Factorial analysis describing the effect of PPGDMA, PO, PLS, and their interactions on required injection force of experimental bone composites. Error bars are 95% CI (n=3).

## 8.7.2 Monomer conversion

### 8.7.2.1 Inhibition time

Longest and shortest inhibition time were observed with  $P_{25}PO_{12.5}PLS_{2.5}$  ( $41 \pm 12$  s) and  $P_{75}PO_{50}PLS_{2.5}$  ( $517 \pm 13$  s) (Fig 8-3 A). The inhibition time of Simplex ( $403 \pm 2$  s) was comparable with that of  $P_{75}PO_{50}PLS_{10}$  ( $421 \pm 36$  s). Additionally, the inhibition time of Cortoss ( $155 \pm 5$  s) was comparable with that of  $P_{75}PO_{12.5}PLS_{2.5}$  ( $138 \pm 1$  s). The average inhibition time of experimental bone composites (191 s) was higher than the result from the intermediate formulation ( $P_{50}PO_{25}PLS_5$ ;  $98 \pm 14$  s).

Factorial analysis indicated that inhibition time was strongly affected by PPGDMA and PO levels (Fig 8-3 B). The inhibition time was increased by  $342 \pm 24$  % and  $125 \pm 8$  % upon increasing PPGDMA and PO levels. The effect of PLS was negligible.

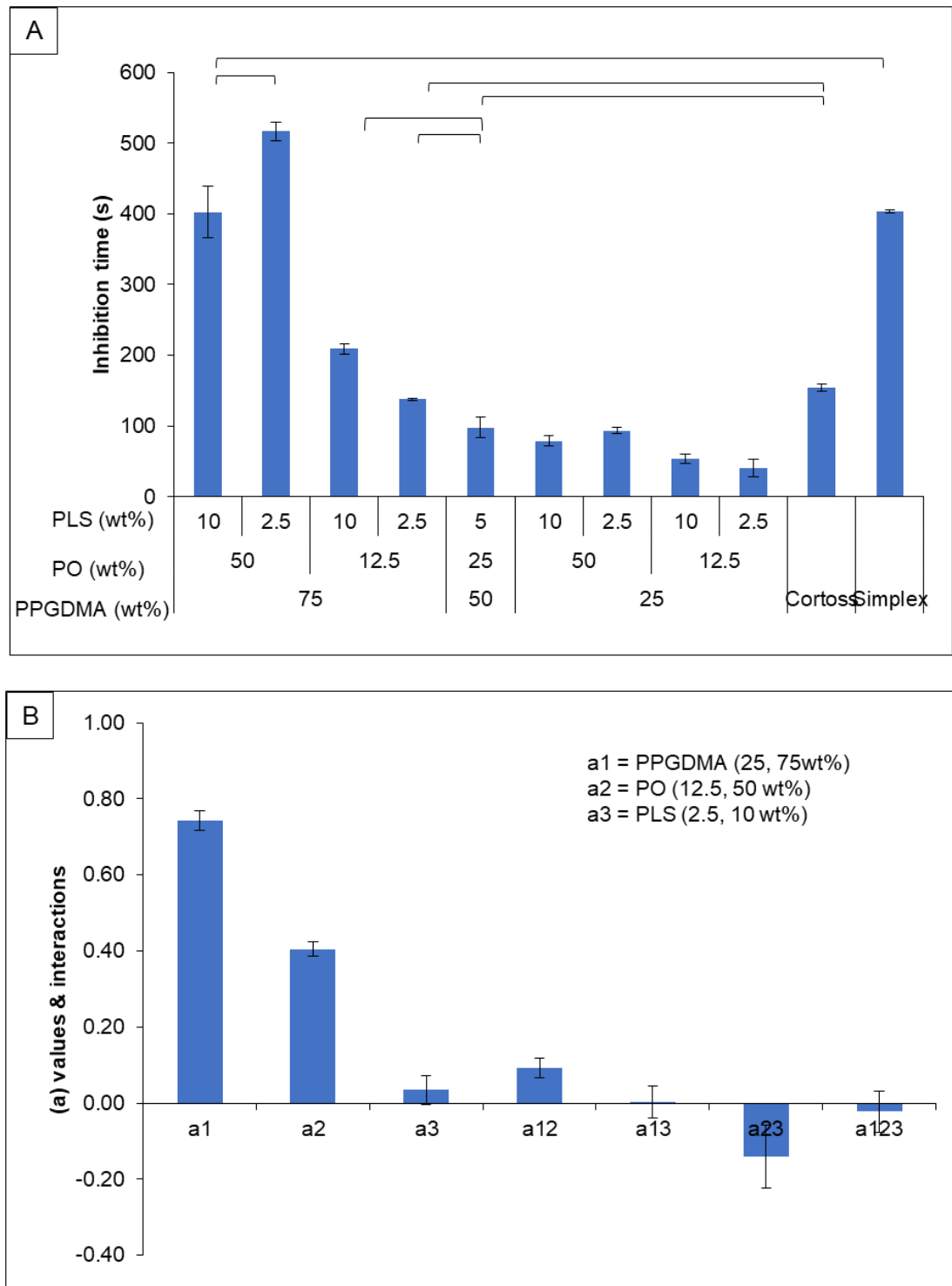


**Fig 8-3 A)** Inhibition time of each material. Lines indicate no significant difference ( $p > 0.05$ ). **B)** Factorial analysis describing the effect of PPGDMA, PO, PLS, and their interactions on inhibition time of experimental bone composites. Error bars are 95% CI ( $n=3$ ).

### 8.7.2.2 Maximum rate of polymerisation ( $R_p^{\max}$ )

Lowest and highest  $R_p^{\max}$  were obtained from  $P_{75}PO_{50}PLS_{2.5}$  ( $0.26 \pm 0.01 \text{ \%} \cdot \text{s}^{-1}$ ) and  $P_{50}PO_{25}PLS_5$  ( $0.62 \pm 0.02 \text{ \%} \cdot \text{s}^{-1}$ ) respectively (Fig 8-4 A).  $R_p^{\max}$  of all experimental bone composites was not significantly different with that of Cortoss ( $0.36 \pm 0.03 \text{ \%} \cdot \text{s}^{-1}$ ).  $R_p^{\max}$  of  $P_{75}PO_{50}PLS_{2.5}$  was significantly higher than that of Simplex ( $0.49 \pm 0.02 \text{ \%} \cdot \text{s}^{-1}$ ). Additionally,  $R_p^{\max}$  of Simplex was significantly higher than that of  $P_{75}PO_{50}PLS_{10}$  ( $0.28 \pm 0.04 \text{ \%} \cdot \text{s}^{-1}$ ) and  $P_{75}PO_{50}PLS_{2.5}$ . The average  $R_p^{\max}$  of experimental bone composites ( $0.43 \text{ \%} \cdot \text{s}^{-1}$ ) was lower than the result from the intermediate formulation ( $P_{50}PO_{25}PLS_5$ ;  $0.62 \pm 0.02 \text{ \%} \cdot \text{s}^{-1}$ ).

Factorial analysis revealed that the primary factor influencing  $R_p^{\max}$  of experimental bone composites was PPGDMA level (Fig 8-4 B).  $R_p^{\max}$  of the composites was increased by  $50 \pm 2 \text{ \%}$  upon decreasing PPGDMA level. Additionally,  $R_p^{\max}$  of the composites with high PPGDMA level was increased by  $36 \pm 8 \text{ \%}$  upon decreasing PO level. The effect of PLS was negligible.

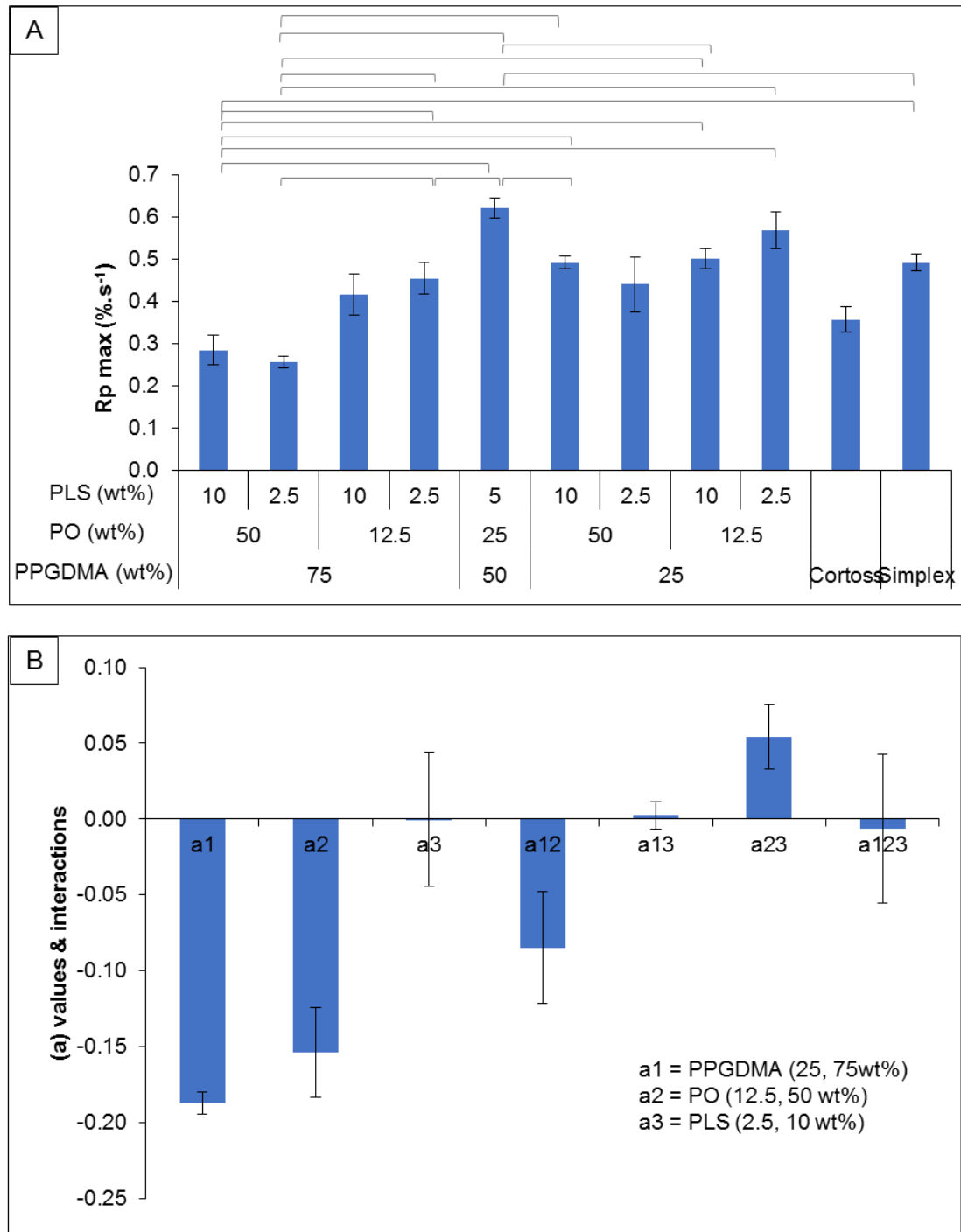


**Fig 8-4 A) Maximum rate of polymerisation ( $R_p^{\text{max}}$ ) of experimental bone composites and commercial materials. Lines indicate significant difference ( $p < 0.05$ ). B) Factorial analysis describing the effect of PPGDMA, PO, PLS, and their interactions on  $R_p^{\text{max}}$  of experimental bone composites. Error bars are 95% CI ( $n=3$ ).**



### 8.7.2.3 Final monomer conversion

Final monomer conversions of experimental bone composites were significantly higher than that of Cortoss ( $64 \pm 1$  %) (Fig 8-5 A). Highest and lowest monomer conversion of experimental bone composites were obtained from  $P_{75}PO_{12.5}PLS_{10}$  ( $99 \pm 3$  %) and  $P_{25}PO_{50}PLS_{2.5}$  ( $79 \pm 0$  %) respectively. The experimental bone composites containing 50 or 75 wt% of PPGDMA exhibited significant higher final monomer conversion than Simplex ( $78 \pm 1$  %). Additionally, the conversion of Simplex was comparable to that of the experimental composites containing 25 wt% PPGDMA. Monomer conversion of the intermediate formulation ( $P_{50}PO_{25}PLS_5$ ;  $95 \pm 1$  %) was higher than the average monomer conversion of experimental bone composites (89 %).

Factorial analysis revealed that final monomer conversion of experimental bone composites was primarily governed by level of PPGDMA (Fig 8-5 B). The conversion was increased by  $20 \pm 0$  % upon raising PPGDMA level.

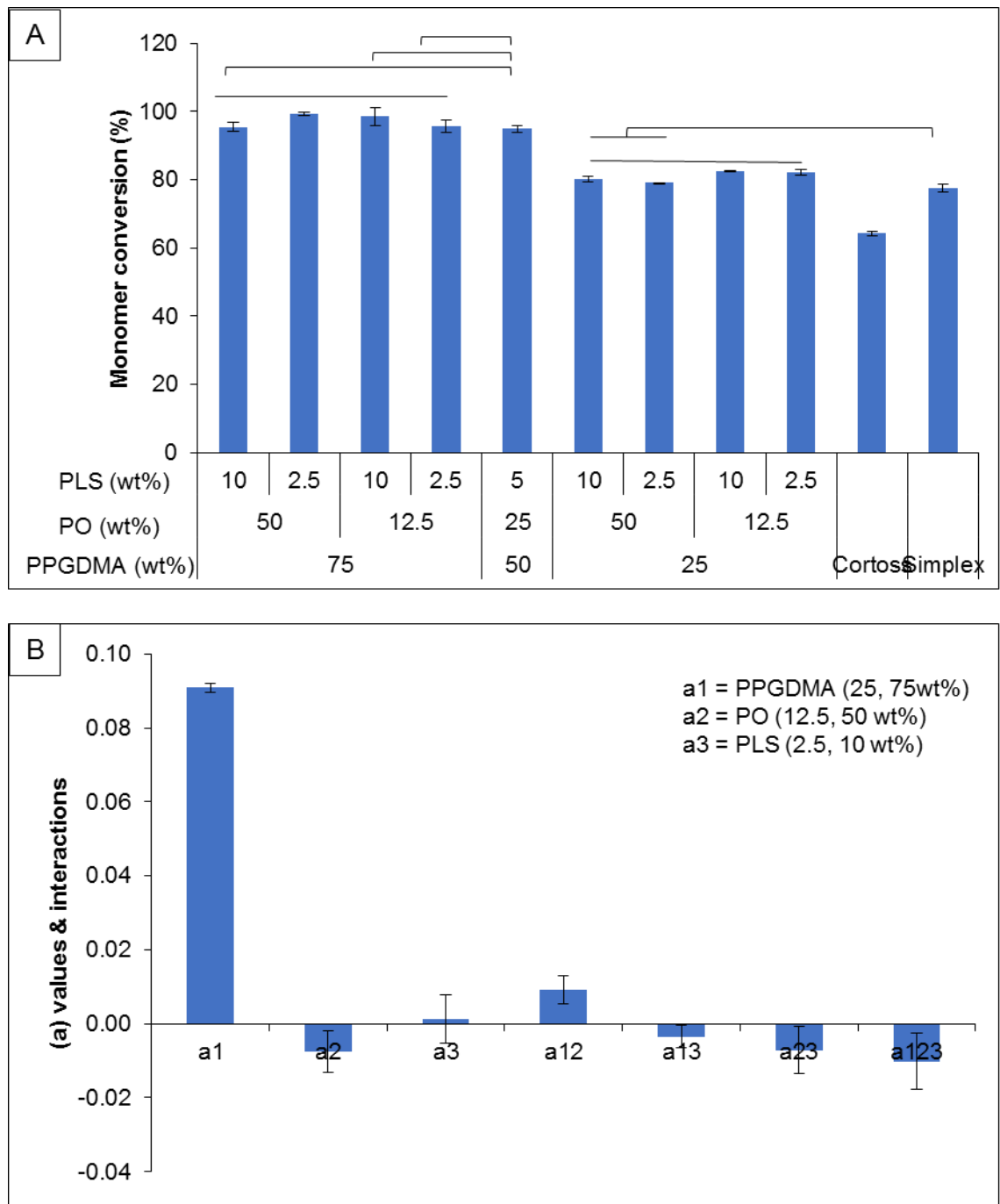


**Fig 8-5 A) Final monomer conversion of experimental bone composites and commercial products.** Lines indicate no significant difference ( $p > 0.05$ ). **B) Factorial analysis describing the effect of PPGDMA, PO, PLS, and their interactions on final monomer conversion of experimental bone composites.** Error bars are 95% CI ( $n=3$ ).

#### 8.7.2.4 Calculated polymerisation shrinkage and heat generation

Highest and lowest calculated polymerisation shrinkage and heat generation were obtained from  $P_{50}PO_{25}PLS_5$  ( $4.10 \pm 0.04$  vol%,  $0.098 \pm 0.006$  kJ/cc) and  $P_{25}PO_{50}PLS_{2.5}$  ( $3.43 \pm 0.00$  vol%,  $0.085 \pm 0.000$  kJ/cc) (Fig 8-6 A). The calculated polymerisation shrinkage and heat generation of the experimental bone composites containing 75 wt% PPGDMA, except for  $P_{75}PO_{50}PLS_{2.5}$ , were not significantly different from those of the composites containing 25 wt%. Calculated polymerisation shrinkage and heat generation of the intermediate formulation ( $P_{50}PO_{25}PLS_5$ ) was slightly higher than average results of experimental bone composites (3.6 vol%, 0.09 kJ/cc).

Factorial analysis revealed that PPGDMA level was the primary factor controlling calculated polymerisation shrinkage and heat generation (Fig 8-6 B). The shrinkage and heat generation was increased by  $6 \pm 1$  % upon raising PPGDMA level. The effect of PO and PLS were negligible.

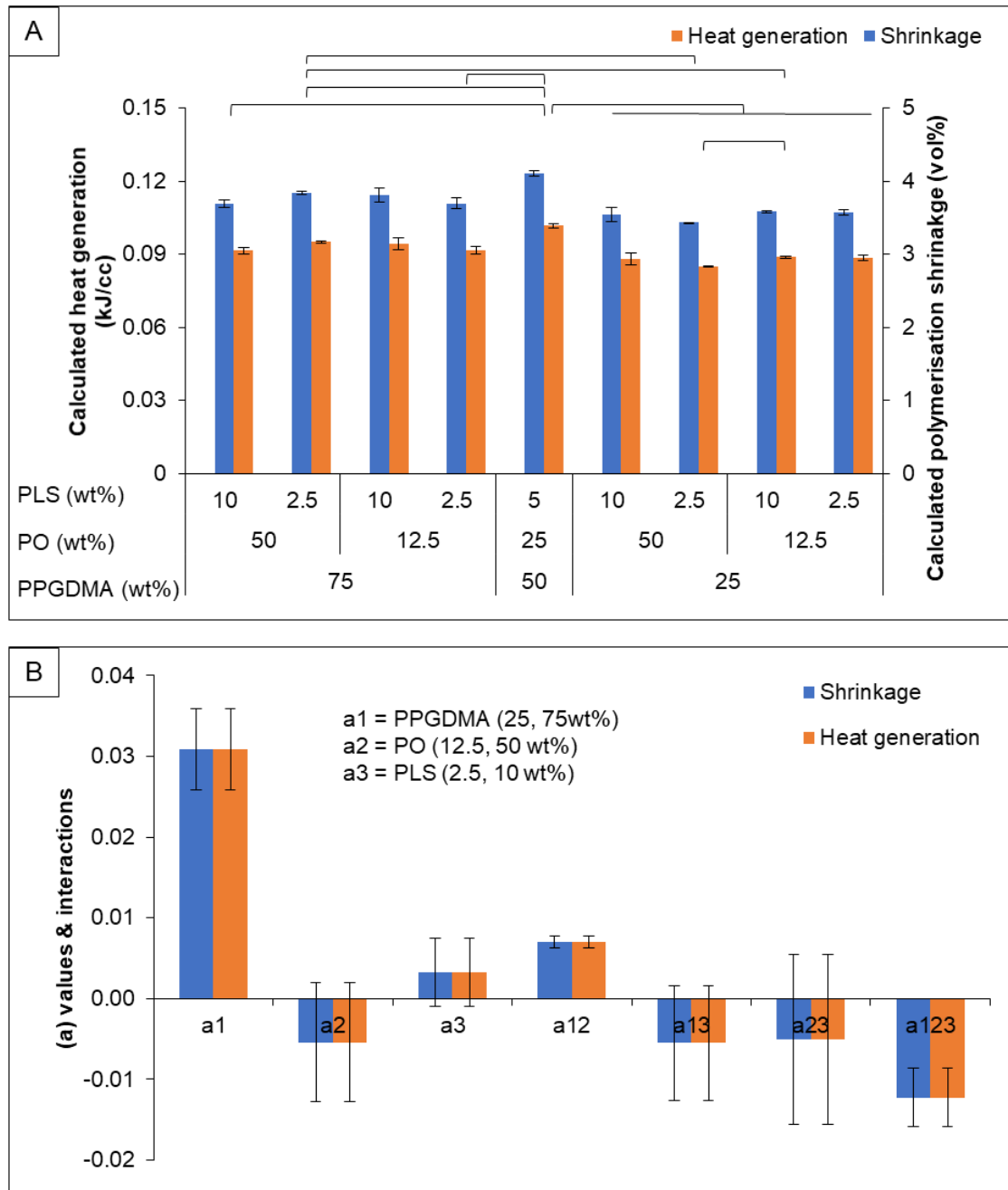


**Fig 8-6 A) Calculated polymerisation shrinkage and heat generation. Lines indicate significant difference ( $p < 0.05$ ). B) Factorial analysis describing the effect of increasing PPGDMA, PO, PLS, and their interactions on calculated polymerisation shrinkage and heat generation of experimental bone composites. Error bars are 95% CI ( $n=3$ ).**

### 8.7.3 Mass and volume changes

#### 8.7.3.1 Mass change

Mass of experimental composites increased linearly with square root of time (hr) at early time (Fig 8-7). For the composites containing high PPGDMA, their masses peaked at 2 or 3 days before levelling off. At 1 day,  $P_{75}PO_{12.5}PLS_{10}$  and  $P_{75}PO_{50}PLS_{10}$  reached maximum mass of  $0.9 \pm 0.1$  wt% and  $2.3 \pm 1.0$  wt%. At 4 weeks, mass of these composites slowly declined to final values of  $-0.4 \pm 0.1$  wt% for  $P_{75}PO_{12.5}PLS_{10}$  and  $0.5 \pm 0.2$  wt% for  $P_{75}PO_{50}PLS_{10}$ . Upon decreasing PLS, mass of the composites continued to increase for longer.  $P_{75}PO_{12.5}PLS_{2.5}$  and  $P_{75}PO_{12.5}PLS_{2.5}$  reached a maximum level of  $1.7 \pm 0.3$  wt% and  $4.0 \pm 0.3$  wt%. Their masses then slightly decreased to final values of  $1.6 \pm 0.3$  wt% and  $3.0 \pm 0.8$  wt% respectively.

For the experimental bone composites containing low PPGDMA, their masses increased and reached final values at 1 to 2 weeks. The final values were  $2.0 \pm 0.1$  wt% for  $P_{25}PO_{12.5}PLS_{2.5}$  and  $3.0 \pm 0.4$  wt% for  $P_{25}PO_{12.5}PLS_{10}$ . Mass changes of the composites were increased upon raising PO. For  $P_{25}PO_{50}PLS_{2.5}$  and  $P_{25}PO_{50}PLS_{10}$ , their final mass changes were  $9.0 \pm 0.4$  wt% and  $9.0 \pm 0.1$  wt% respectively.

The highest and lowest rate of mass increase ( $\% \cdot hr^{-0.5}$ ) with time were observed from  $P_{25}PO_{50}PLS_{10}$  ( $0.7 \pm 0.1$   $\% \cdot hr^{-0.5}$ ) and  $P_{25}PO_{12.5}PLS_{10}$  ( $0.1 \pm 0.0$   $\% \cdot hr^{-0.5}$ ) respectively (Fig 8-8 A). The average rate of mass increase of experimental bone composites ( $0.3$   $\% \cdot hr^{-0.5}$ ) was comparable to the result from the intermediate formulation ( $P_{50}PO_{25}PLS_5$ ;  $0.3 \pm 0.0$   $\% \cdot hr^{-0.5}$ ). The average maximum mass increase of the composites (3.8 wt%) was, however, slightly lower than the result obtained from the intermediate formulation ( $4.4 \pm 4$  wt%).

Factorial analysis indicated that the primary factor that affect rate of mass increase was PO (Fig 8-8 B). The rate of mass increase of experimental bone composites was increased by  $171 \pm 40$  % upon increasing PO. Maximum mass increase of the composites was affected by PPGDMA and PO levels. The maximum mass increase was raised by  $194 \pm 32$  % and  $180 \pm 28$  % upon decreasing PPGDMA and increasing PO respectively.

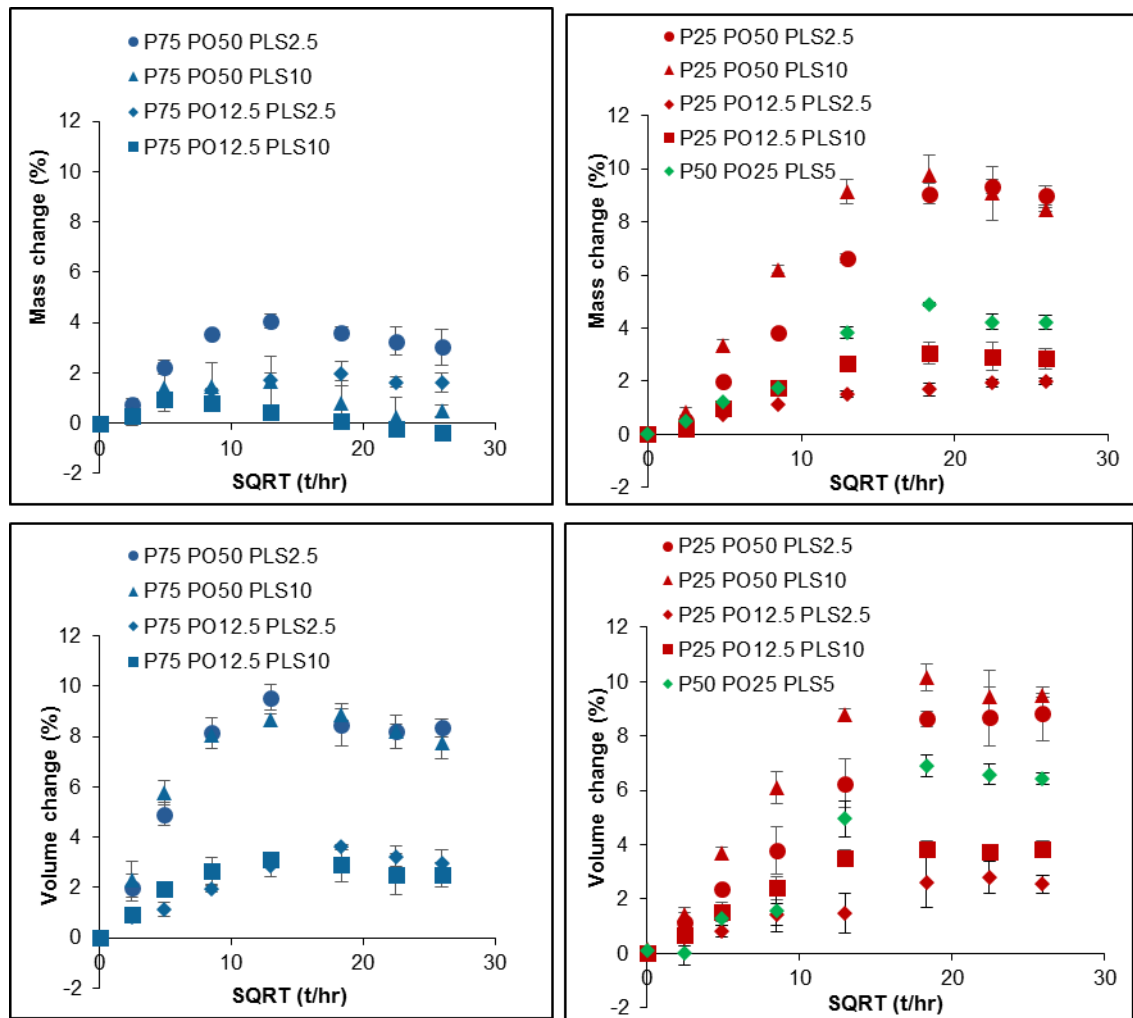


Fig 8-7 Mass and volume changes of experimental bone composites in SBF versus square root of time. Error bars are 95% CI (n=3).

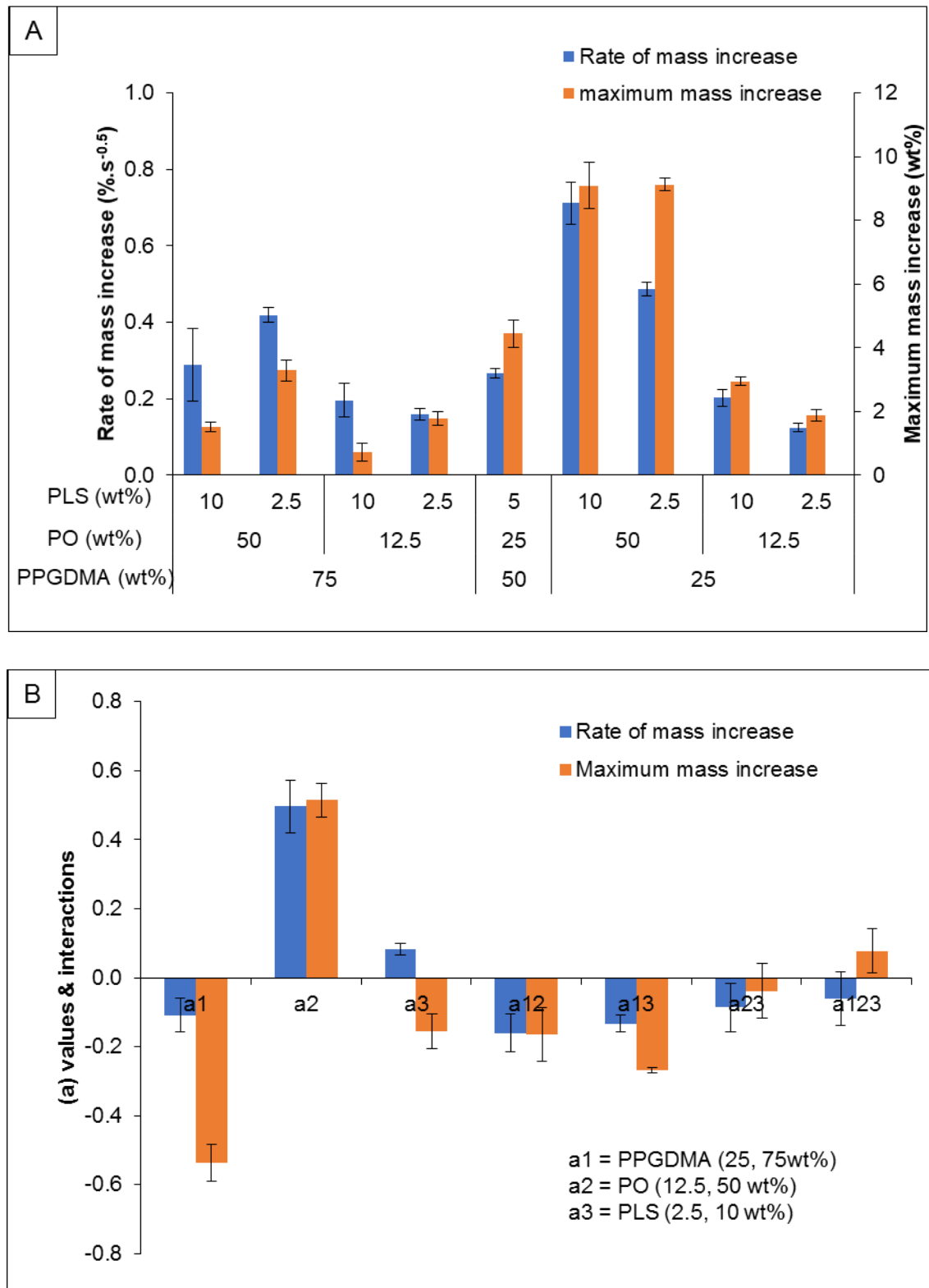


Fig 8-8 A) Rate of mass increase (%.hr<sup>-0.5</sup>) and maximum mass increase. B) Factorial analysis describing the effect PPGDMA, PO, PLS, and their interactions on rate of mass increase and maximum mass increase of experimental bone composites. Error bars are 95% CI (n=3).

### 8.7.3.2 Volume change

Volume changes of the experimental bone composites reached a plateau at 1 week (Fig 8-6). With low phosphates, the volume changes at late time were  $3.3 \pm 0.4$  vol%,  $2.6 \pm 0.3$  vol%,  $3.8 \pm 0.1$  vol%,  $2.7 \pm 0.1$  vol% for  $P_{75}PO_{12.5}PLS_{2.5}$ ,  $P_{25}PO_{12.5}PLS_{10}$ ,  $P_{25}PO_{12.5}PLS_{2.5}$ , and  $P_{25}PO_{12.5}PLS_{10}$  respectively (Fig 8-9 A). Volume changes of composites were increased upon raising phosphates. These volume changes at late time were  $8.3 \pm 0.6$  vol% for  $P_{75}PO_{50}PLS_{2.5}$ ,  $8.3 \pm 0.2$  vol% for  $P_{75}PO_{50}PLS_{2.5}$ ,  $9.7 \pm 0.4$  vol% for  $P_{25}PO_{50}PLS_{2.5}$ , and  $8.7 \pm 0.1$  vol% for  $P_{25}PO_{50}PLS_{2.5}$ . Highest and lowest rate of volume change were obtained from  $P_{75}PO_{75}PLS_{10}$  ( $1.0 \pm 0.0$  vol%.hr<sup>-0.5</sup>) and  $P_{25}PO_{12.5}PLS_{10}$  ( $0.2 \pm 0.0$  vol%.hr<sup>-0.5</sup>) respectively (Fig 8-9 A). The average rate of volume increase ( $0.5$  vol%.hr<sup>-0.5</sup>) and volume changes at late time ( $5.9$  vol%) of experimental bone composites were comparable to the results obtained from the intermediate formulation ( $P_{50}PO_{25}PLS_5$ ;  $0.4 \pm 0.0$  vol%.hr<sup>-0.5</sup> and  $6.6 \pm 0.3$  vol%).

Factorial analysis indicated that rate of volume increase and volume changes at late time was affected by level of PPGDMA, PO, and PLS (Fig 8-9 B). Rate of volume increase was raised by  $59 \pm 8$  %,  $206 \pm 53$  % and  $46 \pm 5$  % upon increasing PPGDMA, PO, and PLS respectively. Final volume change at late time of experimental bone composites was governed primarily by PO. Raising PO level increased final volume by  $186 \pm 8$  %.



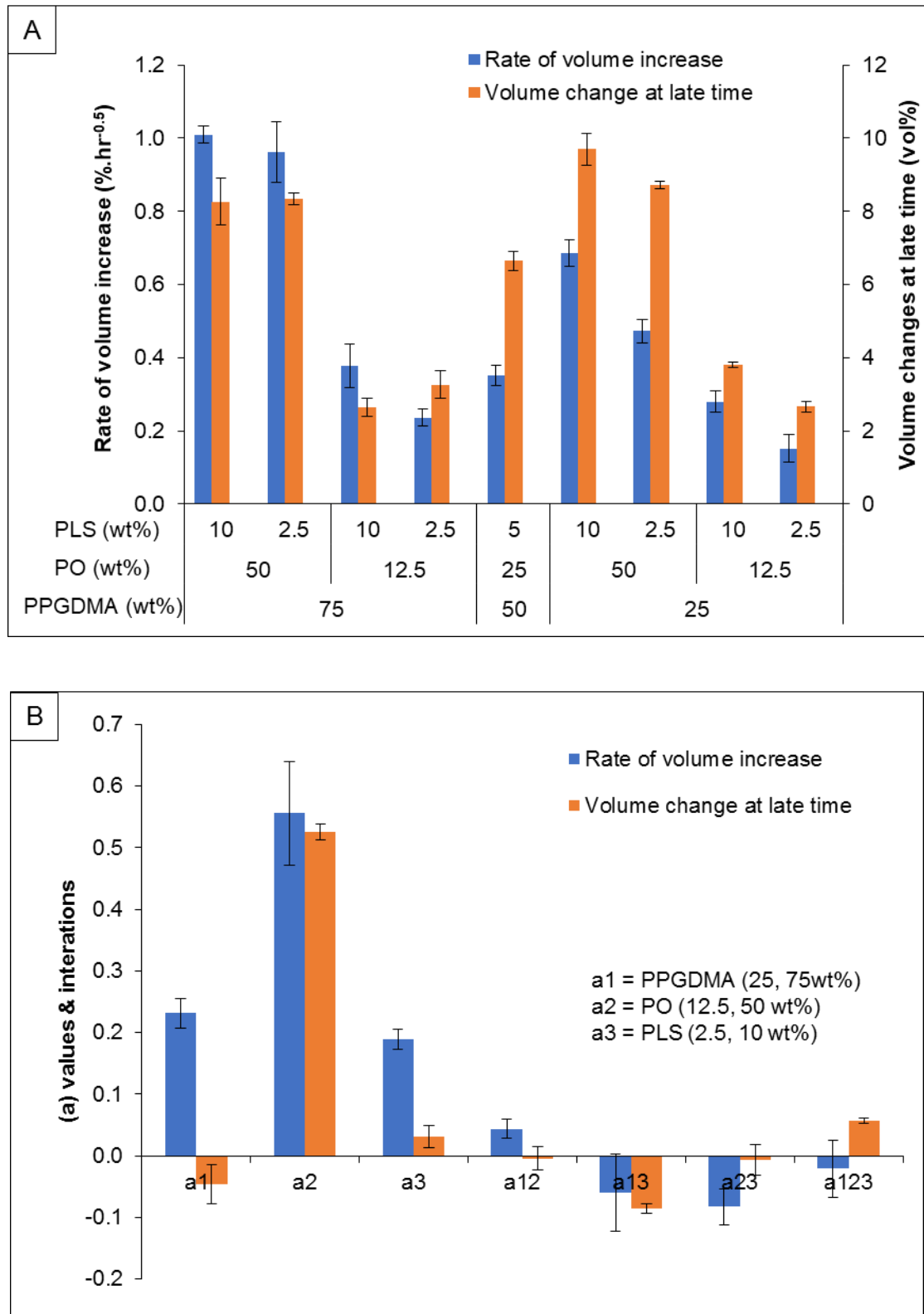


Fig 8-9 A) Rate of volume increase (%.hr<sup>-0.5</sup>) and volume changes at late time, B) factorial analysis describing the effect of increasing PPGDMA, PO, PLS, and their interactions on rate of volume increase and volume changes at late time of experimental bone composites. Error bars are 95% CI (n=3).

## 8.7.4 Polylysine release

### 8.7.4.1 Delay time ( $t_d$ )

The release of PLS increased linearly with square root of time, reaching a plateau at late time (Fig 8-10). Time when PLS could be first detected after immersion in deionised water (delay time,  $t_d$ ) was obtained from intercepts on the x axis of the linear regression lines (equation 2-19). An average of delay time of experimental bone composites containing 75 wt% PPGDMA (6 hr) was shorter than that of the composites containing 25 wt% PPGDMA (32 hr) (Fig 8-11 A). The shortest and longest  $t_d$  were obtained from  $P_{75}PO_{50}PLS_{10}$  ( $5 \pm 1$  hr) and  $P_{25}PO_{50}PLS_{2.5}$  ( $42 \pm 9$  hr). The  $t_d$  obtained from the intermediate formulation ( $P_{50}PO_{25}PLS_5$ ;  $30 \pm 1$  hr) was longer than the average  $t_d$  of experimental bone composites (19 hr).

Factorial analysis indicated that PPGDMA is the primary factor that affect  $t_d$  of PLS release (Fig 8-11 B). The analysis indicated that  $t_d$  of the composites was increased by  $496 \pm 290$  % upon reducing PPGDMA level. The effect of PO and PLS were negligible.

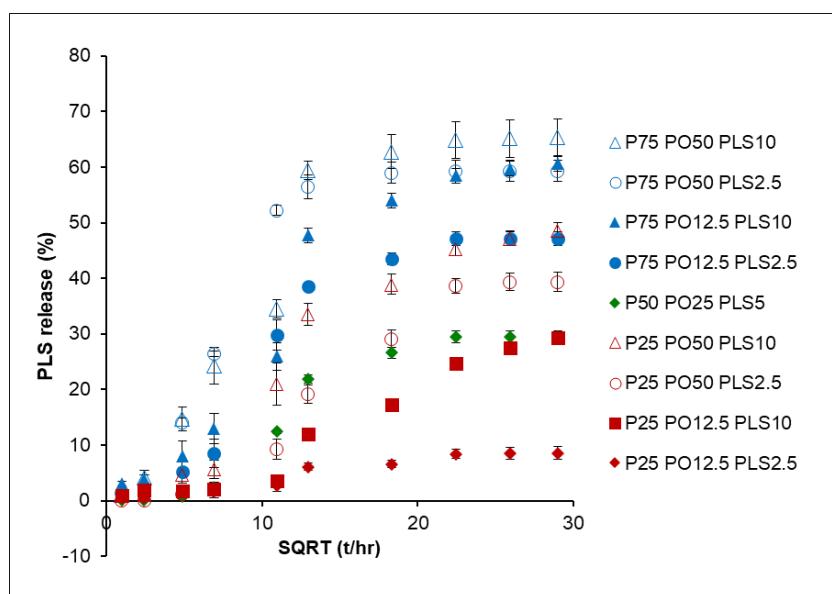


Fig 8-10 PLS release in deionised water versus square root of hour. Error bars are 95% CI (n=3).

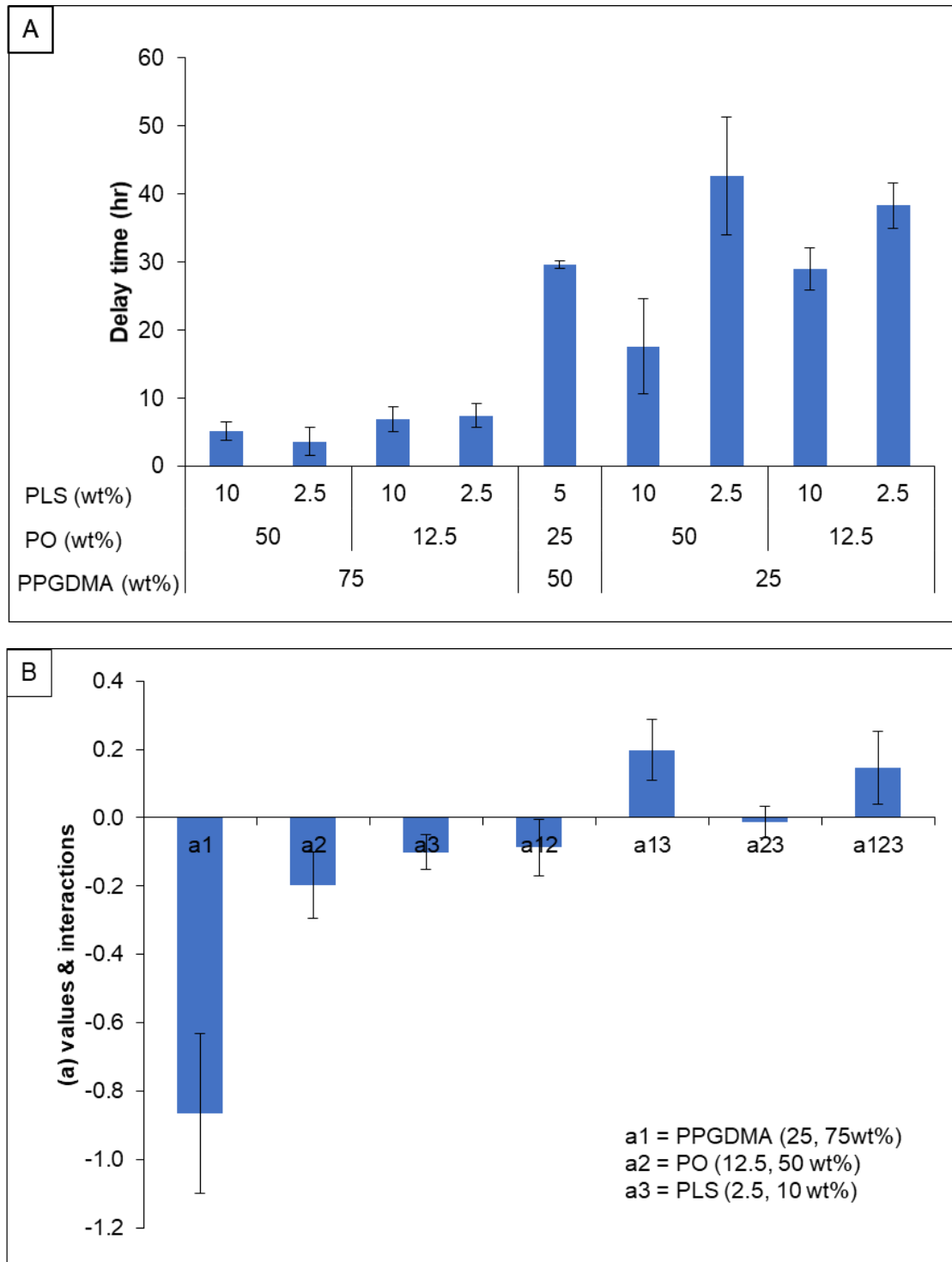
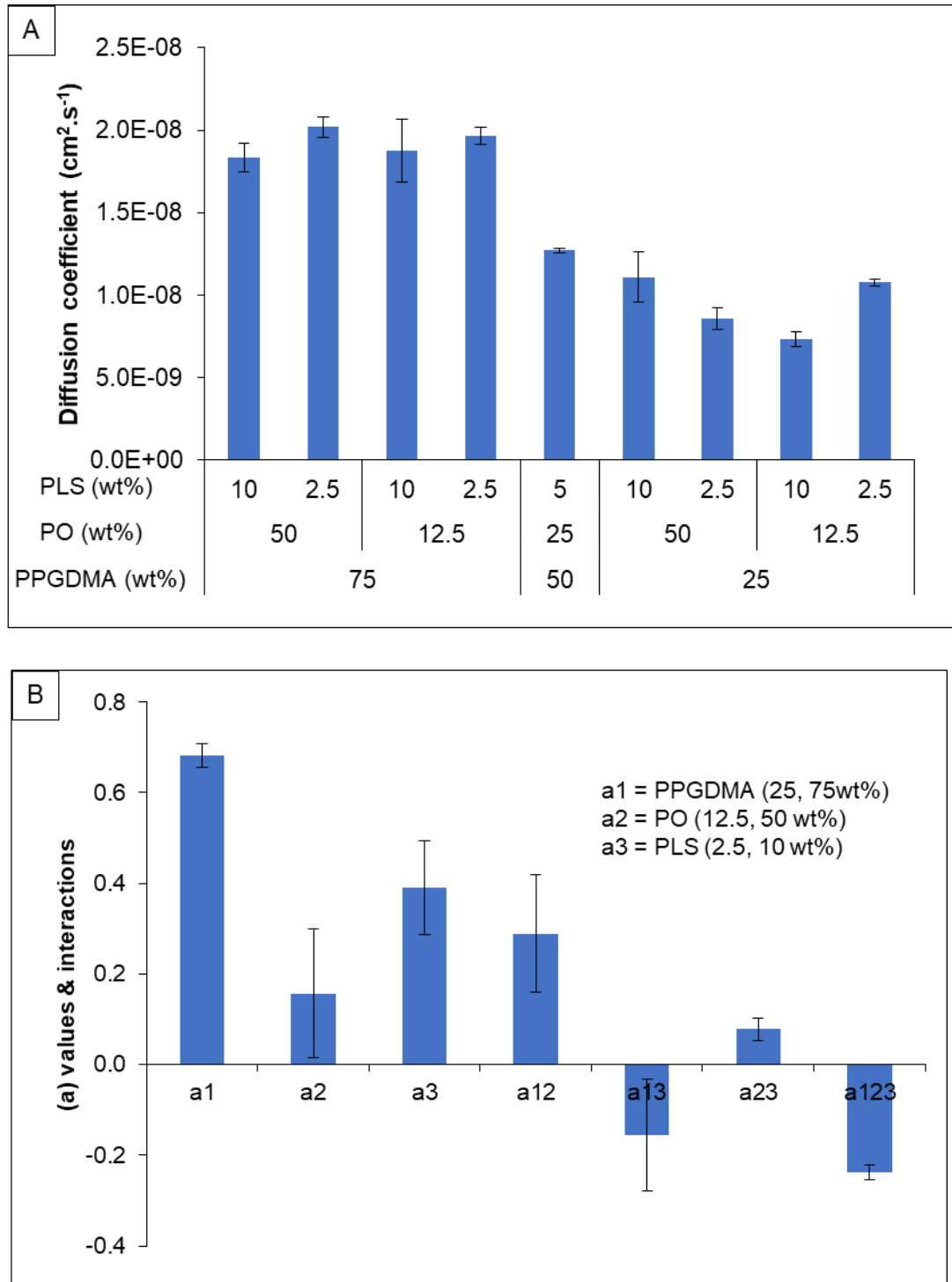


Fig 8-11 A) Delay time ( $t_d$ ) of each formulation and B) factorial analysis describing the effect of PPGDMA, PO, PLS, and their interactions on the  $t_d$  of PLS. Error bars are 95% CI (n=3).

#### 8.7.4.2 Diffusion coefficient

The average diffusion coefficient for PLS through composites containing 75 wt% of PPGDMA ( $1.9 \times 10^{-8} \text{ cm}^2.\text{s}^{-1}$ ) was higher than that of the composites containing 25 wt% of PPGDMA ( $9.4 \times 10^{-9} \text{ cm}^2.\text{s}^{-1}$ ) (Fig 8-12 A).  $\text{P}_{75}\text{PO}_{50}\text{PLS}_{2.5}$  exhibited the highest diffusion coefficient ( $2.0 \times 10^{-8} \pm 6.4 \times 10^{-10} \text{ cm}^2.\text{s}^{-1}$ ). The lowest coefficient was obtained from  $\text{P}_{25}\text{PO}_{50}\text{PLS}_{10}$  ( $7.3 \times 10^{-9} \pm 4.6 \times 10^{-10} \text{ cm}^2.\text{s}^{-1}$ ). The coefficient obtained from the intermediate formulation ( $\text{P}_{50}\text{PO}_{25}\text{PLS}_5$ ;  $1.3 \times 10^{-8} \pm 1.6 \times 10^{-10} \text{ cm}^2.\text{s}^{-1}$ ) was comparable to the average coefficient of experimental bone composites ( $1.4 \times 10^{-8} \text{ cm}^2.\text{s}^{-1}$ ).

Factorial analysis showed that PPGDMA level had strong effect on diffusion coefficient of experimental bone composites (Fig 8-12 B). The diffusion coefficient was increased by  $107 \pm 20 \%$  upon increasing PPGDMA level. The effect of PO and PLS were negligible.



**Fig 8-12 A) Diffusion coefficient PLS, and B) factorial analysis describing the effect of PPGDMA, PO, PLS, and interactions on the diffusion coefficient of PLS release. Lines indicated no significant difference ( $p > 0.05$ ) Error bars are 95% CI ( $n=3$ ).**

#### 8.7.4.3 Cumulative PLS release

Cumulative PLS release at specific time points (1 day, 1 week, and 4 weeks) are presented in Fig 8-13 A. The cumulative release at each time point was decreased upon lowering PPGDMA, PO, and PLS. For experimental bone composites containing 75 wt% PPGDMA, their average cumulative release at 1 day (13 %) increased and reached a maximum at 1 week (55 %). At 4 weeks, the release levels were only slightly enhanced (58 %). For the composites containing 25 wt% of PPGDMA, the average of cumulative PLS release at 1 day was 4 %. These increased to 22 % and 31 % at 1 week and 4 weeks respectively.

The cumulative PLS release obtained from the intermediate formulation ( $P_{50}PO_{25}PLS_5$ ) was ( $3 \pm 1$ ), ( $27 \pm 1$ ), and ( $30 \pm 1$ ) % at 1 day, 1 week, and 4 weeks respectively. These were lower than the average cumulative PLS release of experimental bone composites at 1 day (9 %), 1 week (38 %), and 4 weeks (44 %).

Factorial analysis showed that PPGDMA was the primary factor affecting accumulative PLS release at all time points (Fig 8-13 B). The PLS release at 1 day was increased by  $260 \pm 76$  % upon increasing PPGDMA level. The effect of increasing PPGDMA gradually declined to  $175 \pm 21$  % at 1 week and  $108 \pm 17$  % at 4 weeks. The PLS release was increased on average by 76 % and 58 % upon raising PO and PLS levels respectively.

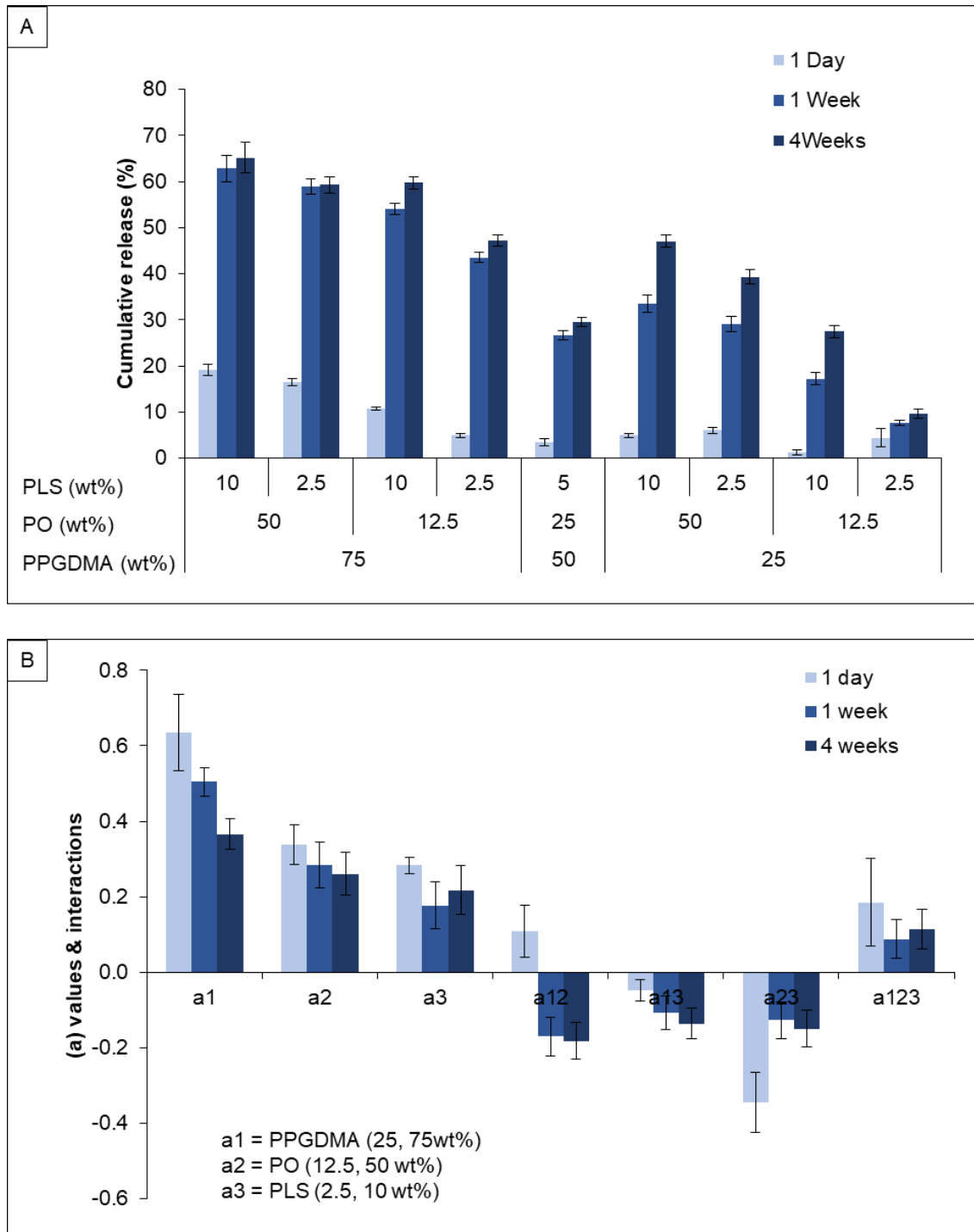


**Fig 8-13 A) Cumulative release of PLS at 1 week, and B) factorial analysis describing the effect of increasing PPGDMA, PO, and PLS on the cumulative release of PLS. Error bars are 95% CI (n=3).**

### 8.7.5 Apatite formation

Surface apatite precipitation on experimental bone composites and Cortoss upon immersion in SBF for up to 4 weeks is shown in Figs 8-14,15.  $P_{25}PO_{12.5}PLS_{10}$  and  $P_{25}PO_{12.5}PLS_{2.5}$  exhibited only patches of precipitate at all time points. Additionally, no precipitation was not observed on Simplex. Ca/P and Ca/Si ratios of Cortoss was not shown due to the high variability of ions across the surface.

At 1 day, brushite was detected on the surface of  $P_{75}PO_{50}PLS_{10}$  and  $P_{75}PO_{50}PLS_{2.5}$  (Fig 8-14). At the same time point, the surface of  $P_{25}PO_{50}PLS_{2.5}$  and  $P_{50}PO_{25}PLS_5$  (Fig 8-14) were covered by thin layers of apatite ( $\sim 1 \mu m$  in thickness). Ca/P ratio of these precipitates was lower than 1.

At 1 week, precipitates of brushite on  $P_{75}PO_{50}PLS_{10}$  were increased (Fig 8-14). In contrast, brushite previously seen of  $P_{75}PO_{50}PLS_{2.5}$  was replaced by an apatite layer ( $\sim 5-10 \mu m$  in thickness) with the Ca/P ratio of  $1.3 \pm 0.1$  (Fig 8-16A). At the same time point, surfaces of  $P_{75}PO_{12.5}PLS_{2.5}$ ,  $P_{50}PO_{25}PLS_5$ , and  $P_{25}PO_{50}PLS_{2.5}$  were fully covered by apatite precipitates (Figs 8- 14,15). Ca/P ratio of these precipitates were  $1.2 \pm 0.1$ ,  $1.3 \pm 0.1$ , and  $1.2 \pm 0.0$  respectively (Fig 8-16A).

At 4 weeks, the surface brushite previously seen on  $P_{75}PO_{50}PLS_{10}$  was replaced by dense apatite layer (Ca/P ratio =  $1.4 \pm 0.1$ ) (Fig 8-16A). The thickness of the apatite layers previously observed at 1 week in  $P_{75}PO_{50}PLS_{2.5}$ ,  $P_{75}PO_{12.5}PLS_{2.5}$ ,  $P_{50}PO_{25}PLS_5$ , and  $P_{25}PO_{50}PLS_{2.5}$  was also increased to approximately 10 - 20  $\mu m$  (Figs 8-14,15). The Ca/P ratio of these precipitates was 1.2 to 1.3 (Fig 8-16A). At this time point, thin apatite layer started to become visible on the surface of  $P_{75}PO_{12.5}PLS_{10}$  (Fig 8-13). Furthermore, Cortoss encouraged precipitation of apatite at 4 weeks (Fig 8-14).



Ca / Si ratio of surface apatite on experimental bone composites correlated with the increase in thickness of the apatite layers (Fig 8-17 A).

The average Ca/P (0.7) and Ca/Si (23) ratios at all time points of experimental bone composites were comparable to the results obtained from the intermediate formulation ( $P_{50}PO_{25}PLS_5$ ; 0.9 and 19 for Ca/P and Ca/Si ratios respectively).

Ca/P and Ca/Si ratios were affected by PPGDMA, PO, PLS levels (Figs 8-16B, 17B). Ca/P ratio of experimental bone composites at all time points was increased on average by 110 % and 81 % upon raising PPGDMA and PO levels. The effect of PLS was observed at 1 week as Ca/P ratio was increased by  $124 \pm 49$  % upon decreasing PLS level.

For Ca/Si ratio, the ratio was increased on average by 30 (3,128 %) and 274 (27,477 %) folds upon raising PPGDMA and PO. At 1 week, however, Ca/Si ratio was increased by 94 folds ( $9,431 \pm 2,944$  %) upon decreasing PLS level.

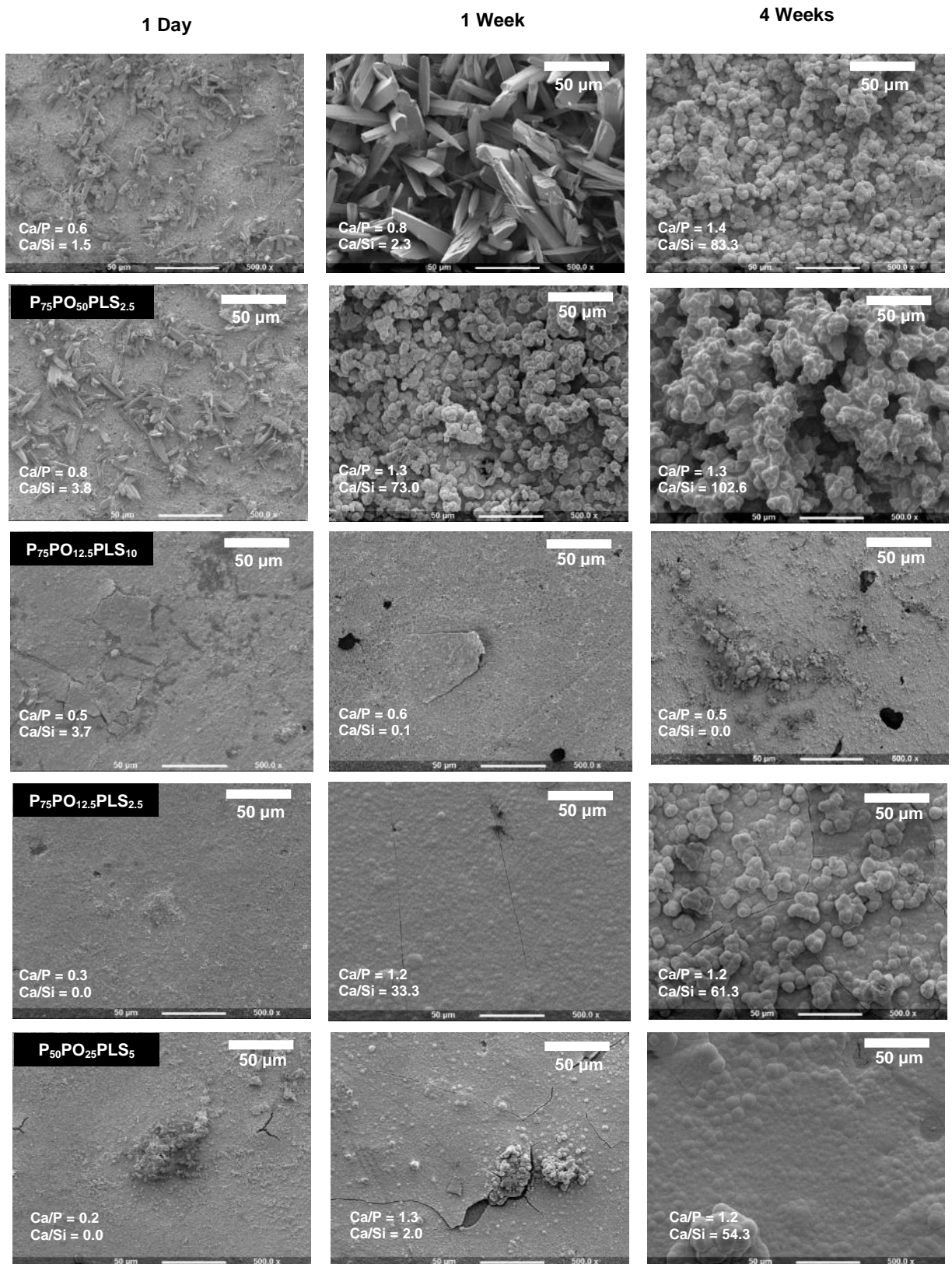
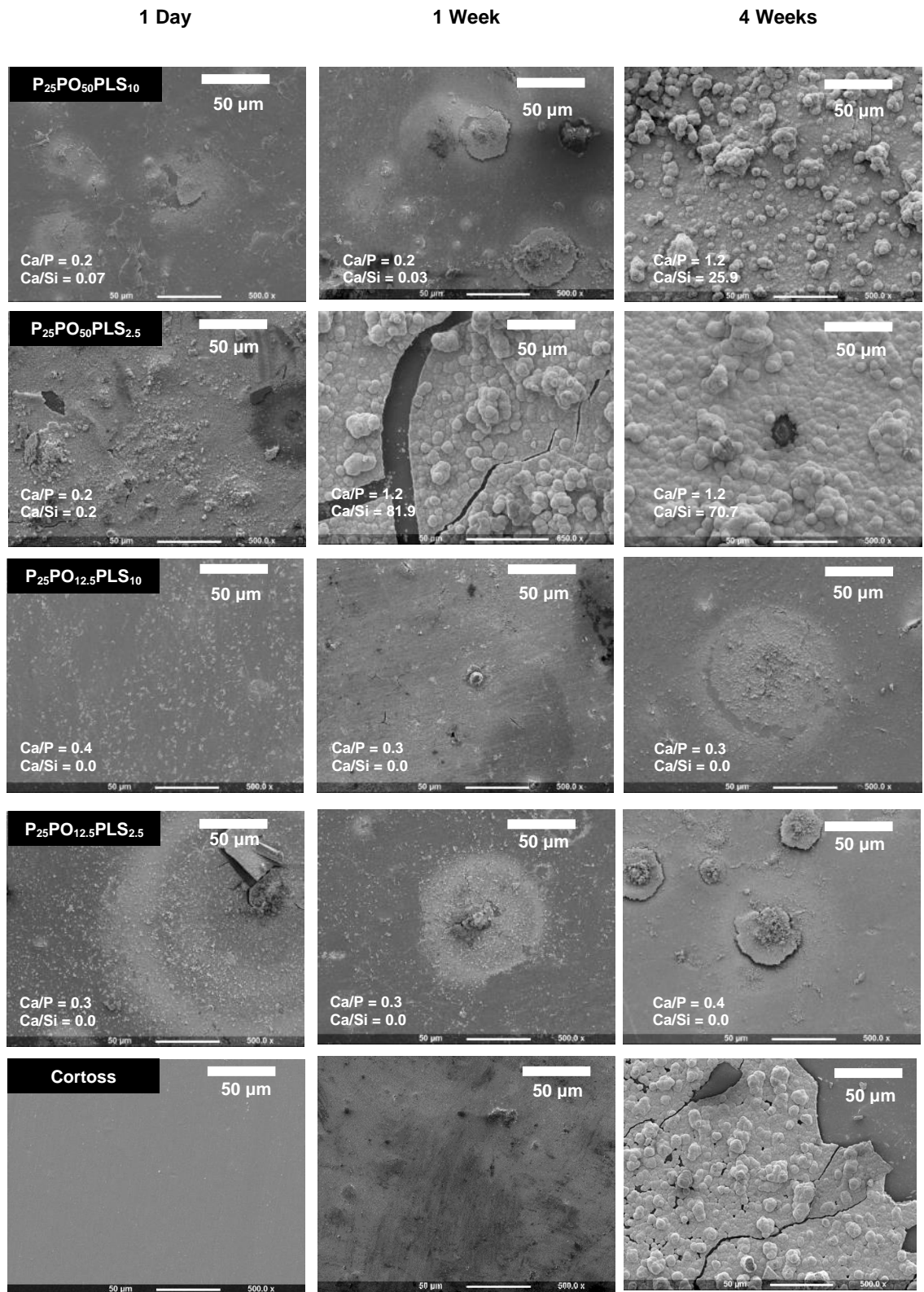
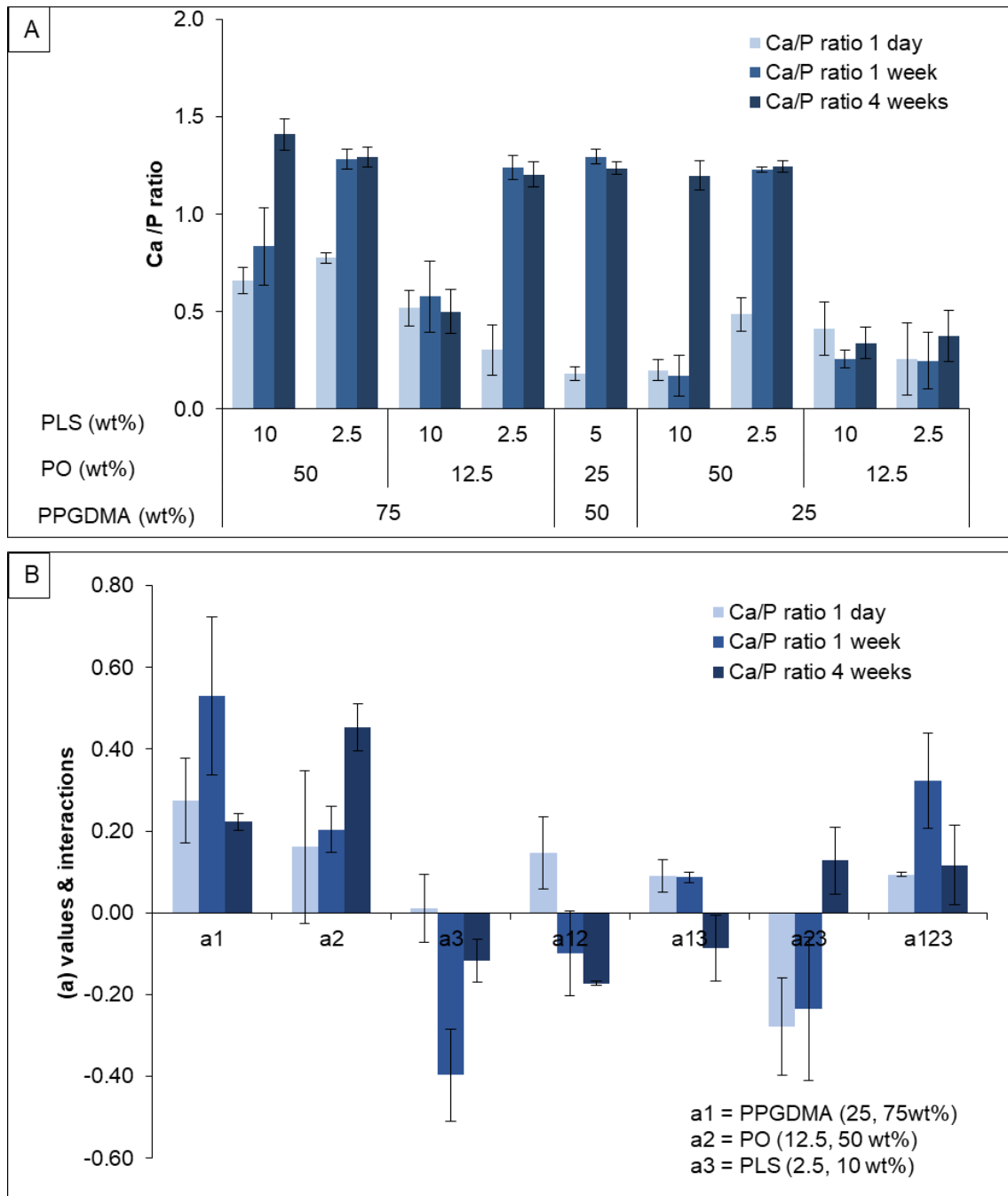


Fig 8-14 Representative of surface SEM images of composite discs after immersion in SBF for 1 day, 1, and 4 weeks (n=1).



**Fig 8-15** Representative of surface SEM images of disc samples from experimental bone composites and Cortoss after immersion in SBF for 1 day, 1, and 4 weeks (n=1). Ca/Si and Ca/P ratio of Cortoss did not show due to the large variation in Ca, Si, and P ions across the surface.



**Fig 8-16 A) Ca/P ratio of representative surface precipitates. B) Factorial analysis describing the effect of increasing PPGDMA, PO, and PLS on Ca / P ratio. Error bars are 95% CI (n=3).**

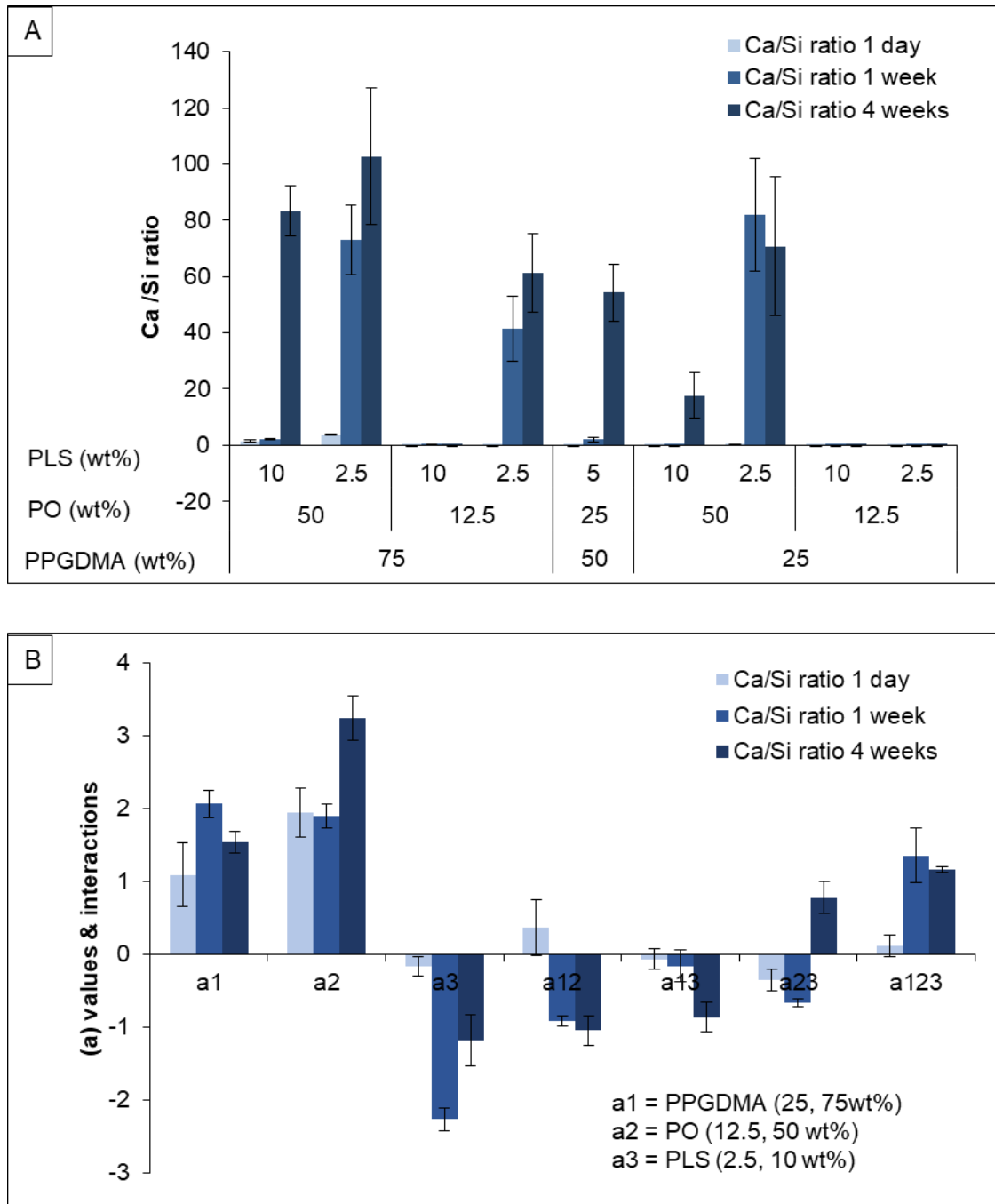


Fig 8-17 A) Ca/Si ratio of representative surface precipitates. B) Factorial analysis describing the effect of increasing PPGDMA, PO, and PLS on Ca / Si ratio. Error bars are 95% CI (n=3).

## 8.7.6 Mechanical properties

### 8.7.6.1 Compressive strength

The average compressive strength of experimental bone composites containing 75 wt% of PPGDMA (106 MPa) was lower than that of the composites containing 25 wt% of PPGDMA (155 MPa). Lowest and highest compressive strength was observed with  $P_{75}PO_{50}PLS_{10}$  ( $49 \pm 10$  MPa) and  $P_{25}PO_{12.5}PLS_{2.5}$  ( $238 \pm 30$  MPa) respectively (Fig 8-18 A). The highest strength was significantly higher than that of Simplex ( $86 \pm 7$  MPa) and Cortoss ( $160 \pm 11$  MPa).

The compressive strength of Simplex was comparable to that of  $P_{75}PO_{50}PLS_{2.5}$  ( $97 \pm 10$  MPa),  $P_{75}PO_{12.5}PLS_{10}$  ( $102 \pm 12$  MPa),  $P_{25}PO_{50}PLS_{10}$  ( $90 \pm 9$  MPa), and  $P_{25}PO_{50}PLS_{2.5}$  ( $113 \pm 10$  MPa). Additionally, compressive strength of  $P_{75}PO_{12.5}PLS_{2.5}$  ( $179 \pm 16$  MPa),  $P_{50}PO_{25}PLS_5$  ( $161 \pm 18$  MPa), and  $P_{25}PO_{12.5}PLS_{10}$  ( $178 \pm 9$  MPa) were comparable to that of Cortoss. The average result of experimental bone composites (130 MPa) was lower than the result from the intermediate formulation ( $P_{50}PO_{25}PLS_5$ ,  $167 \pm 18$  MPa).

All composite formulations except for  $P_{75}PO_{50}PLS_{10}$  showed compressive strength greater than 70 MPa required from the BS ISO 5833. Factorial analysis indicated that the PPGDMA, PO, and PLS strongly affected compressive strength of experimental bone composites (Fig 8-17 B). The compressive strength was increased by  $50 \pm 10$  %,  $101 \pm 13$  %, and  $56 \pm 15$  % upon decreasing PPGDMA, PO, and PLS levels respectively.

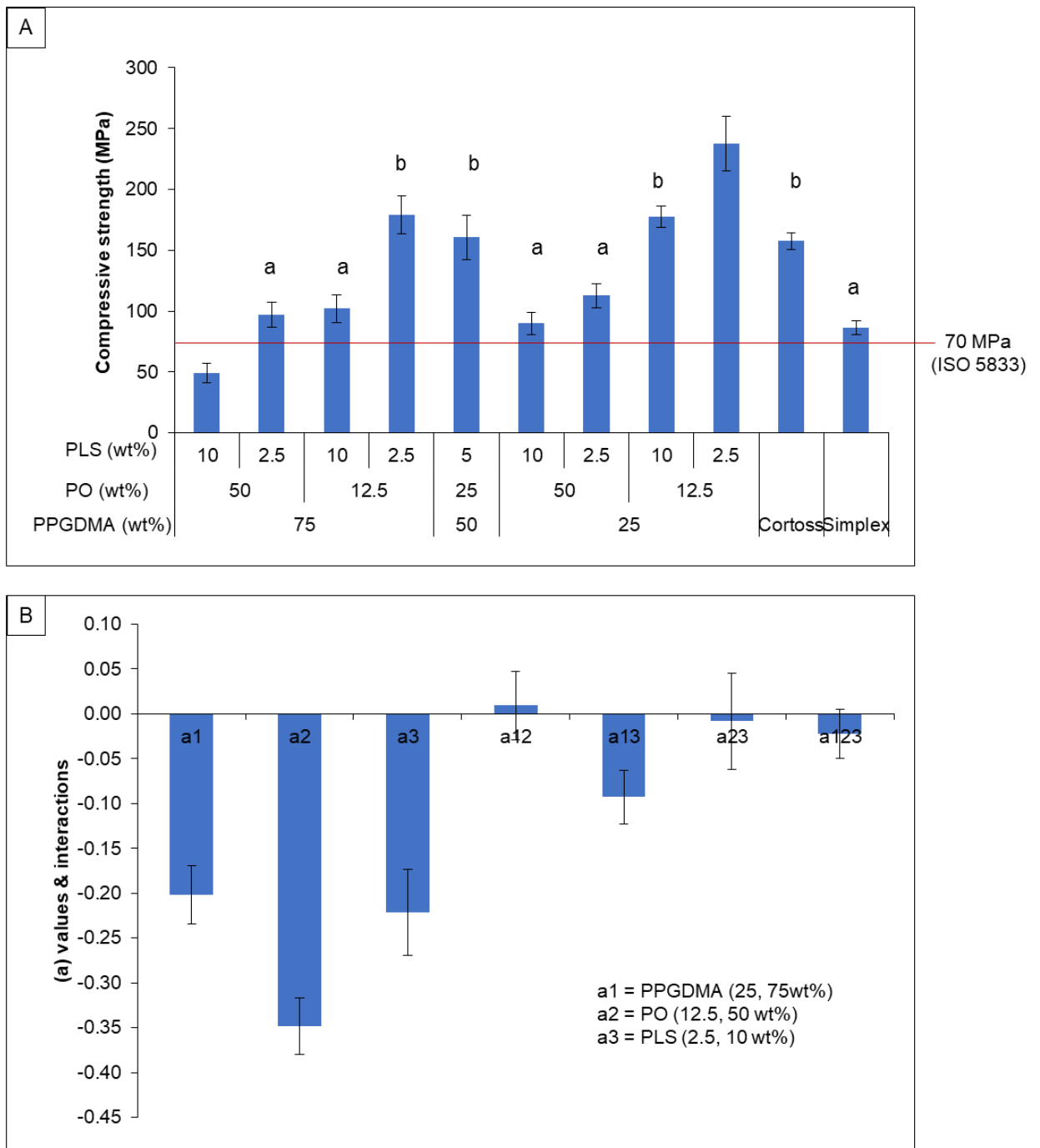


**Fig 8-18 A) Compressive strength and B) factorial analysis describing the effect of PPGDMA, PO, and PLS on compressive strength. Error bars are 95% CI (n = 5). Same letters indicate statistically insignificance ( $p > 0.05$ ).**

### 8.7.6.2 Biaxial flexural strength

BFS and modulus of elasticity of all materials decreased upon enhancing immersion time. The highest and lowest BFS at all immersion time points (1 day, 1 week, 4 weeks) were observed with  $P_{25}PO_{12.5}PLS_{2.5}$  ( $141 \pm 14$ ,  $124 \pm 9$ ,  $124 \pm 12$  MPa) and  $P_{75}PO_{50}PLS_{10}$  ( $34 \pm 2$ ,  $31 \pm 1$ ,  $27 \pm 2$  MPa) (Fig 8-19).

At 1 day, an average BFS of experiment bone composites containing 75 wt% PPGDMA (54 MPa) was ~ 50 % lower than that of the composites containing 25 wt% of PPGDMA (105 MPa). Additionally, BFS of all composites containing 75 wt% PPGDMA composites was significant lower than that of Cortoss ( $83 \pm 9$  MPa) and Simplex ( $129 \pm 15$  MPa). Furthermore, BFS of  $P_{25}PO_{12.5}PLS_{2.5}$  was comparable to that of Simplex but was significantly higher than that of Cortoss. A reduction of BFS from 1 day to 1 week was observed with all materials. The average BFS at 1 week and 4 weeks were 45 and 46 MPa for composites containing 75 wt%. These of composites containing 25 wt% of PPGDMA were 89 and 86 MPa at 1 week and 4 weeks respectively.

The BFS at 1 week and 4 weeks of all materials was not significantly different. BFS after immersion in SBF for 24 hr of all experimental bone composites except for  $P_{75}PO_{50}PLS_{10}$  ( $34 \pm 2$  MPa) were higher than that of 50 MPa required from BS ISO 5833 (Implants for surgery-acrylic resin cements).

At 4 weeks, BFS of Simplex ( $117 \pm 7$  MPa) was comparable with that of  $P_{25}PO_{12.5}PLS_{2.5}$  ( $124 \pm 12$  MPa) and  $P_{25}PO_{12.5}PLS_{10}$  ( $100 \pm 6$  MPa). Furthermore, BFS of  $P_{75}PO_{12.5}PLS_{10}$  ( $51 \pm 4$  MPa),  $P_{75}PO_{12.5}PLS_{2.5}$  ( $63 \pm 3$  MPa), and  $P_{25}PO_{50}PLS_{2.5}$  ( $68 \pm 5$  MPa) were comparable with that of Cortoss ( $61 \pm 3$  MPa).



The average BFS of experimental bone composites at 1 day (80 MPa) was lower than the result from the intermediate formulation ( $P_{50}PO_{25}PLS_5$ ;  $98 \pm 4$  MPa). The average result of the composites at 1 week (67 MPa) and 4 weeks (66 MPa) were however higher than the result from the intermediate formulation ( $59 \pm 4$  and  $49 \pm 2$  MPa at 1 and 4 weeks respectively).

Factorial analysis showed that BFS of experimental bone composites was strongly affected PPGDMA, PO, and PLS levels at all immersion time points (Fig 8-20). The BFS of the composites increased on averaged by 88 %, 74 %, and 52 % upon decreasing PPGDMA, PO, and PLS levels.

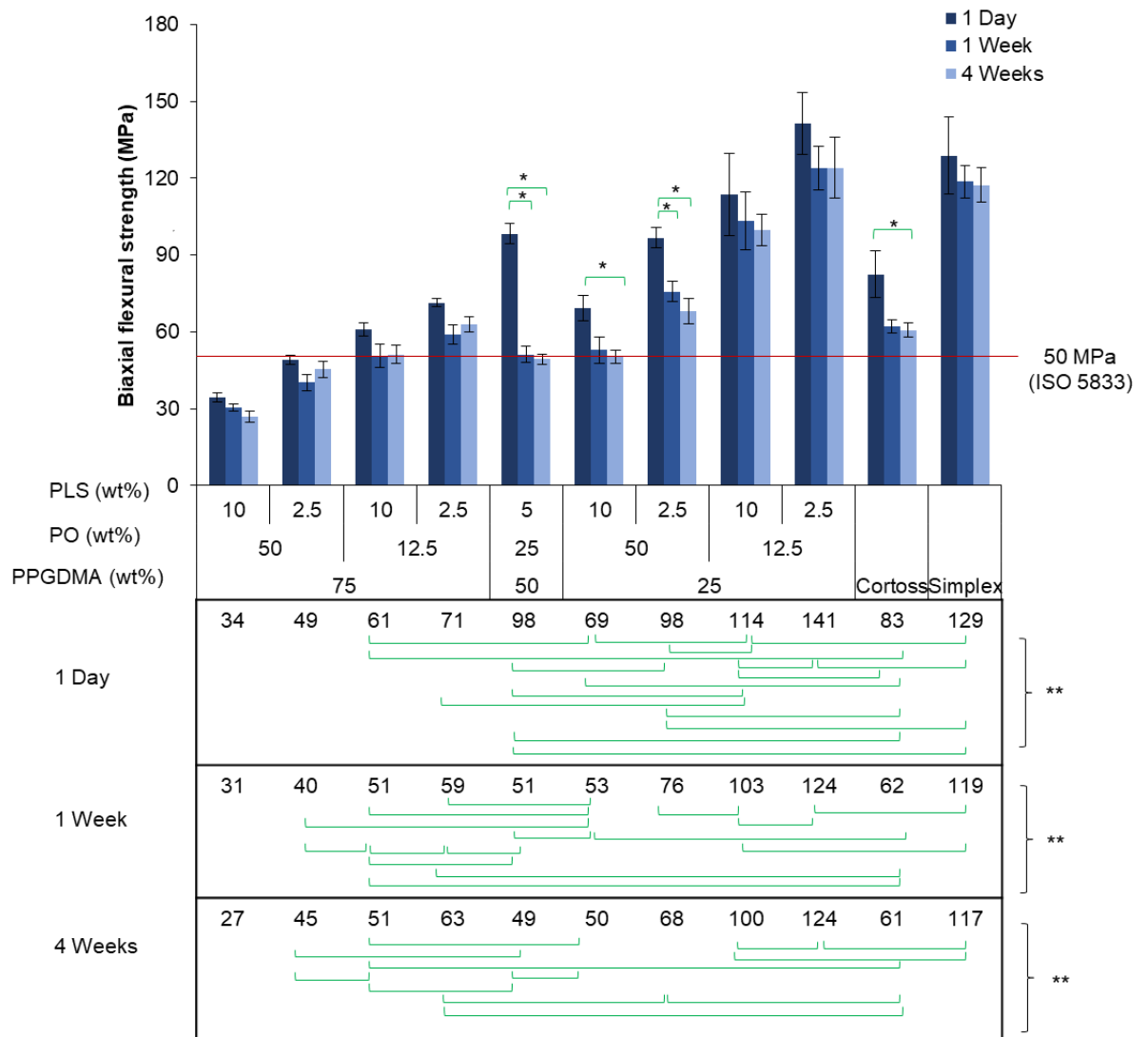


**Fig 8-19 BFS of all materials after immersion in SBF for 1 day and 4 weeks. Error bars are 95% CI (n=5). (\*) and (\*\*) indicate statistical significance ( $p < 0.05$ ) and statistical not significance ( $p > 0.05$ ) respectively.**

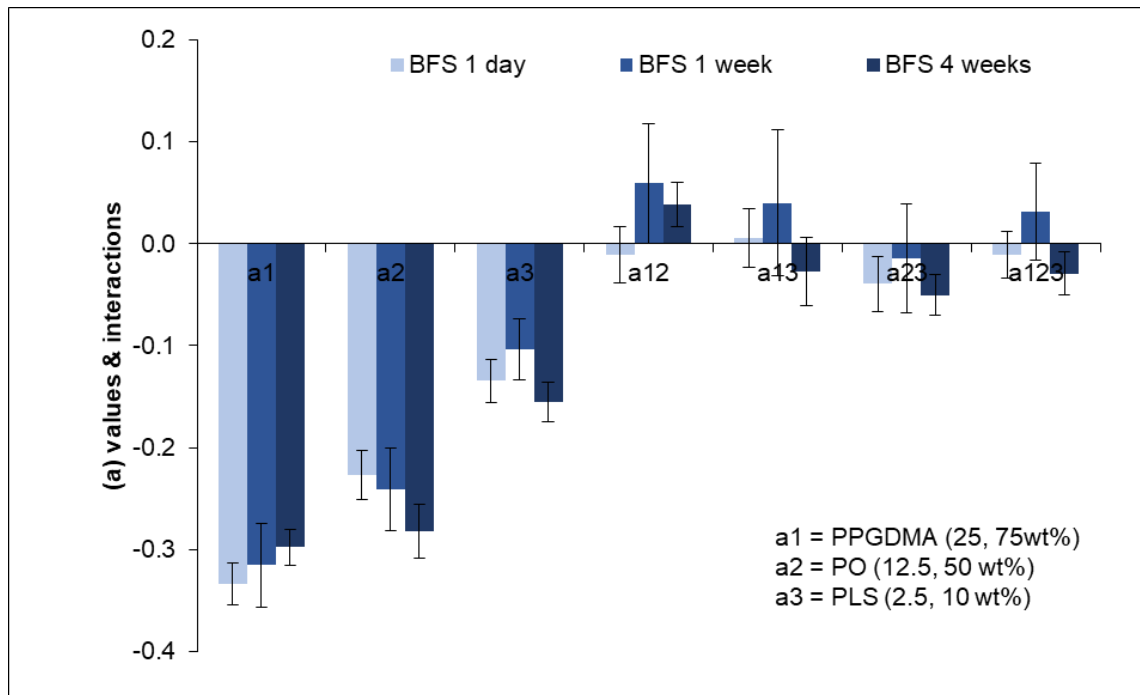


**Fig 8-20** Factorial analysis describing the effect of decreasing PPGDMA, PO, and PLS on biaxial flexural strength of the composites after immersion in SBF up to 4 weeks. Error bars are 95% CI (n=5).

### 8.7.6.3 Modulus of elasticity

At 1 day, the average modulus of elasticity of experimental bone composites containing 75 wt% of PPGDMA (0.7 GPa) was three times lower than that of the composites containing 25 wt% of PPGDMA (2.1 GPa). The highest and lowest modulus of elasticity at 1 day were observed from  $P_{25}PO_{12.5}PLS_{2.5}$  ( $3.1 \pm 0.4$  GPa) and  $P_{75}PO_{50}PLS_{10}$  ( $0.3 \pm 0.0$  GPa) (Fig 8-21). At this time point, the modulus of elasticity of all experimental bone composites containing 75 wt% PPGDMA were significantly lower than that of Cortoss ( $2.3 \pm 0.2$  GPa). Furthermore, the modulus of elasticity of  $P_{75}PO_{50}PLS_{10}$ ,  $P_{75}PO_{50}PLS_{2.5}$  ( $0.5 \pm 0.1$  GPa),  $P_{75}PO_{12.5}PLS_{10}$  ( $0.9 \pm 0.0$  GPa), and  $P_{25}PO_{50}PLS_{10}$  ( $1.1 \pm 0.2$  GPa) were significantly lower than that of Simplex ( $1.7 \pm 0.2$  GPa).  $P_{25}PO_{12.5}PLS_{2.5}$  exhibited modulus of elasticity comparable to Cortoss but significantly higher than Simplex. Additionally, experimental bone composites that showed modulus of elasticity comparable or greater the flexural modulus at 24 hr required from BFS ISO 5833 (1.8 GPa) included  $P_{50}PO_{25}PLS_5$  ( $1.8 \pm 0.2$  GPa),  $P_{25}PO_{12.5}PLS_{10}$  ( $2.6 \pm 0.4$  GPa), and  $P_{25}PO_{12.5}PLS_{2.5}$  ( $3.1 \pm 0.4$  GPa).

The significant reduction in modulus of elasticity from 1 day to 1 week was observed with  $P_{50}PO_{25}PLS_5$ . At this time point, the composites containing 75 wt% PPGDMA (0.3 – 0.9 GPa) exhibited significantly lower modulus elasticity compared with Simplex ( $1.8 \pm 0.1$  GPa). The modulus of Simplex also significantly higher than that of  $P_{50}PO_{25}PLS_5$  ( $0.9 \pm 0.1$  GPa) and  $P_{25}PO_{50}PLS_{10}$  ( $0.8 \pm 0.1$  GPa). No significant reduction of modulus of elasticity from 1 week to 4 weeks was observed. At 4 weeks, the composites containing 75 wt% PPGDMA (0.3 – 1.0 GPa),  $P_{50}PO_{25}PLS_5$  ( $0.9 \pm 0.1$  GPa), and  $P_{25}PO_{50}PLS_5$  ( $0.7 \pm 0.1$  GPa) exhibited lower modulus of elasticity compared with that of Simplex ( $1.5 \pm 0.0$  GPa) and Cortoss ( $2.0 \pm 0.2$  GPa).

The experimental bone composites that showed modulus of elasticity close to that of cancellous bone ( $< 0.7$  GPa) were  $P_{75}PPG_{50}PLS_{10}$  ( $0.3 \pm 0.0$  GPa),  $P_{75}PO_{50}PLS_{2.5}$  ( $0.5 \pm 0.1$  GPa),  $P_{75}PO_{12.5}PLS_{10}$  ( $0.7 \pm 0.0$  GPa), and  $P_{25}PO_{50}PLS_{10}$  ( $0.7 \pm 0.1$  GPa).

The average modulus of elasticity of experimental bone composites at 1 day (1.4 GPa) was lower than the result from the intermediate formulation ( $P_{50}PO_{25}PLS_5$ ;  $2.1 \pm 0.2$  MPa). The average result of the composites at 1 and 4 weeks (1.2 GPa) were however higher than the result from the intermediate formulation ( $1.1 \pm 1$  and  $0.9 \pm 0.1$  GPa at 1 and 4 weeks respectively).

Factorial analysis indicated that modulus of elasticity of experimental bone composites was affected PPGDMA, PO, and PLS levels (Fig 8-22). The modulus was increased on average by 196 %, 129 %, and 52 % upon decreasing PPGDMA, PO, and PLS respectively.

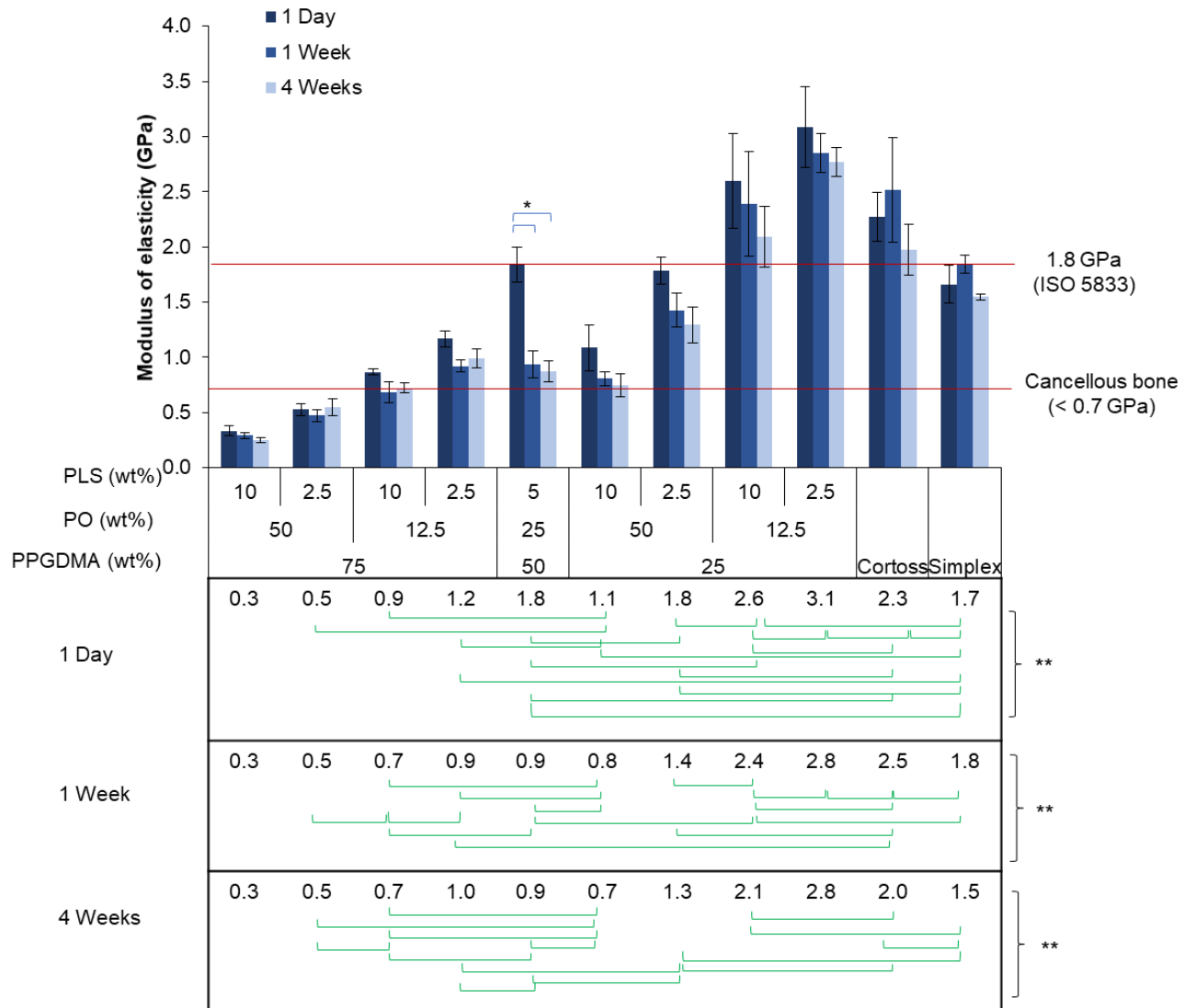


**Fig 8-21 Modulus of elasticity of all materials for 1 day and 4 weeks. Error bars are 95% CI (n=5). (\*) and (\*\*) indicate statistical significance ( $p < 0.05$ ) and statistically not significance ( $p > 0.05$ ) respectively.**

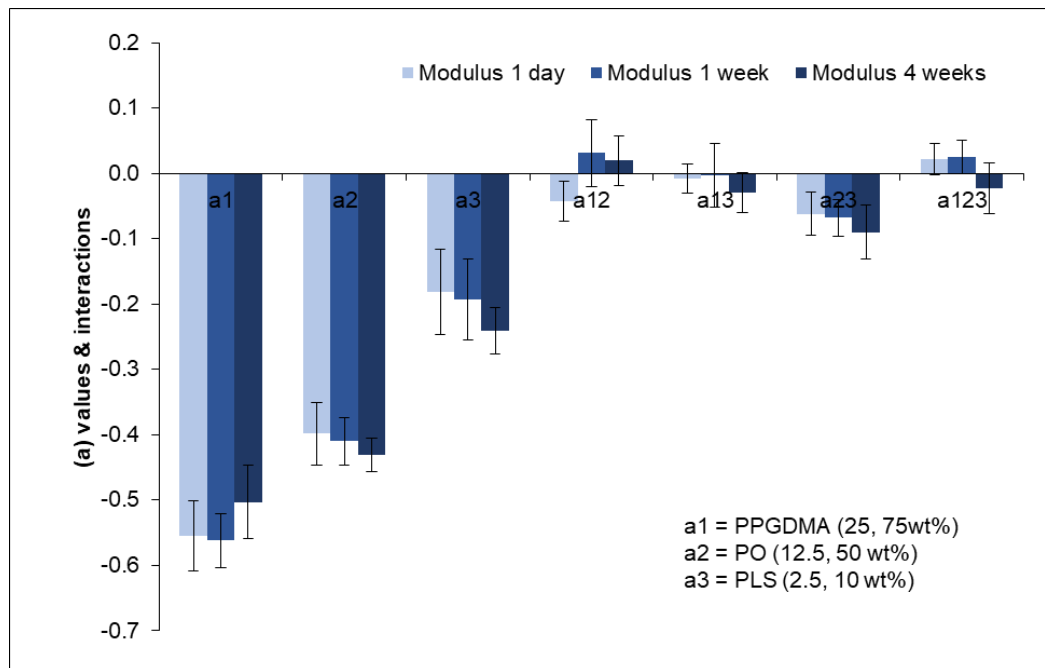


**Fig 8-22** Factorial analysis describing the PPGDMA, PO, PLS, and their interactions on modulus of elasticity of the composites after immersion in SBF for up to 4 weeks. Error bars are 95% CI (n=3).

#### **8.7.6.4 Biaxial flexural fatigue**

##### **8.7.6.4.1 Biaxial flexural strength tested at 37 °C in SBF**

All formulations being pre-stored for 4 weeks in SBF. BFS of all experimental bone composites tested in SBF at a controlled temperature of 37 °C using a hydraulic testing machine (Dartec HC10) was however lower than that obtained in air at room temperature using an universal testing machine (Shimadzu AGSX) (Fig 8-23 A). Result from the intermediate formulation ( $P_{50}PO_{25}PLS_5$ ;  $40 \pm 4$  MPa) was comparable to the average result of experimental bone composites (43 MPa/cycle).

At higher temperature and wet conditions, the effect of PPGDMA dominated other variables, whilst the effect of PPGDMA and PO were comparable for BFS tested in dry condition (Fig 8-23 B). Factorial analysis indicated that BFS of the composites measured wet was increased by  $100 \pm 13$  %,  $49 \pm 3$  %, and  $27 \pm 5$  % upon decreasing PPGDMA, PO, and PLS levels respectively.

##### **8.7.6.4.2 Stress versus failure cycles**

Plots of BFS versus failure cycles (S/N curve) are presented in Figs 8-24,25. Gradients of the S/N curve obtained from the experimental bone composites (3.7 – 7.2 MPa/log cycle) were comparable with that of Cortoss ( $6.0 \pm 0.3$  MPa/log cycle) but significantly lower than that of Simplex ( $16.6 \pm 0.8$  MPa/log cycle) (Fig 8-26 A). The average result of experimental bone composites (5.7 MPa/cycle) was lower than the result from the intermediate formulation ( $P_{50}PO_{25}PLS_5$ ;  $7.0 \pm 1.0$  log cycle).

No primary factor affecting the gradient of S-N curve of experimental bone composites was observed (Fig 8-26 B). The gradient of S-N curve was, however, increased by  $33 \pm 16$  % and  $26 \pm 19$  % upon decreasing PPGDMA and PO levels respectively.



#### 8.7.6.4.3 Predicted fatigue life

The extrapolated fatigue life of the composites upon the applied flexural stress of 10 MPa increased upon the reduction of PPGDMA, PO, and PLS (Fig 8-27 A). The longest and shortest fatigue life was observed with  $P_{25}PO_{12.5}PLS_{2.5}$  ( $9.2 \pm 0.7$  log cycle) and  $P_{75}PO_{50}PLS_{10}$  ( $5.3 \pm 0.3$  log cycle). The fatigue life of  $P_{25}PO_{12.5}PLS_{10}$  ( $7.6 \pm 0.6$  log cycle) was comparable with that of Simplex ( $7.8 \pm 0.5$  log cycle) and Cortoss ( $8.0 \pm 0.2$  log cycle). Result from the intermediate formulation ( $P_{50}PO_{25}PLS_5$ ;  $6.3 \pm 1.2$  log cycle) was comparable to the average result of experimental bone composites (6.4 log cycle).

Factorial analysis showed that primary factor affecting the fatigue life of experimental bone composites was PPGDMA level (Fig 8-27 B). The fatigue life of the composites was increased by  $58 \pm 9\%$ ,  $17 \pm 3\%$ , and  $18 \pm 4\%$  upon decreasing PPGDMA, PO, and PLS levels respectively.

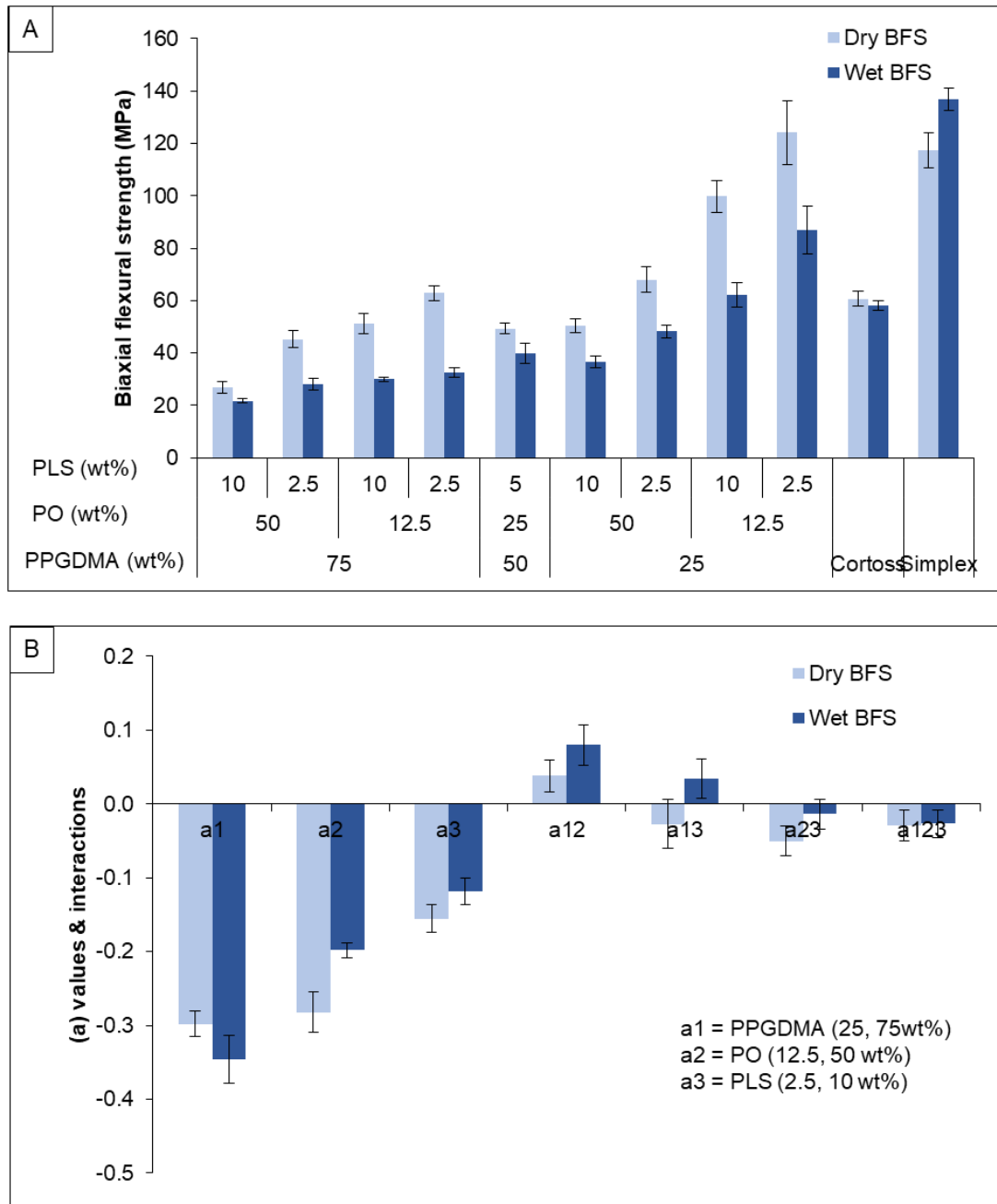


**Fig 8-23 A) BFS of materials tested in air at room temperature from Fig 8-19 and in SBF at 37 °C after immersion in SBF for 4 weeks. B) Factorial analysis describing the effect of PPGDMA, PO, and PLS on BFS of the experimental bone composites. Error bars are 95% CI (n = 5).**

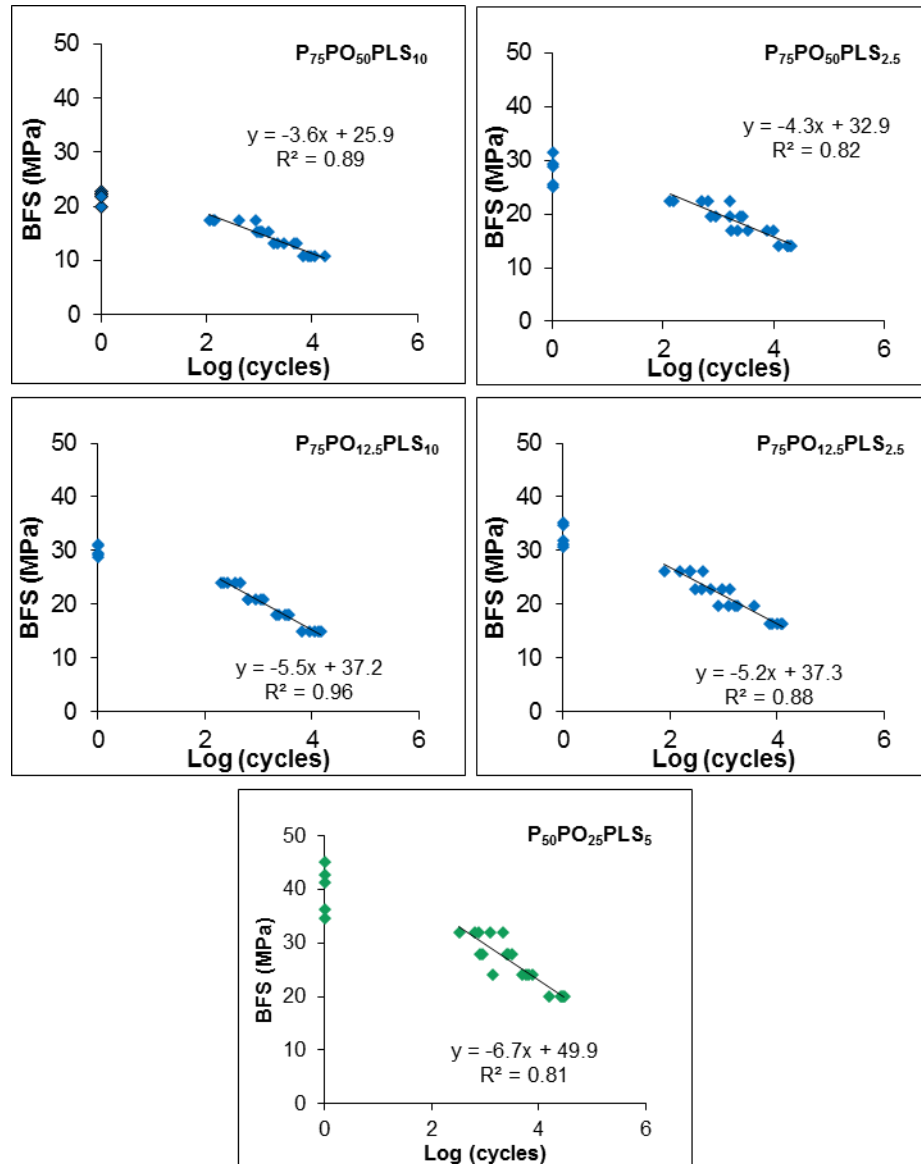


Fig 8-24 Plots of BFS versus log (cycle) of experimental bone composites containing 75 or 50 wt% of PPGDMA (n=20).

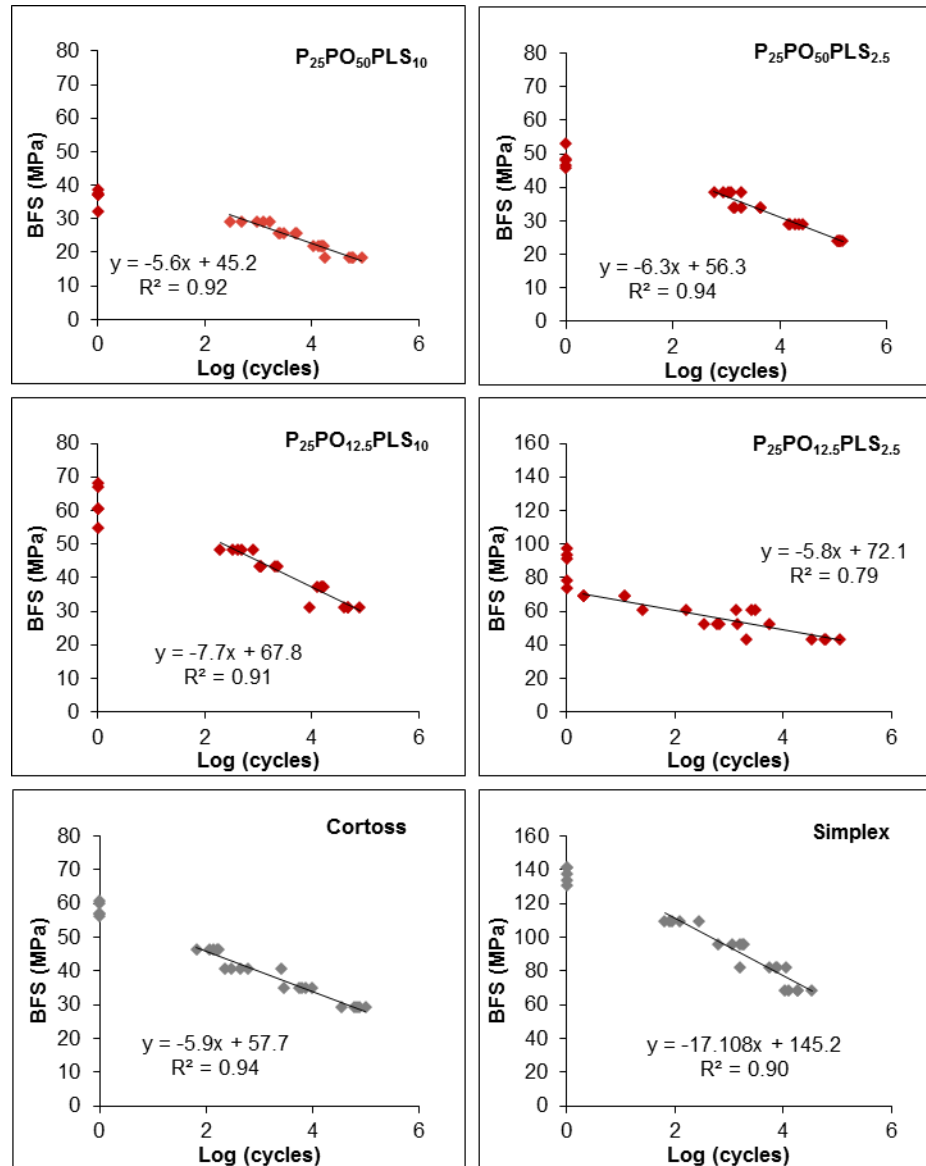


Fig 8-25 Plots of BFS versus log (cycle) of experimental bone composites containing 25 wt% of PPGDMA and commercial materials (n=20).

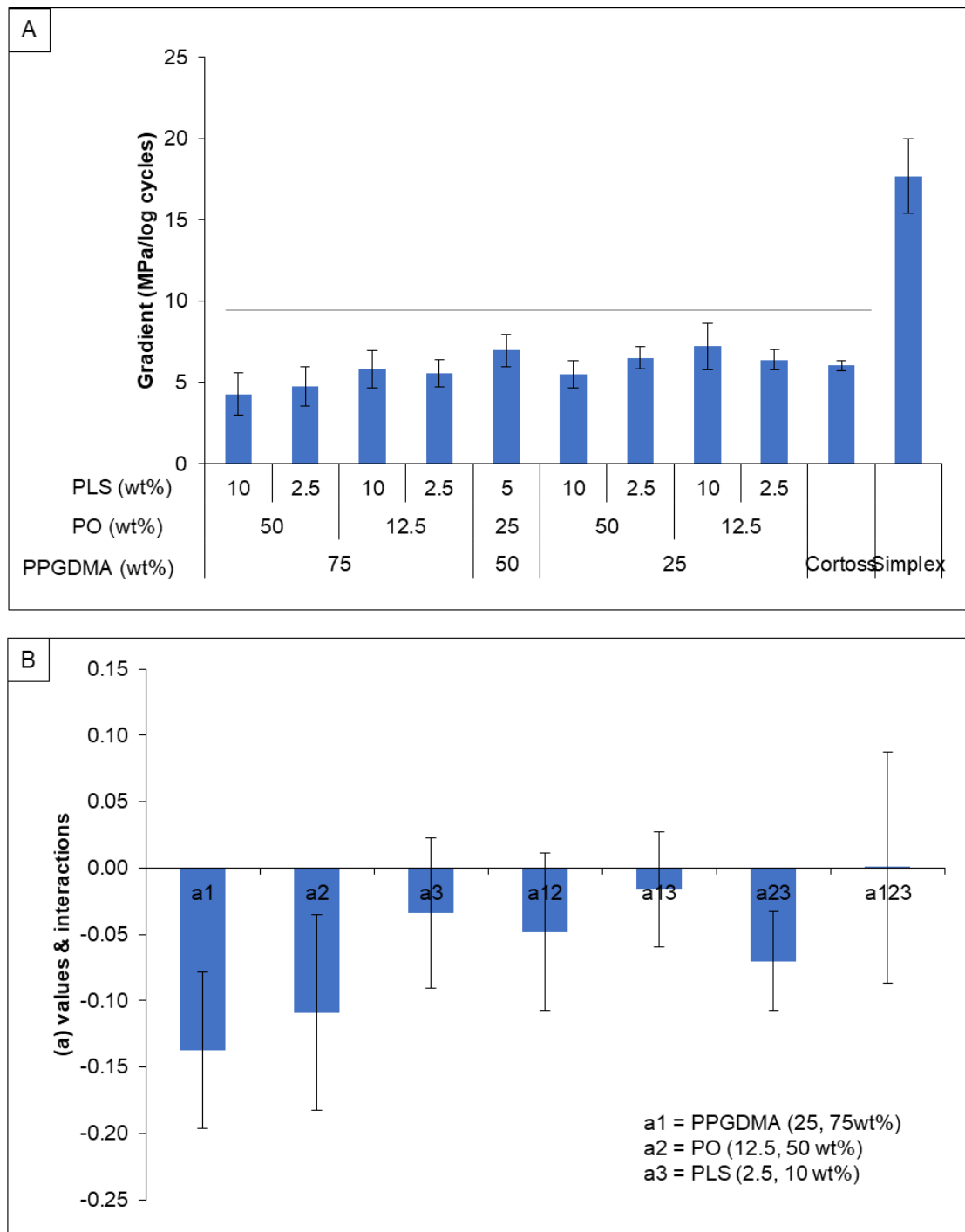
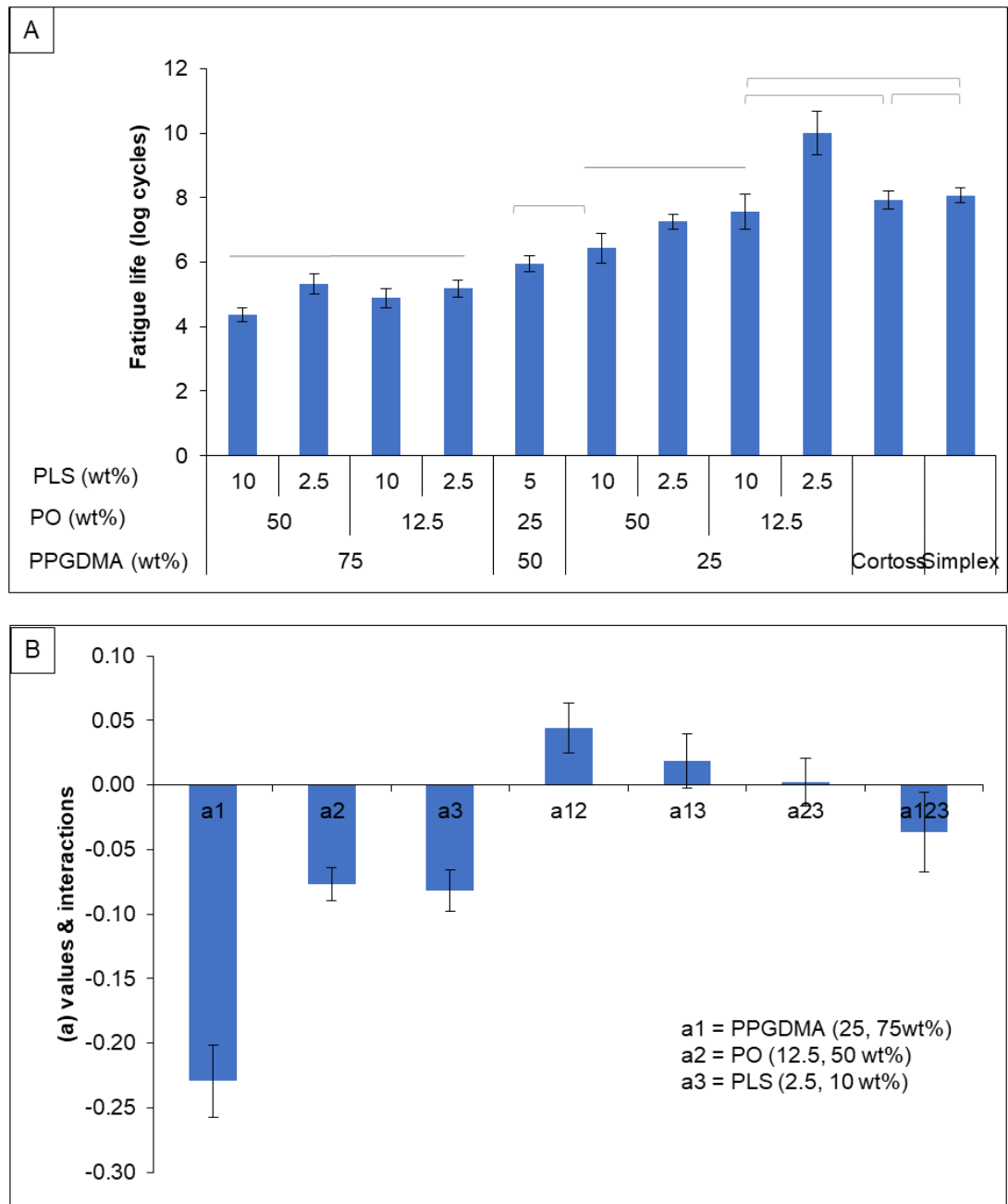


Fig 8-26 A) Gradient of S / N curve and B) Factorial analysis describing the effect of PPGDMA, PO, PLS, and their interactions on gradient of S/N curve. Error bars are 95% CI (n=5). Line indicates no statistically significant difference ( $p > 0.05$ ).



**Fig 8-27 A) Fatigue life of materials upon BFS of 10 MPa and B) factorial analysis describing the effect of PPGDMA, PO, PLS, and their interactions on fatigue life of the experimental bone composites. Error bars are 95% CI (n=3). Line indicates no statistically significant difference ( $p > 0.05$ ).**

### 8.7.7 Cytocompatibility test

The cytocompatibility test was performed by Dr Caitriona O'Rourke. Metabolic activity of surviving MSCS cultured in solutions containing 24 hr storage extracts from composite discs compared with that of a control with no extracts is presented in Fig 8-28 A. Highest and lowest relative metabolic activity of MSCS were observed with the solutions that had contained  $P_{25}PO_{12.5}PLS_{10}$  ( $78 \pm 8 \%$ ) and  $P_{75}PO_{50}PLS_{2.5}$  ( $14 \pm 3 \%$ ) respectively. The relative metabolic activity of MSCS in the solution previously containing  $P_{25}PO_{12.5}PLS_{10}$  was also comparable to that of the solutions in which  $P_{25}PO_{12.5}PLS_{2.5}$  ( $78 \pm 8 \%$ ) and  $P_{50}PO_{25}PLS_5$  ( $66 \pm 12 \%$ ) had been placed. The solution which contained  $P_{75}PO_{50}PLS_{10}$  inhibited metabolic activity of MSCS to a comparable degree with the storage solutions of  $P_{75}PO_{50}PLS_{10}$  ( $18 \pm 6 \%$ ),  $P_{25}PO_{50}PLS_{10}$  ( $19 \pm 3 \%$ ), and  $P_{25}PO_{50}PLS_{2.5}$  ( $29 \pm 8 \%$ ). The relative metabolic activity of MSCS cultured in the solution containing extracts from the intermediate formulation ( $P_{50}PO_{25}PLS_5$ ,  $66 \pm 12 \%$ ) was greater than the average result that from experimental bone composites ( $41 \%$ ).

Factorial analysis indicated that PO was the primary factor affecting metabolic activity of MSCS (Fig 8-28 B). The metabolic activity was increased by  $59 \pm 17 \%$  and  $258 \pm 54 \%$  upon reducing PPGDMA and PO levels respectively. The effect of PLS was negligible.

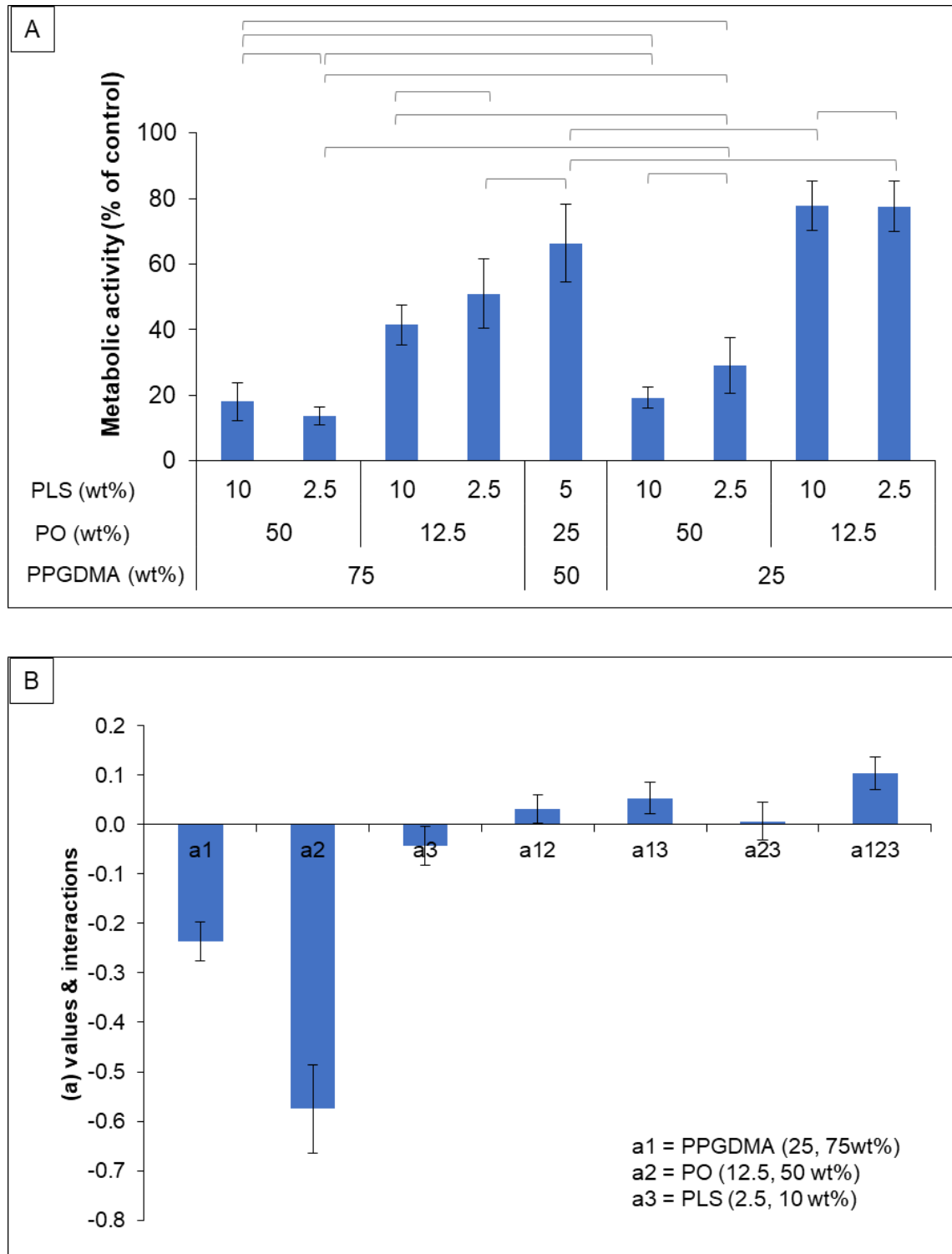


**Fig 8-28 A)** Metabolic activity (relative to the corresponding control) of surviving MSCs after cultured in solutions previously immersed by experimental bone composite discs for 24 hr. **B)** Factorial analysis describing the effect of PPGDMA, PO, PLS, and their interactions on the metabolic activity (relative to the corresponding control) of MSCs. Lines indicate no significant difference ( $p > 0.05$ ). Error bars are 95% CI (n=5).



## **8.8 Discussion**

Injectable bone composites that exhibited low stiffness, high PLS release in addition to apatite precipitation were developed. The effect of PPGDMA, PO, and PLS on the following properties were assessed.

### **8.8.1 Injectability**

Injection biomechanics of bone cements is affected by viscosity of the cements, applied pressure, speed of injection, volume injected, and bone morphology (Boger et al., 2009). A bone composite that can be easily injected and shows no phase separation is expected to facilitate injection of the material during vertebroplasty.

Chapter 4 demonstrates that the viscosity of bone composites is affected by PLR and PPGDMA levels. Higher injection force was therefore required for the experimental bone composites prepared with high powder to liquid ratio (3:1), as was expected. The diameter of the tip of hypodermic syringe (internal tip diameter of 2 mm), used in the current study, was slightly larger than that of a 13 gauge vertebroplasty needle (internal diameter of 1.8 mm) (Dadkhah et al., 2017). Hence, the experimental bone composites may require greater injection force in a clinical situation than that obtained in the above study.

In the current study, more than 90% of the composite pastes were successfully injected through the syringe. Additionally, separation of powder and liquid phase during the injection (i.e. filter pressing) was not observed in any experimental bone composites. This indicated a homogenous mixing between the liquid and powder phase.

The high injection force of composites prepared with PLR of 3:1 suggests these composite formulations may not be suitable with a simple hand injection system. Injection force was reduced upon increasing PPGDMA or PO. This was primarily due to the decreased level of high viscosity UDMA and replacing of small glass fillers with larger phosphate fillers in the composites respectively. Low viscosity and injection force should enable easier placement of the material. The use of low viscosity cement may, however, consequently increase the risk of cement extravasation. Nevertheless, a clinical study showed no association between cement extravasation and viscosity of the cements (Nieuwenhuijse et al., 2010).

### **8.8.2 Monomer conversion**

An ideal bone composite should exhibit sufficient inhibition time (4-8 min), high polymerisation rate to prevent materials being washout, high monomer conversion to ensure good strength and reduce risk of uncured monomer leeching. Furthermore, polymerisation shrinkage and heat generation should be as low as possible to ensure bone adaptation and prevent fibrous encapsulation.

Raising PPGDMA level increased inhibition time of experimental bone composites on average from 1 to 5 min. The increase of inhibition time upon raising PPGDMA was in accordance with previous work from Main (2013). PPGDMA:UDMA wt% in Main's study was comparable to the current study but with lower or higher PLR (1.5:1 for low PPGDMA or 4:1 for high PPGDMA), different level of initiator and activator (0.5 wt% BP and 0.5 wt% DMPT), and no active fillers. Final monomer conversion of the composites in the previous study was slightly lower than that observed with the current study by ~ 10%. The previous work demonstrated that the inhibition time of the composites was governed by inhibitor concentration and initiator efficiency ( $f$ ) at a given initiator and activator concentration. Therefore, the increase of inhibition time upon raising PPGDMA level

could be a consequence of greater amount of inhibitor or higher initiator efficacy in UDMA compared with those of PPGDMA. Raising PO also increased inhibition time. This could be due to high oxygen incorporation resulting from air bubbles entrapment or incomplete wetting of these nonsilanated PO fillers in the hydrophobic monomers. The increase of inhibition time also correlated with decrease in reaction rate (Main, 2013).

The increase of PPGDMA may lower the glass transition temperature of the polymerising mixture, thereby increasing monomer conversion (Sideridou et al., 2002). This high final monomer conversion of the composites may lower the risk of toxic monomer release. Raising of PPGDMA only slightly increased calculated polymerisation shrinkage and heat generation due possibly to the high molecular weight of PPGDMA compensating for increased monomer conversion.

One limitation of the current study was that monomer conversion was measured at room temperature. Future work should assess the monomer conversion at body temperature (37 ° C). The increase in temperature would accelerate the reaction which could affect setting kinetics of the experimental bone composites.

### **8.8.3 Mass and volume change**

Mass and volume of the experimental composites increased linearly with the square root of time indicating a diffusion-controlled mechanism (Leung et al., 2005). Raising hydrophilic components such as phosphate and PLS in composites containing 25 wt% PPGDMA substantially increased their mass change. In contrast, the addition of these additives did not significantly increase mass of the composites containing 75 wt%. This might be due to the high flexibility of PPGDMA polymer led to rapid release of components, thereby resulting in mass loss of the composites.

The loss of mass of the composites containing 75 wt% PPGDMA can be compensated by mass gain due to the formation of dicalcium phosphates in the bulk of specimen or the precipitation of surface apatite as previously described in Chapter 3. The negative final mass change observed in  $P_{75}PO_{12.5}PLS_{10}$  suggested an imbalance of its mass loss and mass gain. This correlated with the SEM image of this composite, (Fig 8-14) where apatite precipitation was not evident, which could probably due to the low level of phosphates.

Mass changes of the composites containing 25 wt% PPGDMA were approximately equal to their volume changes. This suggests that the mass increase of these composites was partially due to water filling pores inside the specimen (Mehdawi et al., 2013). In contrast, mass changes of the composites containing 75 wt% PPGDMA were lower than their volume changes. This was probably due to the rapid loss of components.

Volume expansion ( $\sim 8$  vol%) of the experimental bone composites was higher than their calculated polymerisation shrinkage ( $\sim 4$  vol%). This net increase in volumetric expansion may be beneficial by improving adaptation and interlocking between the composites and the porous bone (Muller et al., 2002).

#### **8.8.4 Polylysine release**

Drug release of polymer-based material is affected by several factors including physicochemical properties of drug, structural characteristics of the resin matrix, and the release environment (Fu and Kao, 2010). Generally, the release of antibiotic from a bone cement is a two stages process including initial burst release from the surface followed by the low and sustained release from the bulk of the cement (Neut et al., 2010; Mori et al., 2011). The benefit of long-term release of antibiotic from a bone cement is

controversial as it might lead to the development of antibiotic resistance (Walker et al., 2016).

Burst release of PLS, which was previously observed with dental composites in Chapter 3, was not seen with experimental bone composites in this chapter. This could be due to that the bone composites exhibited higher monomer conversion (~ 90 %) compared to the dental composites (~ 70 %). Hence, PLS on the surface of experimental bone composites may not be readily released upon exposure to water leading to a delay of PLS release observed in this chapter.

Resin matrix of experimental bone composites became more flexible upon rising PPGDMA level. This then enhanced the PLS diffusion shortening the delay time before release on average from 32 to 6 hr and increased the total release of PLS on average from 31 to 58 %. This high release at early time (within 4 weeks) may help to prevent the infection acquired during hospitalisation which could occur within 1 month (Abdelrahman et al., 2013). This will be of benefit for patients who have high potential to develop infection. Furthermore, the release of PLS from the experimental bone composites containing high PPGDMA could not be detected after reaching their maximum release. This may help to prevent developing of antibiotic resistance to PLS.

Khan (2015) revealed that PLS of 32 ppm is the minimum bactericidal concentration for MSSA (methicillin sensitive *Staphylococcus aureus*), MSSE (methicillin sensitive *Staphylococcus epidermidis*), and MRSA (methicillin resistance *Staphylococcus aureus*). The most common causative organism of infected vertebroplasty was *Staphylococcus aureus* (Abdelrahman et al., 2013). The concentration of PLS released from experimental bone composites after immersion in deionised water for 24 hr was 100 to 2,649 ppm. These were much higher than the minimum bactericidal concentration

of PLS (32 ppm) suggesting that the composites would provide antibacterial effects. This could potentially prevent post-operative infection which is a life-threatening complication after vertebroplasty. In the body, however, physiological fluids or blood perfusion around the injected bone composite may wash out PLS thereby reducing concentration of PLS around the composite.

#### **8.8.5 Apatite formation**

As mentioned earlier, the ability of materials to promote surface apatite precipitation is known to promote bone-bonding ability of the materials. Brushite precipitation was detected in the experimental bone composites containing high PO and PPGDMA. This could be due to the high level of MCPM producing acid upon reacting with water. The acid may be released and lower pH of the solution. This acidic condition ( $\text{pH} < 6.5$ ) is favourable for brushite precipitation (Arifuzzaman and Rohani, 2004; Navarro da Rocha et al., 2017).

After 1 and 4 weeks, calcium and phosphate ions may release from the experimental bone composites slower than the acidic protons. The phosphates then subsequently provided a saturated condition that is favourable for precipitation of low solubility and high Ca/P ratio apatite at late time (after 1 or 4 weeks). The Ca/P ratio ( $\sim 1.3$ ) of the precipitates observed in the above study was lower than that of stoichiometric HA (1.67). This suggests that the precipitates were calcium-deficient hydroxyapatite (CDHA), which is commonly found in biological hard tissues (Yan et al., 2011; Hurle et al., 2014). CDHA was observed with composites containing 25 wt% PPGDMA earlier than with composites containing 75 wt% PPGDMA. The low level of flexible PPGDMA polymers may lower the rate of MCPM disproportionation, thereby promoting a more suitable condition for precipitation of the apatite. The high level of MCPM, however, may cause toxicity to human cells.

It can be seen that the composites in the current studies provided greater surface apatite precipitation than the composites in Chapter 7. Additionally, most formulations showed apatite precipitation quicker (within 1 week) than Cortoss. Raising PLS level, however, did not enhance apatite precipitation as was expected. The reason for this may be that hydrophilic PLS also enhance water sorption leading to a rapid release of acid. Furthermore, according to the finding in Chapter 7, increasing PPGDMA and PO would promote the release of  $\text{Sr}^{2+}$  release and enhance the radiopacity to aid visualisation of the composites during vertebroplasty.  $\text{Sr}^{2+}$  release and its effects on cell responses need to be investigated in future works.

## **8.8.6 Mechanical properties**

### **8.8.6.1 Compressive strength, biaxial flexural strength, and modulus of elasticity**

As mentioned earlier, an injectable bone cement that has comparable stiffness with cancellous bone is required to reduce adjacent vertebral fractures. The results of Chapter 7 demonstrated that a decrease in stiffness of the experimental bone composites could be achieved by raising the level of PPGDMA. This, however, was associated with decreased strength. The experimental bone composites should be able to provide sufficient strength to stabilise fractures. Additionally, their mechanical properties should be higher than that required by ISO 5833. Modulus of elasticity of the composite decreasing with time to match with that of cancellous bone might be beneficial.

The results regarding the compressive strength of Cortoss and Simplex were in accordance to previously published studies (Boyd et al., 2008; Arora et al., 2013). The majority of experimental bone composites exhibited higher compressive strength (70

MPa) and flexural strength (50 MPa) than those required from the BS ISO 5833 (British Standard, 2008). It has to be pointed out that the BS ISO 5833 is generally used for assessing an acrylic cement for cementation of prostheses. A standard for bone composites for bone application has yet to be established.

Strength of experimental bone composites was decreased upon raising flexible monomers and hydrophilic fillers (PO and PLS). Most of the experimental bone composites exhibited strength at early time greater than the compressive strength (23 MPa) and flexural strength (10 – 20 MPa) of cancellous bone (White and Best, 2009). The modulus of elasticity of most experimental composites was, however, lower than that required from ISO 5833 (1.8 GPa). The modulus of elasticity was also comparable to that of cancellous bone (0.1 - 0.7 GPa) (Banse et al., 2002). This was more evident for the composites containing 75 wt% PPGDMA. The application of these composites may help reduce the risk of adjacent vertebral fractures.

Despite modulus of elasticity of Cortoss being greater than that of Simplex, one study revealed that patients with no history of fractures treated with Cortoss developed adjacent vertebral fractures (10 %) lower than the patients treated with PMMA cement (18 %) (Gilula and Persenaire, 2013). The possible explanation for this might be that an average volume of Cortoss (2.3 mL) used per vertebra was less than that of PMMA (3.5 mL). Another reason could be that Cortoss can encourage surface apatite precipitation (Fig 8-14), which may help to improve integration with bone (Sanus et al., 2013). This allowed a more efficient load transfer and more uniformly distributed deformation of the threatened and neighbouring vertebra (Wang et al., 2012), which may subsequently minimise the risk of adjacent vertebral fracture.



The reduction of modulus of elasticity in the experimental bone composite could be due to: 1) the increase of flexible monomer reducing the modulus of the composites according to Rule of mixture (equation 6-1); 2) hydrophilic compounds (PO, PLS) enhancing water sorption which may consequently reduce glass transition temperature of the composite. The effect of raising PPGDMA, PO, and PLS on the reduction in modulus was relatively greater than the reduction in BFS which is in good agreement with results from Chapter 6. This is desirable as the composites would still provide sufficient strength to support fractures.

Interestingly, the formulation containing intermediate level of all variables passed all of the requirements mentioned above. This formulation exhibited sufficient mean compressive strength (160 MPa), flexural strength (98 MPa), and modulus of elasticity (1.8 GPa) for passing ISO requirements. Its modulus was also decreased to the value of 0.9 GPa after 1 week. Therefore, this formulation could be selected for further investigations in future works.

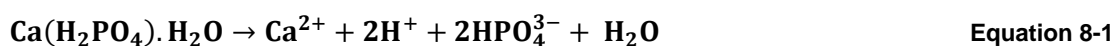
#### **8.8.6.2 Biaxial flexural fatigue**

The strength tested in wet environment and body temperature may be more clinically relevant than that tested in dry condition. BFS of the experimental bone composite in the current study tested in SBF at body temperature was lower than that tested in air at room temperature. This could be due to that wet environment and high temperature enhancing water plasticisation of resin matrix thereby decreasing strength of the composites (Curtis et al., 2009). Furthermore, servo-hydraulic (Dartec HC10) and standard (Shimadzu AGSX) universal testing machine were used to measure BFS in wet and dry condition respectively. Another possible explanation of different BFS result could be therefore a variability between mechanical testing machines.

All experimental bone composites exhibited gradients of S/N curve lower than Simplex as was expected. The extrapolated results were mainly governed by the initial BFS of the composites. Hence, fatigue life of most of these composites was much lower than that observed with experimental bone composites in the previous chapter. It has been shown that vertebra injected with modified low modulus PMMA cement exhibited comparable fatigue properties to that of a vertebra injected with a standard PMMA cement (Boger et al., 2007; Kolb et al., 2013b). Therefore, the fatigue life of these composites in the clinical situation may be longer than that of predicted in the above study. Therefore, future work is needed to assess fatigue properties of *ex vivo* vertebra injected with these low modulus bone composites.

### 8.8.7 Cytocompatibility test

A bone composite with good cytocompatibility is preferable to ensure surviving of bone cells that may facilitate new bone formation and integration with the material. Generally, it is believed that unbound monomers can be leached out from composites. High level of PPGDMA and PO in composites decreased metabolic activity of MSCs. This could probably due to high flexibility PPGDMA polymer that promoted rapid water sorption and subsequently enhanced the dissolution of MCPM. MCPM in experimental bone composites produce calcium ions, phosphate ions, and protons upon exposure to absorbed water (equation 8-1)(Ishikawa, 2011).



These protons may release from the composites leading to a reduction of local pH which could affect cell viability (Van den Vreken et al., 2010). Furthermore, increasing environmental calcium and phosphate ions also affected oxidative mechanisms and induced cell apoptosis (Mansfield et al., 2003; Orrenius et al., 2003). According to *in vitro* studies, calcium phosphate cements have generally low toxicity to human cells

(Carey et al., 2005; Xu et al., 2007). This could be due to that after setting, high soluble phosphates in the cements being transformed to the low soluble biological calcium-deficient apatite/hydroxyapatite.

Experimental bone composites in the current study were immersed in culture media which may have contained lower phosphate ions compared to SBF. Hence, the level of phosphate ions in the solution might not have been sufficient to promote a saturated environment, favourable for the precipitation of the low soluble calcium-deficient hydroxyapatite. The solution, which was subsequently used as a culture medium for MSCS, may consist of high level of leached ions and protons. These conditions may therefore reduce metabolic activity of MSCS.

The release of PLS was expected to provide buffering effects which could improve cytocompatibility of the materials. Nevertheless, PLS itself is hydrophilic that can enhance water sorption to facilitate the release of components. In addition, it was speculated that high PLS concentration may induce cytotoxic effects to MSCS.

This MTS assay provided preliminary information of cell-composite interactions and acted as a pilot study for future projects. This MTS assay was however unable to simulate physiologic conditions where materials will be exposed to complex environments. It is therefore suspected that the effect from rapid release of ions and the alteration of local pH in the culture medium could be mitigated by fluid exchange at the injected site in body (Klammert et al., 2009). Future works may need to assess cytocompatibility of composites at different time points.

## 8.9 Conclusions

Low stiffness, polylysine - releasing, and apatite - forming bone composites were successfully developed. The following conclusions could be drawn.

- 1) The decrease of PLR and increase of PPGDMA lowered injection force.
- 2) High level of PPGDMA led to an increase of inhibition time and monomer conversion for the composites above 90%. This was associated with a small increase of calculated polymerisation shrinkage and heat generation.
- 3) Increasing PPGDMA and PO also enhanced volume expansion which could potentially compensate the polymerisation shrinkage.
- 4) PPGDMA increase enhanced diffusion of PLS. Additionally, increased PPGDMA, PO, and PLS enhanced release of PLS above 50 % at 4 weeks.
- 5) Increase of PPGDMA and PO promoted rapid surface apatite precipitation.
- 6) The increase of PPGDMA and the additives lowered strength of the materials but provided stiffness more comparable to cancellous bone.
- 7) The increase of PPGDMA and PO reduced metabolic activity of MSCS.

## Chaper 9 Summary

The aim of this chapter is to summarise key findings of each chapter.

Chapter 1 provided the background and reviewed the current situation of dental caries and osteoporotic vertebral fracture. Similarities of these diseases include the nature of affected tissues and the currently used therapeutic materials. One major drawback of dental composites is the high risk of secondary caries due to bacterial microleakage. The limitations of the currently used bone cements include toxicity, low monomer conversion, high shrinkage / heat generation, excessive stiffness, and lack of bone-bonding potential. The aim of this Thesis was to test various aspects of novel formulations of either dental or bone composites, with the objective to overcome the aforementioned shortcomings of the currently available materials.

Chapter 2 included a detailed discussion of the general materials and characterisation methods and techniques which were used throughout the Thesis in order to assess various chemical, structural and mechanical properties of the experimental dental and bone composites.

Chapter 3 demonstrated the development of remineralising and antibacterial polylysine-releasing dental composites. These composites exhibited high monomer conversion, and a calculated polymerisation shrinkage comparable with their hygroscopic expansion. The addition of remineralising agents (MCPM and TSrP) promoted surface apatite precipitation within 24 hr. The addition of PLS enhanced this precipitation and enabled burst release of polylysine followed by a linear release versus square root of time. Furthermore, the flexural strength of the composites was greater than that required by the BS ISO 4049 ( $> 80$  MPa).

Chapter 4 demonstrated the development of injectable bone composite by decreasing PLR of dental composites from 4:1 to 3:1, 2.6:1, or 2.3:1. Effects of glass particle size (7, 0.7 $\mu$ m, or equal mass of 0.7 and 7  $\mu$ m), and diluent monomer PPGDMA (25, 50, and 75 wt%) on rheological properties were examined. The experimental bone composites can be characterised as viscoelastic fluids. A solid-like behavior was observed when low strain and frequency were applied. The composites became more liquid-like upon increasing strain and frequency. The increase of PLR and use of small glass filler size enhanced solid-like behaviour of the composite pastes which may help to ensure paste stability at rest or during transportation. Increasing of PLR and reducing PPGDMA led to an increase of viscosity. Viscosities of the composites, however, decreased with increasing shear rate (shear-thinning behaviour) which is desirable for injectable materials.

Chemical initiator (BP) and polymersable amine activator (NTGGMA) were added in the experimental bone composites in Chapter 5 to enable chemical activated polymerisation. Stability of active ingredients (MCPM, TSrP, PLS) in monomers and the initiator and activator pastes containing PPGDMA or TEGDMA upon accelerated temperature ageing were assessed. The active ingredients were stable upon the ageing. The initiator paste of PPGDMA based composite exhibited longer shelf life than the TEGDMA based composite. Additionally, the effect of aging composite at various storage temperatures (4, 23, 37 °C) was also assessed. Replacing TEGDMA with PPGDMA enhanced monomer conversion of the composites. Inhibition time and rate of polymerisation of the composites were slightly increased upon aging for 12 months. Final monomer conversion of the composites, however, remained unchanged.

In Chapter 6 the effects of different glass filler size (0.7 or 7  $\mu$ m), MCPM level (5 or 10 wt%), and fibres (0 or 20 wt%) on strength at early time (24 hr) were investigated. The

use of small glass filler and fibre addition improved biaxial flexural strength and fracture toughness respectively. The effect of increasing PPGDMA on strength of the composites was also examined. The modulus of elasticity of the composites containing low level of PPGDMA was too high compared with cancellous bone but could be optimised by increasing the level of PPGDMA.

In Chapter 7, experimental bone composites with different diluent monomer (PPGDMA versus TEGDMA) and MCPM level (0, 5, and 10 wt%) were developed. Replacing TEGDMA with PPGDMA enhanced monomer conversion and decreased calculated polymerisation shrinkage/heat generation. The use of PPGDMA and increased MCPM level promoted water sorption induced volume expansion which was comparable to polymerisation shrinkage. The composites promoted  $\text{Sr}^{2+}$  release that was enhanced by increasing MCPM or using PPGDMA. The increase of MCPM enhanced surface apatite precipitation. The use of PPGDMA and increase MCPM level decreased strength of the composite. However, the fatigue properties of the experimental bone composites compared favourably with commercial PMMA cement and bone composite.

Chapter 8 focused on the effect of increasing PPGDMA, phosphates (MCPM and TSrP), and PLS on various properties of the experimental bone composites. Increasing PPGDMA increased inhibition time and monomer conversion of the composites. The increase of PPGDMA and phosphates also enabled rapid PLS release in addition to enhanced diffusion and increased total release of polylysine. The increase of PPGDMA and PO also promoted rapid apatite formation and enhanced calcium-deficient hydroxyl apatite precipitation. Increasing PPGDMA, PO, and PLS decreased mechanical properties of the composites. The effect of increased components on BFS was smaller than that observed on modulus of elasticity which is preferable. Additionally, increasing PPGDMA and PO reduced the metabolic activity of mesenchymal stem cells. The

experimental bone composite containing intermediate levels of PPGDMA, PO, and PLS exhibited results in a range that was reasonably acceptable. Therefore, this formulation could be selected for further investigations in future works.

It has to be pointed out that the major limitation of experimental bone composites in this thesis was their inhibition time that were too short ( $< 4$  min) or too long ( $> 8$  min). This inhibition time, however, can be optimised based on results from previous thesis of Khan (2015). Khan demonstrated predictable relationships between inhibition time, rate of reaction, final monomer conversion, mechanical properties and concentration of initiator and activator.

Overall, the project has been successful in its stated aims to produce novel formulations of dental and bone composites to overcome the multiple limitations of current materials. High monomer conversion may improve physical and mechanical properties and decrease the risk of toxic monomer release. Hygroscopic expansion and apatite formation of the novel dental composites may minimise gap formation due to polymerisation shrinkage. The release of PLS was expected to kill residual bacteria. This could potentially help to reduce bacterial microleakage of dental composite restorations.

The good paste stability and optimised rheological properties of the novel bone composites may ensure long shelf-life and ease of application. High monomer conversion with low shrinkage and low heat generation could potentially reduce the risk of thermal damage to surrounding bone. The apatite formation of experimental bone composites may enhance the bone-bonding potential of the materials. High release of PLS upon increasing PPGDMA and phosphates may prevent post-operative infection after vertebroplasty in addition to reducing risk of developing antimicrobial resistance.



The release of  $\text{Sr}^{2+}$  may help to repair the surrounding osteoporotic bone. The reduction of composite's stiffness by increasing PPGDMA may help to maintain load transfer from adjacent vertebra. This could potentially lower the risk of the adjacent vertebral fracture. Furthermore, from a manufacturer's perspective, the modification of bone composite based on dental composite may facilitate the regulatory approval for bone composite.

## Chaper 10 Future Projects

The major areas that should be investigated in future projects are as follows.

### 1) Novel dental composites

- Develop dental caries model to assess the effectiveness of remineralising and antibacterial properties on simulated dental cares model.
- Cytocompatiblity and antibacterial properties of experimental dental composites.
- Long-term mechanical properties and wear resistance of the composites.
- Effect of diets on colour and translucency of the composites
- Radiopacity of the experimental composites.

### 2) Novel bone composites

- Viscosity changes upon paste aging.
- Develop an injection model to assess the risk of cement leakage.
- Optimisation of BP and NTGGMA levels to allow inhibition time of the composites to be 4 - 8 min at 25 °C and 2-4 min at 37 °C.
- Monomer conversion of the experimental bone composites tested at body temperature.
- Radiopacity of the composites to ensure the visibility of the materials during clinical application.
- Develop a vertebroplasty model to assess the effectiveness of low stiffness cement on adjacent vertebral.
- Cytocompatibility of experimental bone composites at longer time
- Proliferation and function of mesenchymal stem cells or other types of relevant cells on experimental bone composite surfaces.
- Incorporation of bisphosphonate into the experimental bone composites to provide local release to the surrounding bone. This may help to increase bone mass of the

osteoporotic bone and prevent complication from systemic administration such as osteonecrosis of the jaw.

## Bibliography

- Abbas G., Fleming G. J., Harrington E., Shortall A. C. & Burke F. J. 2003. Cuspal movement and microleakage in premolar teeth restored with a packable composite cured in bulk or in increments. *Journal of Dentistry*, 31(6), 437-444.
- Abdelrahman H., Siam A. E., Shawky A., Ezzati A. & Boehm H. 2013. Infection after vertebroplasty or kyphoplasty. A series of nine cases and review of literature. *The Spine Journal*, 13(12), 1809-1817.
- Abou Neel E. A., Aljabo A., Strange A., Ibrahim S., Coathup M., Young A. M., Bozec L. & Mudera V. 2016. Demineralization-remineralization dynamics in teeth and bone. *International Journal of Nanomedicine*, 11, 4743-4763.
- Agnihotry A., Fedorowicz Z. & Nasser M. 2016. Adhesively bonded versus non-bonded amalgam restorations for dental caries. *Cochrane Database of Systematic Reviews*, 3(3), CD007517.
- Ahn D. K., Lee S., Choi D. J., Park S. Y., Woo D. G., Kim C. H. & Kim H. S. 2009. Mechanical properties of blood-mixed polymethylmetacrylate in percutaneous vertebroplasty. *Asian Spine Journal*, 3(2), 45-52.
- Al-Ahdal K., Silikas N. & Watts D. C. 2014. Rheological properties of resin composites according to variations in composition and temperature. *Dental Materials*, 30(5), 517-524.
- Al Sunbul H., Silikas N. & Watts D. C. 2016. Polymerization shrinkage kinetics and shrinkage-stress in dental resin-composites. *Dental Materials*, 32(8), 998-1006.
- Alenezi S., Jerban S. & Elkoun S. 2017. Importance of the PMMA viscoelastic rheology on the reduction of the leakage risk during osteoporotic bone augmentation: A numerical leakage model through a porous media. *Journal of the Mechanical Behavior of Biomedical Materials*, 65, 29-41.
- Ali U., Abd Karim K. J. B. & Buang N. A. 2015. A Review of the Properties and Applications of Poly (Methyl Methacrylate) (PMMA). *Polymer Reviews*, 55(4), 678-705.
- Aljabo A., Abou Neel E. A., Knowles J. C. & Young A. M. 2016. Development of dental composites with reactive fillers that promote precipitation of antibacterial-hydroxyapatite layers. *Materials Science and Engineering C: Materials for Biological Applications*, 60, 285-292.

- Aljabo A., Xia W., Liaqat S., Khan M. A., Knowles J. C., Ashley P. & Young A. M. 2015. Conversion, shrinkage, water sorption, flexural strength and modulus of remineralizing dental composites. *Dental Materials*, 31(11), 1279-1289.
- Alshali R. Z., Silikas N. & Satterthwaite J. D. 2013. Degree of conversion of bulk-fill compared to conventional resin-composites at two time intervals. *Dental Materials*, 29(9), e213-217.
- Alves N. M., Leonor I. B., Azevedo H. S., Reis R. L. & Mano J. F. 2010. Designing biomaterials based on biomineralization of bone. *Journal of Materials Chemistry*, 20(15), 2911-2921.
- American Society for Testing and Materials. 2013. ASTM E1823-13 Standard Terminology Relating to Fatigue and Fracture Testing. West Conshohocken. PA: ASTM International.
- Anagnostakos K. 2017. Therapeutic Use of Antibiotic-loaded Bone Cement in the Treatment of Hip and Knee Joint Infections. *Journal of Bone and Joint Infection*, 2(1), 29-37.
- Anagnostakos K. & Kelm J. 2009. Enhancement of antibiotic elution from acrylic bone cement. *Journal of Biomedical Materials Research Part B: Applied Biomaterials*, 90(1), 467-475.
- André C. B., Gomes B. P. F. A., Duque T. M., Rosalen P. L., Chan D. C. N., Ambrosano G. M. B. & Giannini M. 2017. Antimicrobial activity, effects on *Streptococcus mutans* biofilm and interfacial bonding of adhesive systems with and without antibacterial agent. *International Journal of Adhesion and Adhesives*, 72, 123-129.
- Ang S. F., Bortel E. L., Swain M. V., Klocke A. & Schneider G. A. 2010. Size-dependent elastic/inelastic behavior of enamel over millimeter and nanometer length scales. *Biomaterials*, 31(7), 1955-1963.
- Anselmetti G. C., Manca A., Kanika K., Murphy K., Eminefendic H., Masala S. & Regge D. 2009. Temperature measurement during polymerization of bone cement in percutaneous vertebroplasty: an in vivo study in humans. *CardioVascular and Interventional Radiology*, 32(3), 491-498.
- Antonucci J. M., Fowler B. O. & Venz S. 1991. Filler systems based on calcium metaphosphates. *Dental Materials*, 7(2), 124-129.
- Aoba T. 2004. Solubility properties of human tooth mineral and pathogenesis of dental caries. *Oral Diseases*, 10(5), 249-257.
- Aquarius R., Zijden A. M., Homminga J., Verdonschot N. & Tanck E. 2013. Does bone cement in percutaneous vertebroplasty act as a stress riser? *Spine (Phila Pa 1976)*, 38, 2092-2097.

- Arifuzzaman S. M. & Rohani S. 2004. Experimental study of brushite precipitation. *Journal of Crystal Growth*, 267(3-4), 624-634.
- Armas L. A. & Recker R. R. 2012. Pathophysiology of osteoporosis: new mechanistic insights. *Endocrinology and Metabolism Clinics of North America*, 41(3), 475-486.
- Arnaiz-Garcia M. E., Dalmau-Sorli M. J. & Gonzalez-Santos J. M. 2014. Massive cement pulmonary embolism during percutaneous vertebroplasty. *Heart (British Cardiac Society)*, 100(7), 600.
- Arora M., Chan E. K., Gupta S. & Diwan A. D. 2013. Polymethylmethacrylate bone cements and additives: A review of the literature. *World Journal of Orthopedics*, 4(2), 67-74.
- Asmusen S., Arenas G., Cook W. D. & Vallo C. 2009. Photobleaching of camphorquinone during polymerization of dimethacrylate-based resins. *Dental Materials*, 25(12), 1603-1611.
- Ates A., Gemalmaz H. C., Deveci M. A., Simsek S. A., Cetin E. & Senkoylu A. 2016. Comparison of effectiveness of kyphoplasty and vertebroplasty in patients with osteoporotic vertebra fractures. *Acta Orthopaedica et Traumatologica Turcica*, 50(6), 619-622.
- Austin R., Eliyas S., Burke F. J., Taylor P., Toner J. & Briggs P. 2016. British society of prosthodontics debate on the implications of the minamata convention on mercury to dental amalgam—should our patients be worried? *Dental Update*, 43(1), 8-10, 12-4, 16-8.
- Ayre W. N., Denyer S. P. & Evans S. L. 2014. Ageing and moisture uptake in polymethyl methacrylate (PMMA) bone cements. *Journal of the Mechanical Behavior of Biomedical Materials*, 32, 76-88.
- Azam M. T., Khan A. S., Muzzafar D., Faryal R., Siddiqi S. A., Ahmad R., Chauhdry A. A. & Rehman I. U. 2015. Structural, surface, in vitro bacterial adhesion and biofilm formation analysis of three dental restorative composites. *Materials*, 8(6), 3221-3237.
- Badaoui Najjar M., Kashtanov D. & Chikindas M. L. 2009. Natural Antimicrobials  $\epsilon$ -Poly-L-lysine and Nisin A for Control of Oral Microflora. *Probiotics and Antimicrobial Proteins*, 1(2), 143.
- Bae H., Hatten H. P., Jr., Linovitz R., Tahernia A. D., Schaufele M. K., Mccollom V., Gilula L., Maurer P., Benyamin R., Mathis J. M. & Persenaire M. 2012. A prospective randomized FDA-IDE trial comparing Cortoss with PMMA for vertebroplasty: a comparative effectiveness research study with 24-month follow-up. *Spine (Phila Pa 1976)*, 37(7), 544-50.

- Bae H., Shen M., Maurer P., Peppelman W., Beutler W., Linovitz R., Westerlund E., Peppers T., Lieberman I., Kim C. & Girardi F. 2010. Clinical experience using Cortoss for treating vertebral compression fractures with vertebroplasty and kyphoplasty: twenty four-month follow-up. *Spine (Phila Pa 1976)*, 35(20), E1030-E1036.
- Bakhurji E., Scott T., Mangione T. & Sohn W. 2017. Dentists' perspective about dental amalgam: current use and future direction. *Journal of Public Health Dentistry*, n/a-n/a.
- Bakopoulou A., Papadopoulos T. & Garefis P. 2009. Molecular Toxicology of Substances Released from Resin-Based Dental Restorative Materials. *International Journal of Molecular Sciences*, 10(9), 3861.
- Baleani M., Cristofolini L., Minari C. & Toni A. 2003. Fatigue strength of PMMA bone cement mixed with gentamicin and barium sulphate vs pure PMMA. *Proceedings of the Institution of Mechanical Engineers. Part H*, 217(1), 9-12.
- Banerji S., Mehta S. B. & Millar B. J. 2010. Cracked tooth syndrome. Part 1: aetiology and diagnosis. *British Dental Journal*, 208(10), 459-463.
- Banse X., Sims T. J. & Bailey A. J. 2002. Mechanical properties of adult vertebral cancellous bone: correlation with collagen intermolecular cross-links. *Journal of Bone and Mineral Research*, 17(9), 1621-1628.
- Baroud G., Crookshank M. & Böhner M. 2006. High-viscosity cement significantly enhances uniformity of cement filling in vertebroplasty: An experimental model and study on cement leakage. *Spine (Phila Pa 1976)*, 31(22), 2562-2568.
- Becker S., Franz K., Wilke I. & Ogon M. 2006. Injectable bone cements in the treatment of spinal fractures, osteopromotive capacity and surgical considerations. *16th Interdisciplinary Research Conference On Biomaterials*. Bern, Switzerland.
- Belbakra Z., Cherkaoui Z. M. & Allonas X. 2014. Photocurable polythiol based (meth)acrylate resins stabilization: New powerful stabilizers and stabilization systems. *Polymer Degradation and Stability*, 110, 298-307.
- Belli R., Petschelt A. & Lohbauer U. 2014. Are linear elastic material properties relevant predictors of the cyclic fatigue resistance of dental resin composites? *Dental Materials*, 30(4), 381-391.
- Benetti A. R., Havndrup-Pedersen C., Honore D., Pedersen M. K. & Pallesen U. 2015. Bulk-fill resin composites: polymerization contraction, depth of cure, and gap formation. *Operative Dentistry*, 40(2), 190-200.
- Benneker L. M. & Hoppe S. 2013. Percutaneous cement augmentation techniques for osteoporotic spinal fractures. *European Journal of Trauma and Emergency Surgery*, 39(5), 445-453.

- Benzel E. C. 2012. Vertebroplasty and Kyphoplasty. *Spine Surgery*. 3 ed. Philadelphia: Elsevier Saunders, 1253-1262.
- Bernards C., Chapman J. & Mirza S. Lethality of embolized Norian bone cement varies with the time between mixing and embolization. 50th Annual Meeting of the Orthopaedic Research Society, 2004. pp. 7-10.
- Beun S., Bailly C., Dabin A., Vreven J., Devaux J. & Leloup G. 2009. Rheological properties of experimental Bis-GMA/TEGDMA flowable resin composites with various macrofiller/microfiller ratio. *Dental Materials*, 25(2), 198-205.
- Beun S., Glorieux T., Devaux J., Vreven J. & Leloup G. 2007. Characterization of nanofilled compared to universal and microfilled composites. *Dental Materials*, 23(1), 51-59.
- Black D. M. & Rosen C. J. 2016. Clinical Practice. Postmenopausal Osteoporosis. *New England Journal of Medicine*, 374(3), 254-262.
- Blackham J. T., Vandewalle K. S. & Lien W. 2009. Properties of hybrid resin composite systems containing prepolymerized filler particles. *Operative Dentistry*, 34(6), 697-702.
- Blasco J., Martinez-Ferrer A., Macho J., San Roman L., Pomes J., Carrasco J., Monegal A., Guanabens N. & Peris P. 2012. Effect of vertebroplasty on pain relief, quality of life, and the incidence of new vertebral fractures: a 12-month randomized follow-up, controlled trial. *Journal of Bone and Mineral Research*, 27(5), 1159-1166.
- Bo T., Han P. P., Su Q. Z., Fu P., Guo F. Z., Zheng Z. X., Tan Z. L., Zhong C. & Jia S. R. 2016. Antimicrobial epsilon-poly-L-lysine induced changes in cell membrane compositions and properties of *Saccharomyces cerevisiae*. *Food Control*, 61, 123-134.
- Boaro L. C., Goncalves F., Guimaraes T. C., Ferracane J. L., Pfeifer C. S. & Braga R. R. 2013. Sorption, solubility, shrinkage and mechanical properties of "low-shrinkage" commercial resin composites. *Dental Materials*, 29(4), 398-404.
- Bocalon A. C., Mita D., Narumya I., Shouha P., Xavier T. A. & Braga R. R. 2016. Replacement of glass particles by multidirectional short glass fibers in experimental composites: Effects on degree of conversion, mechanical properties and polymerization shrinkage. *Dental Materials*, 32(9), e204-210.
- Boger A., Bohner M., Heini P., Schwieger K. & Schneider E. 2008. Performance of vertebral cancellous bone augmented with compliant PMMA under dynamic loads. *Acta Biomaterialia*, 4(6), 1688-1693.



- Boger A., Heini P., Windolf M. & Schneider E. 2007. Adjacent vertebral failure after vertebroplasty: a biomechanical study of low-modulus PMMA cement. *European Spine Journal*, 16(12), 2118-2125.
- Boger A. & Wheeler K. 2011. A Medium Viscous Acrylic Cement Enhances Uniformity of Cement Filling and Reduces Leakage in Cancellous Bone Augmentation. *ISRN Materials Science*, 2011, 7.
- Boger A., Wheeler K. D., Schenk B. & Heini P. F. 2009. Clinical investigations of polymethylmethacrylate cement viscosity during vertebroplasty and related in vitro measurements. *European Spine Journal*, 18(9), 1272-1278.
- Bonifacio C. C., Kleverlaan C. J., Raggio D. P., Werner A., De Carvalho R. C. & Van Amerongen W. E. 2009. Physical-mechanical properties of glass ionomer cements indicated for atraumatic restorative treatment. *Australian Dental Journal*, 54(3), 233-237.
- Boonen S., Wahl D. A., Nauroy L., Brandi M. L., Bouxsein M. L., Goldhahn J., Lewiecki E. M., Lyritis G. P., Marsh D., Obrant K., Silverman S., Siris E., Akesson K. & Foundation C. S. a. F. W. G. O. I. O. 2011. Balloon kyphoplasty and vertebroplasty in the management of vertebral compression fractures. *Osteoporosis International*, 22(12), 2915-2934.
- Borhan S., Hesarakhi S. & Nezafati N. 2016. Synthesis and rheological evaluations of novel injectable sodium alginate/chitosan-nanostructured hydroxyapatite composite bone pastes. *Journal of the Australian Ceramic Society*, 52(2), 120-127.
- Bouza C., Lopez-Cuadrado T., Almendro N. & Amate J. M. 2015. Safety of balloon kyphoplasty in the treatment of osteoporotic vertebral compression fractures in Europe: a meta-analysis of randomized controlled trials. *European Spine Journal*, 24(4), 715-723.
- Boyd D., Towler M. R., Wren A. & Clarkin O. M. 2008. Comparison of an experimental bone cement with surgical Simplex® P, Spineplex® and Cortoss®. *Journal of Materials Science: Materials in Medicine*, 19(4), 1745-1752.
- Braga R. R., Ballester R. Y. & Ferracane J. L. 2005. Factors involved in the development of polymerization shrinkage stress in resin-composites: a systematic review. *Dental Materials*, 21(10), 962-970.
- Brauer D. S. 2015. Bioactive glasses-structure and properties. *Angewandte Chemie International Edition*, 54(14), 4160-4181.
- British Standard. 2002. BS ISO 5833:2002 Implants for surgery. *Acrylic resin cements*: BSI Standards Limited.

- British Standard. 2008. BS ISO 16402:2008. *Implants for surgery — Acrylic resin cement — Flexural fatigue testing of acrylic resin cements used in orthopaedics*, Switzerland: BSI Standards Limited.
- British Standard. 2009. BS EN ISO 4049:2009 Dentistry. *Polymer- based restorative materials*, Switzerland: BSI Standards Limited.
- British Standard. 2012. BS ISO 23317:2012 Implants for surgery. *In vitro evaluation for apatite-forming ability of implant materials*, Switzerland: BSI Standards Limited.
- British Standard. 2016. BS ISO 13586:2000+A1:2003(E). *Plastics-Determination of fracture toughness ( and )- Linear elastic fracture mechanics (LEFM) approach*, Geneva: BSI Standards Limited.
- Burge R. T., Worley D., Johansen A., Bhattacharyya S. & Bose U. 2008. The cost of osteoporotic fractures in the UK: projections for 2000–2020. *Journal of Medical Economics*, 4(1-4), 51-62.
- Burke F. J., Lucarotti P. S. & Holder R. 2005a. Outcome of direct restorations placed within the general dental services in England and Wales (Part 4): influence of time and place. *Journal of Dentistry*, 33(10), 837-847.
- Burke F. J., Lucarotti P. S. & Holder R. L. 2005b. Outcome of direct restorations placed within the general dental services in England and Wales (Part 2): variation by patients' characteristics. *Journal of Dentistry*, 33(10), 817-826.
- Buszewski B. & Noga S. 2012. Hydrophilic interaction liquid chromatography (HILIC)--a powerful separation technique. *Analytical and Bioanalytical Chemistry*, 402(1), 231-247.
- Cama G. 2014. 1 - Calcium phosphate cements for bone regeneration. In: Dubruel, P. & Vlierberghe, S. V. (eds.) *Biomaterials for Bone Regeneration*. Woodhead Publishing, 3-25.
- Cardoso S. A., Oliveira H. L., Münchow E. A., Carreño N. L. V., Gonini Junior A. & Piva E. 2014. Effect of shelf-life simulation on the bond strength of self-etch adhesive systems to dentin. *Applied Adhesion Science*, 2(1), 26.
- Carey L. E., Xu H. H. K., Simon Jr C. G., Takagi S. & Chow L. C. 2005. Premixed rapid-setting calcium phosphate composites for bone repair. *Biomaterials*, 26(24), 5002-5014.
- Carlsson E., Mestres G., Treerattrakoon K., Lopez A., Karlsson Ott M., Larsson S. & Persson C. 2015. In Vitro and In Vivo Response to Low-Modulus PMMA-Based Bone Cement. *BioMed Research International*, 2015, 594284.

- Cazzaniga G., Ottobelli M., Ionescu A., Garcia-Godoy F. & Brambilla E. 2015. Surface properties of resin-based composite materials and biofilm formation: A review of the current literature. *American Journal of Dentistry*, 28(6), 311-320.
- Chang H.-H., Chang M.-C., Wang H.-H., Huang G.-F., Lee Y.-L., Wang Y.-L., Chan C.-P., Yeung S.-Y., Tseng S.-K. & Jeng J.-H. 2014. Urethane dimethacrylate induces cytotoxicity and regulates cyclooxygenase-2, hemeoxygenase and carboxylesterase expression in human dental pulp cells. *Acta Biomaterialia*, 10(2), 722-731.
- Chang Y., Tai C.-L., Hsieh P.-H. & Ueng S. W. N. 2013. Gentamicin in bone cement: A potentially more effective prophylactic measure of infection in joint arthroplasty. *Bone & Joint Journal*, 2(10), 220-226.
- Chen A. T., Cohen D. B. & Skolasky R. L. 2013. Impact of nonoperative treatment, vertebroplasty, and kyphoplasty on survival and morbidity after vertebral compression fracture in the medicare population. *Journal of Bone and Joint Surgery: American Volume*, 95(19), 1729-1736.
- Chen F. P., Song Z. Y. & Liu C. S. 2015. Fast setting and anti-washout injectable calcium-magnesium phosphate cement for minimally invasive treatment of bone defects. *Journal of Materials Chemistry B*, 3(47), 9173-9181.
- Chen Y. C. & Lin W. C. 2016. Can anti-osteoporotic therapy reduce adjacent fracture in magnetic resonance imaging-proven acute osteoporotic vertebral fractures? *BMC Musculoskeletal Disorders*, 17(1), 151.
- Cheng L., Weir M. D., Xu H. H., Kraigsley A. M., Lin N. J., Lin-Gibson S. & Zhou X. 2012. Antibacterial and physical properties of calcium-phosphate and calcium-fluoride nanocomposites with chlorhexidine. *Dental Materials*, 28(5), 573-83.
- Cheng L., Zhang K., Weir M. D., Melo M. A., Zhou X. & Xu H. H. 2015. Nanotechnology strategies for antibacterial and remineralizing composites and adhesives to tackle dental caries. *Nanomedicine*, 10(4), 627-641.
- Cheng L., Zhang K., Zhou C. C., Weir M. D., Zhou X. D. & Xu H. H. 2016. One-year water-ageing of calcium phosphate composite containing nano-silver and quaternary ammonium to inhibit biofilms. *International of Oral Sciences*, 8(3), 172-181.
- Cheng Y. J., Zeiger D. N., Howarter J. A., Zhang X., Lin N. J., Antonucci J. M. & Lin-Gibson S. 2011. In situ formation of silver nanoparticles in photocrosslinking polymers. 97(1), 124-31.
- Cho A. R., Cho S. B., Lee J. H. & Kim K. H. 2015. Effect of Augmentation Material Stiffness on Adjacent Vertebrae after Osteoporotic Vertebroplasty Using Finite Element Analysis with Different Loading Methods. *Pain Physician*, 18(6), E1101-1110.

- Clark W., Bird P., Gonski P., Diamond T. H., Smerdely P., Mcneil H. P., Schlaphoff G., Bryant C., Barnes E. & Gebiski V. 2016. Safety and efficacy of vertebroplasty for acute painful osteoporotic fractures (VAPOUR): a multicentre, randomised, double-blind, placebo-controlled trial. *The Lancet*, 388(10052), 1408-1416.
- Claxton L., Taylor M. & Kay E. 2016. Oral health promotion: the economic benefits to the NHS of increased use of sugarfree gum in the UK. *British Dental Journal*, 220(3), 121-127.
- Cornelio R. B., Wikant A., Mjøsund H., Kopperud H. M., Haasum J., Gedde U. W. & Örtengren U. T. 2014. The influence of bis-EMA vs bis GMA on the degree of conversion and water susceptibility of experimental composite materials. *Acta Odontologica Scandinavica*, 72(6), 440-447.
- Costa S. M., Martins C. C., Bonfim Mde L., Zina L. G., Paiva S. M., Pordeus I. A. & Abreu M. H. 2012. A systematic review of socioeconomic indicators and dental caries in adults. *International Journal of Environmental Research and Public Health*, 9(10), 3540-3574.
- Curtis A. R., Palin W. M., Fleming G. J. P., Shortall A. C. C. & Marquis P. M. 2009. The mechanical properties of nanofilled resin-based composites: The impact of dry and wet cyclic pre-loading on bi-axial flexure strength. *Dental Materials*, 25(2), 188-197.
- Cury J. A., De Oliveira B. H., Dos Santos A. P. & Tenuta L. M. 2016. Are fluoride releasing dental materials clinically effective on caries control? *Dental Materials*, 32(3), 323-333.
- Dadkhah M., Pontiroli L., Fiorilli S., Manca A., Tallia F., Tcacencu I. & Vitale-Brovarone C. 2017. Preparation and characterisation of an innovative injectable calcium sulphate based bone cement for vertebroplasty application. *Journal of Materials Chemistry B*, 5(1), 102-115.
- Dall'oca C., Maluta T., Cavani F., Morbioli G. P., Bernardi P., Sbarbati A., Degl'innocenti D. & Magnan B. 2014. The biocompatibility of porous vs non-porous bone cements: a new methodological approach. *European Journal of Histochemistry*, 58(2), 2255.
- Darvell B. W. 2009. *Acrylic. Materials Science for Dentistry*. Cambridge: Woodhead Publishing Limited, 109-127.
- Davis H. B., Gwinner F., Mitchell J. C. & Ferracane J. L. 2014. Ion release from, and fluoride recharge of a composite with a fluoride-containing bioactive glass. *Dental Materials*, 30(10), 1187-1194.
- De Oliveira D. C., Rovaris K., Hass V., Souza-Junior E. J., Haiter-Neto F. & Sinhoreti M. A. 2015. Effect of low shrinkage monomers on physicochemical properties of dental resin composites. *Brazilian Dental Journal*, 26(3), 272-276.

- De Souza M. C., Harrison M. & Marshman Z. 2017. Oral health-related quality of life following dental treatment under general anaesthesia for early childhood caries - a UK-based study. *International Journal of Paediatric Dentistry*, 27(1), 30-36.
- Dean S. W., Soltész U., Schäfer R., Jaeger R., Gopp U. & Kühn K. D. 2005. Fatigue Testing of Bone Cements — Comparison of Testing Arrangements. *Journal of ASTM International*, 2(7), 13105.
- Demarco F. F., Correa M. B., Cenci M. S., Moraes R. R. & Opdam N. J. 2012. Longevity of posterior composite restorations: not only a matter of materials. *Dental Materials*, 28(1), 87-101.
- Deng D., Yang H., Guo J., Chen X., Zhang W. & Huang C. 2014. Effects of different artificial ageing methods on the degradation of adhesive-dentine interfaces. *Journal of Dentistry*, 42(12), 1577-1585.
- Dewaele M., Truffier-Boutry D., Devaux J. & Leloup G. 2006. Volume contraction in photocured dental resins: the shrinkage-conversion relationship revisited. *Dental Materials*, 22(4), 359-365.
- Diamond T. H., Bryant C., Browne L. & Clark W. A. 2006. Clinical outcomes after acute osteoporotic vertebral fractures: a 2-year non-randomised trial comparing percutaneous vertebroplasty with conservative therapy. *The Medical Journal of Australia*, 184(3), 113-117.
- Dorozhkin S. V. 2009. Calcium Orthophosphates in Nature, Biology and Medicine. *Materials*, 2(2), 399-498.
- Dorozhkin S. V. 2011. Calcium orthophosphates: Occurrence, properties, biomineralization, pathological calcification and biomimetic applications. *Biomatter*, 1(2), 121-164.
- Dos Santos Junior V. E., De Sousa R. M., Oliveira M. C., De Caldas Junior A. F. & Rosenblatt A. 2014. Early childhood caries and its relationship with perinatal, socioeconomic and nutritional risks: a cross-sectional study. *BMC Oral Health*, 14, 47.
- Drouet C., Carayon M. T., Combes C. & Rey C. 2008. Surface enrichment of biomimetic apatites with biologically-active ions Mg<sup>2+</sup> and Sr<sup>2+</sup>: A preamble to the activation of bone repair materials. *Materials Science and Engineering C: Materials for Biological Applications*, 28(8), 1544-1550.
- Drummond J. L. 2008. Degradation, fatigue, and failure of resin dental composite materials. *Journal of Dental Research*, 87(8), 710-719.
- Du J., Li X. & Lin X. 2014. Kyphoplasty versus vertebroplasty in the treatment of painful osteoporotic vertebral compression fractures: two-year follow-up in a prospective controlled study. *Acta Orthopaedica Belgica*, 80(4), 477-486.

- Du M. H. & Zheng Y. 2008. Degree of conversion and mechanical properties studies of UDMA based materials for producing dental posts. *Polymer Composite*, 29(6), 623-630.
- Dunnick J. K., Brix A., Sanders J. M. & Travlos G. S. 2014. N,N-dimethyl-p-toluidine, a component in dental materials, causes hematologic toxic and carcinogenic responses in rodent model systems. *Toxicologic Pathology*, 42(3), 603-615.
- Durner J., Obermaier J., Draenert M. & Ilie N. 2012. Correlation of the degree of conversion with the amount of elutable substances in nano-hybrid dental composites. *Dental Materials*, 28(11), 1146-1153.
- Eastell R., O'Neill T. W., Hofbauer L. C., Langdahl B., Reid I. R., Gold D. T. & Cummings S. R. 2016. Postmenopausal osteoporosis. *Nature Reviews Disease Primers*, 2, 16069.
- Ekino S., Susa M., Ninomiya T., Imamura K. & Kitamura T. 2007. Minamata disease revisited: an update on the acute and chronic manifestations of methyl mercury poisoning. *Journal of the Neurological Sciences*, 262(1-2), 131-144.
- Ellakwa A., Cho N. & Lee I. B. 2007. The effect of resin matrix composition on the polymerization shrinkage and rheological properties of experimental dental composites. *Dental Materials*, 23(10), 1229-1235.
- Ender A., Zimmermann M., Attin T. & Mehl A. 2016. In vivo precision of conventional and digital methods for obtaining quadrant dental impressions. *Clinical Oral Investigations*, 20(7), 1495-1504.
- Esposito Corcione C., Frigione M., Maffezzoli A. & Malucelli G. 2008. Photo – DSC and real time – FT-IR kinetic study of a UV curable epoxy resin containing o-Boehmites. *European Polymer Journal*, 44(7), 2010-2023.
- Esposito Corcione C., Malucelli G., Frigione M. & Maffezzoli A. 2009. UV-curable epoxy systems containing hyperbranched polymers: Kinetics investigation by photo-DSC and real-time FT-IR experiments. *Polymer Testing*, 28(2), 157-164.
- Esteban Florez F. L., Hiers R. D., Smart K., Kreth J., Qi F., Merritt J. & Khajotia S. S. 2016. Real-time assessment of *Streptococcus mutans* biofilm metabolism on resin composite. *Dental Materials*, 32(10), 1263-1269.
- European Commission 2010. Medical Devices: Guidance document - Classification of medical devices. In: Directorate B Unit B2 "Cosmetics and Medical Devices" (ed.).
- European Commission 2015. Classification of medical devices. DG Health and Consumer.

- Fahim D. K., Sun K., Tawackoli W., Mendel E., Rhines L. D., Burton A. W., Kim D. H., Ehni B. L. & Liebschner M. A. 2011. Premature adjacent vertebral fracture after vertebroplasty: a biomechanical study. *Neurosurgery*, 69(3), 733-744.
- Farrar D. F. & Rose J. 2001. Rheological properties of PMMA bone cements during curing. *Biomaterials*, 22(22), 3005-3013.
- Favus M. J. 2010. Bisphosphonates for osteoporosis. *New England Journal of Medicine*, 363(21), 2027-2035.
- Ferracane J. L. 2006. Hygroscopic and hydrolytic effects in dental polymer networks. *Dental Materials*, 22(3), 211-222.
- Ferracane J. L. 2008. Buonocore Lecture. Placing dental composites--a stressful experience. *Operative Dentistry*, 33(3), 247-257.
- Ferracane J. L. 2011. Resin composite--state of the art. *Dental Materials*, 27(1), 29-38.
- Ferracane J. L. 2013. Resin-based composite performance: are there some things we can't predict? *Dental Materials*, 29(1), 51-58.
- Ferracane J. L. & Hilton T. J. 2016. Polymerization stress--is it clinically meaningful? *Dental Materials*, 32(1), 1-10.
- Fischer D., Li Y., Ahlemeyer B., Krieglstein J. & Kissel T. 2003. In vitro cytotoxicity testing of polycations: influence of polymer structure on cell viability and hemolysis. *Biomaterials*, 24(7), 1121-1131.
- Fontana M., Young D. A., Wolff M. S., Pitts N. B. & Longbottom C. 2010. Defining dental caries for 2010 and beyond. *Dental Clinics of North America*, 54(3), 423-440.
- Forien J.-B., Fleck C., Krywka C., Zolotoyabko E. & Zaslansky P. 2015. In situ compressibility of carbonated hydroxyapatite in tooth dentine measured under hydrostatic pressure by high energy X-ray diffraction. *Journal of the Mechanical Behavior of Biomedical Materials*, 50, 171-179.
- Frasnelli M., Cristofaro F., Sglavo V. M., Dire S., Callone E., Ceccato R., Bruni G., Cornaglia A. I. & Visai L. 2017. Synthesis and characterization of strontium-substituted hydroxyapatite nanoparticles for bone regeneration. *Materials Science and Engineering C: Materials for Biological Applications*, 71, 653-662.
- Frassetto A., Breschi L., Turco G., Marchesi G., Di Lenarda R., Tay F. R., Pashley D. H. & Cadenaro M. 2016. Mechanisms of degradation of the hybrid layer in adhesive dentistry and therapeutic agents to improve bond durability--A literature review. *Dental Materials*, 32(2), e41-53.

- Frencken J. E., Peters M. C., Manton D. J., Leal S. C., Gordan V. V. & Eden E. 2012. Minimal intervention dentistry for managing dental caries - a review: report of a FDI task group. *International Journal of Dentistry*, 62(5), 223-243.
- Fu S. Y., Feng X. Q., Lauke B. & Mai Y. W. 2008. Effects of particle size, particle/matrix interface adhesion and particle loading on mechanical properties of particulate-polymer composites. *Composites Part B: Engineering*, 39(6), 933-961.
- Fu Y. & Kao W. J. 2010. Drug release kinetics and transport mechanisms of non-degradable and degradable polymeric delivery systems. *Expert Opinion on Drug Delivery*, 7(4), 429-444.
- Fujita K., Nishiyama N., Nemoto K., Okada T. & Ikemi T. 2005. Effect of base monomer's refractive index on curing depth and polymerization conversion of photo-cured resin composites. *Dental Materials Journal*, 24(3), 403-408.
- Gandolfi M. G., Taddei P., Siboni F., Modena E., De Stefano E. D. & Prati C. 2011. Biomimetic remineralization of human dentin using promising innovative calcium-silicate hybrid "smart" materials. *Dental Materials*, 27(11), 1055-69.
- Gbureck U., Dembski S., Thull R. & Barralet J. E. 2005. Factors influencing calcium phosphate cement shelf-life. *Biomaterials*, 26(17), 3691-3697.
- Giannini M., Makishi P., Ayres A. P., Vermelho P. M., Fronza B. M., Nikaido T. & Tagami J. 2015. Self-etch adhesive systems: a literature review. *Brazilian Dental Journal*, 26(1), 3-10.
- Gilula L. & Persenaire M. 2013. Subsequent Fractures Post-Vertebral Augmentation: Analysis of a Prospective Randomized Trial in Osteoporotic Vertebral Compression Fractures. *American Journal of Neuroradiology*, 34(1), 221-227.
- Goldberg M. 2008. In vitro and in vivo studies on the toxicity of dental resin components: a review. *Clinical Oral Investigations*, 12(1), 1-8.
- Goncalves F., Kawano Y., Pfeifer C., Stansbury J. W. & Braga R. R. 2009. Influence of BisGMA, TEGDMA, and BisEMA contents on viscosity, conversion, and flexural strength of experimental resins and composites. *European Journal of Oral Sciences*, 117(4), 442-446.
- Goncalves F., Pfeifer C. S., Ferracane J. L. & Braga R. R. 2008. Contraction stress determinants in dimethacrylate composites. *Journal of Dental Research*, 87(4), 367-371.
- Gonzalez-Cabezas C. 2010. The chemistry of caries: remineralization and demineralization events with direct clinical relevance. *Dental Clinics of North America*, 54(3), 469-478.



- Graves J. L., Jr., Tajkarimi M., Cunningham Q., Campbell A., Nonga H., Harrison S. H. & Barrick J. E. 2015. Rapid evolution of silver nanoparticle resistance in *Escherichia coli*. *Frontiers in Genetics*, 6, 42.
- Griffiths P. R. 2002. Introduction to vibrational spectroscopy. In: Chalmers, J. M. & Griffiths, P. R. (eds.) *Handbook of vibrational spectroscopy*. Wiley, 9.
- Grotzky A., Manaka Y., Fornera S., Willeke M. & Walde P. 2010. Quantification of  $\alpha$ -polylysine: a comparison of four UV/Vis spectrophotometric methods. *Analytical Methods*, 2(10), 1448.
- Guo Y., Landis F. A., Wang Z., Bai D., Jiang L. & Chiang M. Y. 2016. Polymerization stress evolution of a bulk-fill flowable composite under different compliances. *Dental Materials*, 32(4), 578-86.
- Gupta S. K., Saxena P., Pant V. A. & Pant A. B. 2012. Release and toxicity of dental resin composite. *Toxicology International*, 19(3), 225-234.
- Habib M., Serhan H., Marchek C. & Baroud G. 2010. Cement leakage and filling pattern study of low viscous vertebroplastic versus high viscous confidence cement. *SAS Journal*, 4(1), 26-33.
- Hadley C., Awan O. A. & Zoarski G. H. 2010. Biomechanics of vertebral bone augmentation. *Neuroimaging Clinics of North America*, 20(2), 159-167.
- Han B., Ma P.-W., Zhang L.-L., Yin Y.-J., Yao K.-D., Zhang F.-J., Zhang Y.-D., Li X.-L. & Nie W. 2009.  $\beta$ -TCP/MCPM-based premixed calcium phosphate cements. *Acta Biomaterialia*, 5(8), 3165-3177.
- Harmata A. J., Uppuganti S., Granke M., Guelcher S. A. & Nyman J. S. 2015. Compressive fatigue and fracture toughness behavior of injectable, settable bone cements. *Journal of the Mechanical Behavior of Biomedical Materials*, 51, 345-355.
- Harvey N., Dennison E. & Cooper C. 2010. Osteoporosis: impact on health and economics. *Nature Reviews Rheumatology*, 6(2), 99-105.
- Hasenwinkel J. M., Lautenschlager E. P., Wixson R. L. & Gilbert J. L. 2002. Effect of initiation chemistry on the fracture toughness, fatigue strength, and residual monomer content of a novel high-viscosity, two-solution acrylic bone cement. *Journal of Biomedical Materials Research*, 59(3), 411-21.
- Hashimoto M. 2010. A review--micromorphological evidence of degradation in resin-dentin bonds and potential preventional solutions. *Journal of Biomedical Materials Research Part B: Applied Biomaterials*, 92(1), 268-280.
- Hatamleh M. M. & Watts D. C. 2010. Mechanical properties and bonding of maxillofacial silicone elastomers. *Dental Materials*, 26(2), 185-191.

- He Z., Zhai Q., Hu M., Cao C., Wang J., Yang H. & Li B. 2015. Bone cements for percutaneous vertebroplasty and balloon kyphoplasty: Current status and future developments. *3(1)*, 1-11.
- Hidalgo E. & Dominguez C. 2001. Mechanisms underlying chlorhexidine-induced cytotoxicity. *Toxicology in vitro*, 15(4-5), 271-276.
- Higgs W. A., Lucksanasombool P., Higgs R. J. & Swain M. V. 2001. A simple method of determining the modulus of orthopedic bone cement. *Journal of Biomedical Materials Research*, 58(2), 188-195.
- Holmgren C., Gaucher C., Decerle N. & Domejean S. 2014. Minimal intervention dentistry II: part 3. Management of non-cavitated (initial) occlusal caries lesions-non-invasive approaches through remineralisation and therapeutic sealants. *British Dental Journal*, 216(5), 237-243.
- Holub O., Lopez A., Borse V., Engqvist H., Kapur N., Hall R. M. & Persson C. 2015. Biomechanics of low-modulus and standard acrylic bone cements in simulated vertebroplasty: A human ex vivo study. *Journal of Biomechanics*, 48(12), 3258-3266.
- Howard B., Wilson N. D., Newman S. M., Pfeifer C. S. & Stansbury J. W. 2010. Relationships between conversion, temperature and optical properties during composite photopolymerization. *Acta Biomaterialia*, 6(6), 2053-2059.
- Hsu H.-C., Chou W.-K., Chiang C.-K. & Wang J.-L. 2014. Effects of fracture severity and cement viscosity on the risk of cement leakage during percutaneous vertebroplasty. *Journal of Biomechanical Science and Engineering*, 9(2), 13-00184-13-00184.
- Hu L., Xiao Y. H., Fang M., Gao Y., Huang L., Jia A. Q. & Chen J. H. 2015. Effects of type I collagen degradation on the durability of three adhesive systems in the early phase of dentin bonding. *PLoS ONE*, 10(2), e0116790.
- Huang L., Zhou B., Wu H., Zheng L. & Zhao J. 2017. Effect of apatite formation of biphasic calcium phosphate ceramic (BCP) on osteoblastogenesis using simulated body fluid (SBF) with or without bovine serum albumin (BSA). *Materials Science and Engineering C: Materials for Biological Applications*, 70(Pt 2), 955-961.
- Hui L., Trujillo-Lemon M., Junhao G. & Stansbury J. W. 2010. Dental Resins Based on Dimer Acid Dimethacrylates: A Route to High Conversion with Low Polymerization Shrinkage. *Compendium of Continuing Education in Dentistry*, 31, 1-4.
- Hulme P. A., Krebs J., Ferguson S. J. & Berlemann U. 2006. Vertebroplasty and kyphoplasty: a systematic review of 69 clinical studies. *Spine (Phila Pa 1976)*, 31(17), 1983-2001.

- Hurle K., Neubauer J., Bohner M., Doebelin N. & Goetz-Neunhoeffler F. 2014. Effect of amorphous phases during the hydraulic conversion of alpha-TCP into calcium-deficient hydroxyapatite. *Acta Biomaterialia*, 10(9), 3931-3941.
- Hyldgaard M., Mygind T., Vad B. S., Stenvang M., Otzen D. E. & Meyer R. L. 2014. The antimicrobial mechanism of action of epsilon-poly-L-lysine. *Applied and Environmental Microbiology*, 80(24), 7758-7770.
- Hyun H.-K. & Ferracane J. L. 2016. Influence of biofilm formation on the optical properties of novel bioactive glass-containing composites. *Dental Materials*, 32(9), 1144-1151.
- Ilie N. & Hickel R. 2009. Investigations on mechanical behaviour of dental composites. *Clinical Oral Investigations*, 13(4), 427-38.
- Ilie N., Hickel R., Valceanu A. S. & Huth K. C. 2012. Fracture toughness of dental restorative materials. *Clinical Oral Investigations*, 16(2), 489-498.
- Imazato S. 2009. Bio-active restorative materials with antibacterial effects: new dimension of innovation in restorative dentistry. *Dental Materials Journal*, 28(1), 11-19.
- Imazato S., Ma S., Chen J. H. & Xu H. H. 2014. Therapeutic polymers for dental adhesives: loading resins with bio-active components. *Dental Materials*, 30(1), 97-104.
- Imazato S., McCabe J. F., Tarumi H., Ehara A. & Ebisu S. 2001. Degree of conversion of composites measured by DTA and FTIR. *Dental Materials*, 17(2), 178-183.
- Irie M., Hatanaka K., Suzuki K. & Watts D. C. 2006. Immediate versus water-storage performance of Class V flowable composite restoratives. *Dental Materials*, 22(9), 875-883.
- Ishikawa K. 2011. Bioactive Ceramics: Cements. In: Paul Ducheyne (ed.) *Comprehensive Biomaterials*. Italy: Elsevier, 281.
- Janssen I., Ryang Y. M., Gempt J., Bette S., Gerhardt J., Kirschke J. S. & Meyer B. 2017. Risk of cement leakage and pulmonary embolism by bone cement-augmented pedicle screw fixation of the thoracolumbar spine. *The Spine Journal*.
- Javidi H., Tickle M. & Aggarwal V. R. 2015. Repair vs replacement of failed restorations in general dental practice: factors influencing treatment choices and outcomes. *British Dental Journal*, 218(1), E2.
- Jeffers J. R., Browne M. & Taylor M. 2005. Damage accumulation, fatigue and creep behaviour of vacuum mixed bone cement. *Biomaterials*, 26(27), 5532-5541.

- Jiranek W. A., Hanssen A. D. & Greenwald A. S. 2006. Antibiotic-loaded bone cement for infection prophylaxis in total joint replacement. *The Journal of Bone and Joint Surgery: American Volume*, 88(11), 2487-2500.
- Johnell O. & Kanis J. A. 2006. An estimate of the worldwide prevalence and disability associated with osteoporotic fractures. *Osteoporosis International*, 17(12), 1726-1733.
- Jokstad A. 2016. Secondary caries and microleakage. *Dental Materials*, 32(1), 11-25.
- Juhasz J. A., Best S. M., Brooks R., Kawashita M., Miyata N., Kokubo T., Nakamura T. & Bonfield W. 2004. Mechanical properties of glass-ceramic A-W-polyethylene composites: effect of filler content and particle size. *Biomaterials*, 25(6), 949-955.
- Kane R. J., Yue W., Mason J. J. & Roeder R. K. 2010. Improved fatigue life of acrylic bone cements reinforced with zirconia fibers. *Journal of the Mechanical Behavior of Biomedical Materials*, 3(7), 504-511.
- Kassebaum N. J., Bernabe E., Dahiya M., Bhandari B., Murray C. J. & Marcenes W. 2015. Global burden of untreated caries: a systematic review and metaregression. *Journal of Dental Research*, 94(5), 650-658.
- Khan A. S., Azam M. T., Khan M., Mian S. A. & Ur Rehman I. 2015. An update on glass fiber dental restorative composites: a systematic review. *Materials Science and Engineering C: Materials for Biological Applications*, 47, 26-39.
- Khan M. A. 2015. Development of antibacterial and remineralising composite bone cements. Thesis (Ph.D.), University College London.
- Khan M. A., Walters N. J. & Young A. M. 2014. Fibre-reinforced injectable orthopedic composites with improved toughness and cell compatibility. *Pioneering the Future of Biomaterials*. Denver Colorado.
- Khvostenko D., Hilton T. J., Ferracane J. L., Mitchell J. C. & Kruzic J. J. 2016. Bioactive glass fillers reduce bacterial penetration into marginal gaps for composite restorations. *Dental Materials*, 32(1), 73-81.
- Khvostenko D., Mitchell J. C., Hilton T. J., Ferracane J. L. & Kruzic J. J. 2013. Mechanical performance of novel bioactive glass containing dental restorative composites. *Dental Materials*, 29(11), 1139-48.
- Kielbassa A. M., Glockner G., Wolgin M. & Glockner K. 2016. Systematic review on highly viscous glass-ionomer cement/resin coating restorations (Part I): Do they merge Minamata Convention and minimum intervention dentistry? *Quintessence International*, 47(10), 813-823.

- Kim Y. K., Yiu C. K., Kim J. R., Gu L., Kim S. K., Weller R. N., Pashley D. H. & Tay F. R. 2010. Failure of a glass ionomer to remineralize apatite-depleted dentin. *Journal of Dental Research*, 89(3), 230-235.
- Kimes M. 2012. *Bad to the bone: A medical horror story* [Online]. Available: <http://fortune.com/2012/09/18/bad-to-the-bone-a-medical-horror-story/> [Accessed 24 March 2017].
- Kinzl M., Benneker L. M., Boger A., Zysset P. K. & Pahr D. H. 2012a. The effect of standard and low-modulus cement augmentation on the stiffness, strength, and endplate pressure distribution in vertebroplasty. *European Spine Journal*, 21(5), 920-929.
- Kinzl M., Boger A., Zysset P. K. & Pahr D. H. 2012b. The mechanical behavior of PMMA/bone specimens extracted from augmented vertebrae: a numerical study of interface properties, PMMA shrinkage and trabecular bone damage. *Journal of Biomechanics*, 45(8), 1478-1484.
- Klammert U., Reuther T., Jahn C., Kraski B., Kübler A. C. & Gbureck U. 2009. Cytocompatibility of brushite and monetite cell culture scaffolds made by three-dimensional powder printing. *Acta Biomaterialia*, 5(2), 727-734.
- Klazen C. A., Venmans A., De Vries J., Van Rooij W. J., Jansen F. H., Blonk M. C., Lohle P. N., Juttman J. R., Buskens E., Van Everdingen K. J., Muller A., Fransen H., Elgersma O. E., Mali W. P. & Verhaar H. J. 2010. Percutaneous vertebroplasty is not a risk factor for new osteoporotic compression fractures: results from VERTOS II. *American Journal of Neuroradiology*, 31(8), 1447-1450.
- Kokubo T., Kim H.-M. & Kawashita M. 2003. Novel bioactive materials with different mechanical properties. *Biomaterials*, 24(13), 2161-2175.
- Kolb J. P., Kueny R. A., Puschel K., Boger A., Rueger J. M., Morlock M. M., Huber G. & Lehmann W. 2013a. Does the cement stiffness affect fatigue fracture strength of vertebrae after cement augmentation in osteoporotic patients? *European Spine Journal*, 22(7), 1650-1656.
- Kolb J. P., Kueny R. A., Puschel K., Boger A., Rueger J. M., Morlock M. M., Huber G. & Lehmann W. 2013b. Does the cement stiffness affect fatigue fracture strength of vertebrae after cement augmentation in osteoporotic patients? *European Spine Journal*, 22(7), 1650-6.
- Kopperud S. E., Tveit A. B., Gaarden T., Sandvik L. & Espelid I. 2012. Longevity of posterior dental restorations and reasons for failure. *European Journal of Oral Sciences*, 120(6), 539-548.
- Koster U., Jaeger R., Bardts M., Wahnes C., Buchner H., Kuhn K. D. & Vogt S. 2013. Creep and fatigue behavior of a novel 2-component paste-like formulation of

- acrylic bone cements. *Journal of Materials Science: Materials in Medicine*, 24(6), 1395-1406.
- Kuehn K. D., Ege W. & Gopp U. 2005. Acrylic bone cements: composition and properties. *The Orthopedic Clinics of North America*, 36(1), 17-28, v.
- Kulik E. M., Waltimo T., Weiger R., Schweizer I., Lenkeit K., Filipuzzi-Jenny E. & Walter C. 2015. Development of resistance of mutans streptococci and *Porphyromonas gingivalis* to chlorhexidine digluconate and amine fluoride/stannous fluoride-containing mouthrinses, in vitro. *Clinical Oral Investigations*, 19(6), 1547-1553.
- Kumar G. & Shivrayan A. 2015. Comparative study of mechanical properties of direct core build-up materials. *Contemporary Clinical Dentistry*, 6(1), 16-20.
- Kurtz S. M., Villarraga M. L., Zhao K. & Edidin A. A. 2005. Static and fatigue mechanical behavior of bone cement with elevated barium sulfate content for treatment of vertebral compression fractures. *Biomaterials*, 26(17), 3699-712.
- Kyllonen L., D'este M., Alini M. & Eglin D. 2015. Local drug delivery for enhancing fracture healing in osteoporotic bone. *Acta Biomaterialia*, 11, 412-34.
- Lane N. E. 2006. Epidemiology, etiology, and diagnosis of osteoporosis. *American Journal of Obstetrics and Gynecology*, 194(2 Suppl), S3-11.
- Laske M., Opdam N. J., Bronkhorst E. M., Braspenning J. C. & Huysmans M. C. 2016. Longevity of direct restorations in Dutch dental practices. Descriptive study out of a practice based research network. *Journal of Dentistry*, 46, 12-17.
- Layrolle P. 2011. Calcium Phosphate Coatings. In: Ducheyne, P. (ed.) *Comprehensive Biomaterials*. 1 ed. Oxford, UK: Elsevier, 224.
- Lee B., Franklin I., Lewis J. S., Coombes R. C., Leonard R., Gishen P. & Stebbing J. 2009. The efficacy of percutaneous vertebroplasty for vertebral metastases associated with solid malignancies. *European Journal of Cancer*, 45(9), 1597-1602.
- Lee C. B., Kim H. S. & Kim Y. J. 2007. Pyogenic Spondylitis after Vertebroplasty - A Report of Two Cases. *Asian Spine Journal*, 1(2), 106-109.
- Lee I., Chang J. & Ferracane J. 2008. Slumping resistance and viscoelasticity prior to setting of dental composites. *Dental Materials*, 24(12), 1586-1593.
- Lee J.-H., Um C.-M. & Lee I.-B. 2006. Rheological properties of resin composites according to variations in monomer and filler composition. *Dental Materials*, 22(6), 515-526.


- Lee J. S., Kim K. W. & Ha K. Y. 2011. The Effect of Vertebroplasty on Pulmonary Function in Patients With Osteoporotic Compression Fractures of the Thoracic Spine. *Journal of Spinal Disorders & Techniques*, 24(2), E11-E15.
- Lee K.-Y., Aitomäki Y., Berglund L. A., Oksman K. & Bismarck A. 2014. On the use of nanocellulose as reinforcement in polymer matrix composites. *Composites Science and Technology*, 105, 15-27.
- Legeros R. Z. 2008. Calcium phosphate-based osteoinductive materials. *Chemical Reviews*, 108(11), 4742-4753.
- Lempel E., Czibulya Z., Kunsagi-Mate S., Szalma J., Sumegi B. & Boddi K. 2014. Quantification of Conversion Degree and Monomer Elution from Dental Composite Using HPLC and Micro-Raman Spectroscopy. *Chromatographia*, 77(17-18), 1137-1144.
- Leprince J. G., Palin W. M., Hadis M. A., Devaux J. & Leloup G. 2013. Progress in dimethacrylate-based dental composite technology and curing efficiency (vol 29, pg 139, 2013). *Dental Materials*, 29(4), 493-493.
- Leung D., Spratt D. A., Pratten J., Gulabivala K., Mordan N. J. & Young A. M. 2005. Chlorhexidine-releasing methacrylate dental composite materials. *Biomaterials*, 26(34), 7145-7153.
- Lewis G. 2006. Injectable bone cements for use in vertebroplasty and kyphoplasty: state-of-the-art review. *Journal of Biomedical Materials Research Part B: Applied Biomaterials*, 76(2), 456-68.
- Lewis G. 2011. Viscoelastic properties of injectable bone cements for orthopaedic applications: state-of-the-art review. *Journal of biomedical materials research. Part B, Applied biomaterials*, 98(1), 171-91.
- Li Y. A., Lin C. L., Chang M. C., Liu C. L., Chen T. H. & Lai S. C. 2012. Subsequent vertebral fracture after vertebroplasty: incidence and analysis of risk factors. *Spine (Phila Pa 1976)*, 37(3), 179-83.
- Lieberman I. H., Togawa D. & Kayanja M. M. 2005. Vertebroplasty and kyphoplasty: filler materials. *The Spine Journal*, 5(6 Suppl), 305S-316S.
- Lin J., Hsieh Y.-C., Chien L.-N., Tsai W.-L. & Chiang Y. H. 2016. Vertebroplasty Associated with a Lower Risk of Mortality and Morbidity of Aged Patients with Painful Vertebral Compression Fractures: A Population-Based Propensity Score Matching Cohort Study in Taiwan. *The Spine Journal*, 16(10), S262.
- Lippert F. & Hara A. T. 2013. Strontium and caries: a long and complicated relationship. *Caries Research*, 47(1), 34-49.

- Listl S., Galloway J., Mossey P. A. & Marcenes W. 2015. Global Economic Impact of Dental Diseases. *Journal of Dental Research*, 94(10), 1355-1361.
- Liu C., Shao H., Chen F. & Zheng H. 2006. Rheological properties of concentrated aqueous injectable calcium phosphate cement slurry. *Biomaterials*, 27(29), 5003-5013.
- Liu J., Rawlinson S. C., Hill R. G. & Fortune F. 2016. Strontium-substituted bioactive glasses in vitro osteogenic and antibacterial effects. *Dental Materials*, 32(3), 412-422.
- Liu W., Zhang J., Weiss P., Tancret F. & Bouler J. M. 2013. The influence of different cellulose ethers on both the handling and mechanical properties of calcium phosphate cements for bone substitution. *Acta Biomaterialia*, 9(3), 5740-5750.
- Lohbauer U. 2010. Dental Glass Ionomer Cements as Permanent Filling Materials? – Properties, Limitations and Future Trends. *Materials*, 3(1), 76.
- Lopez A., Hoess A., Thersleff T., Ott M., Engqvist H. & Persson C. 2011. Low-modulus PMMA bone cement modified with castor oil. *Bio-Medical Materials and Engineering*, 21(5-6), 323-332.
- Lubbert A., Castelletto V., Hamley I. W., Nuhn H., Scholl M., Bourdillon L., Wandrey C. & Klok H. A. 2005. Nonspherical assemblies generated from polystyrene-b-poly(L-lysine) polyelectrolyte block copolymers. *Langmuir*, 21(14), 6582-6589.
- Lubisich E. B., Hilton T. J., Ferracane J. L., Pashova H. I., Burton B. & Northwest P. 2011. Association between caries location and restorative material treatment provided. *Journal of Dentistry*, 39(4), 302-308.
- Lucarotti P. S., Holder R. L. & Burke F. J. 2005. Outcome of direct restorations placed within the general dental services in England and Wales (Part 3): variation by dentist factors. *Journal of Dentistry*, 33(10), 827-835.
- Luo X., Barbieri D., Duan R., Yuan H. & Bruijn J. D. 2015. Strontium-containing apatite/polylactide composites enhance bone formation in osteopenic rabbits. *Acta Biomaterialia*, 26, 331-337.
- Lynch C. D. & Wilson N. H. 2013. Managing the phase-down of amalgam: Part I. Educational and training issues. *British Dental Journal*, 215(3), 109-113.
- Mackey T. K., Contreras J. T. & Liang B. A. 2014. The Minamata Convention on Mercury: attempting to address the global controversy of dental amalgam use and mercury waste disposal. *The Science of the Total Environment*, 472, 125-129.
- Main K. 2013. Development of composites for bone repair. PhD Thesis, University College London.



- Mansfield K., Pucci B., Adams C. S. & Shapiro I. M. 2003. Induction of Apoptosis in Skeletal Tissues: Phosphate-Mediated Chick Chondrocyte Apoptosis is Calcium Dependent. *Calcified Tissue International*, 73(2), 161-172.
- Marcenes W., Kassebaum N. J., Bernabe E., Flaxman A., Naghavi M., Lopez A. & Murray C. J. 2013. Global burden of oral conditions in 1990-2010: a systematic analysis. *Journal of Dental Research*, 92(7), 592-597.
- Mari R., Seto R., Morris J. F. & Denn M. M. 2014. Shear thickening, frictionless and frictional rheologies in non-Brownian suspensions. *Journal of Rheology*, 58(6), 1693-1724.
- Marovic D., Tarle Z., Hiller K. A., Muller R., Rosentritt M., Skrtic D. & Schmalz G. 2014. Reinforcement of experimental composite materials based on amorphous calcium phosphate with inert fillers. *Dental Materials*, 30(9), 1052-1060.
- Marovic D., Taubock T. T., Attin T., Panduric V. & Tarle Z. 2015. Monomer conversion and shrinkage force kinetics of low-viscosity bulk-fill resin composites. *Acta Odontologica Scandinavica*, 73(6), 474-480.
- Marsh P. D. 2010. Microbiology of dental plaque biofilms and their role in oral health and caries. *Dental Clinics of North America*, 54(3), 441-454.
- Martim G. C., Pfeifer C. S. & Giroto E. M. 2017. Novel urethane-based polymer for dental applications with decreased monomer leaching. *Materials Science and Engineering C: Materials for Biological Applications*, 72, 192-201.
- Matos A. C., Goncalves L. M., Rijo P., Vaz M. A., Almeida A. J. & Bettencourt A. F. 2014. A novel modified acrylic bone cement matrix. A step forward on antibiotic delivery against multiresistant bacteria responsible for prosthetic joint infections. *Materials Science and Engineering C: Materials for Biological Applications*, 38, 218-226.
- May-Pat A., Herrera-Kao W., Cauich-Rodriguez J. V., Cervantes-Uc J. M. & Flores-Gallardo S. G. 2012. Comparative study on the mechanical and fracture properties of acrylic bone cements prepared with monomers containing amine groups. *Journal of the Mechanical Behavior of Biomedical Materials*, 6, 95-105.
- Mcdonald R. J., Lane J. I., Diehn F. E. & Wald J. T. 2017. Percutaneous vertebroplasty: Overview, clinical applications, and current state. *Applied Radiology*, 46(1), 24-30.
- Mcparland H. & Warnakulasuriya S. 2012. Oral lichenoid contact lesions to mercury and dental amalgam--a review. *Journal of Biomedicine and Biotechnology*, 2012, 589569.
- Mehbod A., Aunoble S. & Le Huec J. C. 2003. Vertebroplasty for osteoporotic spine fracture: prevention and treatment. *European Spine Journal*, 12 Suppl 2, S155-S162.

- Mehdawi I., Neel E. A., Valappil S. P., Palmer G., Salih V., Pratten J., Spratt D. A. & Young A. M. 2009. Development of remineralizing, antibacterial dental materials. *Acta Biomaterialia*, 5(7), 2525-2539.
- Mehdawi I. M., Pratten J., Spratt D. A., Knowles J. C. & Young A. M. 2013. High strength re-mineralizing, antibacterial dental composites with reactive calcium phosphates. *Dental Materials*, 29(4), 473-484.
- Melo M. A., Guedes S. F., Xu H. H. & Rodrigues L. K. 2013a. Nanotechnology-based restorative materials for dental caries management. *Trends in Biotechnology*, 31(8), 459-67.
- Melo M. A., Weir M. D., Rodrigues L. K. & Xu H. H. 2013b. Novel calcium phosphate nanocomposite with caries-inhibition in a human in situ model. *Dental Materials*, 29(2), 231-240.
- Meriwether L. A., Blen B. J., Benson J. H., Hatch R. H., Tantbirojn D. & Versluis A. 2013. Shrinkage stress compensation in composite-restored teeth: relaxation or hygroscopic expansion? *Dental Materials*, 29(5), 573-579.
- Miola M., Bistolfi A., Valsania M. C., Bianco C., Fucale G. & Verne E. 2013. Antibiotic-loaded acrylic bone cements: an in vitro study on the release mechanism and its efficacy. *Materials Science and Engineering C: Materials for Biological Applications*, 33(5), 3025-3032.
- Mori R., Nakai T., Enomoto K., Uchio Y. & Yoshino K. 2011. Increased antibiotic release from a bone cement containing bacterial cellulose. *Clinical Orthopaedics and Related Research*, 469(2), 600-606.
- Morisebak E., Ansteinssohn V. & Samuelsen J. T. 2015. Cell toxicity of 2-hydroxyethyl methacrylate (HEMA): the role of oxidative stress. *European Journal of Oral Sciences*, 123(4), 282-287.
- Moszner N. & Hirt T. 2012. New polymer-chemical developments in clinical dental polymer materials: Enamel-dentin adhesives and restorative composites. *Journal of Polymer Science Part A: Polymer Chemistry*, 50(21), 4369-4402.
- Mukherjee S. & Lee Y.-P. 2011. Current Concepts in the Management of Vertebral Compression Fractures. *Operative Techniques in Orthopaedics*, 21(3), 251-260.
- Muller S. D., Green S. M. & McCaskie A. W. 2002. The dynamic volume changes of polymerising polymethyl methacrylate bone cement. *Acta Orthopaedica*, 73(6), 684-687.
- Nagem Filho H., Nagem H. D., Francisconi P. A., Franco E. B., Mondelli R. F. & Coutinho K. Q. 2007. Volumetric polymerization shrinkage of contemporary composite resins. *Journal of Applied Oral Science*, 15(5), 448-452.

- Nakamura T., Yamaji T. & Takayama K. 2013. Effects of packaging and heat transfer kinetics on drug-product stability during storage under uncontrolled temperature conditions. *Journal of Pharmaceutical Sciences*, 102(5), 1495-1503.
- National Patient Safety Agency. 2008. Approval for medical devices research. *Guidance for researchers, manufacturers, research ethics committees and NHS R&D offices*: National Research Ethics Service.
- Navarro Da Rocha D., Cruz L. R., De Campos J. B., Marcal R. L., Mijares D. Q., Coelho P. G. & Prado Da Silva M. H. 2017. Mg substituted apatite coating from alkali conversion of acidic calcium phosphate. *Materials Science and Engineering C: Materials for Biological Applications*, 70(Pt 1), 408-417.
- Nedeljkovic I., De Munck J., Slomka V., Van Meerbeek B., Teughels W. & Van Landuyt K. L. 2016a. Lack of Buffering by Composites Promotes Shift to More Cariogenic Bacteria. *Journal of Dental Research*, 95(8), 875-881.
- Nedeljkovic I., Teughels W., De Munck J., Van Meerbeek B. & Van Landuyt K. L. 2015. Is secondary caries with composites a material-based problem? *Dental Materials*, 31(11), e247-277.
- Nedeljkovic I., Yoshihara K., De Munck J., Teughels W., Van Meerbeek B. & Van Landuyt K. L. 2016b. No evidence for the growth-stimulating effect of monomers on cariogenic Streptococci. *Clinical Oral Investigations*, 1-9.
- Neut D., Kluin O. S., Thompson J., Van Der Mei H. C. & Busscher H. J. 2010. Gentamicin release from commercially-available gentamicin-loaded PMMA bone cements in a prosthesis-related interfacial gap model and their antibacterial efficacy. *BMC Musculoskeletal Disorders*, 11(1), 258.
- NICE 2013. Percutaneous vertebroplasty and percutaneous balloon kyphoplasty for treating osteoporotic vertebral compression fractures. *NICE guidelines [ta279]*. London:  National Institute for Health and Care Excellence.
- Nicholas M. K. D., Waters M. G. J., Holford K. M. & Adusei G. 2007. Analysis of rheological properties of bone cements. *Journal of Materials Science: Materials in Medicine*, 18(7), 1407-1412.
- Nieuwenhuijse M. J., Muijs S. P. J., Van Erkel A. R. & Dijkstra S. P. D. 2010. A Clinical Comparative Study on Low Versus Medium Viscosity PolyMethylMetAcrylate Bone Cement in Percutaneous Vertebroplasty Viscosity Associated With Cement Leakage. *Spine (Phila Pa 1976)*, 35(20), E1037-E1044.
- Nudelman F., Pieterse K., George A., Bomans P. H., Friedrich H., Brylka L. J., Hilbers P. A., De With G. & Sommerdijk N. A. 2010. The role of collagen in bone apatite formation in the presence of hydroxyapatite nucleation inhibitors. *Nature Materials*, 9(12), 1004-1009.

- O'Neill R., McCarthy H. O., Cunningham E., Montufar E., Ginebra M. P., Wilson D. I., Lennon A. & Dunne N. 2016. Extent and mechanism of phase separation during the extrusion of calcium phosphate pastes. *Journal of Materials Science: Materials in Medicine*, 27(2), 29.
- O'hara R., Buchanan F. & Dunne N. 2014. Injectable calcium phosphate cements for spinal bone repair. In: Dubruel, P. & Vlierberghe, S. V. (eds.) *Biomaterials for Bone Regeneration*. Woodhead Publishing, 26-61.
- Ooms E. M., Wolke J. G., Van De Heuvel M. T., Jeschke B. & Jansen J. A. 2003. Histological evaluation of the bone response to calcium phosphate cement implanted in cortical bone. *Biomaterials*, 24(6), 989-1000.
- Opdam N. J., Bronkhorst E. M., Loomans B. A. & Huysmans M. C. 2010. 12-year survival of composite vs. amalgam restorations. *Journal of Dental Research*, 89(10), 1063-1067.
- Opdam N. J., Van De Sande F. H., Bronkhorst E., Cenci M. S., Bottenberg P., Pallesen U., Gaengler P., Lindberg A., Huysmans M. C. & Van Dijken J. W. 2014. Longevity of posterior composite restorations: a systematic review and meta-analysis. *Journal of Dental Research*, 93(10), 943-9.
- Oral O., Lassila L. V., Kumbuloglu O. & Vallittu P. K. 2014. Bioactive glass particulate filler composite: Effect of coupling of fillers and filler loading on some physical properties. *Dental Materials*, 30(5), 570-577.
- Orr J. F., Dunne N. J. & Quinn J. C. 2003. Shrinkage stresses in bone cement. *Biomaterials*, 24(17), 2933-4290.
- Orrenius S., Zhivotovsky B. & Nicotera P. 2003. Regulation of cell death: the calcium-apoptosis link. *Nature Reviews Molecular Biology*, 4(7), 552-565.
- Ozok A. R., Wu M. K. & Wesselink P. R. 2002. Comparison of the in vitro permeability of human dentine according to the dentinal region and the composition of the simulated dentinal fluid. *Journal of Dentistry*, 30(2-3), 107-111.
- Padovani G. C., Feitosa V. P., Sauro S., Tay F. R., Duran G., Paula A. J. & Duran N. 2015. Advances in Dental Materials through Nanotechnology: Facts, Perspectives and Toxicological Aspects. *Trends in Biotechnology*, 33(11), 621-636.
- Pan H., Zhao X., Darvell B. W. & Lu W. W. 2010. Apatite-formation ability--predictor of "bioactivity"? *Acta Biomaterialia*, 6(11), 4181-4188.
- Panpisut P., Liaqat S., Zacharaki E., Xia W., Petridis H. & Young A. M. 2016. Dental Composites with Calcium / Strontium Phosphates and Polylysine. *PLoS One*, 11(10), e0164653.

- Papanastassiou I. D., Filis A., Gerochristou M. A. & Vrionis F. D. 2014. Controversial issues in kyphoplasty and vertebroplasty in osteoporotic vertebral fractures. *BioMed Research International*, 2014, 934206.
- Park J. W. & Ferracane J. L. 2014. Water aging reverses residual stresses in hydrophilic dental composites. *Journal of Dental Research*, 93(2), 195-200.
- Pemberton M. N. 2016. Allergy to Chlorhexidine. *Dental Update*, 43(3), 272-274.
- Peterlik H., Roschger P., Klaushofer K. & Fratzl P. 2006. From brittle to ductile fracture of bone. *Nature materials*, 5(1), 52-55.
- Pick B., Meira J. B., Driemeier L. & Braga R. R. 2010. A critical view on biaxial and short-beam uniaxial flexural strength tests applied to resin composites using Weibull, fractographic and finite element analyses. *Dental Materials*, 26(1), 83-90.
- Pinto Gdos S., Oliveira L. J., Romano A. R., Schardosim L. R., Bonow M. L., Pacce M., Correa M. B., Demarco F. F. & Torriani D. D. 2014. Longevity of posterior restorations in primary teeth: results from a paediatric dental clinic. *Journal of Dentistry*, 42(10), 1248-1254.
- Pisani P., Renna M. D., Conversano F., Casciaro E., Di Paola M., Quarta E., Muratore M. & Casciaro S. 2016. Major osteoporotic fragility fractures: Risk factor updates and societal impact. *World Journal of Orthopedics*, 7(3), 171-181.
- Pittayachawan P., Mcdonald A., Petrie A. & Knowles J. C. 2007. The biaxial flexural strength and fatigue property of Lava Y-TZP dental ceramic. *Dental Materials*, 23(8), 1018-1029.
- Pomrink G. J., Diccico M. P., Clineff T. D. & Erbe E. M. 2003. Evaluation of the reaction kinetics of CORTOSS, a thermoset cortical bone void filler. *Biomaterials*, 24(6), 1023-1031.
- Qin C., Xu J. & Zhang Y. 2011. Tubular Structure and Dentin Hypersensitivity Spectroscopic Investigation of the Function of Aqueous 2-Hydroxyethylmethacrylate/Glutaraldehyde Solution as a Dentin Desensitizer. *Journal of Esthetic and Restorative Dentistry*, 23(6), 413-414.
- Qin C. Y., Xu J. W. & Zhang Y. J. 2006. Spectroscopic investigation of the function of aqueous 2-hydroxyethylmethacrylate/glutaraldehyde solution as a dentin desensitizer. *European Journal of Oral Sciences*, 114(4), 354-359.
- Quinn J. B. & Quinn G. D. 2010. A practical and systematic review of Weibull statistics for reporting strengths of dental materials. *Dental Materials*, 26(2), 135-147.
- Race A., Miller M. A., Ayers D. C. & Mann K. A. 2004. Shrinkage of vacuum mixed cement causes interface gaps: gap distribution depends on stem surface finish. *The Journal of Bone and Joint Surgery: British Volume*, 86-B(SUPP I), 9-9.

- Rachner T. D., Khosla S. & Hofbauer L. C. 2011. Osteoporosis: now and the future. *The Lancet*, 377(9773), 1276-87.
- Raggio D. P., Tedesco T. K., Calvo A. F. & Braga M. M. 2016. Do glass ionomer cements prevent caries lesions in margins of restorations in primary teeth?: A systematic review and meta-analysis. *Journal of American Dental Association*, 147(3), 177-185.
- Rai M., Yadav A. & Gade A. 2009. Silver nanoparticles as a new generation of antimicrobials. *Biotechnology Advances*, 27(1), 76-83.
- Randolph L. D., Palin W. M., Leloup G. & Leprince J. G. 2016. Filler characteristics of modern dental resin composites and their influence on physico-mechanical properties. *Dental Materials*, 32(12), 1586-1599.
- Reginster J. Y., Seeman E., De Vernejoul M. C., Adami S., Compston J., Phenekos C., Devogelaer J. P., Curiel M. D., Sawicki A., Goemaere S., Sorensen O. H., Felsenberg D. & Meunier P. J. 2005. Strontium ranelate reduces the risk of nonvertebral fractures in postmenopausal women with osteoporosis: Treatment of Peripheral Osteoporosis (TROPOS) study. *The Journal of Clinical Endocrinology and Metabolism*, 90(5), 2816-2822.
- Regnault W. F., Icenogle T. B., Antonucci J. M. & Skrtic D. 2008. Amorphous calcium phosphate/urethane methacrylate resin composites. I. Physicochemical characterization. *Journal of Materials Science: Materials in Medicine*, 19(2), 507-515.
- Richert L., Arntz Y., Schaaf P., Voegel J. C. & Picart C. 2004. pH dependent growth of poly(L-lysine)/poly(L-glutamic) acid multilayer films and their cell adhesion properties. *Surface Science*, 570(1-2), 13-29.
- Rizzoli R., Reginster J. Y., Boonen S., Breart G., Diez-Perez A., Felsenberg D., Kaufman J. M., Kanis J. A. & Cooper C. 2011. Adverse reactions and drug-drug interactions in the management of women with postmenopausal osteoporosis. *Calcified Tissue International*, 89(2), 91-104.
- Rodriguez L. C., Chari J., Aghyarian S., Gindri I. M., Kosmopoulos V. & Rodrigues D. C. 2014. Preparation and Characterization of Injectable Brushite Filled-Poly (Methyl Methacrylate) Bone Cement. *Materials*, 7(9), 6779-6795.
- Rohlmann A., Boustani H. N., Bergmann G. & Zander T. 2010. A probabilistic finite element analysis of the stresses in the augmented vertebral body after vertebroplasty. *European Spine Journal*, 19(9), 1585-1595.
- Rozenberg M. & Shoham G. 2007. FTIR spectra of solid poly-L-lysine in the stretching NH mode range. *Biophysical Chemistry*, 125(1), 166-171.

- Sa Y., Yang F., Leeuwenburgh S. C. G., Wolke J. G. C., Ye G., De Wijn J. R., Jansen J. A. & Wang Y. 2015. Physicochemical properties and in vitro mineralization of porous polymethylmethacrylate cement loaded with calcium phosphate particles. *Journal of Biomedical Materials Research Part B: Applied Biomaterials*, 103(3), 548-555.
- Saleem H. G., Seers C. A., Sabri A. N. & Reynolds E. C. 2016. Dental plaque bacteria with reduced susceptibility to chlorhexidine are multidrug resistant. *BMC Microbiology*, 16(1), 214.
- Saleh K. J., El Othmani M. M., Tzeng T. H., Mihalko W. M., Chambers M. C. & Grupp T. M. 2016. Acrylic bone cement in total joint arthroplasty: A review. *Journal of Orthopaedic Research*, 34(5), 737-744.
- Sanus G. Z., Ulu M. O., Ozlen F., Biceroglu H., Kucukyuruk B., Isler C., Yassa M. I., Albayram S., Bas A., Oz B., Kurkcu M. & Tanriverdi T. 2013. Assessment of Osteointegration of Cortoss (TM) in Cranioplasty: An Experimental Study in Rabbits. *Journal of Neurological Sciences (Turkish)*, 30(1), 144-152.
- Schmitt S., Krzypow D. J. & Rimnac C. M. 2004. The effect of moisture absorption on the fatigue crack propagation resistance of acrylic bone cement. *Biomedical Engineering (Berlin)*, 49(3), 61-65.
- Schneider L. F., Cavalcante L. M. & Silikas N. 2010. Shrinkage Stresses Generated during Resin-Composite Applications: A Review. *Journal of Dental Biomechanics*, 2010, 131630.
- Schröder C., Nguyen M., Kraxenberger M., Chevalier Y., Melcher C., Wegener B. & Birkenmaier C. 2016. Modification of PMMA vertebroplasty cement for reduced stiffness by addition of normal saline: a material properties evaluation. *European Spine Journal*, 1-7.
- Schumacher M. & Gelinsky M. 2015. Strontium modified calcium phosphate cements - approaches towards targeted stimulation of bone turnover. *Journal of Materials Chemistry B*, 3(23), 4626-4640.
- Schumacher M., Wagner A. S., Kokesch-Himmelreich J., Bernhardt A., Rohnke M., Wenisch S. & Gelinsky M. 2016. Strontium substitution in apatitic CaP cements effectively attenuates osteoclastic resorption but does not inhibit osteoclastogenesis. *Acta Biomaterialia*, 37, 184-194.
- Schweikl H., Spagnuolo G. & Schmalz G. 2006. Genetic and Cellular Toxicology of Dental Resin Monomers. *Journal of Dental Research*, 85(10), 870-877.
- Sellenet P. H., Allison B., Applegate B. M. & Youngblood J. P. 2007. Synergistic Activity of Hydrophilic Modification in Antibiotic Polymers. *Biomacromolecules*, 8(1), 19-23.

- Serra-Gómez R., Dreiss C. A., González-Benito J. & González-Gaitano G. 2016. Structure and Rheology of Poloxamine T1107 and Its Nanocomposite Hydrogels with Cyclodextrin-Modified Barium Titanate Nanoparticles. *Langmuir*, 32(25), 6398-6408.
- Shah D. U., Schubel P. J., Clifford M. J. & Licence P. 2013. Fatigue life evaluation of aligned plant fibre composites through S-N curves and constant-life diagrams. *Composites Science and Technology*, 74, 139-149.
- Shahid S., Hassan U., Billington R. W., Hill R. G. & Anderson P. 2014. Glass ionomer cements: Effect of strontium substitution on esthetics, radiopacity and fluoride release. *Dental Materials*, 30(3), 308-313.
- Shaini F. J., Fleming G. J., Shortall A. C. & Marquis P. M. 2001. A comparison of the mechanical properties of a gallium-based alloy with a spherical high-copper amalgam. *Dental Materials*, 17(2), 142-148.
- Shepherd J. H., Shepherd D. V. & Best S. M. 2012. Substituted hydroxyapatites for bone repair. *Journal of Materials Science: Materials in Medicine*, 23(10), 2335-2347.
- Shi C., Zhao X., Liu Z., Meng R., Chen X. & Guo N. 2016. Antimicrobial, antioxidant, and antitumor activity of epsilon-poly-L-lysine and citral, alone or in combination. *Food & Nutrition Research*, 60, 31891.
- Shim J. B., Warner S. J., Hasenwinkel J. M. & Gilbert J. L. 2005. Analysis of the shelf life of a two-solution bone cement. *Biomaterials*, 26(19), 4181-4187.
- Shima S., Matsuoka H., Iwamoto T. & Sakai H. 1984. Antimicrobial action of epsilon-poly-L-lysine. *The Journal of Antibiotics (Tokyo)*, 37(11), 1449-55.
- Shukla S. & Rai J. S. P. 2013. Synthesis and kinetic study of diacrylate and dimethacrylate. *International Journal of Plastics Technology*, 1-12.
- Shukla S. C., Singh A., Pandey A. K. & Mishra A. 2012. Review on production and medical applications of  $\epsilon$ -polylysine. *Biochemical Engineering Journal*, 65(0), 70-81.
- Sideridou I., Tserki V. & Papanastasiou G. 2002. Effect of chemical structure on degree of conversion in light-cured dimethacrylate-based dental resins. *Biomaterials*, 23(8), 1819-1829.
- Sideridou I. D., Achilias D. S. & Karava O. 2006. Reactivity of Benzoyl Peroxide/Amine System as an Initiator for the Free Radical Polymerization of Dental and Orthopaedic Dimethacrylate Monomers: Effect of the Amine and Monomer Chemical Structure. *Macromolecules*, 39(6), 2072-2080.



- Sideridou I. D., Karabela M. M. & Bikiaris D. N. 2007. Aging studies of light cured dimethacrylate-based dental resins and a resin composite in water or ethanol/water. *Dental Materials*, 23(9), 1142-1149.
- Sideridou I. D., Karabela M. M. & Vouvoudi E. 2011. Physical properties of current dental nanohybrid and nanofill light-cured resin composites. *Dental Materials*, 27(6), 598-607.
- Sideridou I. D. & Vouvoudi E. C. 2015. Dental Composites: Dimethacrylate-Based. *Encyclopedia of Biomedical Polymers and Polymeric Biomaterials*. CRC Press, 2463-2470.
- Sidhu S. K. 2011. Glass-ionomer cement restorative materials: a sticky subject? *Australian Dental Journal*, 56 Suppl 1, 23-30.
- Sidhu S. K. & Nicholson J. W. 2016. A Review of Glass-Ionomer Cements for Clinical Dentistry. *Journal of Functional Biomaterials*, 7(3), E16.
- Sinnett-Jones P. E., Browne M., Moffat A. J., Jeffers J. R., Saffari N., Buffiere J. Y. & Sinclair I. 2009. Crack initiation processes in acrylic bone cement. *Journal of Biomedical Materials Research Part A*, 89(4), 1088-1097.
- Skrtec D. & Antonucci J. M. 2007. Dental composites based on amorphous calcium phosphate - resin composition/physicochemical properties study. *Journal of Biomaterials Applications*, 21(4), 375-393.
- Slane J. A., Vivanco J. F., Rose W. E., Squire M. W. & Ploeg H. L. 2014. The influence of low concentrations of a water soluble poragen on the material properties, antibiotic release, and biofilm inhibition of an acrylic bone cement. *Materials Science and Engineering C: Materials for Biological Applications*, 42, 168-176.
- Smiline G. A., Pandi S. K., Hariprasad P. & Raguraman R. 2012. A preliminary study on the screening of emerging drug resistance among the caries pathogens isolated from carious dentine. *Indian Journal of Dental Research*, 23(1), 26-30.
- Song W., Seta J., Kast R. E., Auner G. W., Chen L., Markel D. C. & Ren W. P. 2015. Influence of Particle Size and Soaking Conditions on Rheology and Microstructure of Amorphous Calcium Polyphosphate Hydrogel. *Journal of the American Ceramic Society*, 98(12), 3758-3769.
- Suh B. I., Feng L., Pashley D. H. & Tay F. R. 2003. Factors contributing to the incompatibility between simplified-step adhesives and chemically-cured or dual-cured composites. Part III. Effect of acidic resin monomers. *Journal of Adhesive Dentistry*, 5(4), 267-282.
- Sun Z., Voigt T. & Shah S. P. 2006. Rheometric and ultrasonic investigations of viscoelastic properties of fresh Portland cement pastes. *Cement and Concrete Research*, 36(2), 278-287.

- Svedbom A., Alvares L., Cooper C., Marsh D. & Strom O. 2013. Balloon kyphoplasty compared to vertebroplasty and nonsurgical management in patients hospitalised with acute osteoporotic vertebral compression fracture: a UK cost-effectiveness analysis. *Osteoporosis International*, 24(1), 355-367.
- Tadros T. 2004. Application of rheology for assessment and prediction of the long-term physical stability of emulsions. *Advances in Colloid and Interface Science*, 108–109, 227-258.
- Takahara K., Kamimura M., Moriya H., Ashizawa R., Koike T., Hidai Y., Ikegami S., Nakamura Y. & Kato H. 2016. Risk factors of adjacent vertebral collapse after percutaneous vertebroplasty for osteoporotic vertebral fracture in postmenopausal women. *BMC Musculoskeletal Disorders*, 17(1), 12.
- Takahashi N. & Nyvad B. 2011. The role of bacteria in the caries process: ecological perspectives. *Journal of Dental Research*, 90(3), 294-303.
- Takahashi N. & Nyvad B. 2016. Ecological Hypothesis of Dentin and Root Caries. *Caries Research*, 50(4), 422-431.
- Takehige F., Kawakami Y., Hayashi M. & Ebisu S. 2007. Fatigue behavior of resin composites in aqueous environments. *Dental Materials*, 23(7), 893-899.
- Takura T., Yoshimatsu M., Sugimori H., Takizawa K., Furumatsu Y., Ikeda H., Kato H., Ogawa Y., Hamaguchi S., Fujikawa A., Satoh T. & Nakajima Y. 2017. Cost-Effectiveness Analysis of Percutaneous Vertebroplasty for Osteoporotic Compression Fractures. *Clinical Spine Surgery*, 30(3), E205-E210.
- Tamimi F., Sheikh Z. & Barralet J. 2012. Dicalcium phosphate cements: brushite and monetite. *Acta Biomaterialia*, 8(2), 474-487.
- Tan J. H., Koh B. T., Ramruttun A. K. & Wang W. 2016. Compression and flexural strength of bone cement mixed with blood. *Journal of Orthopaedic Surgery (Hong Kong)*, 24(2), 240-244.
- Tanaka H., Mori Y., Noro A., Kogure A., Kamimura M., Yamada N., Hanada S., Masahashi N. & Itoi E. 2016. Apatite Formation and Biocompatibility of a Low Young's Modulus Ti-Nb-Sn Alloy Treated with Anodic Oxidation and Hot Water. *PLoS ONE*, 11(2), e0150081.
- Tanaka M. H., Lima G. M. G. & Ito C. Y. K. 2017. Biology of the oral environment and its impact on the stability of dental and craniofacial reconstructions. *Material-Tissue Interfacial Phenomena*. Woodhead Publishing, 181-202.
- Taylor R. S., Taylor R. J. & Fritzell P. 2006. Balloon kyphoplasty and vertebroplasty for vertebral compression fractures: a comparative systematic review of efficacy and safety. *Spine (Phila Pa 1976)*, 31(23), 2747-2755.

- Tome-Bermejo F., Pinera A. R., Duran-Alvarez C., Lopez-San Roman B., Mahillo I. & Alvarez L. 2014. Identification of Risk Factors for the Occurrence of Cement Leakage During Percutaneous Vertebroplasty for Painful Osteoporotic or Malignant Vertebral Fracture. *Spine (Phila Pa 1976)*, 39(11), E693–E700.
- Vaishya R., Chauhan M. & Vaish A. 2013. Bone cement. *Journal of Clinical Orthopaedics and Trauma*, 4(4), 157-163.
- Vallejo R. & Benyamin R. M. 2010. Vertebral augmentation techniques for the treatment of vertebral compression fractures: A review. *Techniques in Regional Anesthesia and Pain Management*, 14(3), 133-141.
- Vallo C. I. 2002. Theoretical prediction and experimental determination of the effect of mold characteristics on temperature and monomer conversion fraction profiles during polymerization of a PMMA-based bone cement. *Journal of Biomedical Materials Research*, 63(5), 627-642.
- Van Den Vreken N. M. F., Pieters I. Y., Declercq H. A., Cornelissen M. J. & Verbeeck R. M. H. 2010. Characterization of calcium phosphate cements modified by addition of amorphous calcium phosphate. *Acta Biomaterialia*, 6(2), 617-625.
- Van Landuyt K. L., Snauwaert J., De Munck J., Peumans M., Yoshida Y., Poitevin A., Coutinho E., Suzuki K., Lambrechts P. & Van Meerbeek B. 2007. Systematic review of the chemical composition of contemporary dental adhesives. *Biomaterials*, 28(26), 3757-3785.
- Venkatasami G. & Sowa J. R., Jr. 2010. A rapid, acetonitrile-free, HPLC method for determination of melamine in infant formula. *Analytica Chimica Acta*, 665(2), 227-230.
- Walker D. H., Mummaneni P. & Rodts G. E., Jr. 2004. Infected vertebroplasty. Report of two cases and review of the literature. *Neurosurgical Focus*, 17(6), E6.
- Walker L. C., Baker P., Holleyman R. & Deehan D. 2016. Microbial resistance related to antibiotic-loaded bone cement: a historical review. *Knee Surgery, Sports Traumatology, Arthroscopy*, 1-10.
- Walters N. J., Xia W., Salih V., Ashley P. F. & Young A. M. 2016. Poly(propylene glycol) and urethane dimethacrylates improve conversion of dental composites and reveal complexity of cytocompatibility testing. *Dental Materials*, 32(2), 264-277.
- Wang J., Zhu C., Cheng T., Peng X., Zhang W., Qin H. & Zhang X. 2013. A systematic review and meta-analysis of antibiotic-impregnated bone cement use in primary total hip or knee arthroplasty. *PLoS ONE*, 8(12), e82745.
- Wang J. L., Chiang C. K., Kuo Y. W., Chou W. K. & Yang B. D. 2012. Mechanism of fractures of adjacent and augmented vertebrae following simulated vertebroplasty. *Journal of Biomechanics*, 45(8), 1372-8.

- Wang X., Xu S., Zhou S., Xu W., Leary M., Choong P., Qian M., Brandt M. & Xie Y. M. 2016. Topological design and additive manufacturing of porous metals for bone scaffolds and orthopaedic implants: A review. *Biomaterials*, 83, 127-141.
- Wang Y., Spencer P. & Walker M. P. 2007. Chemical profile of adhesive/caries-affected dentin interfaces using Raman microspectroscopy. 81(2), 279-86.
- Wang Z., Shen Y. & Haapasalo M. 2014. Dental materials with antibiofilm properties. *Dental Materials*, 30(2), e1-16.
- Wardlaw D., Cummings S. R., Van Meirhaeghe J., Bastian L., Tillman J. B., Ranstam J., Eastell R., Shabe P., Talmadge K. & Boonen S. 2009. Efficacy and safety of balloon kyphoplasty compared with non-surgical care for vertebral compression fracture (FREE): a randomised controlled trial. *The Lancet*, 373(9668), 1016-1024.
- Wegener B., Zolyniak N., Gülecyüz M. F., Büttner A., Von Schulze Pellengahr C., Schaffer V., Jansson V. & Birkenmaier C. 2012. Heat distribution of polymerisation temperature of bone cement on the spinal canal during vertebroplasty. *International Orthopaedics*, 36(5), 1025-1030.
- Wei Y. J., Silikas N., Zhang Z. T. & Watts D. C. 2011. Hygroscopic dimensional changes of self-adhering and new resin-matrix composites during water sorption/desorption cycles. *Dental Materials*, 27(3), 259-266.
- Wei Y. J., Silikas N., Zhang Z. T. & Watts D. C. 2013. The relationship between cyclic hygroscopic dimensional changes and water sorption/desorption of self-adhering and new resin-matrix composites. *Dental Materials*, 29(9), e218-226.
- White A. A. & Best S. M. 2009. Properties and characterisation of bone repair materials. In: Planell, J. A. (ed.) *Bone repair biomaterials*. Florida, USA: Woodhead Publisher, 125.
- Wiegand A., Buchalla W. & Attin T. 2007. Review on fluoride-releasing restorative materials--fluoride release and uptake characteristics, antibacterial activity and influence on caries formation. *Dental Materials*, 23(3), 343-362.
- Wilke H. J., Mehnert U., Claes L. E., Bierschneider M. M., Jaksche H. & Boszczyk B. M. 2006. Biomechanical evaluation of vertebroplasty and kyphoplasty with polymethyl methacrylate or calcium phosphate cement under cyclic loading. *Spine (Phila Pa 1976)*, 31(25), 2934-41.
- Wong C. C. & McGirt M. J. 2013. Vertebral compression fractures: a review of current management and multimodal therapy. *Journal of Multidisciplinary Healthcare*, 6, 205-214.
- Wu C. C., Hsu L. H., Sumi S., Yang K. C. & Yang S. H. 2016a. Injectable and biodegradable composite bone filler composed of poly(propylene fumarate) and

calcium phosphate ceramic for vertebral augmentation procedure: An in vivo porcine study. *Journal of Biomedical Materials Research Part B: Applied Biomaterials*.

- Wu K., Chen Y. C., Hsu Y. M. & Chang C. H. 2016b. Enhancing Drug Release From Antibiotic-loaded Bone Cement Using Porogens. *The Journal of the American Academy of Orthopaedic Surgeons*, 24(3), 188-195.
- Wynn-Jones G., Shelton R. M. & Hofmann M. P. 2014. Injectable citrate-modified Portland cement for use in vertebroplasty. *Journal of Biomedical Materials Research Part B: Applied Biomaterials*, 102(8), 1799-1808.
- Xie D., Brantley W. A., Culbertson B. M. & Wang G. 2000. Mechanical properties and microstructures of glass-ionomer cements. *Dental Materials*, 16(2), 129-138.
- Xin L., Bungartz M., Maenz S., Horbert V., Hennig M., Illerhaus B., Gunster J., Bossert J., Bischoff S., Borowski J., Schubert H., Jandt K. D., Kunisch E., Kinne R. W. & Brinkmann O. 2016. Decreased extrusion of calcium phosphate cement versus high viscosity PMMA cement into spongy bone marrow-an ex vivo and in vivo study in sheep vertebrae. *The Spine Journal*, 16(12), 1468-1477.
- Xu B. S., Hu Y. C., Yang Q., Xia Q., Ma X. L. & Ji N. 2012. Long-term results and radiographic findings of percutaneous vertebroplasties with polymethylmethacrylate for vertebral osteoporotic fractures. *Chinese Medical Journal*, 125(16), 2832-2836.
- Xu H. H., Moreau J. L., Sun L. & Chow L. C. 2010a. Novel CaF<sub>2</sub> nanocomposite with high strength and fluoride ion release. *Journal of Dental Research*, 89(7), 739-745.
- Xu H. H., Weir M. D., Sun L., Moreau J. L., Takagi S., Chow L. C. & Antonucci J. M. 2010b. Strong nanocomposites with Ca, PO<sub>4</sub>, and F release for caries inhibition. *Journal of Dental Research*, 89(1), 19-28.
- Xu H. H. K., Carey L. E., Simon Jr C. G., Takagi S. & Chow L. C. 2007. Premixed calcium phosphate cements: Synthesis, physical properties, and cell cytotoxicity. *Dental Materials*, 23(4), 433-441.
- Yalcin F., Korkmaz Y. & Baseren M. 2006. The effect of two different polishing techniques on microleakage of new composites in Class V restorations. *Journal of Contemporary Dental Practice*, 7(5), 18-25.
- Yan S., Yin J., Cui L., Yang Y. & Chen X. 2011. Apatite-forming ability of bioactive poly(l-lactic acid)/grafted silica nanocomposites in simulated body fluid. *Colloids and Surfaces B: Biointerfaces*, 86(1), 218-224.

- Yang H. & Zou J. 2011. Filling materials used in kyphoplasty and vertebroplasty for vertebral compression fracture: a literature review. *Artificial Cells, Blood Substitutes, and Immobilization Biotechnology*, 39(2), 87-91.
- Yang Y., Dubois A., Qin X. P., Li J., El Haj A. & Wang R. K. 2006. Investigation of optical coherence tomography as an imaging modality in tissue engineering. *Physics in Medicine and Biology*, 51(7), 1649-1659.
- Ye R., Xu H., Wan C., Peng S., Wang L., Xu H., Aguilar Z. P., Xiong Y., Zeng Z. & Wei H. 2013. Antibacterial activity and mechanism of action of epsilon-poly-L-lysine. *Biochemical and Biophysical Research Communications*, 439(1), 148-153.
- Yimin Y., Zhiwei R., Wei M. & Jha R. 2013. Current status of percutaneous vertebroplasty and percutaneous kyphoplasty--a review. *Medical Science Monitor*, 19, 826-836.
- Ying R. 2015. Extraction and Analysis of Strontium in Water Sample Using a Sr (2+) Selective Polymer as the Absorbent Phase. *International Journal of Analytical Chemistry*, 2015, 425084.
- Yli-Urpo H., Vallittu P. K., Narhi T. O., Forsback A. P. & Vakiaparta M. 2004. Release of silica, calcium, phosphorus, and fluoride from glass ionomer cement containing bioactive glass. *Journal of Biomaterials Applications*, 19(1), 15-20.
- Yoshida T. & Nagasawa T. 2003. epsilon-Poly-L-lysine: microbial production, biodegradation and application potential. *Applied Microbiology and Biotechnology*, 62(1), 21-26.
- Yoshida Y., Van Meerbeek B., Nakayama Y., Snauwaert J., Helleman L., Lambrechts P., Vanherle G. & Wakasa K. 2000. Evidence of chemical bonding at biomaterial-hard tissue interfaces. *Journal of Dental Research*, 79, 709-714.
- Young A. M. 2010. 11 - Antibacterial releasing dental restorative materials. In: Lewis, A. (ed.) *Drug-Device Combination Products*. Woodhead Publishing, 246-279.
- Young A. M., Ng P. Y., Gbureck U., Nazhat S. N., Barralet J. E. & Hofmann M. P. 2008. Characterization of chlorhexidine-releasing, fast-setting, brushite bone cements. *Acta Biomaterialia*, 4(4), 1081-1088.
- Young A. M., Rafeeka S. A. & Howlett J. A. 2004. FTIR investigation of monomer polymerisation and polyacid neutralisation kinetics and mechanisms in various aesthetic dental restorative materials. *Biomaterials*, 25(5), 823-833.
- Yu L., Li Y., Zhao K., Tang Y., Cheng Z., Chen J., Zang Y., Wu J., Kong L., Liu S., Lei W. & Wu Z. 2013. A novel injectable calcium phosphate cement-bioactive glass composite for bone regeneration. *PLoS ONE*, 8(4), e62570.
- Yu P., Yap A. & Wang X. Y. 2017. Degree of Conversion and Polymerization Shrinkage of Bulk-Fill Resin-Based Composites. *Operative Dentistry*, 42(1), 82-89.

- Zhan Y., Jiang J., Liao H., Tan H. & Yang K. 2017. Risk Factors for Cement Leakage After Vertebroplasty or Kyphoplasty: A Meta-Analysis of Published Evidence. *World Neurosurgery*, 101, 633-642.
- Zhang K., Li F., Imazato S., Cheng L., Liu H., Arola D. D., Bai Y. & Xu H. H. 2013. Dual antibacterial agents of nano-silver and 12-methacryloyloxydodecylpyridinium bromide in dental adhesive to inhibit caries. *Journal of Biomedical Materials Research Part B: Applied Biomaterials*, 101(6), 929-938.
- Zhang L., Weir M. D., Chow L. C., Antonucci J. M., Chen J. & Xu H. H. 2016a. Novel rechargeable calcium phosphate dental nanocomposite. *Dental Materials*, 32(2), 285-293.
- Zhang M., Puska M. A., Botelho M. G., Sailyoja E. S. & Matinlinna J. P. 2016b. Degree of conversion and leached monomers of urethane dimethacrylate-hydroxypropyl methacrylate-based dental resin systems. *Journal of Oral Sciences*, 58(1), 15-22.
- Zhang N., Melo M., Weir M., Reynolds M., Bai Y. & Xu H. 2016c. Do Dental Resin Composites Accumulate More Oral Biofilms and Plaque than Amalgam and Glass Ionomer Materials? *Materials*, 9(11), 888.
- Zhang W., Shen Y., Pan H., Lin K., Liu X., Darvell B. W., Lu W. W., Chang J., Deng L., Wang D. & Huang W. 2011. Effects of strontium in modified biomaterials. *Acta Biomaterialia*, 7(2), 800-808.
- Zhang Y. R., Du W., Zhou X. D. & Yu H. Y. 2014. Review of research on the mechanical properties of the human tooth. *International Journal of Oral Science*, 6(2), 61-69.
- Zhou Y., Yue W., Li C. & Mason J. J. 2009. Static and fatigue mechanical characterizations of variable diameter fibers reinforced bone cement. *Journal of Materials Science: Materials in Medicine*, 20(2), 633-641.
- Zorzin J., Maier E., Harre S., Fey T., Belli R., Lohbauer U., Petschelt A. & Taschner M. 2015. Bulk-fill resin composites: polymerization properties and extended light curing. *Dental Materials*, 31(3), 293-301.